REPORT OF TECHNICAL COOPERATION FOR RESEARCH AND DEVELOPMENT AND IMPLEMENTATION OF RAILWAY INSPECTION AND MONITORING TECHNOLOGY

Propose to

Thailand International Cooperation Agency (TICA)

Undertake by

RAIL TRANSPORTATION SYSTEM TESTING CENTER (RTTC)

THAILAND INSTITUTE OF SCIENTIFIC AND TECHNOLOGICAL RESEARCH (TISTR)

Contents

Introduction to Operating Organization

Railway Transportation System Testing Center (RTTC) is an organization in Thailand Institute of Scientific and Technological Research (TISTR). TISTR is a State-Owned Enterprise institution under the Ministry of Higher Education Science Research and Innovation (MHESI). TISTR plays an important role in applying Science, Technology, and Innovation to support government policies in rail transport. TISTR has continuously developed the country's capability in testing and inspecting the safety performance of materials and products in the rail industry. Currently, TISTR has successfully developed an ISO/IEC17025 certified laboratory to provide testing service for rail materials and components with International Laboratory Accreditation Certification (ILAC) Testing number 0507. TISTR has been providing testing and inspection services for materials and products for rail construction projects in Thailand such as double-track railway projects, mass transit electric train construction projects, monorail construction projects, and high-speed train construction projects, etc. TISTR is also a major stakeholder in upgrading the National Quality Infrastructure (NQI) system to be a key tool in supporting the country's rail industry to grow sustainably. TISTR collaborates with institutes, universities, and private agencies domestically and internationally to conduct research and development that can sustainably solve problems in the rail transport industry, including personnel development by providing practical upskill programs and enhancing local production (Local Content) in the rail industry.

RTTC-TISTR

ISO/IEC accredited logo of RTTC-TISTR

Within the framework of the Thai-Germany cooperation in 1993, knowledge and experiences in advanced technologies were transferred to RTTC staff through several training programs held in many renowned testing laboratories in Germany such as TUV, Audi, BMW, IABG, etc. Through the expertise and in-depth knowledge of advanced technologies gained from many renowned testing laboratories in Germany, RTTC has built up a strong reputation over two decades in providing professional services and consultancies to several industries such as.

- Automobile (passenger car, light truck, heavy truck)
- Rail & Track (railway infrastructure and rolling stock)
- Civil Engineering and Construction
- Bridge & Deck
- Highway engineering

RTTC has been working mainly in five areas as follows.

1. The National key Laboratory in railway testing

RTTC has been developing test infrastructure specializing in Testing and Certification of materials and products for the rail transport sector covering Rail track and Rolling stock. Most of the tests and certifications follow Project specifications, Contract References, and regional/international standards. Over a decade RTTC was well known as a leading ILAC and ISO/IEC accredited testing laboratory in Thailand and ASEAN.

2. Promote Local Manufacturing

RTTC works with 14 Thai organizations formed as “Railway Alliance” to promote the railway local manufacturing in Thailand and promote the regional rail industry.

3. Develop National Railway standards

RTTC utilizes its expertise in railway testing in developing drafted railway product standards to support Local Manufacturing by working as a standard drafting organization (SDO) and as a committee member for railway product development.

4. Research and Development

RTTC has been conducting industrial/applied research and development in railway transport focusing on Operation and Maintenance (O&M) application. Some successful and ongoing developments in railway applications such as combined Inspection & Monitoring technologies for rail and road transport in Thailand, the development of predictive maintenance platforms for freight wagons, Life Cycles Cost of railway infrastructure and components, etc.

5. Technology Transfer

By utilizing RTTC's modern test facilities, RTTC collaborates with domestic and international railway expert organizations to develop technology transfer programs for governmental institutions, academic railway curriculums for universities, and professional training courses for engineers and researchers.

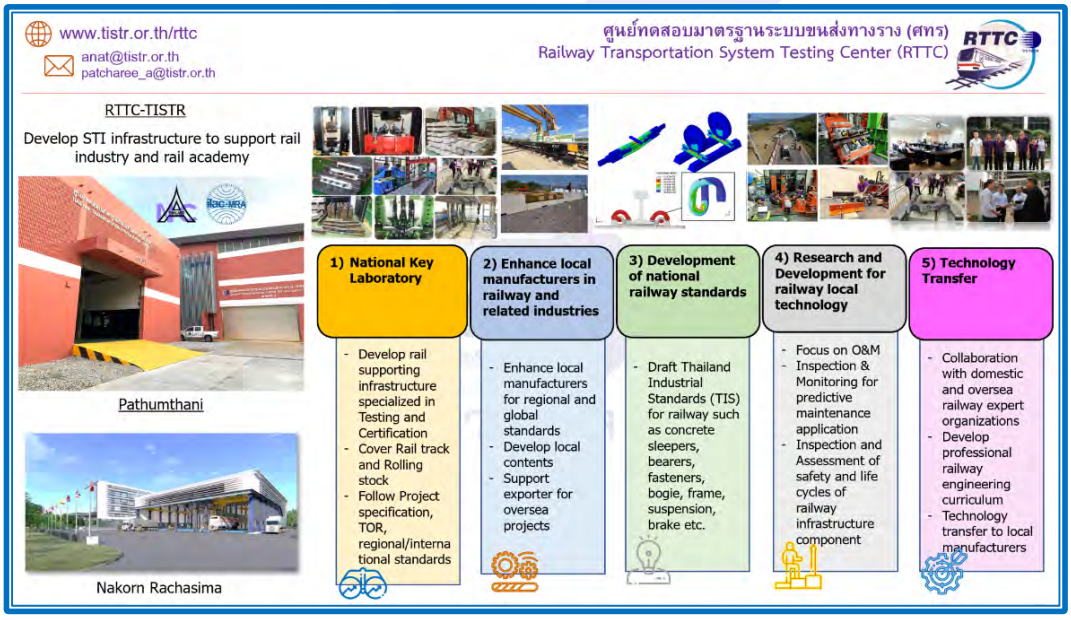

Summary of the main activity of RTTC-TISTR.

More details about the RTTC can be explored by downloading this document.
https://drive.google.com/file/d/1NfjHkgIIAqFhxxUbClaVqIuzrr5y9ysp/view?usp=sharing

Introduction of the project

Improving the economic situation is the main concern of developing countries. One of the attempts that will certainly guarantee more income for developing countries is to develop their railway transportation. As the cheapest, most energy-efficient, and most reliable land transportation. As the cheapest, most energy efficient, and most reliable land transportation, the railway is the hope of many developing countries to raise more income whether from improving connectivity to its neighboring countries for more export of goods or from increasing more reliable way to transport people in and outside their countries to promote their tourism. However, railway sectors in ASEAN developing countries have been neglected and left to deteriorate for decades. Many railway lines are under speed restrictions due to their conditions and many aged rolling stock units are still operating despite their service age. This massively handicapped the ability of the railway sector to provide the expected level of efficiency and reliability in transporting goods and people so most passengers and manufacturers chose other less time-consuming and safer but costly modes of transportation thus resulting in transportation cost increases for freight transportation and passenger travel. Furthermore, with many upcoming railway projects in developing countries, this problem will become more visible as there is a need to restore the old railway lines to accommodate new rolling stock technology. With current railway inspection technology in ASEAN developing countries, assuring the safety of the old railway lines will not be easy as maintenance personnel must do the inspection manually on the rail. As new train technology is being implemented enabling faster-speed trains, the amount of damage and loss it could generate in the event of an accident can also become more devastating. To prevent accidents, monitoring technology has to be implemented to detect potential problems as fast as possible to avoid damage and loss from railway accidents.

At the present time, there are several new efficient technologies available in the market for railway inspection and monitoring. These technologies collectively contribute to safer, more reliable, and efficient railway systems, ensuring they meet the demands of modern transportation. Some benefits of modern technology over conventional technology are such as.

- Increased Safety: Early detection of defects prevents accidents.
- Cost Savings: Efficient inspection methods reduce maintenance costs.

- Enhanced Efficiency: Automation minimizes human intervention and speeds up processes.
- Sustainability: Optimized maintenance extends the lifespan of infrastructure.

1. Non-Destructive Testing (NDT): NDT methods assess the condition of railway infrastructure without causing damage. These techniques ensure the integrity of tracks, wheels, and other components. Some examples of NDT techniques are Ultrasonic Testing (UT), Magnetic Particle Inspection (MPI), and Eddy Current Testing. Some descriptions of this technique are as follows.

- Ultrasonic Testing (UT):
    - Uses high-frequency sound waves to penetrate materials.
    - Detects internal defects like cracks, voids, and inclusions.
    - Performed with hand-held devices or automated rail-mounted systems.
    - Example: Ultrasonic rail flaw detection cars.
- Magnetic Particle Inspection (MPI):
    - Utilized for ferromagnetic materials.
    - Detects surface and near-surface cracks by applying magnetic fields and fine iron particles.
- Eddy Current Testing:
    - Ideal for detecting surface cracks in conductive materials.
    - Commonly used for inspecting wheel treads, axles, and rails.

2. Automated Track Inspection Systems: these advanced automated systems offer precise and continuous monitoring of rail tracks, such as.

- Track Geometry Measurement Systems (TGMS):
    - Uses lasers, gyroscopes, and accelerometers to assess alignment, curvature, and elevation.
    - Mounted on inspection cars or high-speed trains.
- Rail Profiling Systems:
    - Employ laser or video technologies to measure rail wear and cross-sectional profiles.
    - Helps plan grinding and replacement activities.
- Gauge Restraint Measurement Systems (GRMS):
    - Measures the strength and flexibility of the track gauge, especially in curves.

3. Machine Vision and AI-Based Inspection: The vision-based systems leverage high-resolution cameras and artificial intelligence for automated analysis. Some elements of machine vision and AI-based inspection are as follows.

- High-Speed Cameras:
    - Capture images of track components at speeds up to 300 km/h.
    - Identify surface defects, missing fasteners, or ballast irregularities.
- AI and Machine Learning:
    - Algorithms analyzed images to detect defects in real time.
    - Continuously improve accuracy with more data.
- Thermal Imaging:
    - Identifies overheating components such as bearings or brakes.

4. Drones and UAVs: Currently, unmanned aerial vehicles (UAVs) are increasingly used for many applications. In railway inspection, the UAVs are likely gaining more interest due to their ability to access many restricted access areas, especially the way-side infrastructures. Some applications of UAVs are as follows.

- Applications:
    - Inspect hard-to-access areas like bridges, tunnels, and viaducts.
    - Monitor vegetation encroachment and landslide risks.
    - Thermal imaging for detecting heat anomalies.
- Advantages:
    - Cost-effective and quick deployment.
    - Reduces human risk in dangerous locations.

5. Laser and LiDAR Technology: These technologies provide highly accurate measurements and 3D mapping ability. Some railway applications are as follows.

- Laser Scanners:
    - Analysed track irregularities, rail profiles, and clearance envelopes.
    - Useful for precise measurements of track alignment.
- LiDAR (Light Detection and Ranging):
    - Generates 3D models of tracks and surrounding environments.
    - Detects infrastructure deformation and vegetation encroachment.

6. Acoustic and Vibration Monitoring: Acoustic and vibration technologies monitor the dynamic performance of railway components.

- Acoustic Emission Testing:
  - Detects stress waves produced by crack formation and propagation.
  - Helps identify wheel cracks and rail fractures.
- Vibration Sensors:
  - Monitor wheel-rail interaction for irregularities.
  - Identify track settlement or defective sleepers.

7. Ground Penetrating Radar (GPR): The GPR is mainly used to examine subsurface conditions beneath tracks.

- Applications:
  - Detects ballast fouling, water ingress, and voids.
  - Maps layers of ballast, subgrade, and soil.
- Benefits:
  - Provides insights into issues not visible on the surface.
  - Helps plan track maintenance.

8. Real-Time Monitoring Systems: The Real-time systems collect continuous data for immediate analysis and action.

- Trackside Monitoring Devices:
  - Wheel Impact Load Detectors (WILD): Measure impact forces caused by defective wheels.
  - Hot Box Detectors (HBD): Detect overheating in axle boxes.
- Onboard Monitoring Systems:
  - Equipped on trains to detect anomalies in track geometry, rail wear, and ride quality.
  - Data can be shared with the Operation Control Center (OCC) for immediate action.

9. Satellite and Remote Sensing: Satellites and remote sensors are used to monitor railway networks over vast areas.

- Applications:
  - Detect landslides, erosion, or flooding risks near tracks.

    - Monitor settlement or deformation in railway embankments.
- Benefits:
    - Provides large-scale monitoring with minimal ground intervention.
    - Supports disaster risk assessment.

10. Digital Twin and Predictive Maintenance: The latest modern railways increasingly rely on digital technology and data-driven predictions.

- Digital Twin Technology:
    - Creates a virtual model of the railway system.
    - Simulates real-world conditions to test maintenance scenarios.
- Predictive Analytics:
    - Uses historical and real-time data to predict failures.
    - Enables proactive maintenance, reducing unplanned outages.

One of the most critical and practical techniques in railway inspection and monitoring is the dynamic weighing of wagon and wheel loads, often achieved using some weighing devices such as Loadcell, Wheel Impact Load Detectors (WILD), etc. Wagon and wheel loads play a vital role in ensuring the safety, efficiency, and longevity of railway infrastructure and rolling stock. The following photographs show some examples of the currently available technology for WILD.

Example photograph of Loadcell installed on the rail.

Example photograph of WILD system installed on the way-side of track.

Example photograph: The Tamtron Scalex Wild wheel impact measuring system

The weighing of the wagon can be achieved in static and dynamic. Even though static weighing will give more accurate and reliable data, dynamic weighing is preferable due to the advantages of un-interrupt the rail operation. The weighing of wagons is a cornerstone of safe and efficient modern railway operations. By monitoring wheel loads in real-time, operators can address issues before they escalate, ensuring smooth and reliable train operations. Its integration with other advanced technologies, such as predictive maintenance systems and digital twins, makes it indispensable for modern railway management.

Dynamic weighing measures the force exerted by a train's wheels on the track while the train is in motion. Unlike static weighing systems, dynamic systems assess wheel loads at operational speeds, providing real-time insights into wheel-rail interaction under actual service conditions.

The weighing system could comprise Trackside Sensors, usually strain gauges or load cells installed in the track bed to measure the vertical forces applied by passing wheels. Sensors are typically placed at strategic locations along the track where data collection is most effective. The data collection takes place as the train moves over the sensors; the system records the load exerted by each wheel in real time. The data is then analyzed to detect imbalances, overloads, or irregular force distributions. The analysis of the data and subsequent action is achieved by processing the Algorithms to identify wheels or axles with abnormally high impact forces. The alerts are either warning messages or triggered for maintenance if the forces exceed predefined safety thresholds. The key applications of the dynamic weighing system are as follows.

- Detection of wheel defects: Identifies flat spots, cracks, or uneven wear on wheels that can cause excessive impact forces.
- Overload monitoring: Detects overloaded wagons that could damage the track or compromise stability.
- Wheel-Rail interaction analysis: Helps optimize wheel profiles and track geometry for smoother operations.
- Preventive maintenance: Enables targeted repairs, reducing the risk of derailments and minimizing infrastructure damage.

The benefits of the dynamic weighing system are as follows:

- Improved safety: Prevents derailments by identifying hazardous wheel conditions or overloaded wagons.
- Reduced maintenance Costs: Minimizes track wear and damage caused by uneven or excessive forces.
- Enhanced efficiency: Real-time monitoring allows for immediate action, reducing delays and service disruptions.
- Extended asset lifespan: Protects both rolling stock and track infrastructure from premature degradation.

One of the practical benefits of the dynamic weighing of wagons is the understanding of the weight balance of the wagon. Unbalanced wheel loads in rail transport can lead to various types of damage to both the infrastructure and rolling stock. These damages not only compromise the safety and efficiency of railway operations but also result in increased maintenance costs and

reduced service life for components. Typically, railway operators should employ technologies like dynamic wheel load monitoring (e.g., Wheel Impact Load Detectors) and predictive maintenance systems to identify and address unbalanced loads before significant damage occurs.

There are some common types of damage caused by unbalanced wagon wheel loads:

1. Rail infrastructure damage such as

- Track Wear and Deformation: Uneven wheel loads accelerate wear on rail heads and cause asymmetrical deformation. Corrugation, pitting, and spalling on the rail surface such as Rail Cracks and Fractures: The concentrated stress from overloaded wheels can cause fatigue cracks. If undetected, these can propagate, leading to rail fractures and potential derailments.
- Ballast Damage: Excessive forces from unbalanced loads can crush or displace ballast, reducing its ability to distribute weight evenly. This can lead to track instability and increased risk of derailment.
- Sleeper Damage: Overloaded wheels can cause cracking or breakage of concrete sleepers or even wooden sleepers.
- Degrades track integrity and alignment.

2. Rolling Stock Damage such as

- Flat Spots on Wheels: Unbalanced loads increase the likelihood of wheel slippage and skidding, leading to flat spots. Flat spots cause further uneven loading, creating a feedback loop of damage.
- Bearing and Axle Stress: Overloaded wheels place extra strain on axle bearings and the axle itself, thus increasing the risk of bearing failure or axle fatigue, which can result in catastrophic derailments.
- Uneven Suspension Wear: Suspension systems are designed to distribute loads evenly; unbalanced forces accelerate wear and reduce their effectiveness.

3. Structural Damages such as

- Bridge and Viaduct Stress: Concentrated forces from unbalanced loads can create localized stress points on bridges and viaducts. Over time, this can compromise structural integrity.

- Turnouts and Switches Damage: Unbalanced loads cause excessive wear on critical track components like turnouts and switches, thus leading to misalignments and operational hazards.

4. Operational Challenges such as

- Increased Noise and Vibration: Imbalanced loads cause abnormal noise and vibrations, leading to discomfort for passengers and higher stress on components.
- Reduced Train Stability: Overloaded or unevenly loaded wheels reduce the train's dynamic stability, increasing the risk of derailment on curves or at high speeds.

5. Economic Impacts such as

- Higher Maintenance Costs: Frequent repairs or replacements of damaged infrastructure and rolling stock.
- Service Interruptions: Damage caused by unbalanced loads often results in unexpected downtime for repairs, disrupting schedules and reducing network efficiency.

Thus, understanding the behavior of the wagon wheel load can mitigate these issues.

As above mentioned, for reasons for the safety of railway operation, RTTC-TISTR is interested in the development of local railway weight measurement technology to support the railway operation of State Railway of Thailand (SRT) and to promote this technology among rail operators in ASEAN countries.

There are several technologies have emerged for weighing wagon weight, each with its strengths and applications, such as Static Weighing Systems and Dynamic Weighing Systems.

- Static Weighing Systems such as Platform Scales and Load Cells

Platform Scales: Traditional platform scales are used for measuring stationary trains. While accurate, they require trains to stop and can delay operations.

Load Cells: These sensors measure the weight exerted by the train on the track or platform. Load cells provide high accuracy and can be integrated into existing infrastructure.

- Dynamic Weighing Systems such as Track-Based Weighing and Weigh In Motion (WIM)

- Track-Based Weighing: This technology measures the weight of trains as they pass over specially designed sensors embedded in the track. It allows for continuous monitoring without stopping trains and is beneficial for high-traffic routes.
- Weigh In Motion (WIM): This system combines sensors and data processing technologies to calculate the weight of moving trains in real time. WIM systems are increasingly popular for their ability to automate weight monitoring and improve traffic flow.

Standards for weighing trains vary by country but generally focus on ensuring accuracy, safety, and interoperability. The International Union of Railways (UIC) and other organizations provide guidelines for implementing effective weighing systems. Training for personnel involved in weight measurement and compliance with national regulations is also critical for effective weighing operations.

Weighing technology for trains is essential for the safe and efficient operation of rail transport. Ongoing innovations in dynamic weighing systems, sensor technologies, and data management are transforming how weight is monitored in the railway industry. Addressing current challenges and embracing future trends will enhance safety and operational efficiency, ultimately leading to more effective rail freight systems. Continued research and development in this field will be vital as the industry seeks to meet evolving demands and regulatory requirements.

From the literature and technology review above, there are several techniques available for determining the weight of wagons, including advanced and highly efficient methods. However, considering economic factors, the simplest and most practical option is often preferred. Techniques such as strain gauge-based systems are widely chosen due to their cost-effectiveness, practicality, and familiarity among most engineers. This research project will select a technology that is accurate, inexpensive, and self-developed for self-reliance, which is based on the conventional strain gauge technique. The Train Weight Device (TWD) is named for this technology.

Seeing the need for a solution Thailand Institute of Scientific and Technological Research (TISTR) aims to develop a mutual platform of railway inspection and monitoring technology to improve railway situation in ASEAN and implement a common standard of safety and efficiency in railway operations. Train Weight Device (TWD) was developed by the Railway Transportation

System Testing Centre (RTTC) under the Thailand Institute of Scientific and Technological Research (TISTR), which operates under the Ministry of Higher Education, Science, Research, and Innovation (MHESI), by using the concept from the principle of strain gauge.

A strain gauge is a sensor used to measure the amount of deformation or strain in an object. The principle behind a strain gauge is based on the relationship between mechanical deformation and electrical resistance.

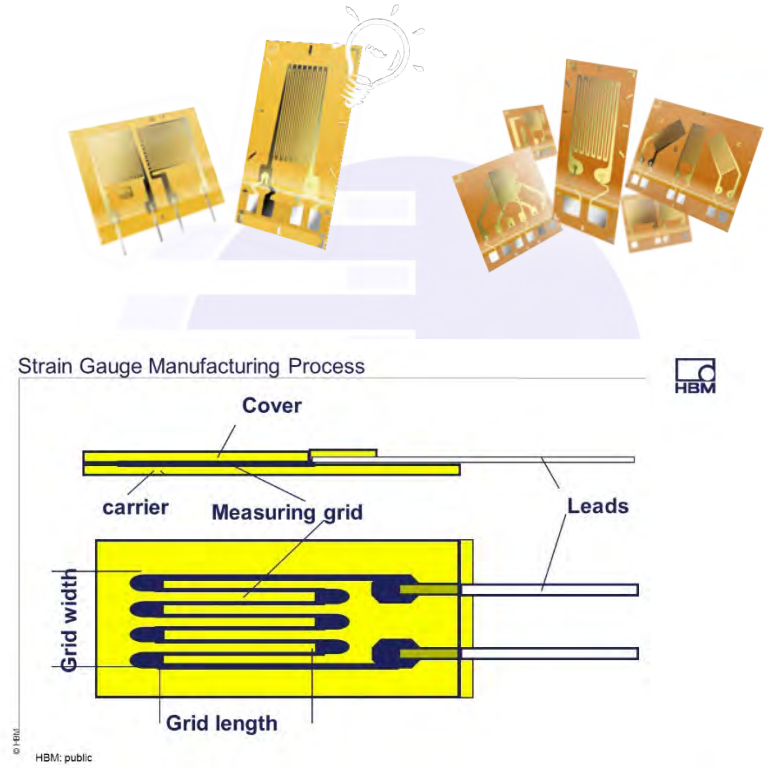

Strain gauge (Courtesy of HBK)

The basic principle of strain gauge is as follow:

1. Basic Concept of strain: When a material is subjected to any type of stress (tension, compression, shear, bending or combined stress), it deforms due to the elasticity following Hook's law. This deformation can be measured as "Strain", which is the change in length divided by the original length.

2. Electrical Resistance Change: A strain gauge consists of a thin wire or foil arranged in a grid pattern. When the material to which the strain gauge is attached deforms, the strain gauge

also deforms. This deformation causes a change in the length and cross-sectional area of the wire or foil, which in turn changes its electrical resistance.

3. Gauge Factor: The sensitivity of a strain gauge is quantified by the gauge factor, which is defined as the ratio of relative change in electrical resistance to the mechanical strain. It is typically around 2.00 for metallic strain gauges.

4. Measurement: The change in resistance is measured using a Wheatstone bridge circuit, which allows for precise measurement of small changes in resistance. The output of the bridge can be calibrated to provide a direct reading of strain.

5. Applications: Strain gauges are widely used in various fields, including civil engineering (to monitor structural integrity), mechanical engineering (to test materials), aerospace (to measure stress on aircraft components), etc.

In summary, the principle of a strain gauge relies on the relationship between mechanical strain and the change in electrical resistance, allowing for accurate measurement of deformation in any materials.

The TWD system is a train weight device from each train wheel passing on the track at the measurement spot. The data from the measurement spot will be sent to a cloud database and monitored with a software developed by RTTC.

The overview of TWD is as follows;

1. The TWD can be quickly installed in the existing track, without removing the sleeper or modifying the track.

2. TWD helps to record each wheel weight of the train making it easy to know weight data and fault of the train wheel.

3. This system can record wheel weight for processing and convert it to axel weight, bogie weight, wagon weight, and total weight of the train. The result from data processing will be converted to statistical data for evaluating the behavior of train transportation and detecting faults in speed and weight according to requirements or standards.

4. This system works with real-time monitoring and fault detection when a fault is detected from a train, it can set an alarm to an operator via an E-mail.

5. TWD could be further developed to identify the identification number of the train when passing with an automatic camera in the future.

The TWD is developed to increase the safety and efficiency of maintenance to reduce cost and maintenance time, and especially to reduce the import of products from abroad and promote domestic production.

Action activities (twelve (12) activities)

This technical cooperation for the research and development and implementation of railway inspection and monitoring technology is scheduled to be conducted in 12 activities as follows.

1. Sign the contract between 3 parties (TISTR, TICA and UNDP).
2. Coordinate with ASEAN participating countries to join the research projects via the online system.
3. Survey the location for installation of the railway inspection and monitoring technology and organize a workshop in Indonesia.
4. Survey the location for installation of the railway inspection and monitoring technology and organize a workshop in Malaysia.
5. Development of Train Weight Device (TWD).
6. Calibration and test of the TWD system in State Railways of Thailand (SRT).
7. Onsite seminar and workshop to share knowledge of the TWD principle and demonstrate the operation of TWD in Thailand.
8. Travel to Malaysia to onsite demonstrate and test the TWD system and transfer inspection and monitoring technology to the Construction Research Institute of Malaysia (CREAM) and Keretapi Tanah Melayu Berhad (KTMB), Malaysia.
9. Travel to Indonesia to onsite demonstrate and test the TWD system and transfer inspection and monitoring technology to Universitas Sumatera Utara (USU) and PT Kereta Api Indonesia (KAI), Indonesia.
10. An online summary of the project, sharing knowledge, assessment of satisfaction, and discussion of the future development of the TWD technology.
11. Seminar and publication of the research project results in Thailand.
12. Project conclusion report.

The action activities plan for this project is shown in the following table.

	Activity	Location	2023												2024											
			Quarter 1			Quarter 2			Quarter 3			Quarter 4			Quarter 1			Quarter 2			Quarter 3			Quarter 4		
			Jan	Feb	Mar	Apr	May	Jun	Jul	Aug	Sep	Oct	Nov	Dec	Jan	Feb	Mar	Apr	May	Jun	Jul	Aug	Sep	Oct	Nov	Dec
1	Sign the contract between 3 parties (during 2021)	Thailand	At 2021																							
2	Coordinate with agencies in participating ASEAN countries in research projects via an online system (during 2022)	Thailand	At 2022																							
3	Survey the location for installation of the railway inspection and monitoring technology and organize a workshop in Indonesia	Indonesia																								
4	Survey the location for installation of the railway inspection and monitoring technology and organize a workshop in Malaysia	Malaysia																								
5	To develop modern inspection and monitoring technologies	Thailand																								
6	Calibration and testing on the railway of SRT at ICD Lad Krabang Station	Thailand																								
7	Onsite workshop to demonstrate prototypes of the modern inspection and monitoring technology in railway systems	Thailand																								
8	Installation, operation, and training the modern inspection and monitoring techniques. in Malaysia	Malaysia																								
9	Installation, operation, and training the modern inspection and monitoring techniques. in Indonesia	Indonesia																								

	Activity	Location	2023												2024											
			Quarter 1			Quarter 2			Quarter 3			Quarter 4			Quarter 1			Quarter 2			Quarter 3			Quarter 4		
			Jan	Feb	Mar	Apr	May	Jun	Jul	Aug	Sep	Oct	Nov	Dec	Jan	Feb	Mar	Apr	May	Jun	Jul	Aug	Sep	Oct	Nov	Dec
10	Online meeting to present a summary of the results and discuss the results of the research project	Thailand																								
11	Seminar and publication of the research project results	Thailand																								
12	Project conclusion	Thailand																								

However, some activities may have their schedules changed due to political, budgetary, and virus infection issues.

Activity 1: Sign the contract between three (3) parties

This project, Technical Cooperation for Research and Development and Implementation of Railway Inspection and Monitoring Technology is co-funded by the Perez-Guerrero Trust Fund for South-South Cooperation (PGTF) year 2021. In this project, all three parties sign the contract to jointly support; (i) United Nations Development Programme (UNDP), (ii) Thailand International Cooperation Agency (TICA) and (iii) Thailand Institute of Scientific and Technological Research (TISTR). TISTR is the undertaking organization in this project. The first page of the signed contract is shown below.The three agencies signed a joint agreement on November 3, 2021. Once the signing is complete, TISTR starts to do research following the research schedule.

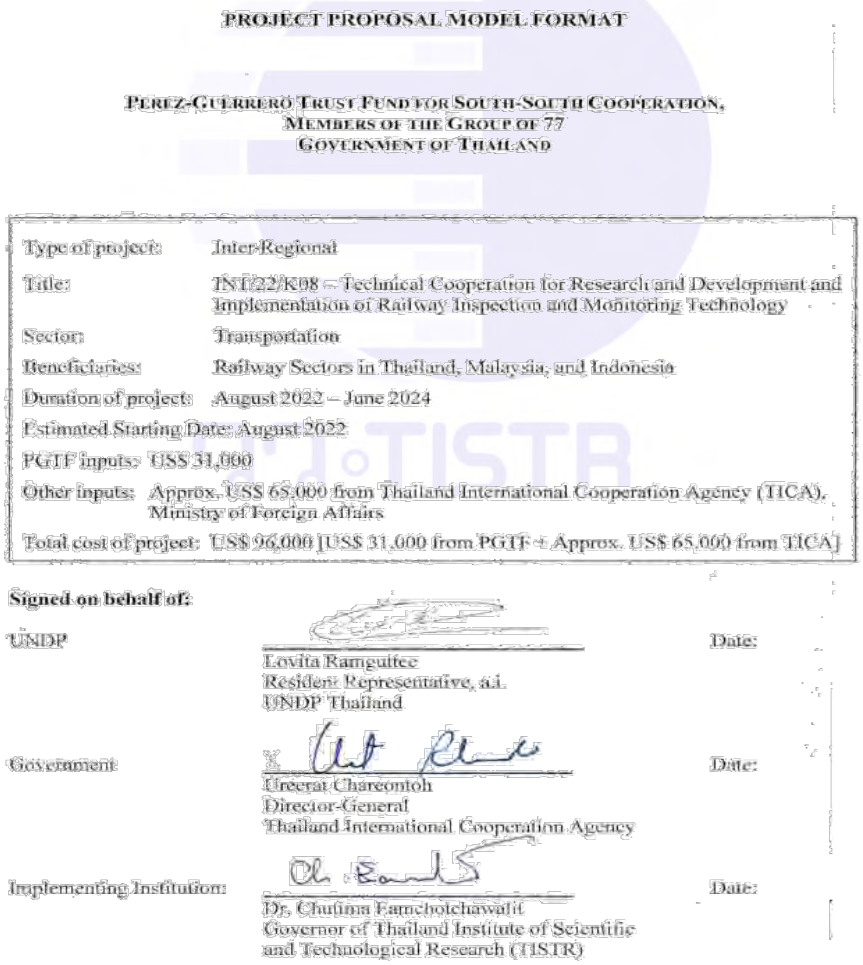

PROJECT PROPOSAL MODEL FORMAT

PEREZ-GUERRERO TRUST FUND FOR SOUTH-SOUTH COOPERATION,
MEMBERS OF THE GROUP OF 77
GOVERNMENT OF THAILAND

Type of project:	Inter-Regional
Title:	INT22/K08 – Technical Cooperation for Research and Development and Implementation of Railway Inspection and Monitoring Technology
Sector:	Transportation
Beneficiaries:	Railway Sectors in Thailand, Malaysia, and Indonesia
Duration of project:	August 2022 – June 2024
Estimated Starting Date:	August 2022
PGTF inputs:	US$ 31,000
Other inputs:	Approx. US$ 65,000 from Thailand International Cooperation Agency (TICA), Ministry of Foreign Affairs
Total cost of project:	US$ 96,000 [US$ 31,000 from PGTF + Approx. US$ 65,000 from TICA]

Signed on behalf of:

UNDP — Date:
Lovita Ramguttee
Resident Representative, a.i.
UNDP Thailand

Government — Date:
Ureerat Charoentoh
Director-General
Thailand International Cooperation Agency

Implementing Institution: — Date:
Dr. Chulinn Famcholchawalit
Governor of Thailand Institute of Scientific and Technological Research (TISTR)

The first page of the signed contract between TISTR, TICA and UNDP

Activity 2: Coordinate with agencies in participating ASEAN countries in research projects via the online system

This activity is an online meeting with the organization related to railway inspection and monitoring technology in Malaysia and Indonesia which consists of CREAM and KTMB from Malaysia, USU and KAI from Indonesia. The online meeting is shown in following **Figure 1**.

Figure 1a Online meeting with Malaysia, CREAM and UiTM

Figure 1b Online meeting with Indonesia.

From this meeting, every organization agreed that they are interested in joining the research project by cooperating and supporting the survey, demonstration, and installation of the railway inspection and monitoring technology in their country. This leads to the next activity.

Activity 3: Survey the location for installation of the railway inspection and monitoring technology and organize a workshop in Indonesia

From 22 - 27 May 2023, TISTR went to Indonesia to survey the location for the installation of the railway inspection and monitoring technology and organize a TWD workshop. By carrying out the following activities:

1. TISTR discussions with KAI to cooperate the research on technical cooperation for research and implementation of railway inspection and monitoring technology to enhance safety and improve maintenance efficiency for rail transport systems in ASEAN countries.
2. TISTR discussions with USU to cooperate the research on technical cooperation for research and implementation of railway inspection and monitoring technology to develop this project together. In addition, the research on Finite Element Analysis (FEA) in Railway Transportation and Green Logistics for Transportation was presented.
3. TISTR discussions with PT INDUSTRI KERETA API (Persero), PT INKA, to cooperate the research on technical cooperation for research and implementation of railway Inspection and monitoring technology to enhance safety and improve maintenance efficiency for rail transport systems in ASEAN countries.

The survey and discussion are shown in **Figure 2 – 4**. The outcome of this collaboration was positive. When the Train Weight Device (TWD) technology is fully operational, there will be seminars and workshops and onsite installation demonstrations.

Figure 2 The survey in Indonesia

Figure 3 The discussion in Indonesia

Figure 4 The slide presentation from RTTC-TISTR

Activity 4: Survey the location for installation of the railway inspection and monitoring technology and organize a workshop in Malaysia

From 19 - 22 June 2023, TISTR went to Malaysia to survey the location for the installation of the railway inspection and monitoring technology and organize a TWD workshop. By carrying out the following activities:

1. TISTR discussions with CREAM to cooperate the research on technical cooperation for research and implementation of railway Inspection and monitoring technology to enhance safety and improve maintenance efficiency for rail transport systems in ASEAN countries.
2. TISTR discussions with Universiti Teknologi MARA (UiTM) to cooperate the research on technical cooperation for research and implementation of railway Inspection and monitoring technology to develop this project together.
3. TISTR discussions with KTMB to cooperate the research on technical cooperation for research and implementation of railway Inspection and monitoring technology to enhance safety and improve maintenance efficiency for rail transport systems in ASEAN countries.

The survey and discussion are shown in **Figures 5** and **6**. The outcome of this collaboration was positive. When the Train Weight Device (TWD) technology is fully operational, there will be seminars and workshops and onsite installation demonstrations.

Figure 5 The survey and discussion in Malaysia

Figure 6 The slide presentation from RTTC-TISTR

Activity 5: Development of Train Weight Device (TWD)

This activity is a project developed by the Railway Transportation System Testing Centre (RTTC) under the Thailand Institute of Scientific and Technological Research (TISTR), which operates under the Ministry of Higher Education, Science, Research, and Innovation (MHESI). The focus of this project is on the invention and utilization of domestically sourced materials (local content) to create a Train Weight Device (TWD) technology.

Several literature indicates that there are many technologies to detect the weight of trains such as Weight in Motion System (WIM) but it is expensive and must be imported. For this reason, RTTC-TISTR is to develop local railway inspection technology to promote self-reliance.

The working principle of TWD technology is the strain gauge's theory to measure a tension bar and bending bar. Which can be explained as follows:

When tensile force P is applied to a material, it has stress σ that corresponds to the applied force. In proportion to the stress, the cross-section contracts and the length elongates by ΔL from the length L the material had before receiving the tensile force (**Figure 7**).

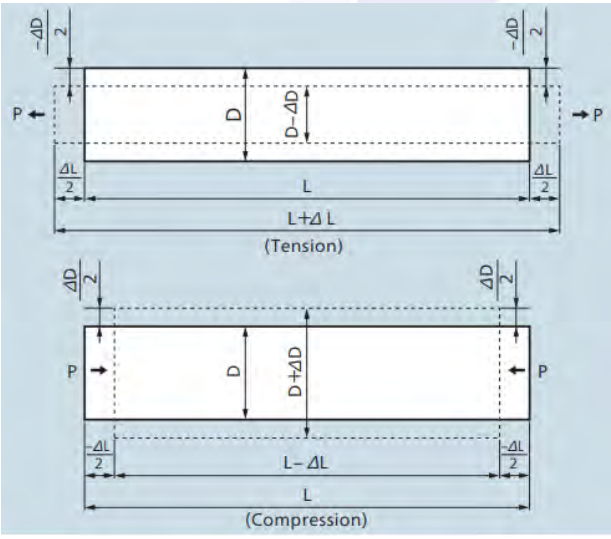

Figure 7 The cross-section contracts and the length elongates by ΔL from the length L of the material

The ratio of the elongation to the original length is called a tensile strain and is expressed as follows:

$$\varepsilon = \frac{\Delta L}{L}$$

If the material receives compressive force, it bears compressive strain expressed as follows:

$$\varepsilon = -\frac{\Delta L}{L}$$

where; ε is Strain, ΔL is Elongation and L is original length

Based on Hooke's law, the relation between stress and the strain initiated in a material by the applied force is expressed as follows:

$$\sigma = E \cdot \varepsilon$$

Where; σ is Stress, E is Young's modulus and ε is Strain

Stress is thus obtained by multiplying strain by Young's modulus. When a material receives tensile force P, it elongates in the axial direction while contracting in the transverse direction. Elongation in the axial direction is called longitudinal strain and contraction in the transverse direction is called transverse strain. The absolute value of the ratio between the longitudinal strain and transverse strain is called Poisson's ratio, which is expressed as follows:

$$\nu = \left|\frac{\varepsilon_1}{\varepsilon_2}\right|$$

Where; ν is Poisson's ratio, ε_1 is Longitudinal strain $\frac{\Delta L}{L}$ or $-\frac{\Delta L}{L}$ and ε_2 is Transverse strain $-\frac{\Delta D}{D}$ or $\frac{\Delta D}{D}$

Poisson's ratio differs depending on the material. For major industrial materials and their mechanical properties including Poisson's ratio.

If external tensile force or compressive force increases or decreases, the resistance proportionally increases or decreases. Suppose that the original resistance R changes by ΔR because of strain ε: the following equation is set up

$$\frac{\Delta R}{R} = Ks \cdot \varepsilon$$

Where; Ks is a gauge factor, expressing the sensitivity coefficient of strain gauges. General-purpose strain gauges use copper-nickel or nickel-chrome alloy for the resistive elements, and the gauge factor provided by these alloys is approximately 2.

The strain-initiated resistance change is extremely small. Thus, for strain measurement, a Wheatstone bridge is formed to convert the resistance change to a voltage change. Resistances (Ω) are R_1, R_2, R_3, and R_4 and the excitation voltage (V) is E. Then, the output voltage e_0 is obtained by the following equation:

$$e_0 = \frac{R_1 R_3 - R_2 R_4}{(R_1 + R_2)(R_3 + R_4)} \cdot E$$

Suppose the resistance R_1 is a strain gauge and it changes by ΔR due to strain. Then, the output voltage is

$$e_0 = \frac{(R_1 + \Delta R) R_3 - R_2 R_4}{(R_1 + \Delta R + R_2)(R_3 + R_4)} \cdot E$$

If $R_1 = R_2 = R_3 = R_4 = R$ in the initial condition,

$$e_0 = \frac{R^2 + R\Delta R - R^2}{(2R + \Delta R)2R} \cdot E$$

Since R may be regarded as extremely larger than ΔR,

$$e_0 = \frac{1}{4} \cdot \frac{\Delta R}{R} \cdot E = \frac{1}{4} \cdot Ks \cdot \varepsilon \cdot E$$

Thus, obtained is an output voltage that is proportional to a change in resistance, i.e. a change in strain. This microscopic output voltage is amplified for analog recording or digital indication for strain measurement.

A strain gauge Wheatstone bridge (strain gauge wiring system) is configured with the full bridge used in this research. The full-bridge system has 4 strain gauges connected one each to all 4 legs of the bridge as shown in **Figure 8**. This circuit ensures a large output of strain-gauge

transducers, improves temperature compensation, and eliminates strain components other than the target strain.

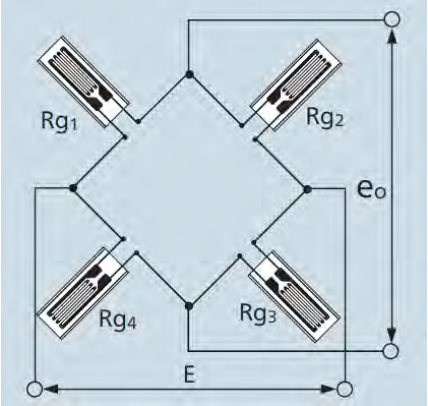

Figure 8 Full bridge system

With the measurements on a tension bar, with a tension bar shown in **Figure 9**, a strain $\boldsymbol{\varepsilon_1 = \frac{\sigma}{E}}$ in the direction of the force applied will occur. In the transverse direction, a transverse contraction $\boldsymbol{\varepsilon_2 = -\nu \cdot \varepsilon_1}$ will occur. From this, a change of resistance $\boldsymbol{\Delta R_1 = \varepsilon_1 \cdot k \cdot R_1}$ will be found in strain gauge no. 1. For strain gauge no. 2, this difference will be $\boldsymbol{\Delta R_2 = -\nu \cdot \varepsilon_1 \cdot k \cdot R_2}$. Accordingly, this is also true for strain gauge no. 3 and no. 4 respectively.

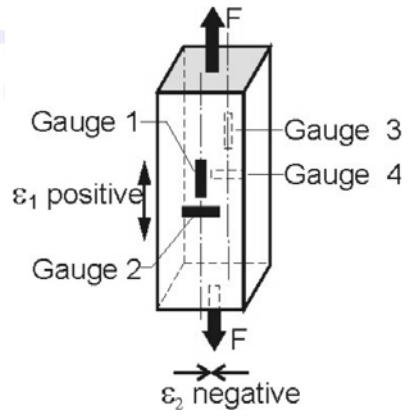

Figure 9 Tension bar

The factor $\boldsymbol{\nu}$, also called Poisson's ratio, depends on the material and is valid in the material's elastic deformation range only. It has a value of around 0.3 for metals.

If all four strain gauges are connected in the sequence of their indices to form a full bridge (**Figure 8**) an output signal as described by the equation is produced

$$\frac{U_A}{U_E} = \frac{k}{4}(\varepsilon_1 - \varepsilon_2 + \varepsilon_3 - \varepsilon_4) = \frac{k}{4}[\varepsilon_1 - (-\varepsilon_1) + \varepsilon_3 - (-\nu\varepsilon_3)].$$

Introducing v = 0.3 and with $\varepsilon_1 = \varepsilon_3 = \varepsilon$ and $\varepsilon_2 = \varepsilon_4 = -0.3 \cdot \varepsilon$, the net signal will be

$$\frac{U_A}{U_E} \approx \frac{k}{4} \cdot 2.6 \cdot \varepsilon_1$$

A bridge circuit with four active strain gauges gives a signal 2.6 times the value of the strain ε_1 in the tension bar's main direction of stress. Sometimes this factor is also called the bridge factor “B”. Therefore, a general form of the equation is also

$$\frac{U_A}{U_E} = \frac{k}{4} \cdot B \cdot \varepsilon_1$$

If compressive forces are to be measured, the opposite signs of the strains ε_1 to ε_4 are valid. If the strain ε_1 in the main stress direction is unknown, this can be derived by transformation from the previous equation:

$$\varepsilon_1 = \frac{4}{2{,}6 \cdot k} \cdot \frac{U_A}{U_E}$$

or, in the more general form of the previous equation, transformed into

$$\varepsilon_1 = \frac{4}{B \cdot k} \cdot \frac{U_A}{U_E}$$

A combination of R_1 and R_3 formed by active strain gauges and R_2 and R_4 with fixed resistors is also possible and gives B = 2. But this is without automatic compensation of the thermal expansion and other influences. However, bending forces that are superimposed will be compensated.

With the measurements on a bending beam, **Figure 10** shows the bending beam

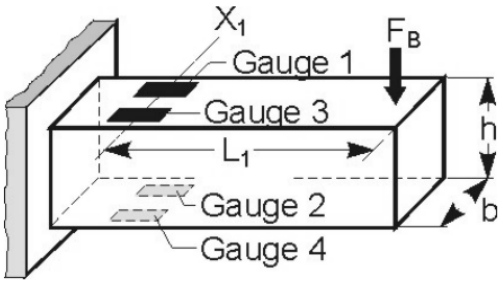

Figure 10 The bending beam

The conditions in the case of the bending beam are a bit simpler and more favorable. Here strain values are of the same absolute value but with the opposite sign. This means that strain values on the upper side and on the underside of the beam are the same but with the opposite sign. We get particularly favorable conditions when adding the measured values according to this equation:

$$\frac{U_A}{U_E} = \frac{k}{4}[\varepsilon_1 - (-\varepsilon_2) + \varepsilon_3 - (-\varepsilon_4)]; \text{ assuming } |\varepsilon_1| = |\varepsilon_2| = |\varepsilon_3| = |\varepsilon_4|$$

B = 4 was used, therefore the equation is:

$$\frac{U_A}{U_E} = \frac{k}{4} \cdot B \cdot |\varepsilon| = k \cdot |\varepsilon|$$

The absolute value of the strain is then $|\varepsilon| = \frac{U_A / U_E}{k}$

Its sign is then positive on the tensile side and negative on the compressive side. If the directions of stress are not evident, then the signs can be derived from the rules given in the previous equation. If the bending beam can only be equipped with two active strain gauges, the bridge arms no. 1 and no. 2 should be used. The bridge factor is then B = 2.

From the strain gauge's theory above, The TWD sensor was developed by the strain gauge principle that relies on the relationship between mechanical strain and the change in electrical resistance, allowing for accurate measurement of material deformation.

The TWD sensor has a simple structure a combination of strain gauges and mechanical springs, it is assembled on the rail support attached to the bottom of the rail shown in **Figure 11**. TWD sensor designed for gauge lengths of 50 mm was using for weight measurement. This sensor is used to measure the stain occurring within rail expansion on the surface at the bottom of the rail.

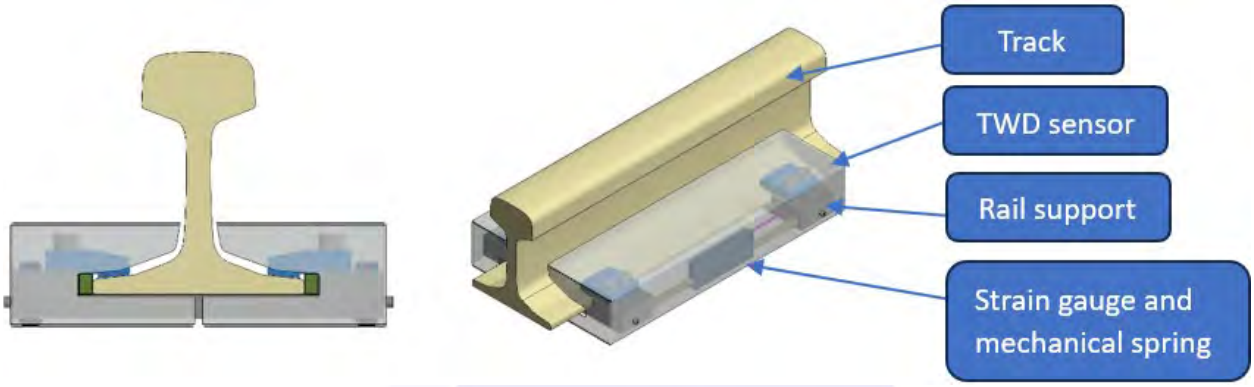

Figure 11 The TWD sensor structure.

The TWD sensor is calibrated with a constant voltage excitation with a full bridge circuit connected to DAQ. The rated output and sensitivity shown on the TWD sensor specification in **Table 1** are found with an instrument gauge factor of 2.0. The TWD sensor is connected with DAQ set to direct measure mode in strain value and can be calculated wheel weight with the calibration coefficient using the following equation:

$$\text{Wheel weight [tons]} = \text{Measure value [}\mu\varepsilon\text{]} \times \text{Calibration coefficient}$$

Table 1 TWD sensor specification

TWD sensor parameter	Value
Sensor type	Strain gauge
Sensor structure	Mechanical spring and Rail support
Gauge length	50 mm.
Gauge factor	2.0
Rated output	Tension: +2000 μV/V
	Compression: -2000 μV/V
Input impedance	350 Ω
Output impedance	350 Ω
Insulation resistance	> 1000 M Ω (DC50V)

The TWD system consists of TWD sensors with cover boxes (as shown in **Figure 12**), it has been simulated using an ANSYS Finite Element Analysis (FEA) program to ensure structural safety against typical loadings and vibration during the service on the track. The TWD is installed on the railway tracks to collect raw data that is then converted into useful data via the Data Acquisition system (DAQ) and Industrial PCs (as shown in **Figures 13** and **14**, respectively). Both devices are housed in the TWD Remote enclosure. The enclosure has been proven to its waterproof by conducting water tightness testing in RTTC, as depicted in **Figure 15**.

The operational principle of the system is illustrated in **Figure 16**. When the train passes the measuring point on the track. The sensors get the signal from the weight of each wheel and the DAQ converts the signal to a physical value such as strain in micro-strain, velocity in meter/second, Lafo in N, etc. The data will be monitored and recorded in the software which is completely developed by RTTC. This software summarizes the raw data and displays the data in several patterns according to the user's preferences, such as statistical data, warning messages, fault data, etc. If the software detects a fault, the user can configure it to send fault information or alarm to the operator by e-mail for a quick response to the problem detected.

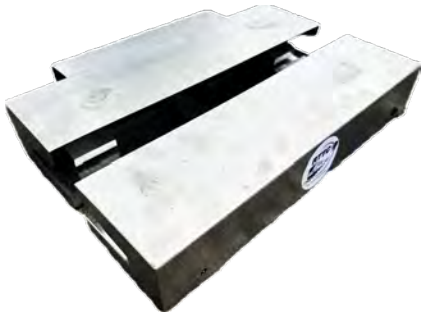

Figure 12 TWD Sensor

Figure 13 Data acquisition (DAQ)

Figure 14 Industrial PC

Figure 15 TWD Remote enclosure

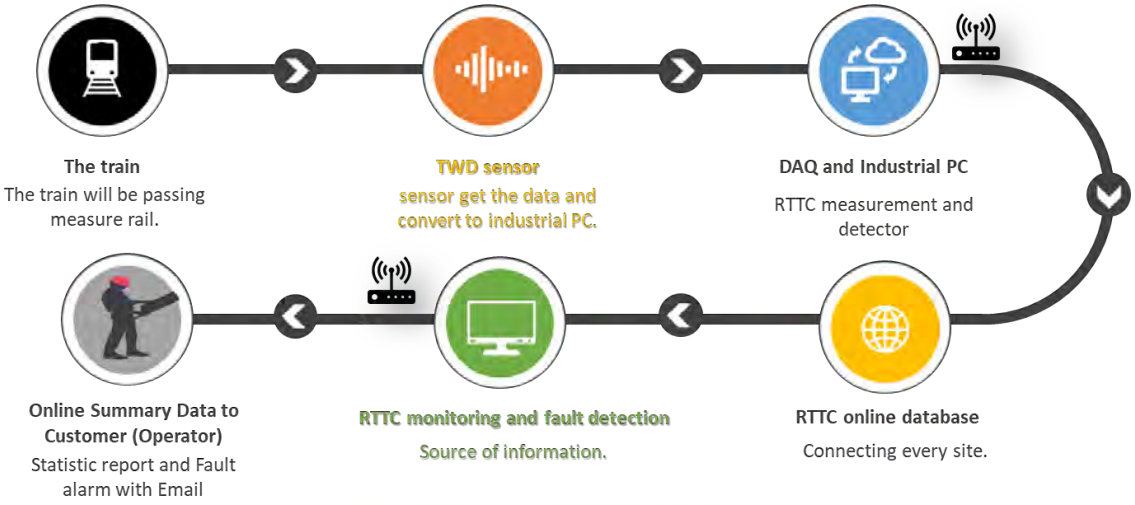

Figure 16 The operational principle of TWD

Activity 6: Calibration and test of operations on State Railways of Thailand (SRT)

During the development of the TWD, the TWD sensors were validated in RTTC's laboratory and the entire TWD system was tested on the State Railway of Thailand's track to verify its performance and reliability. The validation process in RTTC's laboratory is summarized as follows.

1.) The static validation of the TWD was performed by applying a static load from a servo-hydraulic actuator (calibrated according to ISO/IEC 17025 Class 1). The load was applied in steps with a loading rate of 20kN/step to a maximum load of 120 kN as shown in **Figure 17**. **Table 2** presents the validation results with an indicated maximum error of 1.02%.

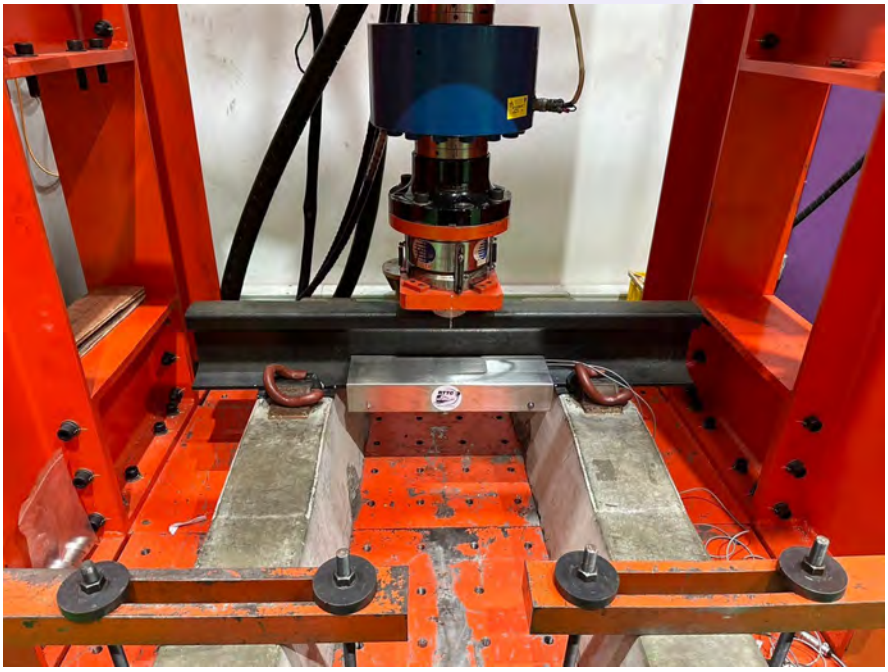

Figure 17 Static validation test in RTTC laboratory.

Table 2 Result from Static Validation test

Standard force(kN)	Measuring Force (kN)			
	Test no.1 SG1+2 (RTTC Lab)	Test no.2 SG1+2 (RTTC Lab)	Test no.3 SG1+2 (RTTC Lab)	Test no.4 SG1+2 (RTTC Lab)
0	0	0	0	0
20	19.86	19.86	19.93	20.02
40	39.71	39.75	40.33	40.32
60	59.60	59.60	60.25	60.42
80	79.46	79.55	80.29	80.28
100	99.11	99.31	100.21	100.05
120	118.84	118.78	119.52	119.46

2.) The dynamic validation of TWD sensors was performed by applying dynamic load between 5 kN to 100 kN at various frequencies between 1 – 5 Hz, as shown in **Figure 18**. The maximum error obtained from this dynamic validation test was 0.48%.

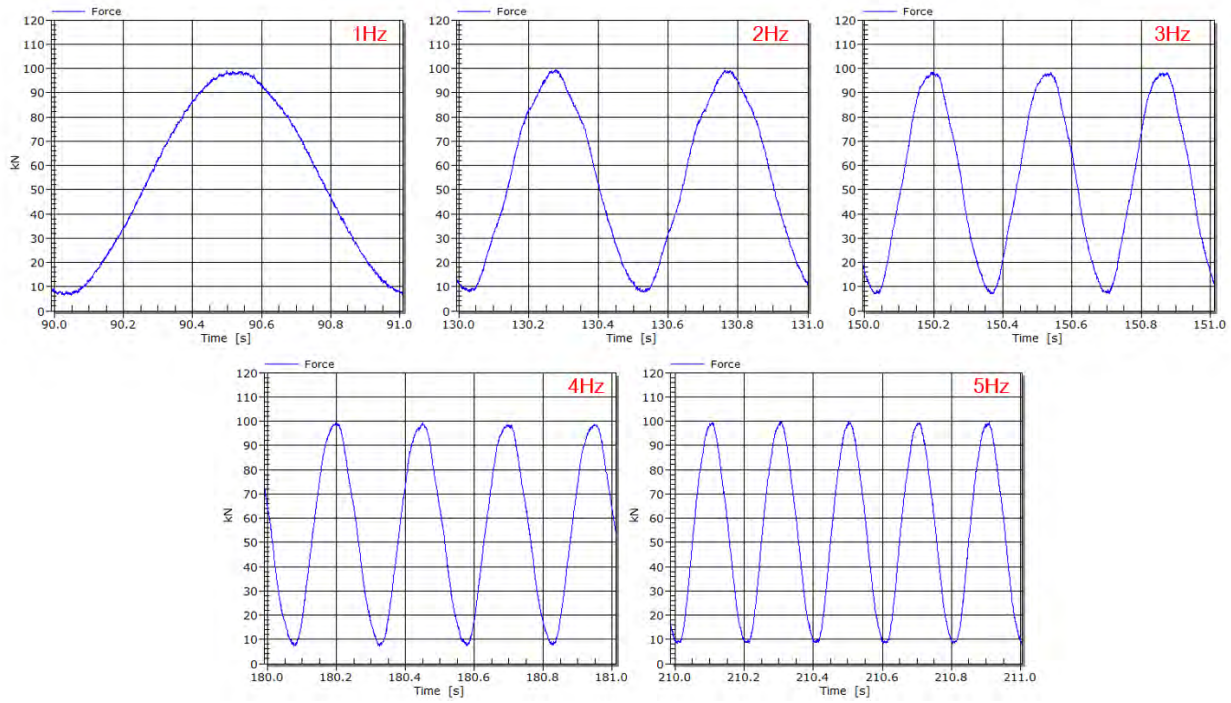

Figure 18 Dynamic validation result of TWD

3.) The TWD sensors were tested under simulated train wheel load at various load values to simulate the train operation, as shown in **Figure 19**. The maximum simulated wheel load

applied to the TWD sensor was between 5 to 100 kN. The test results showed that the maximum error for simulated train wheel load is 1.3%.

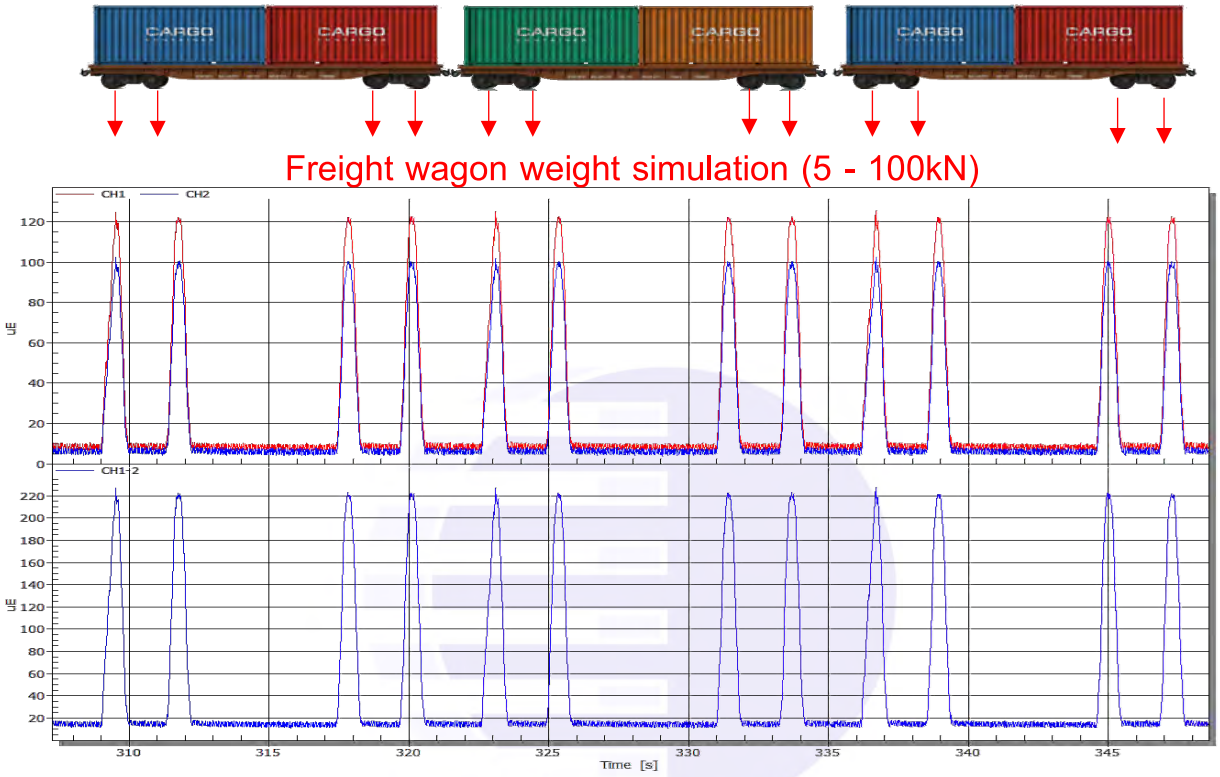

Figure 19 Train wheel load simulation result of TWD

4. The entire TWD system was tested on the experiment test track of RTTC. The experiment test track is a permanent meter gauge track having 45 meters track distance similar to the track of SRT, as shown in **Figure 20**. This validation process required the TWD system installed on the track and an electrical trolley having a total weight of around 500 kg moved passing the measuring point.

Figure 20 The experiment test track

Figure 21 shows the results of the test track validation (the red line is the right wheel of the trolley and the blue line is the left wheel of the trolley). The upper figure shows the strain values from the TWD system and the lower figure is the equivalent wheel load reading from the TWD system. The results show that the TWD can display the weight of the trolley with reasonable accuracy.

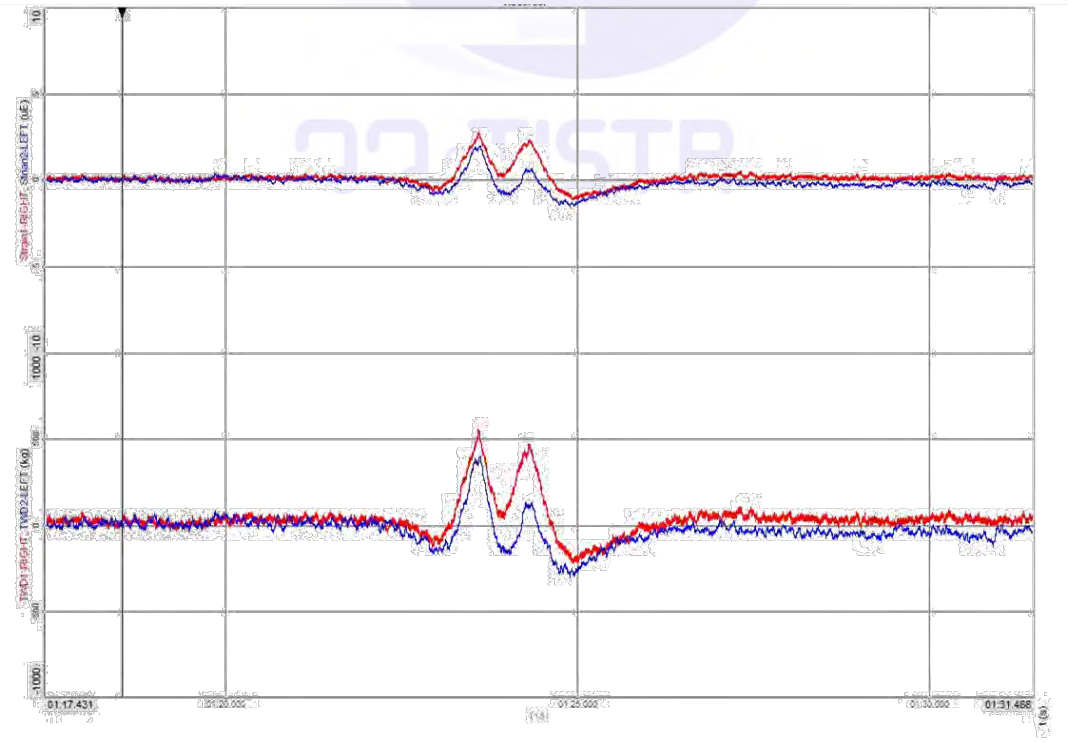

Figure 21 The results of the test track validation

After having been validated in the RTTC laboratory, the TWD was verified on-site on the SRT's track. The installation procedure of the TWD on site is as follows.

1.) Select the installation location for the TWD system, including the sensor and the control cabinet. Prepare appropriate space under the rail foot for the cable wiring as shown in **Figure 22**.

Figure 22 The installation procedure (1)

2.) Securely install the control cabinet on a concrete base. The TWD Sensors, a total of four (4) sets are prepared for installation on the left and right rails, as shown in **Figure 23**.

Figure 23 The installation procedure (2)

3.) Proceed with the installation of the TWD sensor by removing the cover of the TWD device as shown in **Figure 24**. Detach four clamps and install insulators according to relevant rail sizes, such as UIC 60, 54E1, and BS100A, as illustrated in **Figure 25**.

Figure 24 The installation procedure (3)

Figure 25 The installation procedure (4)

4.) Install the TWD to the foot of the rail and securely tighten all four clamps in place (once this step is completed, the train can pass without affecting its operation), as shown in **Figure 26**.

Figure 26 The installation procedure (5)

5.) Install the sensor, close the cover, and check for interference signals (after completing this step, the train can run without affecting its operations), as shown in **Figure 27**.

Figure 27 The installation procedure (6)

6.) Connect the signal wires, apply waterproof silicone, and check for interference signals (once this step is completed, the train can operate without affecting service) as shown in **Figure 28**.

Figure 28 The installation procedure (7)

Once the TWD Sensor system has been installed at all four locations and the signal wires have been properly connected to the TWD Remote enclosure, the setup will appear as shown in **Figure 29**.

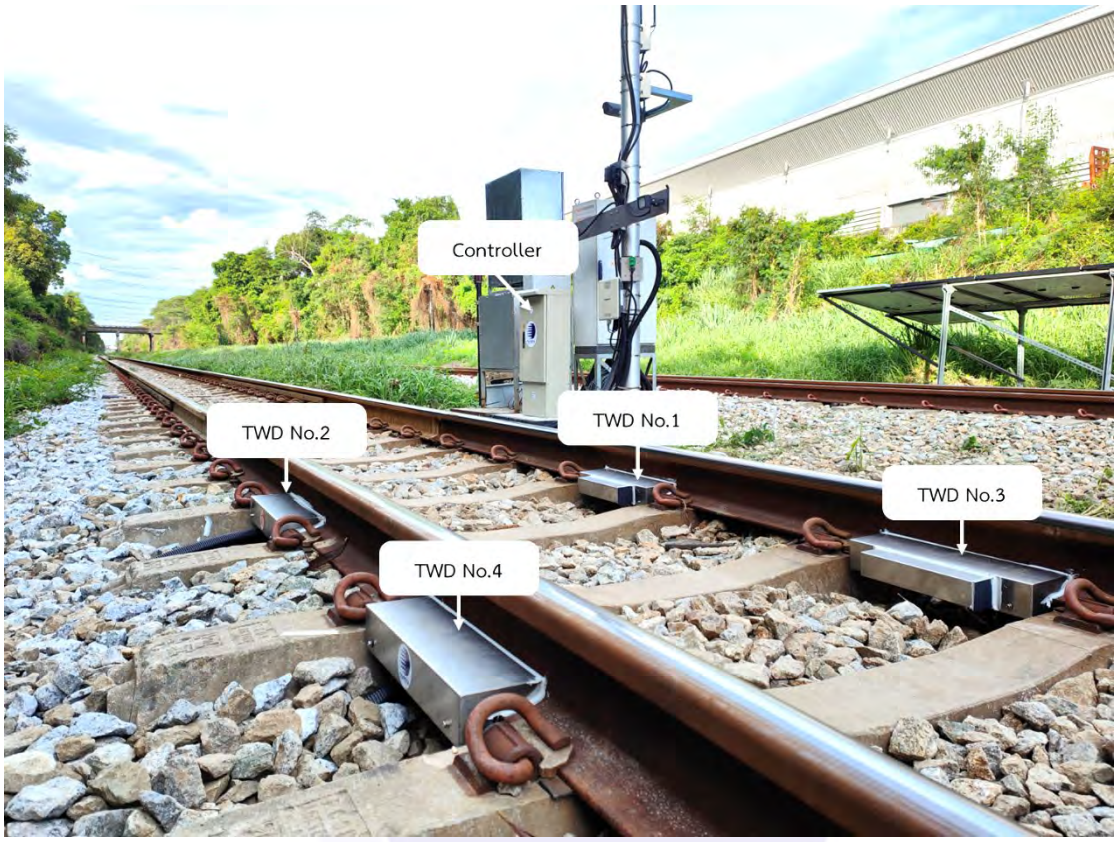

Figure 29 The TWD system is installed and ready for use.

The data processing of the TWD with the software is shown in **Figure 30.** The process can be explained as follows.

1. After the train is passed, raw data is transferred to the cloud database.
2. The TWD software gets the data and does some calculation processes such as signal filtering, peak load detection, and calculation of statistical values such as each wheel load, the total load of the wagon, wheel load, unbalance of each wheel, etc.
3. **Figure 30** shows the graph of the raw data in blue and green lines, the peak weight detected is shown in the red dot. It can be seen that the first six peak loads represent the wheel load of the locomotive while the next four peak loads are the first wagon of the fleet. Every wagon will be detected for its left and right wheel load using this algorithm and finally, the weight of the whole fleet will be reported.
4. The table in **Figure 30** summarizes every wagon weight with labeling according to the running number of wagons. The software shows only the wagon weight on the left and right wheels. However, this information can be utilized to calculate the bogie

unbalance. The bogie unbalance is defined by the maximum deviated weight compared with the average weight. All of this statistical wagon weight information re used for the evaluation of the loading behavior of the fleet.

Figure 30 RTTC's software

The recording results (total of 3 days and 10 trains passed) from the TWD system were compared with a commercially available system called RAWLOC system (Switzerland made from Hastema Gmbh.) and the results are shown in **Figure 31.**

Figure 31, indicates that the TWD system can give the load reading reasonably close to the RAWLOC system. The average difference is approximately 7%. **Figure 32** shows the correlation between the value from the RAWLOC system and the TWD system. The correlation is relatively linear, the TWD system gives satisfactory measuring results.

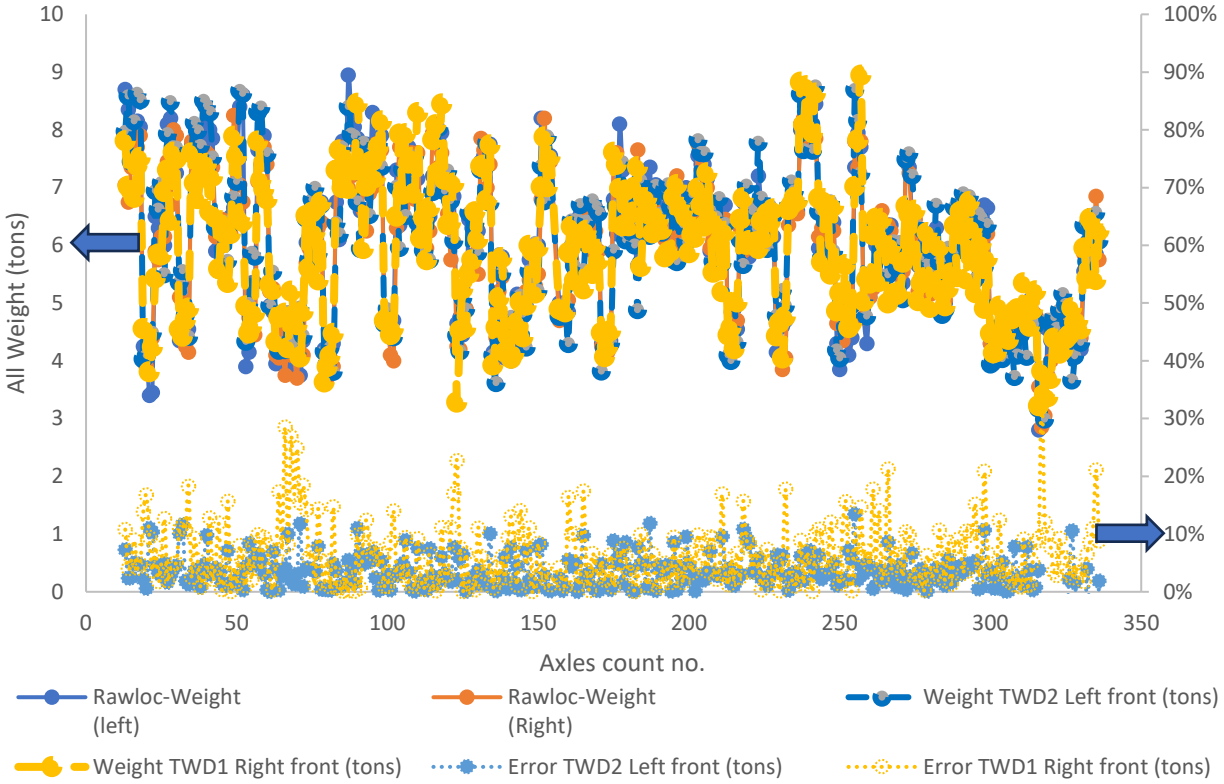

Figure 31 The verification of the TWD system on-site compared with the RAWLOC system

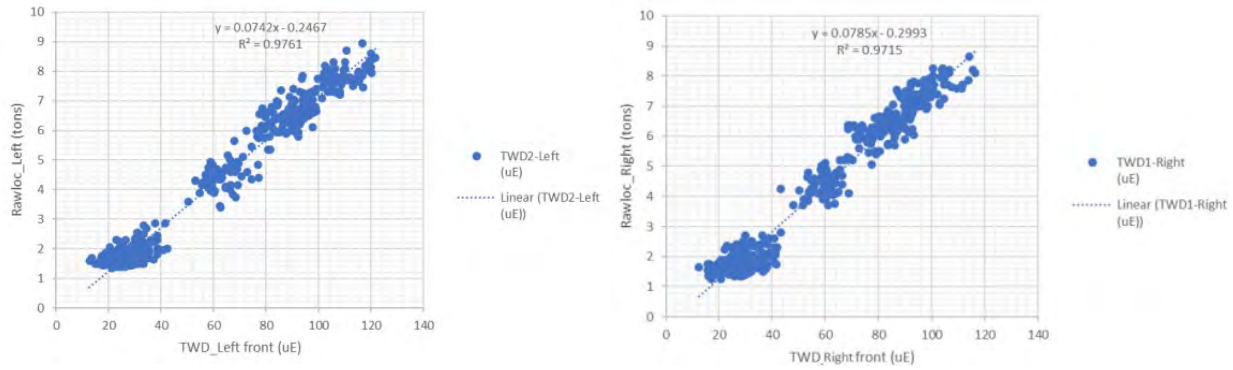

Figure 32 The relationship between the RAWLOC system and the TWD system

Activity 7: Onsite workshop seminar demonstrating the operation of TWD and sharing principles and methods of use in Thailand

After RTTC completed activity 6, they organized an onsite workshop seminar to demonstrate the operation of TWD and share the TWD principles and operation with ASEAN countries. This took place at the Rail Transport Standard Testing Center (RTTC) of the Thailand Institute of Scientific and Technological Research (TISTR) on June 10-11, 2024. The objectives of the seminar are as follows:

1. To promote cooperation for railway technology transfer in the ASEAN region.
2. To enhance the safety level of railway operations by developing local railway technologies and implementation in ASEAN countries.
3. To develop the railway research network and implementation in ASEAN countries through the sharing of knowledge and infrastructures, co-research, and promoting self-reliant railway technologies.
4. To enhance regional connectivity and sustainable development.

Several keynote speakers from developed countries such as Australia and China, including university professors and experts in Thailand as well as participants from ASEAN region countries, including the Philippines, Laos, Malaysia, and Indonesia joined the seminar and workshop. The seminar featured topics and experts presenting on various subjects are as follows.

1.) Safety policy of rail transit in Thailand by Dr. Tayakorn Chandrangsu, Director of Safety Standard and Maintenance Division, Department of Rail Transport as shown in **Figure 33**.

Figure 33 Presentation of Safety policy of rail transit in Thailand

2.) Modern Technology for track inspection by Mr. Yuhao Cai, Project Director of Rail Technology International (RTI), Australia as shown in **Figure 34**.

Figure 34 Presentation of Modern Technology for Track Inspection

3.) Monitoring inspection system by Dr. Hafnee Lateh, a Specialist in railway surveillance and safety as shown in **Figure 35**.

Figure 35 Presentation of Monitoring Inspection System

4.) Implementing of metrology for safety and quality of rail transit by Dr. Sivinee Sawatdiaree, Head of NIMT's electrical metrology department, National Institute of Metrology Thailand (NIMT) as shown in **Figure 36**.

Figure 36 Presentation of Implementing of metrology for safety and quality of rail transit

5.) Structural Health Monitoring (SHM) technology for rail transit and high-speed train by Mr. Wang Guangjun, Senior Engineering of CRRC Qingdao Sifang, China as shown in **Figure 37**.

Figure 37 Presentation of Structural Health Monitoring (SHM) technology for rail transit and high-speed train

6.) Demonstration and workshop of SHM technology by Mr. Wang Guangjun, Senior Engineering of CRRC Qingdao Sifang and TISTR as shown in **Figure 38**.

Figure 38 Demonstration and workshop of SHM technology Structural Health Monitoring (SHM) technology

7.) The development of local technology for Train Weight Devices (TWD) in Thailand by Mr.Phanasindh Paitekul, Director of railway and transportation technology testing and development laboratory of RTTC as shown in **Figure 39**.

Figure 39 Presentation of the development of local technology for Train Weight Devices (TWD) in Thailand

8.) The development of railway inspection by Assoc. Prof. Dr. Wichai Siwakosit, Department of Mechanical Engineering, Faculty of Engineering, Kasetsart University as shown in **Figure 40**.

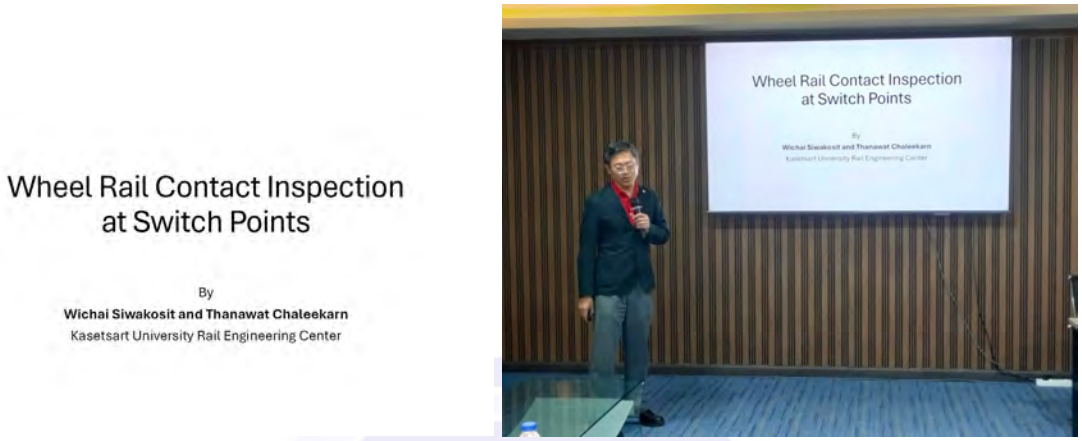

Figure 40 Presentation of the development of railway inspection

9.) Demonstration of railway inspection technology by RTI, TISTR, and Laboratory tour at TISTR as shown in **Figure 41**.

Figure 41 Demonstration of railway inspection technology in RTTC's laboratory

The seminar successfully met all the objectives of the event, and the overall activities are shown in **Figure 42**. The presentation materials are in **Appendix 1**.

Figure 42 Seminar activities

Activity 8: Travel to Malaysia to onsite demonstrate and test the TWD system and transfer inspection and monitoring technology to the Construction Research Institute of Malaysia (CREAM) and Keretapi Tanah Melayu Berhad (KTMB), Malaysia

After the TWD system is validated and verified, it will be demonstrated on-site in Malaysia. With a good cooperation and kind support from Keretapi Tanah Melayu Berhad (KTMB), the TWD system was demonstrated by installing on track in the depot at Ipoh railway station as shown in **Figure 43**.

Figure 43 The TWD system is installed in the depot at Ipoh railway station.

To ensure that the measurement results obtained are accurate, the TWD system is required to be calibrated with a portable calibration frame (as shown in **Figure 44**). However, due to the limitations of the shipment of portable calibration frames, the calibration of the TWD system could not be conducted on-site. Therefore, the TWD system was validated with a KTM fleet with known weight (the weight information of each wagon was from KTM). The scaling factor

obtained from the validation was then utilized to measure the dynamic weight of the other KTM fleets during the demonstration.

Figure 44 The calibration frame

The validation was performed with a wagon with known weight (in this case, a train fleet having 1 locomotive, 19 wagons, and 82 axles) and the TWD scaling factor was obtained by using the regression method (least square method) of the obtained data.

The result of validation is shown in **Figure 45**. It can be seen that the scaling factor of TWD1 (right side) and TWD2 (left side) are as follows; TWD1 = 0.095013 ton/micro-strain, TWD2 = 0.094386 ton/micro-strain.

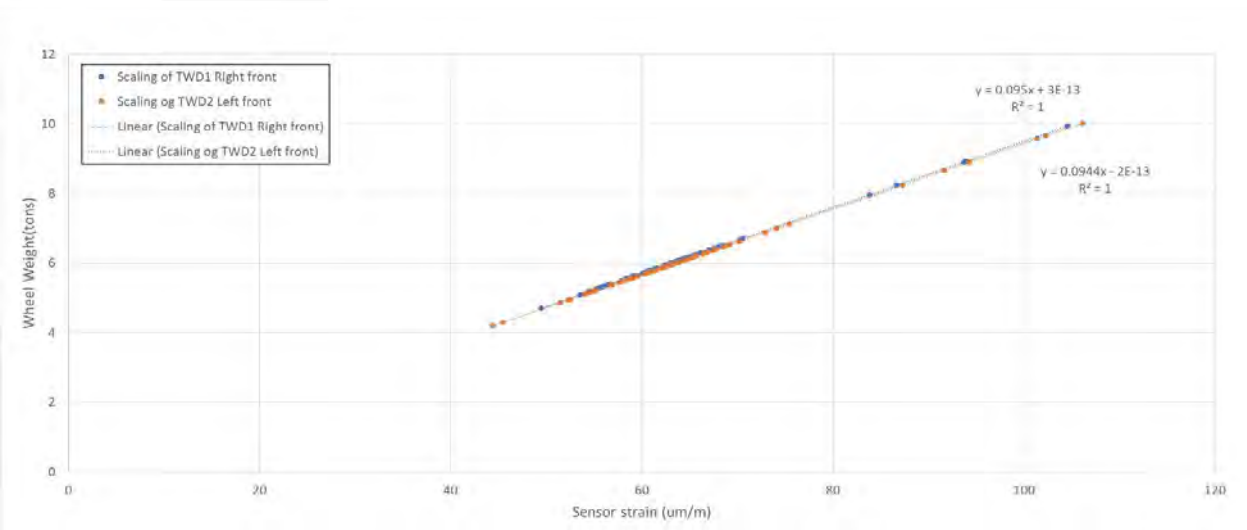

Figure 45 The result of the validation

Then the TWD with a scaling factor is used to re-check the weight of the KTM fleet to verify the validation. **Figure 46** shows the data for each axle weight and wagon weight by comparing the known weight and the TWD result. The validation result is as follows;

Locomotive average wheel weight from TWD1 (Right) = 9.17 tons

Locomotive average wheel weight from TWD2 (Left) = 8.81 tons

Locomotive average total weight from TWD = 107.92 tons

Wagon average wheel weight from TWD1 (Right) = 5.81 tons

Wagon average wheel weight from TWD2 (Left) = 5.83 tons

Wagon average total weight from TWD = 46.59 tons

Wagon average wheel weight information from KTM (Right) = 5.78 tons

Wagon average wheel weight information from KTM (Left) = 5.78 tons

Wagon average total weight information from KTM = 46.27 tons

From the result above, the average error of the wagon weight from the TWD is -0.69%.

The scaling factor obtained from the validation was assumed to be accurate and then utilized to measure the dynamic weight of the other KTM fleets during the demonstration.

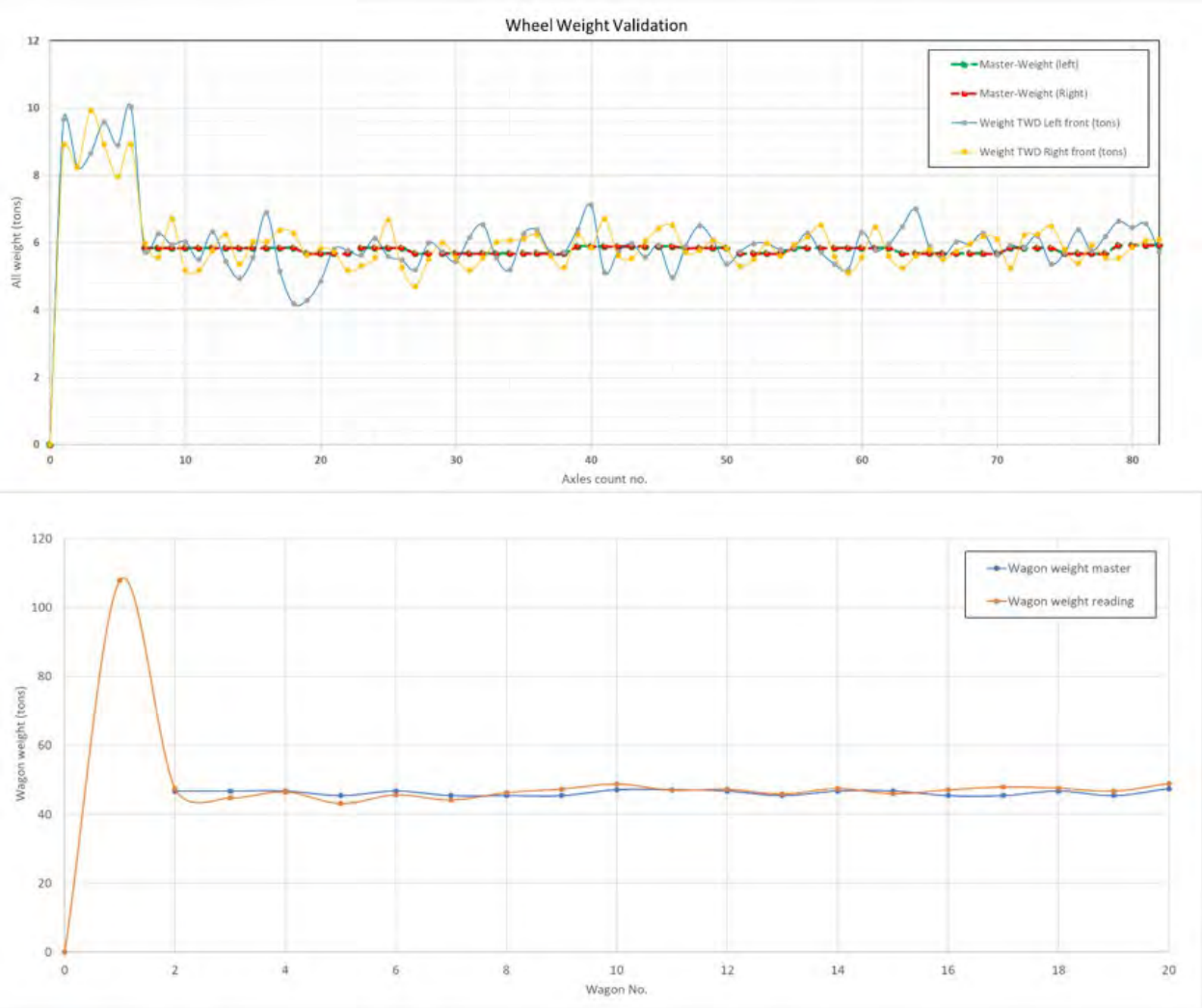

Figure 46 The data for each axle weight and wagon weight

The following part will describe the result of the TWD system in the depot at Ipoh railway station, Malaysia from the 20th to the 21st of August 2024. After the validation was performed and re-checked the TWD system was used to monitor and measure every coming train fleet from the 20th to the 21st of August 2024. During the demonstration, there were only two (2) train fleets coming to Ipoh station during the measurement.

The working summary of the TWD measurement at Ipoh station in Malaysia is summarized in **Figure 47**. RTTC has performed validation on one (1) train fleet and performed measurements on two (2) coming train fleets.

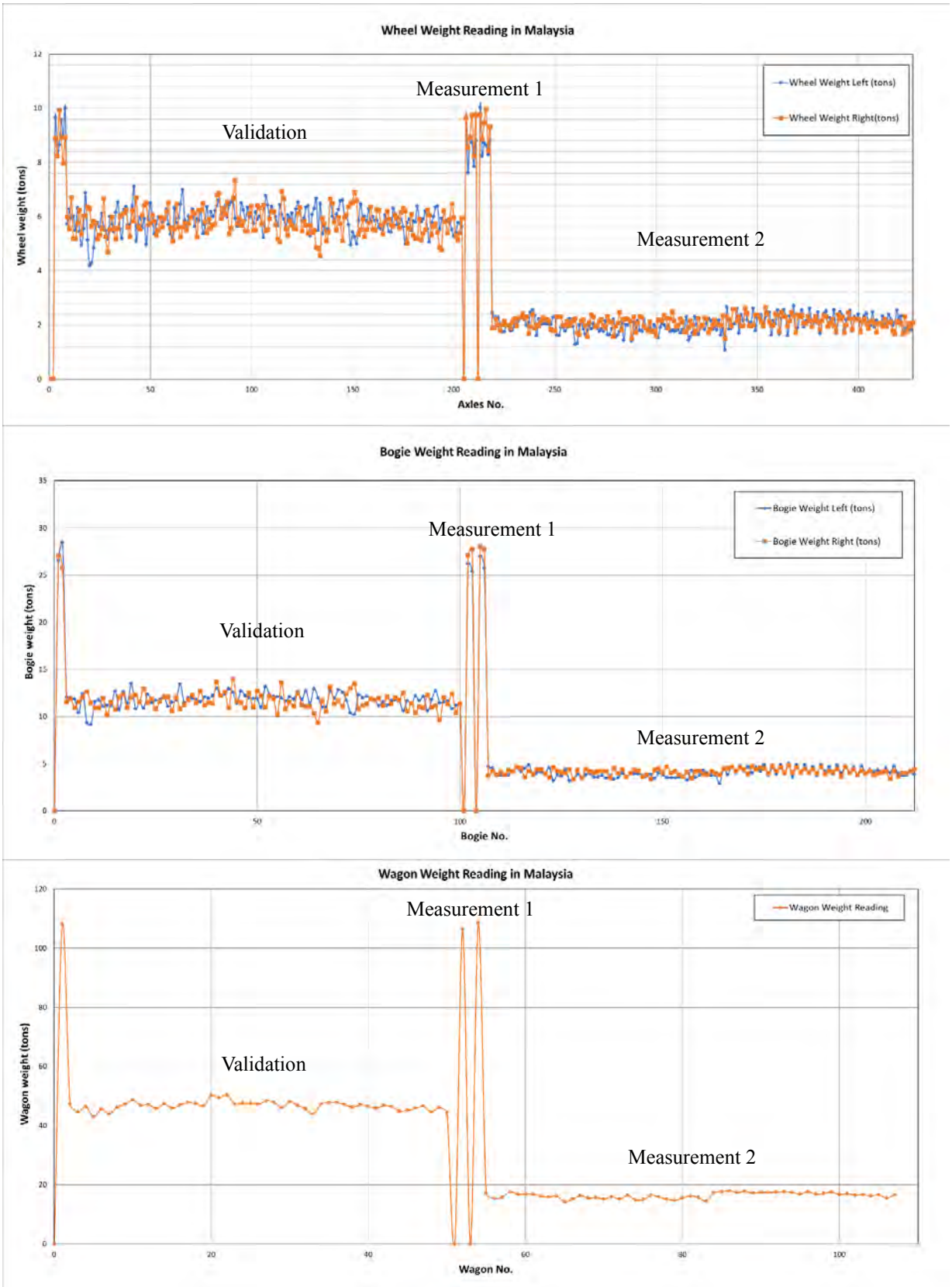

Figure 47 The working summary at Ipoh station

At Ipoh railway station from the 20th to the 21st of August 2024, the TWD system can detect only two (2) train fleets.

The result of the first train detected (6 axles, 2 bogies, and 1 locomotive) is shown in **Figure 48** with the following measurement result;

Locomotive = 1 car, Wagon = 0 car, Total axles = 6 axles, and Total bogies = 2 bogies

Bogie unbalance (%) = 8.62% and 10.11% (value of each bogie is shown in **Figure 48**)

The maximum bogie unbalance occurs at the rear bogie of the locomotive

Locomotive total weight from TWD = 106.51 tons

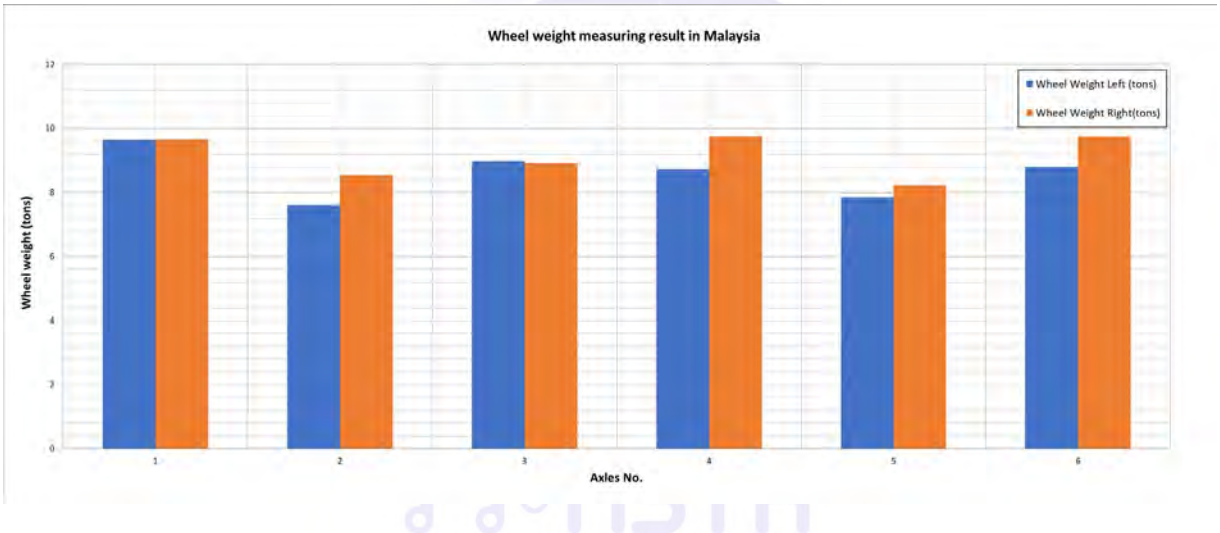

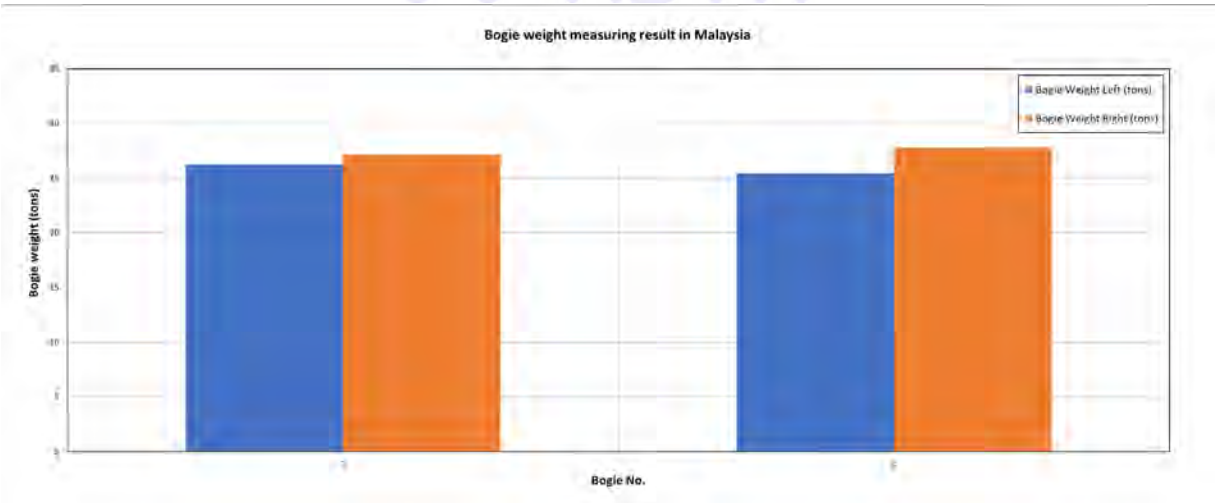

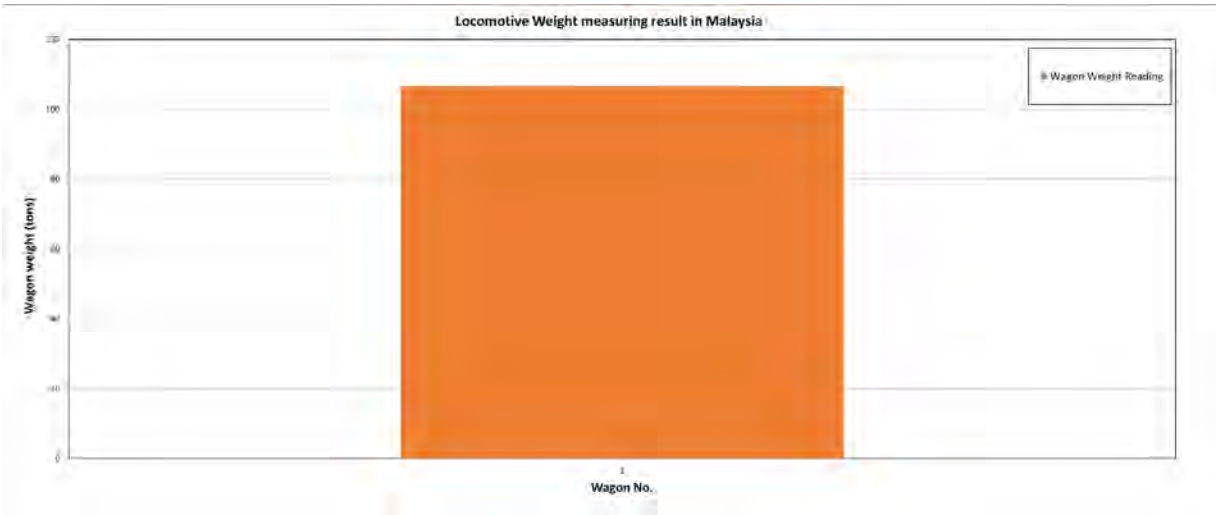

Figure 48 The result of the first train

The result of the second train detected (54 wagons, 108 bogies, and 218 axles) is shown in **Figure 49** with the following measurement result;

Locomotive = 1 car, Wagon = 54 cars, Total bogies = 108 bogies, and Total axles = 218 axles

Locomotive total weight from TWD = 108.55 tons

Bogie unbalance (%) = 1.43% - 38.81% (the value of each bogie is shown in **Figure 49**)

The maximum bogie unbalance occurs at the rear bogie of wagon number 30

Train total weight = 980.61 tons

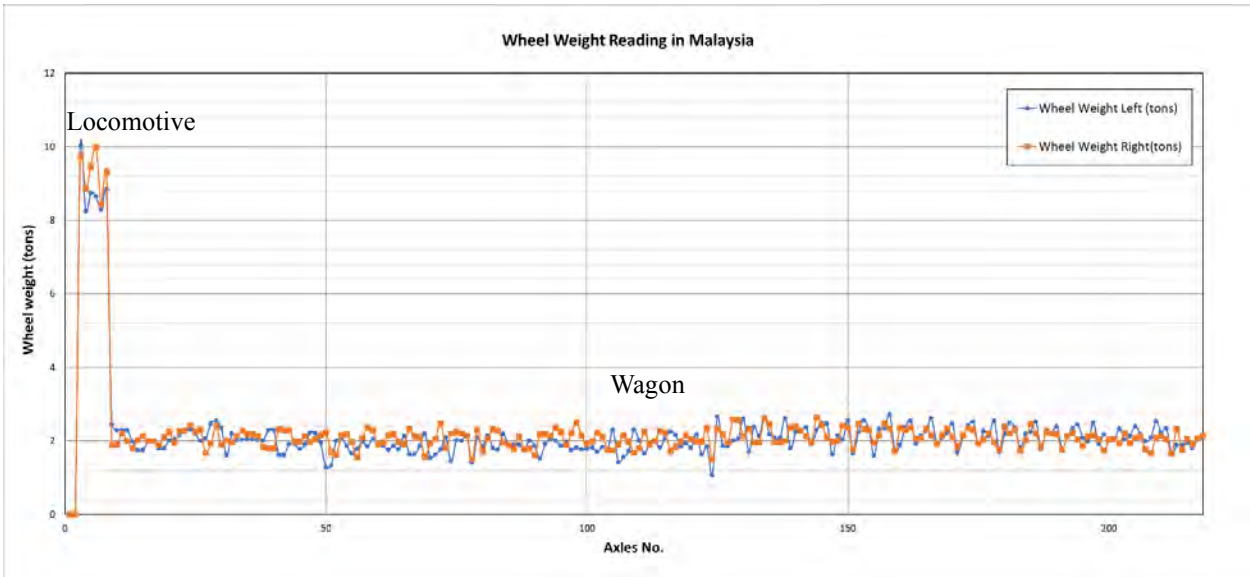
Wheel Weight Reading in Malaysia
Locomotive
Wagon
Wheel Weight Left (tons)
Wheel Weight Right(tons)
Wheel weight (tons)
Axles No.
0
2
4
6
8
10
12
0
50
100
150
200

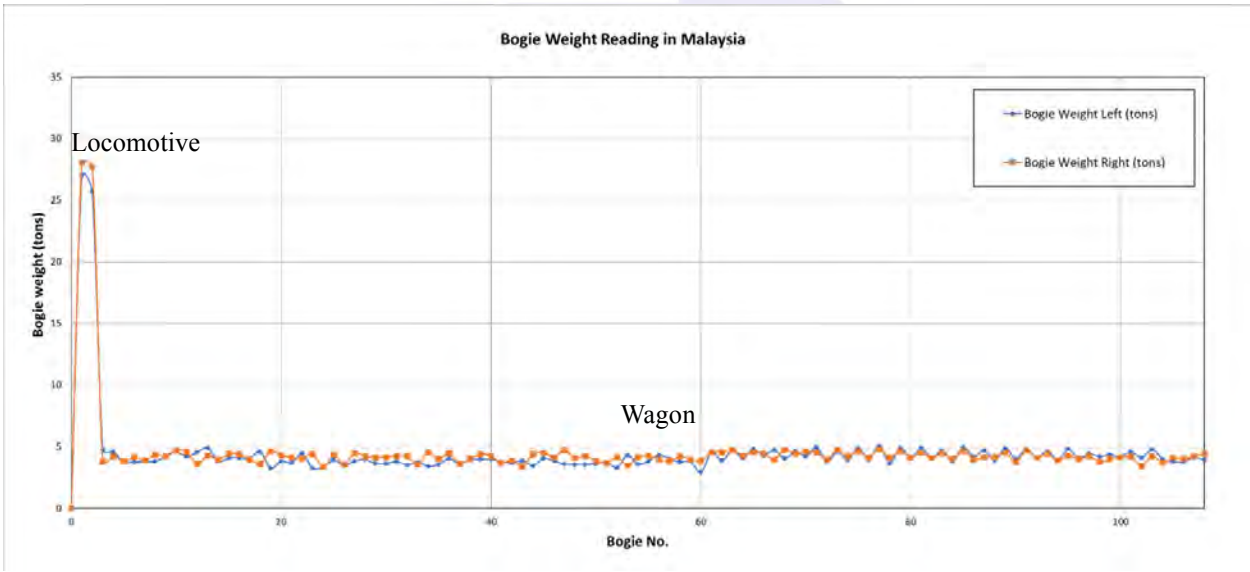
Bogie Weight Reading in Malaysia
Locomotive
Wagon
Bogie Weight Left (tons)
Bogie Weight Right (tons)
Bogie weight (tons)
Bogie No.
0
5
10
15
20
25
30
35
0
20
40
60
80
100

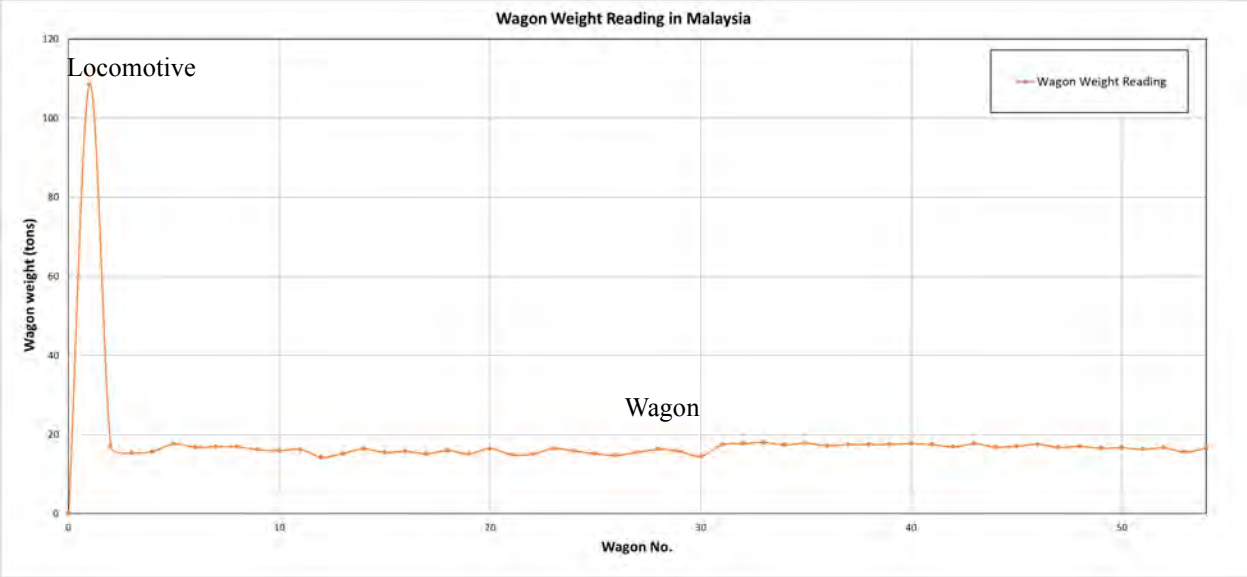

Figure 49 The result of the second train

Activity 9: Travel to Indonesia to onsite demonstrate and test the TWD system and transfer inspection and monitoring technology to Universitas Sumatera Utara (USU) and PT Kereta Api Indonesia (KAI), Indonesia

After finishing the demonstration and testing of the TWD system from the 20th to the 21st of August 2024. RTTC-TISTR continued the demonstration to Indonesia at KAI Medan and organizing a training workshop at Universitas Sumatera Utara (USU) from the 26th to the 30th of August 2024.

The onsite TWD demonstration is shown in **Figure 50**. The demonstration comprised of an introduction to the TWD technology, the working principle of TWD technology, and analysis of the measurement results.

Figure 50 The onsite demonstration in KAI.

The training workshop is shown in **Figure 51**. The workshop featured topics and experts presenting on various subjects from the RTTC-TISTR team as follows.

1. The Development of Transport Testing and Research Infrastructures for Domestic and International Cooperation by Dr. Anat Hasap, the director of RTTC-TISTR
2. The research on the mitigation of transport (green transportation) emissions in Thailand by Dr. Worawat Songkitti, technical officer of RTTC-TISTR
3. The development of local technology for Train Weight Devices (TWD) by Mr. Sarawut Saengvichien, technical officer of RTTC-TISTR
4. The vibration monitoring technology for inspection of rail abnormality by Mr. Winai Tumthong, technical officer of RTTC-TISTR

Figure 51 The workshop at USU.

Activity 10: An online summary of the project, sharing knowledge, assessment of satisfaction, and discussion of the future development of the TWD technology.

This activity is an online technical meeting for a summary of the project, assessment of satisfaction, and discussion of details in the future development of the technology and knowledge with Malaysia and Indonesia as shown in **Figure 52**.

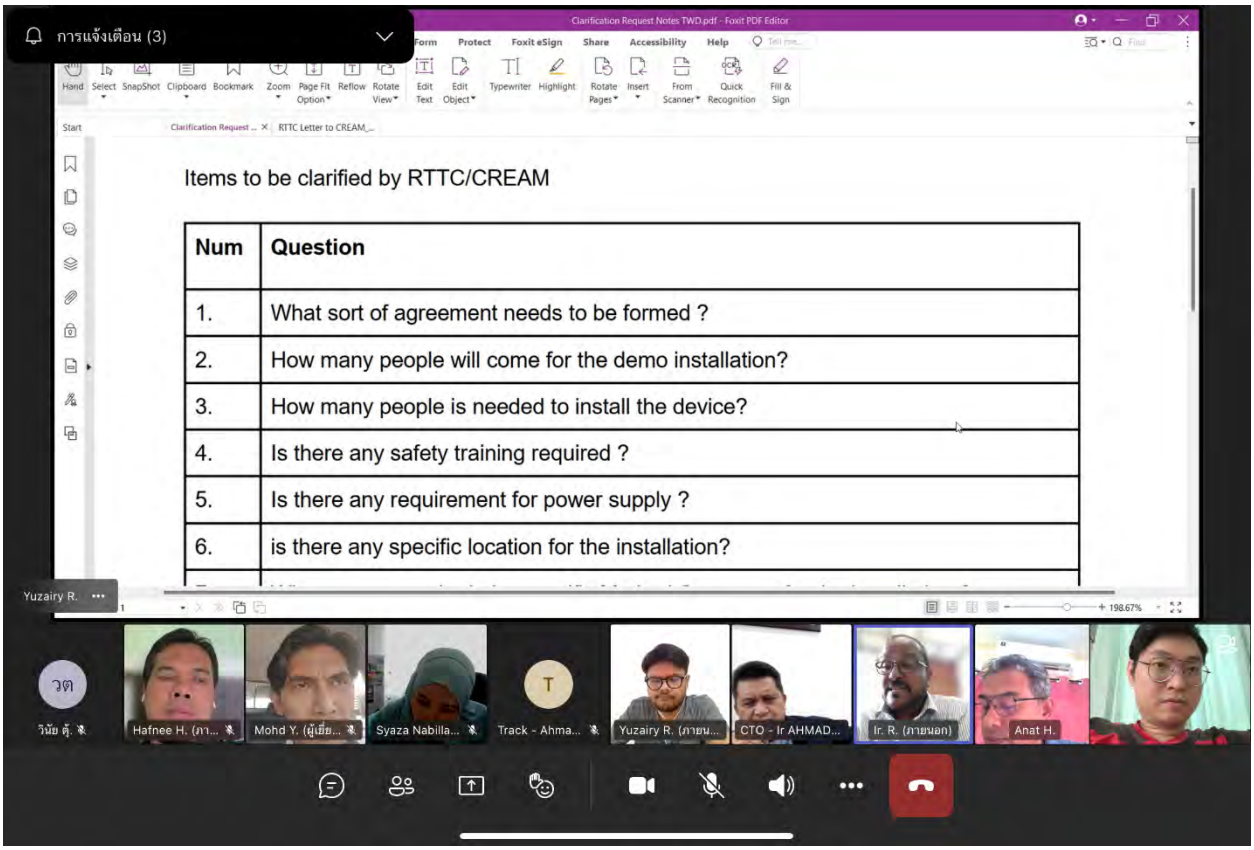

Figure 52 Online technical meeting

The TWD system completed in this research project can be concluded as follows:

1. The TWD system calibration in the laboratory shows a maximum error of 1.3% in the train wheel load simulation case.

2. The TWD system can be easily installed in the existing track without track modification.

3. The TWD system can be calibrated with portable tools on site to obtain maximum accuracy.

4. The TWD system uses an automatic record and transfer of real-time data to a cloud database which can be accessed at any time. Moreover, it can be easily configured and programmed with remote access.

5. The TWD system enclosure design is water-resistant under normal rainy conditions and suitable for outdoor installation.

6. The TWD is good for measuring dynamic weight without interrupting the train operation.

7. The TWD system results from installation on live track can be summarized in the following:

- The TWD system can automatically detect the passing train and automatically measure and record data in the cloud database with transferred data time around 1 – 3 minutes.

- The TWD system software can automatically summarize and display statistical data.

- The TWD system has a dynamic accuracy of around 4.7%.

8. The TWD can be further developed for smart and predictive maintenance concepts. The accuracy can be improved by extending more measuring points and employing image processing technology to accurately identify every single wagon to efficiently complement the maintenance plan in the future.

Finally, the currently developed TWD has satisfactory acceptable accuracy for low-speed dynamic weighting of the wagon. However, the accuracy can be further improved for higher speed measurement. The TWD is proven to be utilized as a very easy and efficient local technology in supporting the maintenance of rolling stock to enhance safety and efficiency for sustainability.

Activity 11: Seminar and publication of the research project results

After all the research activities are completed, RTTC organized an onsite workshop and seminar to perform publication of the research project results and share the knowledge and principles of the TWD technology. This seminar, Publication of Technical Cooperation for Research and Development and Implementation of Railway Inspection and Monitoring Technology, took place at the Maruay Garden Hotel, Bangkok on September 24, 2024. The objectives of the seminar are as follows:

1. To publish and promote cooperation for railway technology transfer in the ASEAN region.
2. To enhance the safety level of railway operations by developing local railway technologies and implementation in ASEAN countries.
3. To develop the railway research network and implementation in ASEAN countries through the sharing of knowledge and infrastructures, co-research, and promoting self-reliant railway technologies.
4. To enhance regional connectivity and sustainable development.

The seminar invited speakers representing many countries, United Kingdom, China, and Singapore, including university professors and experts in Thailand as well as participants from ASEAN region countries, including Laos, Malaysia, and Indonesia. The seminar featured topics and experts presenting on various subjects are as follows.

1.) Project overview and introduction to railway inspection technology by Dr. Anat Hasap, Director of the Railway Transportation System Testing Centre (RTTC) as shown in **Figure 53**.

Figure 53 Presentation of Project overview and introduction to railway inspection technology

2.) TWD technology the development implementation and future application by Dr. Worawat Songkitti and Mr. Sarawut Saengvichien, technical officer of the Railway Transportation System Testing Centre (RTTC) as shown in **Figure 54**.

Figure 54 Presentation of TWD technology the development implementation and future application

3.) The dynamic behavior and monitoring technology for the safety of train structures by Prof. Dr. John Roberts, the Chairman of KU-Rail at Kasetsart University as shown in **Figure 55**.

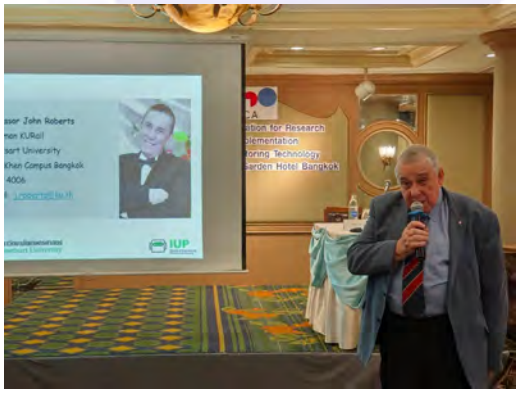

Figure 55 Presentation of the dynamic behavior and monitoring technology for the safety of train structures

4.) The Inspection and Monitoring Research in Earthquake in China by Prof. Dr. Zhong Tao, Faculty of Civil Engineering Mechanics, Kunming University of Science and Technology (KUST) as shown in **Figure 56**.

Figure 56 Presentation of the Inspection and Monitoring Research in Earthquake in China

5.) Rail Noise and Vibration, Mechanisms and Means of Controls, for Prediction by Dr. Sorawit Limthongkul, Department of Mechanical Engineering, Faculty of Engineering, Kasetsart University as shown in **Figure 57**.

Figure 57 Presentation of Rail Noise and Vibration, Mechanisms and Means of Controls, for Prediction

6.) Monitoring and Seismic Retrofit of Reinforced Concrete Buildings to Resistance Future Earthquakes for Sustainable Cities by Assist. Prof. Dr. Panumas Saingam, Department of Civil Engineering, Faculty of Engineering, King Mongkut's Institute of Technology Ladkrabang as shown in **Figure 58**.

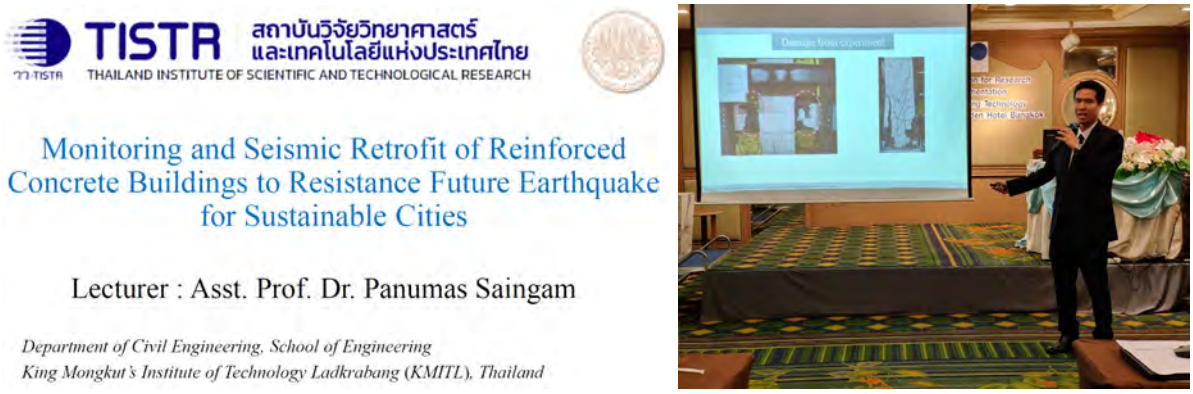

Figure 58 Presentation of Monitoring and Seismic Retrofit of Reinforced Concrete Buildings to Resistance Future Earthquakes for Sustainable Cities

7.) Enabling Integrated Measurement and Control Solutions for Railway by Garry Tjhin, Axiometrix Solutions as shown in **Figure 59**.

Figure 59 Presentation of Enabling Integrated Measurement and Control Solutions for Railway

The seminar successfully met all the objectives of the event, and the overall activities are shown in **Figure 60**. The presentation materials are in **Appendix 2**.

Figure 60 The seminar activity

Activity 12: Project conclusion

This research project, the technical cooperation for the research and development and implementation of railway inspection and monitoring technology, was successfully conducted. The success of the project can be summarized into three parts. The first part is the background of the research project which can be concluded as follows:

1. TISTR proposed a research project proposal titled Technical Cooperation for Research and Development and Implementation of Railway Inspection and Monitoring Technology to PGTF for South-South Cooperation in April 2021.
2. TISTR was rewarded a grant from PGTF for South-South Cooperation and TICA in November 2021. The research contract (2022 – 2024) was signed between TISTR, UNDP and TICA.
3. The objectives of the research project are: (1) to promote cooperation in railway technology transfer in the ASEAN region, (2) to enhance the safety level of railway operations by developing local railway technologies and implementation in ASEAN countries, (3) to develop railway research network and implementation in ASEAN countries through the sharing of knowledge and infrastructures, co-research, and promoting self-reliant railway technologies, and (4) to enhance regional connectivity for sustainable development
4. TISTR conducted the project in Thailand and cooperated with partners in Malaysia and Indonesia and also other ASEAN countries.

The second part is the overview of the TWD technology which can be concluded as follows:

1. The TWD system calibration in the laboratory has a reasonable error with a maximum error of 1.3% in the train wheel load simulation case.
2. The TWD system can be easily installed in the existing track without track modification.
3. The TWD system can be calibrated with portable tools on site to obtain maximum accuracy.

4. The TWD system uses an automatic record and transfer of real-time data to a cloud database which can be accessed at any time. Moreover, it can be easily configured and programmed with remote access.
5. The TWD system and its enclosure are water-resistant under normal rainy conditions and suitable for outdoor installation.
6. The TWD is good for measuring dynamic weight without interrupting the train operation.
7. The TWD system results from installation on live track can be summarized in the following:

   - The TWD system can automatically detect the passing train and automatically measure and record data in the cloud database with transferred data time around 1 – 3 minutes.

   - The TWD system software can automatically summarize and display data statistically.

   - The TWD system has a dynamic accuracy of around 4.7%.

The third part is the positive feedback and recommendations from experts in railway systems for future development of the TWD technology which can be concluded as follows:

Recommendations :

After the study and successful development of the first prototype TWD system as an efficient local technology for the measurement of train weight, the prototype TWD system was demonstrated in the real environment (live railway track) in Thailand and overseas. It was confirmed that the prototype TWD system functions properly and can be used efficiently for the measurement of the train weight.

Future development:

Nowadays technology is developing rapidly. The trend of using modern and smart technology, such as using network technology integrating digital processing such as AI and big data to increase accuracy and advance prediction, and reduce the time and the cost of operations. In addition, every country has several railway operators, resulting in a variety of maintenance requirements and practices. The TWD technology is then recommended by rail operators to be

further developed to fulfill these new requirements and to achieve maximum efficiency in the future as follows:

1. The TWD should be further developed for smart and predictive maintenance concepts. The accuracy can be improved by extending more measuring points and employing image processing technology to accurately identify every single wagon to efficiently complement the maintenance plan in the future.
2. The TWD technology should be further promoted to every ASEAN country that has a railway operator to achieve a safe and efficient regional railway network.
3. The TWD should be further developed by integrating into a network and employing intelligent technology such as AI, and big data to enhance processing efficiency and advance prediction capability.
4. The sensor of TWD can be further developed to increase resolutions to cover every category of railway vehicle such as passenger trains, freight wagons, diesel multiple-unit, electrical trains, etc.
5. The TWD system should be further developed to have some additional features to fulfill the specific requirements of the railway operators.

Appendix 1: Presentation slides of onsite workshop seminar demonstrating the operation of TWD and sharing principles and methods of use in Thailand

Safety policy of rail transit in Thailand by Dr. Tayakorn Chandrangsu

กรมการขนส่งทางราง
Department of Rail Transport

Policy of Rail Transit in Thailand

Presented by Dr.Tayakorn Chandrangsu

June 2024

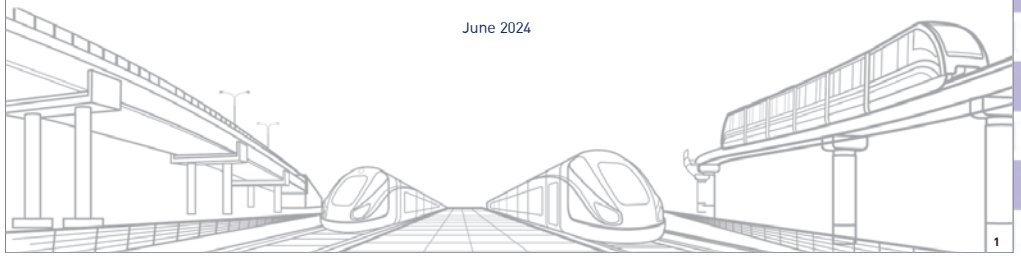

1

History of DRT

The Department of Rail Transport was established in accordance with The Ministry and Departments Revision Act (No.18), B.E. 2562, which is listed in the Royal Gazette Volume 136 section 49 page 9 on 14 April 2019, and is effective on the day following the date of its publication in the Royal Gazette(i.e.15 April 2019). The establishment was by raising and transferring business rights, liabilities and obligations including government officials and employees of the Rail Project Development Office.

2

Department of Rail Transport (DRT) mission

OUR MISSION

1. RAILWAY NETWORK DEVELOPMENT
To plan and develop railway network that passengers can easily access.

2. STANDARDIZATION OF RAILWAY
To set the standards for railway construction, operation, and maintenance.

3. REGULATION
To regulate railway according to the standards, and make sure that the railway system is efficient, convenient, and safe for passengers.

4. ECONOMIC INVESTMENT
To set the appropriate railway fare and fee for rail transport.

5. EVALUATE
To check and mitigate issues on railway projects

3

Rail Transport Players in Thailand

Formulate transportation plans in accordance with government policies

Develop the national strategy for railway technology, focusing on research and development as well as human resource development.

Budget allocation and the establishment of regulatory policies.

Construction management, concession contract oversight, and infrastructure ownership. Operation and maintenance (O&M)

Construction management, concession contract oversight, and infrastructure ownership.

Railway Plan , Regulate Level of Service and Safety Ensure consistent and standardized rail transport nationwide.

OPERATORs Secure government contracts for railway operation and maintenance.

Bangkok holds a majority share of 99.98% and manages facilities and infrastructures within Bangkok.

Concession contract oversight, and infrastructure ownership.

4

Overview Introduction to the Department of Rail Transport

Bangkok Expressway and Metro Public Company Limited — BEM
State Railway of Thailand — SRT
(Operators)
Mass Rapid Transit Authority of Thailand — MRTA
S.R.T. Electrified Train Co., Ltd. — SRTET
Bangkok Mass Transit System Public Company Limited — BTSC
Asia Era One Company Limited — ERA1

Railway Sector

DRT
Department of Rail Transport
(Regulator)

MOT
Ministry of Transport

Other Sectors
- Department of Airports
- Department of Land Transport
- Department of Highway
- Department of Rural Roads
- Marine Department

The DRT was established in 2019 (4 years ago) to regulate and set the railway standards in Thailand.

5

The Rail Transport Act (Draft)

The current draft of the Rail Transport Act consists of 11 chapters and 152 sections.

- General Provisions Section 1-4
- Part 1 Policy Committee Section 5-15 — Roles and Powers
- Part 2 Section 16-20 — The development of rail transport projects — The preparation of a rail transport development plan; The implementation of rail transport projects
- Part 3 Section 21-26 — Rail transport system area And Rail transport system safety zone
- Part 4 Section 27-52 — The operation of rail transport services — Applying for a license to operate rail transport services; Responsibilities of the rail transport operator; Setting passenger fares and service fees
- Part 5 Section 53-66 — Railway track sharing — Shared use of railway tracks for rail transport; Capacity allocation, timetable, and route planning for rail transport
- Part 6 Section 67-80 — Investigation of accidents and incidents — Accidents and Incidents Investigation Committee; Accident and Incident Investigation
- Part 7 Section 81-86 — Rail Transport Inspector — Authorities and Responsibility
- Part 8 Section 87-96 — Officer — Qualifications of the Officer
- Part 9 Section 97-106 — Registration of rail transport vehicles — Application for registration of rail transport vehicles; Specifications of rail transport vehicles
- Part 10 Section 107-111 — Protection of passengers and service users
- Part Section 112-143 — Penalties — Administrative Penalties; Regulatory Fines; Criminal Punishments
- TRANSITORY PROVISIONS Section 144-152 — Policy Committee; Issuance of licenses for rail transport operations

6

Traffic conditions in Bangkok

Population 16.92 million people

Visitor 22 million people/year

- Passenger cars 5.55 million
- Pickup Truck 1.49 million
- Motorcycle 4.25 million
- Taxi 77,232
- Tuk Tuk 8,768
- Motorcycle taxi 68,458
- Bus 34,000
- Truck 159,097

Source : MMAP2, DRT

The development and utilization in Bangkok area

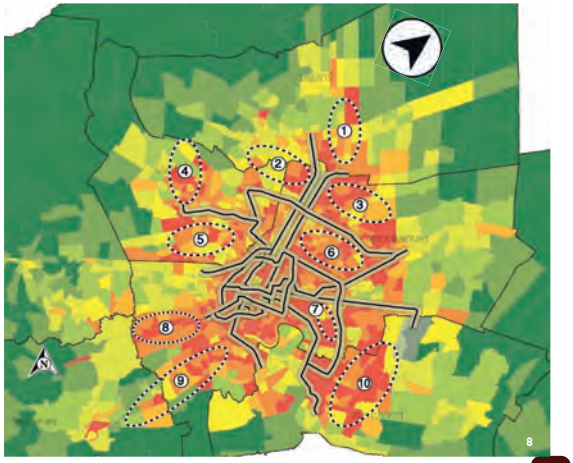

8

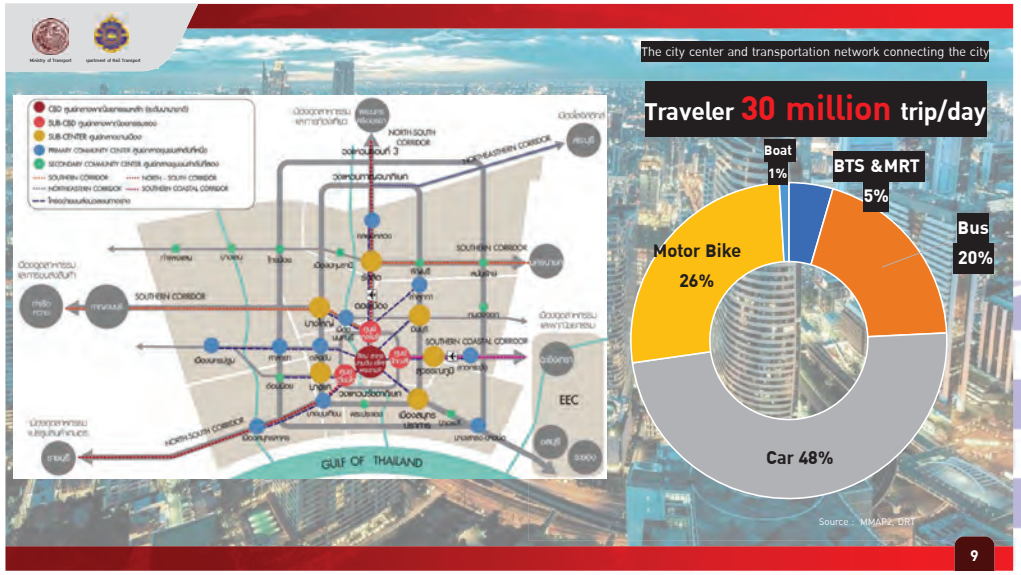

9

Introduce the Mass Rapid Transit Master Plan (M-Map) as a comprehensive strategy for Bangkok's transit network.(2010-2029)

14 routes 553.41 KM

- The Master Plan for Mass Transit System in Bangkok (M-Map 1) was approved in 2010 and covers a total distance of 509 km across 12 routes.
- In 2016, the Cabinet approved for implementing the **Gold Line (Krung Thon Buri - Klong San - Prachadhipok).**
- In 2019, the Cabinet allowed MRTA to develop the **Brown Line (Khae Rai - Lam Salee (Bueng Kum)** as part of M-Map 1.

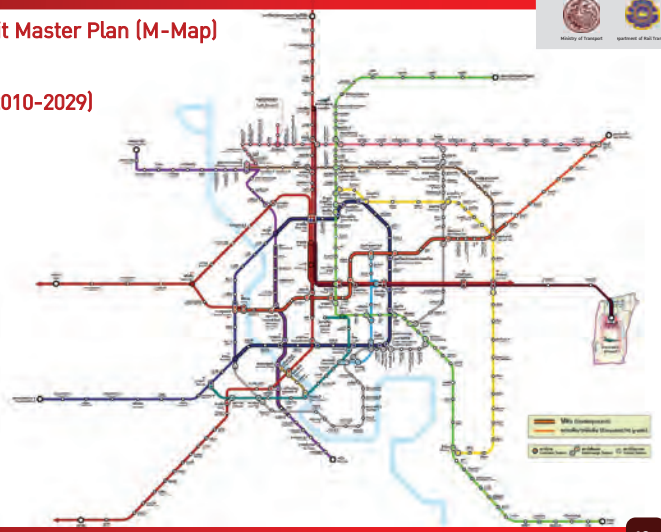

10

In service

13 Routes 276.84 KM

Green (Sukhumvit)
1. **Mo Chit - Samut Prakan** (37.10 KM)
   Mo Chit - On Nut opened on 5 Dec.1999
   On nut- Bearing opened on 12 Aug 2011
   Bearing - Samut Prakan opened on 6 Dec. 2018
2. **Mo Chit - Saphan Mai - Khu Khot** (18.70 KM)
   Mo Chit - Lat Phrao opened on 9 Aug 2019
   Lat Phrao - Kasetsart U opened on 4 Dec. 2019
   Kasetsart U - Wat Phra Si Mahathat opened on service 5 June 2020
   Wat Phra Si Mahathat - Khu Khot opened on 16 Dec. 2020

Green (Silom)
3. **National Stadium - Bang Wa** (14 KM)
   National Stadium - Taksin Bridge opened on 5 Dec. 1999
   Saphan Taksin - Wongwian Yai opened on15 May 2009
   Wongwian Yai - Bang Wa Open opened on 5 Dec. 2013

Blue
4. **Bang Sue - Hua Lamphong** (20 KM)
   Opened on 3 Jul. 2004
   (Bang Sue - Tao Poon 1.2 KM opened on 11 Aug. 2017)
5. **Hua Lamphong - Bang Khae** (14 KM)
   Opened on 29 Sep 2019
6. **Bang Sue - Tha Phra** (13 KM)
   Opened on 30 Mar. 2020

ARL
7. **Phayathai-Suvarnabhumi** (28.70 KM)
   Opened on 23 Aug. 2010

Purple
8. **Bang Yai-Tao Poon** (23 KM)
   Opened on 6 Aug 2016

Gold
9. **Krungthonburi-Khlongsan** (1.88 KM)
   Opened on 16 Dec. 2020

Red (North)
10. **Bang Sue - Rangsit** (26.30 KM)
    Opened on 29 Nov 2021

Red (West)
11. **Bang Sue - Taling Chan** (15.26 KM)
    Opened on 29 Nov 2021

Yellow
12. **Lat Phrao - Samrong** (30.40 KM)
    Opened on 19 Jun 2023

Pink
13. **Khae Rai-Min Buri** (34.50 KM)
    Open on 21 Nov 2023

11

Under construction

4 Projects 70.90 KM

Pink
1. **Si Rat - Muang Thong Thani** (3 KM)
   Civil work 47.87% E&M 28.75%
   Overall progress 41.44% Open in 2025

Orange
3. **Cultural Center – Minburi** (22.50 KM)
   Civil works 100% Open in 2026

ARL
4. **Phaya Thai - Don Mueang**(21.80 KM)
   Included in HSR linking 3 airports, open in 2028

Purple
5. **Taopoon - Ratburana** (23.60 KM)
   MRTA signed a contract for civil works on March 11, 2022.
   Civil works 24.60% Open in 2028

12

Bidding

1 Project 13.40 KM

Orange — **Cultural Center - Bang Khun Non** (13.40 KM) Open in 2028

proposing to the Cabinet to approve the project.

3 Projects 29.34 KM

Red (North)
1. Rangsit-Thammasat University, Rangsit (8.84 KM)

Red (west)
3. Taling Chan - Salaya(14.80 KM)
4. Taling Chan-Siriraj (5.70 KM)

Project Preparation

12 Projects 162.93 KM

- Red (South) — 1 Bang Sue - Hua Lamphong (5.76 KM)
- Red (East) — 2 Bang Sue - Makkasan – Hua Mak (20.14 KM)
- Brown — 3 Khae Rai-Lam Sali (Bueng Kum) (22.10 KM)
- Grey — 4 Watcharaphon-Thonglor (16.25 KM)
- Green (Sukhumvit) — 5 Khu Khot-Lam Luk Ka (6.50 km.)
- Green (Sukhumvit) — 6 Samut Prakan-Bang Pu (9.50 km.)
- Blue — 7 Bang Khae - Phutthamonthon Sai 4 (8 KM)
- Red (South) — 8 Hua Lamphong - Wongwian Yai – Mahachai (38 KM)
- Grey — 9 Phra Khanong-Tha Phra (23.66 KM)
- Light blue — 10 Dindaeng-Sathorn (9.50 KM)
- Gold — 11 Khlong San - Prajadhipok Road (0.92 KM)
- Yellow — 12 Ratchada-Lad Phrao-Ratchayothin (2.60 KM)

Timeline

In service = 276.84 KM

1. Green (Sukhumvit) Mo Chit - Samut Prakan (37.10 km.)
2. Green (Silom) National Stadium - Bang Wa (14 km.)
3. Blue Bang Sue - Hua Lamphong (20 km.)
4. ARL Phayathai-Suvarnabhumi (28.70 km.)
5. Si Muang, Bang Yai-Tao Poon (23 km.)
6. Blue Hua Lamphong - Bang Khae (Lak Song) (14 km.)
7. Blue Bang Sue-Tha Phra (13 km.)
8. Green (Sukhumvit) Mo Chit - Saphan Mai - Khu Khot (18.70 km.)
9. Gold Krung Thon Buri-Khlong San (1.88 km.)
10. Red (north) Bang Sue - Rangsit (26.30 km.)
11. Red (West) Bang Sue - Taling Chan (15.26 km.)
12. Yellow Lat Phrao - Samrong (30.40 KM)
13. Pink Khae Rai - Min Buri (34.50 KM)

2025 = 3 KM (279.84 KM)

14. Pink Si Rat - Muang Thong Thani (3 KM)

2026 = 51.84 KM (331.68 KM)

15. Orange Cultural Center - Min Buri (22.50 KM)
16. Red (north) Rangsit-TU Rangsit Center (8.84 KM)
17. Red (West) Taling Chan - Salaya (14.80 KM)
18. Red (West) Taling Chan - Siriraj (5.70 KM)

2028 = 93.40 KM (425.08 KM)

19. Purple Tao Pun - Rat Burana (23.60 KM)
20. ARL Phaya Thai-Don Mueang (21.80 KM)
21. Red (South) Bang Sue - Hua Lamphong (5.76 KM)
22. Red (East) Bang Sue - Makkasan - Hua Mak (20.14 KM)
23. Brown Khae Rai-Lam Wheat (22.10 KM)

2029 = 128.33 KM (553.41 KM)

24. Orange Cultural Center - Bang Khun Non (13.40 KM)
25. Green (Sukhumvit) Samut Prakan-Bang Pu (9.50 km.)
26. Green (Sukhumvit) Lam Luk Ka-Khu Khot (6.50 km.)
27. Blue Bang Khae - Phutthamonthon Sai 4 (8 km.)
28. Red (South) Hua Lamphong - Mahachai (38 km.)
29. Gold Khlong San - Prajadhipok (0.92 km.)
30. Gray Watcharaphon-Thonglor (16.25 km.)
31. Gray Phra Khanong-Tha Phra (23.66 km.)
32. Blue Dindaeng-Sathorn (9.50 km.)
33. Yellow Ratchada-Ratchayothin Extension (2.60 km.)

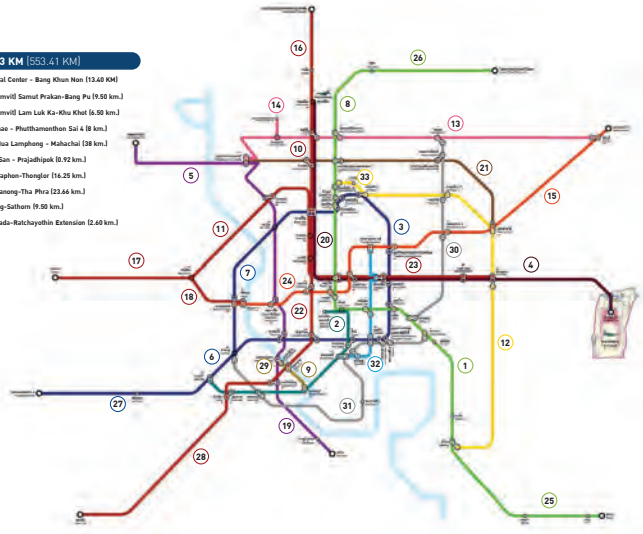

Existing → Future
Railway Network

4,044 km.	Total	4,722 km.
3,310 km. (81.85%)	Single track	1,215 km. (25.73%)
627 km. (15.50%)	Double track	3,400 km. (72%)
107 km. (2.65%)	Triple track	107 km. (2.27%)

17

Development Plan Double track /New Line

Double track

Double track, phase 1 (2018 – 2022)
7 Routes 993 KM
1. Chachoengsao Junction –Khlong Sip Kao-Kaeng Khoi
2. Chira Junction - Khon Kaen
6. Hua Hin-Prachuap Khiri Khan
3. Mab Kabao -Chira Junction
4. Lopburi - Pak Nam Pho
5. Nakhon Pathom - Hua Hin
7. Prachuap Khiri Khan – Chumphon

Double track, phase 2 (2023 – 2027)
7 Routes 1,479 KM
1. Paknampho – Denchai
2. Denchai - Chiang Mai
3. Khon Kaen - Nong Khai
4. Chira - Ubon Ratchathani
5. Chumphon - Suratthani
6. Surat Thani - Hat Yai – Songkhla
7. Hat Yai - Padang Besar

Double track, phase 3 (2028-2037)
2 Routes 391 KM
1. Khlong Sip Kao Junction–Aranya prades
2. Hat Yai Junction –Su ngai Kolok

New Line

New Line (2022– 2027)
2 Routes 677 KM
1. Denchai - Chiang Rai - Chiang Khong
2. Ban Phai - Mukdahan - Nakhon Phanom

New Line phase
1. Kanchanaburi-Suphan Buri – Ban Phachi Junction
2. Si Racha - Rayong
3. Map Ta Phut – Rayong - Chanthaburi - Trat
4. Chumphon-Ranong
5. Surat Thani - Phang Nga - Tha Nun
6. Surat Thani – Don Sak
7. Thap Pu t- Krabi
8. Mukdahan-Amnat Charoen - Ubon Ratchathani

Completed
Under Construction
Ask for Approval/EIA report
Cabinet Approved

18

Planned mass transit in regional cities

Chiang Mai
- The MRTA is studying the Red Line pilot project
- (Nakhon Phing Hospital - Mae Hia - Saman Samakkee)
- Goal is to open in 2028.

Phitsanulok
- The MRTA is studying the Red Line pilot project (University-Department Store)
- Goal is to open for service in 2031.

Nakhon Ratchasima
- The MRTA is studying for Green Line pilot project (Save One Market - career center)
- Goal is to open for service in 2028

Khon Kaen
- The Khon Kaen Province has finished study on the Red Line pilot project (Samran-Tha Phra)
- The EIA report is being revised.

Hat Yai
- Khlong Wa - Van station studied by Local administration
- PPP report being revised
- EIA report approved on January 25, 2021

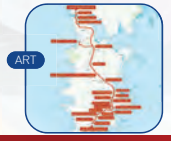

Phuket
- The MRTA is studying for Airport – Chalong (1st Phase)
- 1st Phase is planned to open in 2027.

19

Planned High Speed Rail

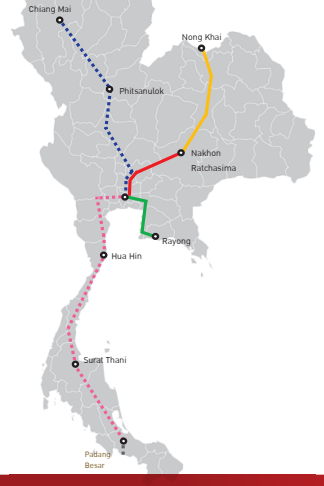

5 Routes in 2032

- Bangkok - Nakhon Ratchasima 253 km. (Under construction)
- Don Muang - U-Tapao (Bangkok-Rayong)* 220 km. (Under construction)
- Nakhon Ratchasima - Nong Khai 355 km.
- Bangkok - Phitsanulok 384 km.
- Bangkok - Padang Besar 970 km.

* Public-Private Partnership (PPP)

20

EMV Contactless Payments

Experience the simplicity of EMV contactless payments, enabling make transactions on various rail lines. Simply spot the contactless symbol on your credit card and you're good to go!

With EMV Contactless payment, you can now pay for MRT Blue Line, Purple Line, Red Line, Yellow Line and Pink Line rides in Bangkok with just a tap. This quick and easy payment method, making your travel experience more efficient and secure.

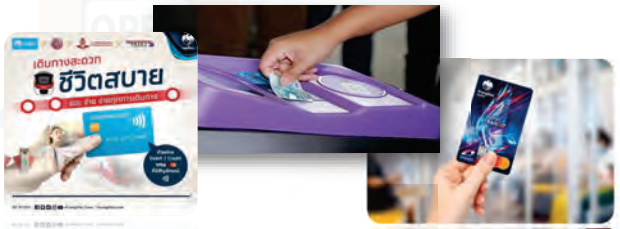

Rail transport system that supports the use of EMV cards.

Credit card
Supports Visa and Mastercard from all banks
VISA

Debit card
Valid only Krungthai bank and UOB bank
UOB

Prepaid card
Supports Visa and Mastercard from all banks
VISA

The route that is eligible for a discount on the initial fare in the rail transport system.

The routh	Discount
MRT connect MRT	14 ฿
MRT connect MRT	14 ฿
MRT connect MRT	15 ฿
MRT connect SRT	In progress
SRT connect MRT	In progress

Economic
Safety
Quality of life
Environment

20 Baht Flat Rate For The Train!

20 baht flat rate train policy
RED & PURPLE

16 October 2023

- The cabinet has approved the policy for red and purple lines flat rate of 20 baht per trip.
  Effective 16 October 2023 – 30 November 2024

30 November 2023

- Interconnecting between two lines
- Using **EMV Cards maximum only 20 baht**
- (Using the same card, and travel across systems must be within 30 minutes.)

Creating opportunitis for the general public, especially for salary workers.

- **Reducing expenses- Increasing purchasing power**
  Decrease the maximum annual burden from 20,224 baht to 9,640 baht.
- **Community expansion -New business district**
  Real estate development projects expanding into urban areas.
- **A new commercial hub has emerged.**
- **Improved quality of life and well-being.**
  Reducing congestion in the city center.
- **Fair taxation**
  - Compensating for transportation fares.
  - Increasing taxes from real estate projects.
  - Windfall Tax, The land value has increased.

Compare the average daily income between the red line, purple line and the combined income of the two lines.
After 20 bath flat rate policy
(Data as of 19 January 2024)

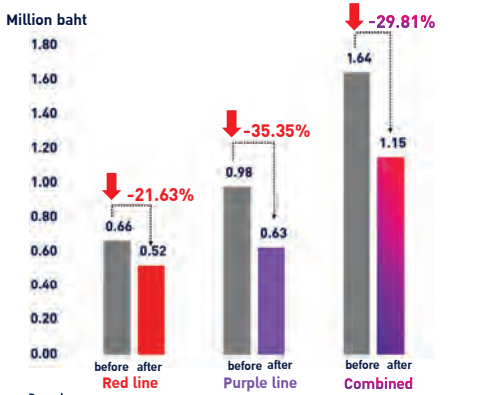

Remark:
1. Average income before the 20 baht policy, data as of September,2023
2. Average income after the 20 baht policy, data as of 16 October 2023 - current)

Compare the number of passenger of the red line, purple line and the combined total of both lines
After 20 bath flat rate policy
(Data as of 19 January 2024)

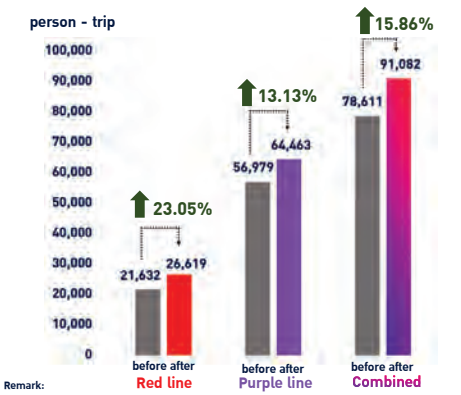

Remark:
1. Average number of passenger before the 20 baht policy, data between 1 – 15 October 2023
2. Average number of passenger after the 20 baht policy, data between 16 October 2023 - 19 January 2024


Target : Efficient Mass Transit System
"Convenient, Safe, On Time, Reasonable Price"
Accessible to everyone
Law
Safety Techniques
Financial Burden
Service Standard
Local Authority
Central Government
Community
University
25

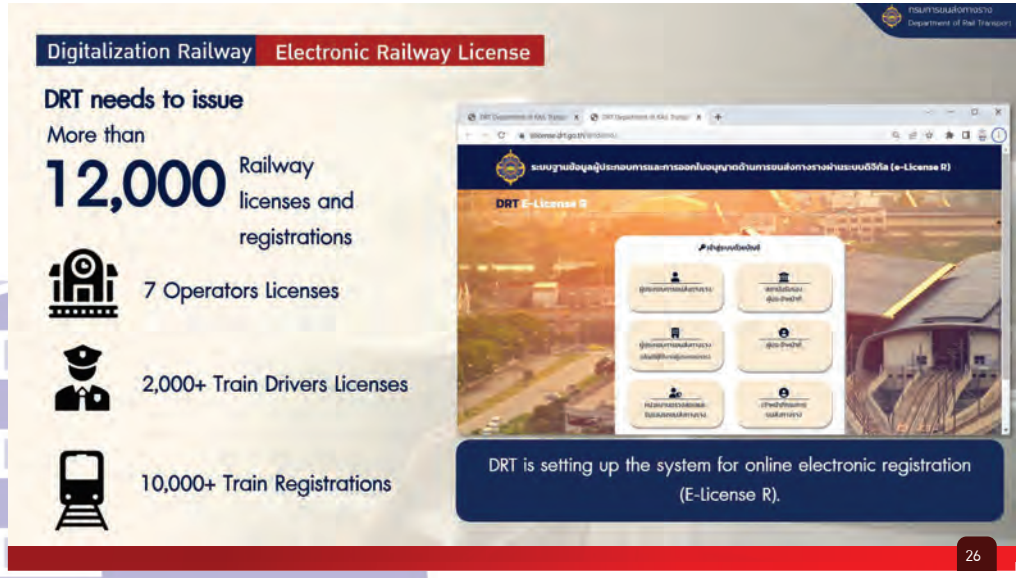
Digitalization Railway
Electronic Railway License
DRT needs to issue
More than
12,000 Railway licenses and registrations
7 Operators Licenses
2,000+ Train Drivers Licenses
10,000+ Train Registrations
DRT is setting up the system for online electronic registration (E-License R).
26


Electronic Railway Licensing System
(E - License R)
1 e-Application
Applicant submits application form and uploads related document online from everywhere.
2 e-Verification
Computer software automatically checks required document.
3 Qualification check
e-License R System sends application form to relevant department, officers check technical qualifications.
4 Online meeting
DRT officer contacts applicant online for further document.
5 e-Payment
Applicant pays license fees via mobile banking.
6 e-License
DRT signs digital signature issuing electronic railway license
Train Driver License
APPROVED
27

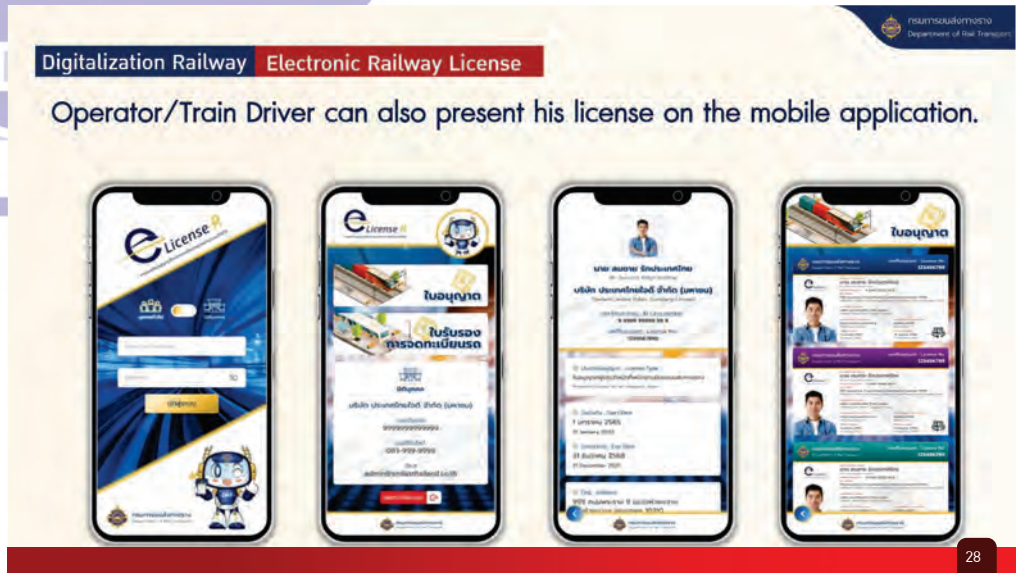
Digitalization Railway
Electronic Railway License
Operator/Train Driver can also present his license on the mobile application.
28

Digitalization Railway — Railway Crossing database and application

There are 2,971 railway crossings in Thailand

Elevated Grade Separated

Underground Grade Separated

619 locations Grade Separation 21%

Grade Crossings 2,135 locations 72%

Suspended 7% 217 locations

Illegal crossing 626 locations (29%)

Authorized crossings 1,509 locations (71%)

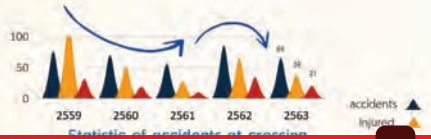

Statistic of accidents at crossing

Digitalization Railway — Railway Crossing database and application

DRT also published database on website and mobile application so that car drivers will know if there is any crossing ahead, and become aware of railroad crossings.

Next phase – DRT tries to sync crossing data with google map and other private companies so that crossing data will be displayed on navigation system in the cars.

Safety and Maintenance Standards

1 Civil and Safety Standards 10

Safety and Maintenance Standards

2 Rolling stock standards 5

Safety and Maintenance Standards

Electrical & signaling system standards 7

- Grounding and Bonding System on Mainline Train
- Transformer Arrangement for AC Electrification System
- AC Electrification System
- SCADA for AC Electrification System for Mainline Train
- Interlocking System on Mainline Train
- Automatic Train Protection System for ETCS Level 1 Mainline Train
- Centralized Traffic Control Standard for Mainline Train

33

กรมการขนส่งทางราง
Department of Rail Transport

Department of Rail Transport
Project in 2024

Work in progress

www.drt.go.th YouTube Channel : กรมการขนส่งทางราง Facebook : กรมการขนส่งทางราง

1 The study on developing standard for railway infrastructure drainage system and preparing risk reduction measures for railway systems

Project Duration 18 Months

"Global Climate Risk Report 2020
Thailand is the 8th highest risk affected by climate change. In the past 20 years, there have been 147 natural disasters and most of them are flooding."

Objective

1. To find the causes and collect flood data
2. To establish guidelines for prevention and problem solving
3. To establish the drainage system standards
4. To establish an analysis handbook for risk reduction measures
5. To establish an application that will notify

Expected Benefits

- guidelines for prevention and problem solving
- Physical improvement requirements
- Infrastructure drainage system standards
- Analysis handbook
- Digital database
- Follow information via APPLICATION

35

2 The study for regulation greenhouse gas emissions and reducing air pollution in rail transport sector

Project Duration 14 Months

Objective

1. To gather statistics on GHG emissions
2. To study guidelines and measures to reduce GHG emissions in the rail system
3. To study guidelines for carbon credits trading in the rail transport system

Expected Benefits

- Possess data on GHG emissions in the rail system
- Possess guidelines and measures to reduce GHG emissions
- Trade carbon credits by using the amount of reduced GHG to be the returned income for the operators

People began to change their travel behaviors from private cars to using the rail system

Study and calculate the GHG reduction from behavior changing to trading carbon credits that will become the returned income to the service provider to further reduce GHG.

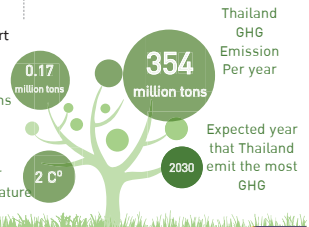

36

3 Monitoring and Evaluation of Thailand-China Railway Cooperation Project under Project Administration Office

Project Duration 12 Months

Objective

Follow up and evaluate project performance and impel the project according to the time frame of plans and goals

Expected Benefits

- Operations of Project Administration Office have specialized experts to implement, monitor and evaluate
- Possess reports to follow up and evaluate performance
- Impel the project according to the time frame of the work plan and the target set by the government

4 The Study of Rail Vehicle Inspection Standard for rail vehicle registration

Project Duration 9 Months

Currently, there's a privation of standard for the vehicles in rail transport sector in Thailand that will be a tool for vehicles readiness checking and provide safety and efficiency during operation.

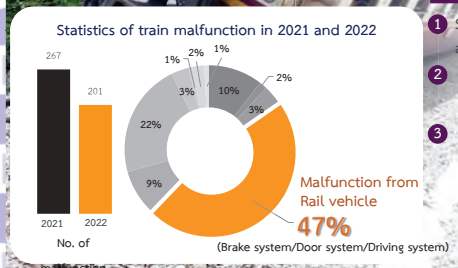

Objective

1. Study the qualifications of the audit agency
2. Prepare (draft) standards and inspection methods and tool
3. Prepare (draft) guidelines for supervision, ministerial regulations, rules or regulations

Expected Benefits

- Possess standards and methods for rail vehicle inspection
- Rail vehicle is safer
- Laws and regulations related to auditing agencies
- Possess information on vehicle inspection from abroad
- Increase the efficiency of operation

5 Analysis of Railway Utilization and Limitations for Enhancing Connectivity on the Singapore-Kunming Rail Link

Project Duration 12 Months

To encourage Thailand to be a hub of rail transport and transportation hub in the region for utilization by using advantages of Thailand's geography

Objective

1. To study the physical characteristics of SKRL
2. To study the regulations and requirements
3. To analyze the rail transport demand of SKRL
4. To propose SKRL operational guidelines
5. To propose guidelines for infrastructure and facilities development

Expected Benefits

- Physical characteristics of infrastructure and facilities for SKRL
- Regulations and requirements
- Transport demand for an evaluation the performance and support of infrastructures and facilities
- SKRL operational guidelines
- Guidelines for infrastructure and facilities development

6 The study on cost structure in determining the ceiling cost and guidelines for reviewing freight rates, railway utility cost and operation cost in rail business

Project Duration 16 Months

Objective

1. To study the cost structure and factors related to logistic costs and railway utility cost
2. To prepare guidelines and determining the ceiling cost including measures to promote the freight transport by train
3. To prepare (Draft) requirements, rules, and relevant laws

Expected Benefits

- Guidelines, measures cost structure and factors related to cost ceiling
- (Draft) requirements, regulations, laws related to cost ceiling
- Operators shift their transportation mode to rail transport

กรมการขนส่งทางราง
Department of Rail Transport

Department of Rail Transport
Upcoming Projects

Proposal for Budget Allocation

www.drt.go.th YouTube Channel : กรมการขนส่งทางราง Facebook : กรมการขนส่งทางราง

1 Develop guidelines for regulating rail transport service providers. and create cyber security measures for DRT in accordance with the Cyber Security Act 2019.

Project Duration 22 months

Expected Benefits

- Make a plan for dealing with cyber threats.
- Formulate guidelines for conducting cyber security assessments.
- Establish guidelines for setting standards for critical information infrastructure to enhance the governance of supervised businesses effectively.

42

2 Railway station service quality assessment (self conduct without procurement)

Project Duration 12 months

Expected Benefits

- Service quality assessment result of railway stations.
- Recommendation to improve the service quality of railway stations.
- Provide service quality assessment checklist in accordance with the international standard.

- Mass Rapid Transit station in Bangkok 11 stations

- Inter-city rail station 8 stations

3 project to create standards and databases for rail transport system areas and Rail transport safety zone

Project Duration 18 months

Expected Benefits

- Set rules for rail zones and safety areas. Use digital tools for checking and managing them
- Digitize the database and inspection records for rail transport system boundaries and safety zones.
- Make rail boundaries and safety zones safer and more efficient.
- Keep train users safe and confident with a user-friendly app system.

44

4 Subsidiary Law Drafting under the draft of the Rail Transport Act

Period 9 Months

Expected Benefits

- There is subsidiary law which is an important factor in explaining the processes and steps that must be complied with the rail transport law.
- Law Enforcement in governing rail transportation operations can be effectively implemented.

45

Thank You

Modern Technology Track Inspection
Rail Flaw Detection

Yuhao Cai – Project Director

Rail Technology International

www.rti-group.com

Company info

Rail Technology International

RTI is an Australian company, currently servicing the worlds most demanding railways in over 20 countries, since our establishment in 1987. We **design, manufacture and engineer** world leading non-destructive automated rail flaw detection systems.

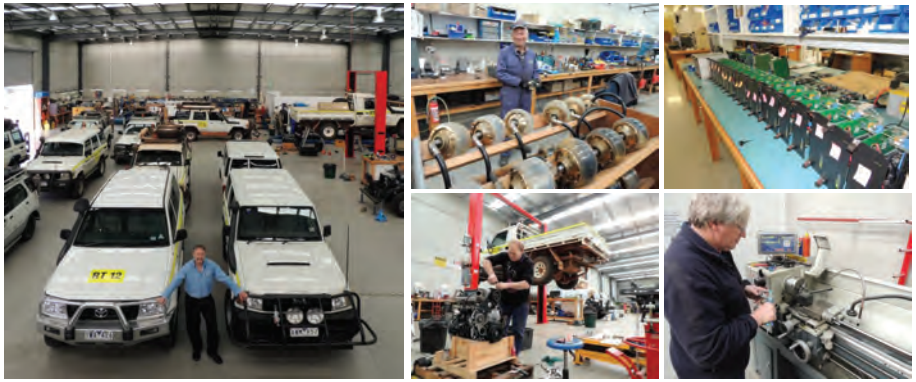

Clients

Rail Technology International

VALE · MTR · bhpbilliton · Downer EDI · Balfour Beatty · PMG · ARMTECH · TISTR · ARTC · RioTinto · BRASTAN · IRT · Brookfield Rail · CN · onesteel · John Holland · AURIZON · Iarnród Éireann Irish Rail · QueenslandRail · tranz · KiwiRail · 中国中车 CRRC · MRS · QUANTUMRail Ltd · 沈阳地铁 Shenyang Metro · 南京地铁 Nanjing Metro

RTI Roadmap

Rail Technology International

First vehicle of RTI in 1988

2000SX **8000SX** **8800SX**

- 1980s	1990s	2000s	2010s	2020s

8800SX SubRack

The Brain of the system

The 8800SX Automated Rail Flaw Detection System was released in 2016. The electronics and racking hardware accommodates the 8800SX **Ultrasonics** and provisions for RTI's Optional **SurfaceMap** System, **3D Cameras** and other options technologies.

- Faster
- More accurate
- More integrated
- More smart
- More capacity

Today, RTI's 8800SX is 65,536 samples per frame.

KEY FEATURES

The limbs of the System

Smart Track Test Carriage on a 4WD Hi Rail

Smart Track Test Carriage on trolley for Rail bound vehicle

Typical test carriage holds two Roller Search Units (RSU's) with a total of 22 transducers (system can take up to 32 channels).

Gauge Tracking System

Maintaining gauge is controlled by RTI's pneumatic gauge rollers.

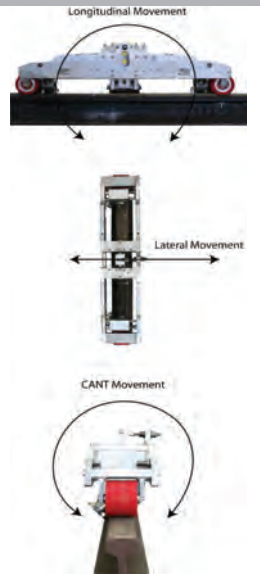

Composition of the RFDV

8800 Subrack

PLC system

Probes

RFDV

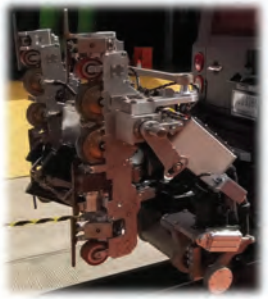

Mechanical system

Software and GUI

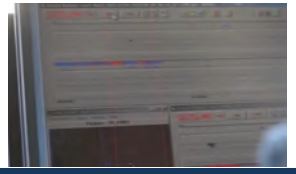

How we test

The GUI that the operator views

Ultrasonic Testing

Rail Technology International

- A and B Scan

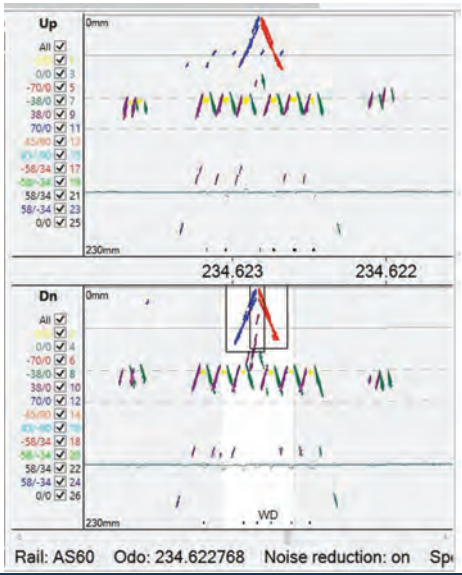

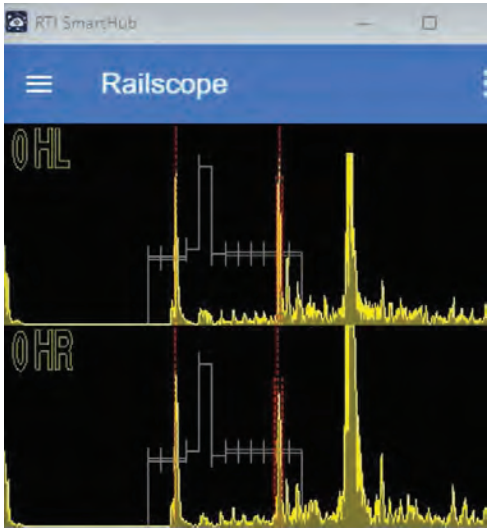

KEY FEATURES

Rail Technology International

Probe Wheel configuration

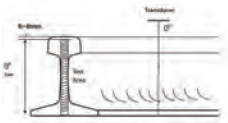
Figure 1 - Scanning Area 0° Type Probe

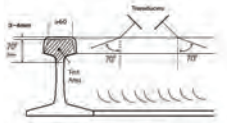
Figure 2 - Scanning Area 70° Type Probe

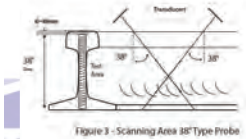
Figure 3 - Scanning Area 38° Type Probe

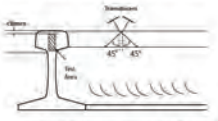
Figure 4 - Scanning Area VSH 45° Type Probe

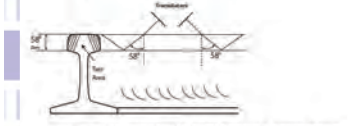
Figure 5 - Scanning Area 58° RHOM Type Probe

Each carriage side mounts two probe wheels containing up to 16 channels (32 in total - can be optioned with more channels if required).

Configuration:

- 0° probes cover the centre section of the rail head, web and foot to detect horizontal split head and rail height.
- 38° probes cover the centre section of the rail head, the web and the centre section of the foot to detect transverse defects, bolt-hole cracks and weld defects.
- 70° probes cover the rail head to detect transverse defects, some surface defects and weld defects. Brush type is used.
- 45° probes cover the part of the rail head to detect vertical split head.
- ROM probes cover the gauge and field corners to detect defects at the corners using second reflections.

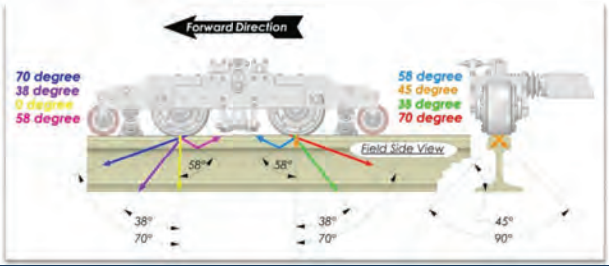

Ultrasonic Testing

Rail Technology International

- Real Time Analysis -- (Hunter)

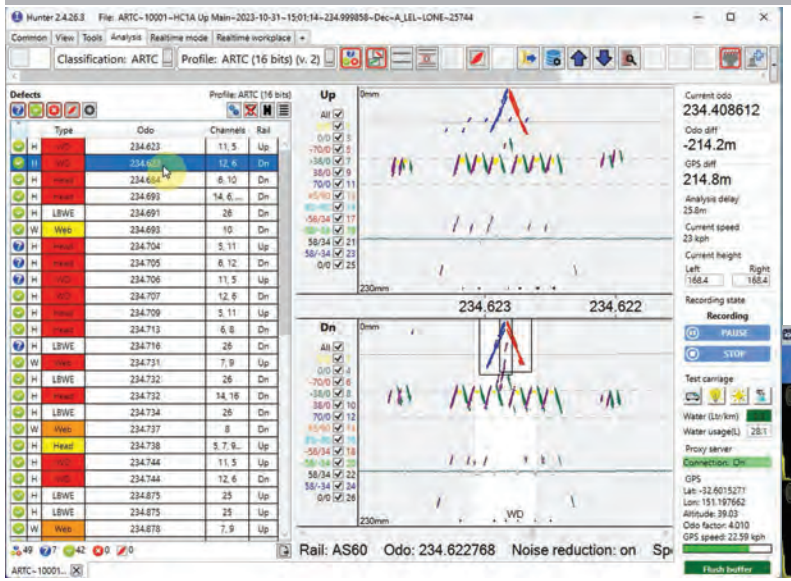

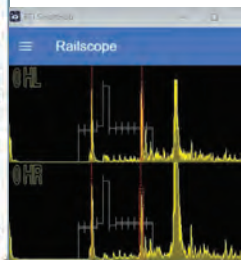

SmartCal

Rail Technology International

The SmartCal system is exclusive to RTI and contributes significantly to both high productivity and high precision of the 8800SX system.

SmartCal™

SmartCal was first introduced in our 8000SX system there was a significant change in detection repeatability and for the first time RTI saw consistently collected data results from survey to survey across operators.

The use of SmartCal into the 8800SX makes it possible to have absolute reference for each channel and for each position of depth by monitoring grain levels at different depths. SmartCal adjusts the Depth Gains (Time Gains) individually for every channel with up to 32 individual gain points per channel.

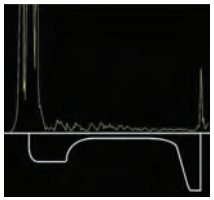
0 Degree no SmartCal

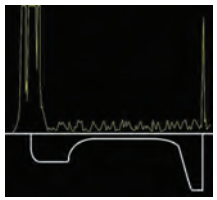
0 Degree with SmartCal

The Benefits of SmartCal™

- **Remove subjectivity of operator**
- **Uniform signal response over the entire height of the rail (compensates for signal attenuation over distance travelled and in rail)**
- **Compensates for signal attenuation to improve detection of TDs under RCF**
- **Transducer gain drift caused by temperature variations is completely eliminated**
- **Fully compensates for non-linearity between transducers**

Detection capabilities TD 13mm

Rail Technology International

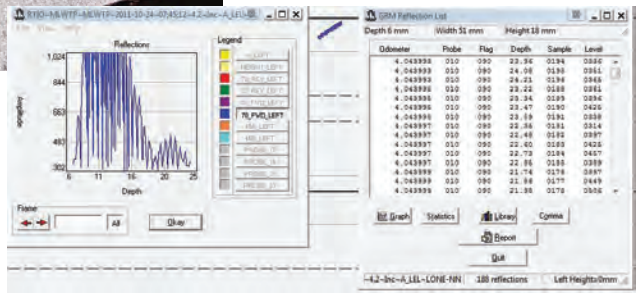

Detection capabilities VSH 3mm long

Rail Technology International

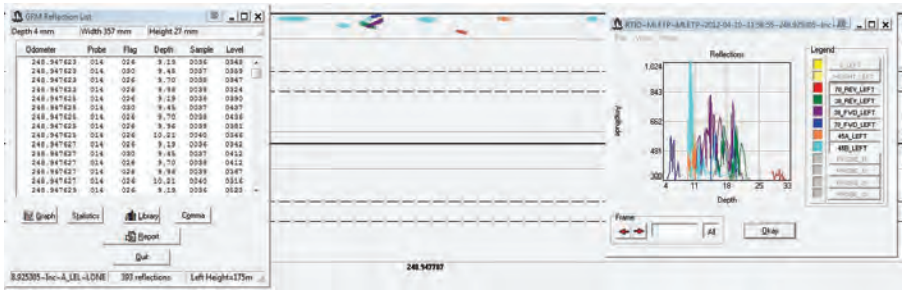

Detection capabilities UHR 4mm

Rail Technology International

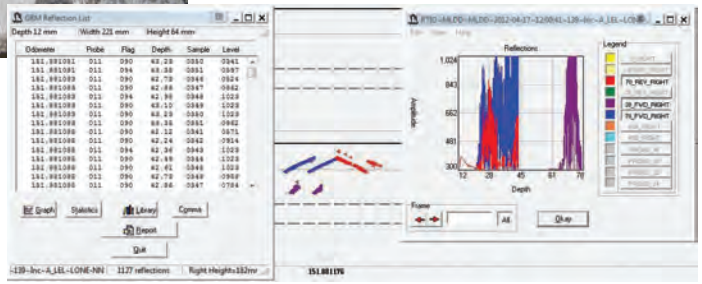

Detection capabilities HSW 135mm

Rail Technology International

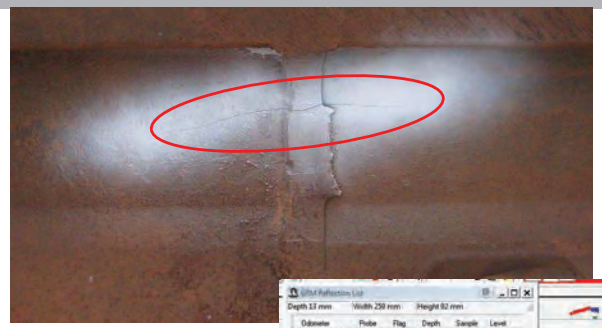

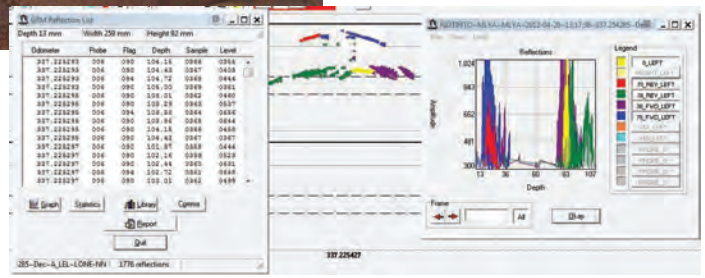

Detection capabilities UHR 3mm

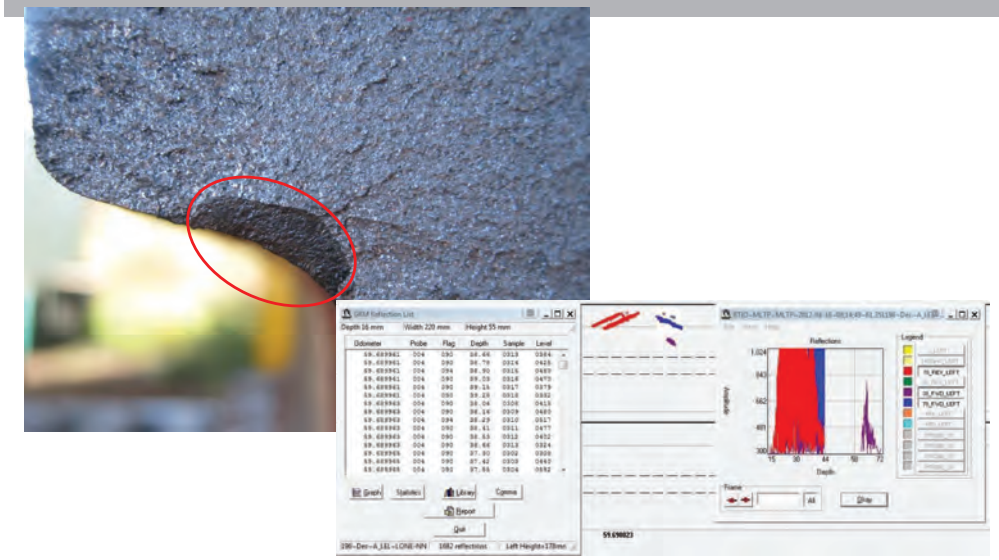

Detection capabilities DW 5mm

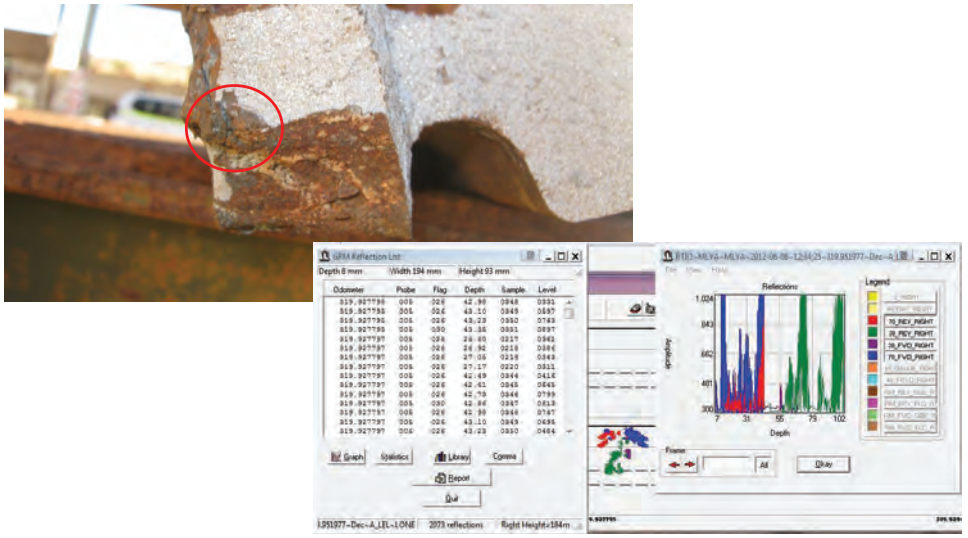

Detection capabilities TD 5mm

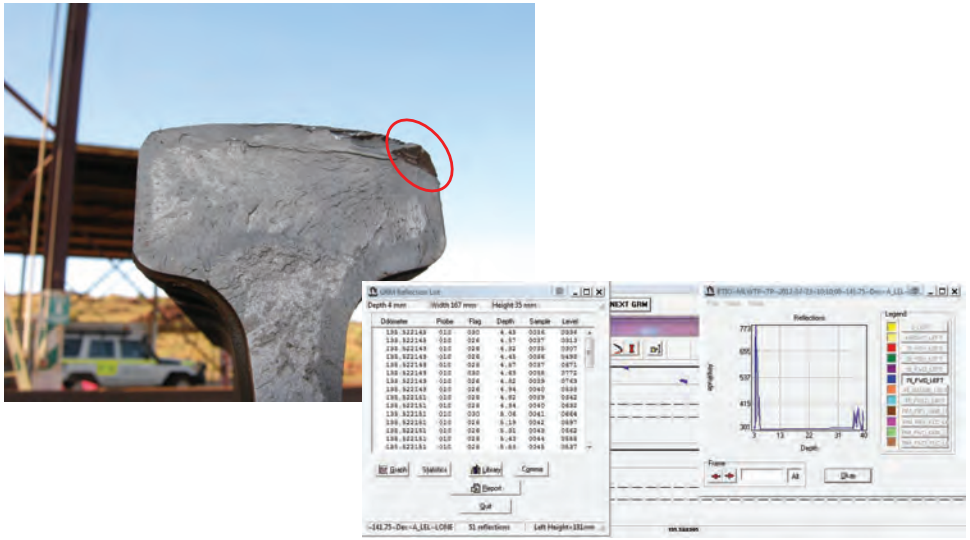

Detection capabilities BHC 6mm

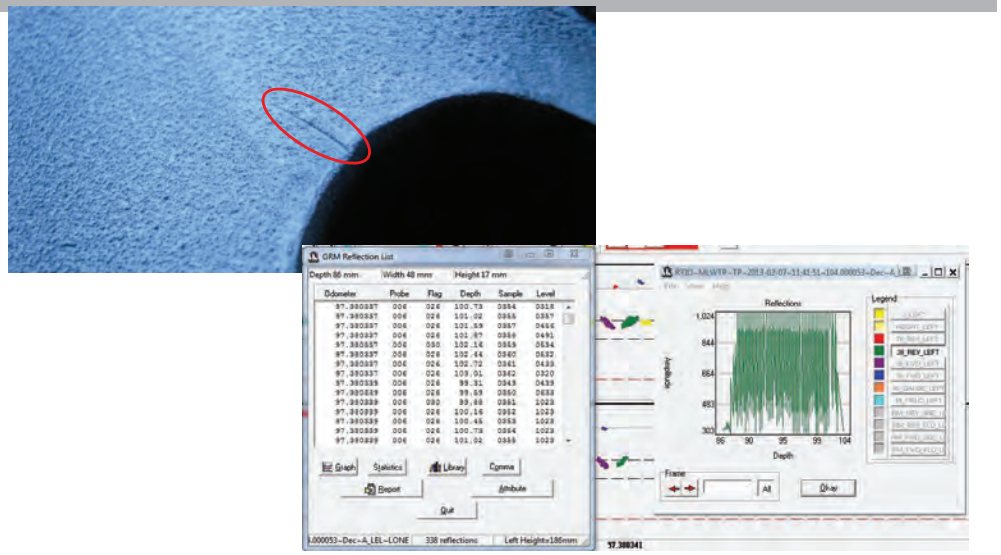

Surface Condition

Rail Technology International

- Surfacemap – (Eddy View)

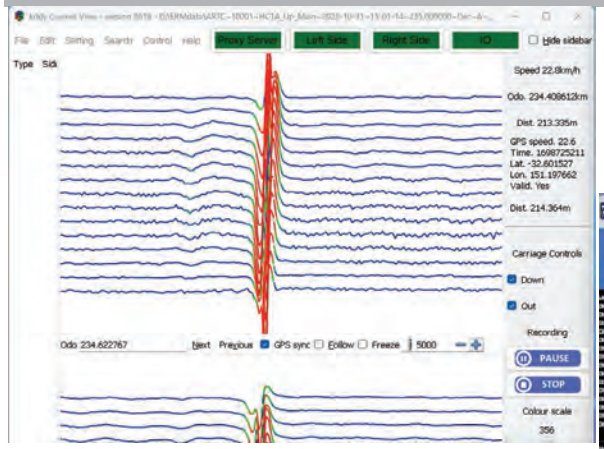

Eddyview

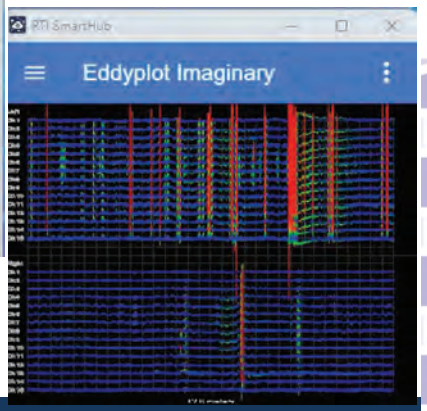

Surface Map Data is mainly for Post analysis

Surface Map - Probe

Rail Technology International

RCF

Rail Technology International

SurfaceMap Detection Capabilities

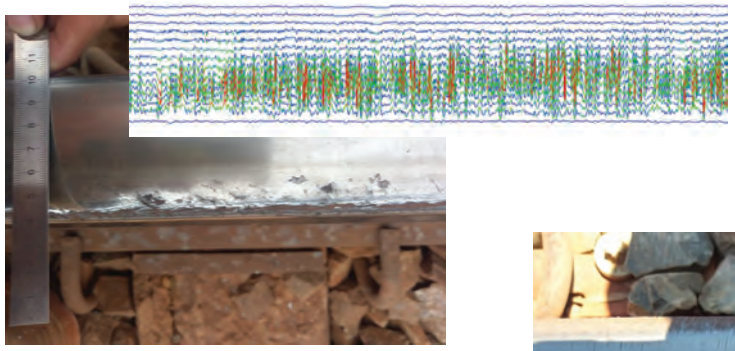

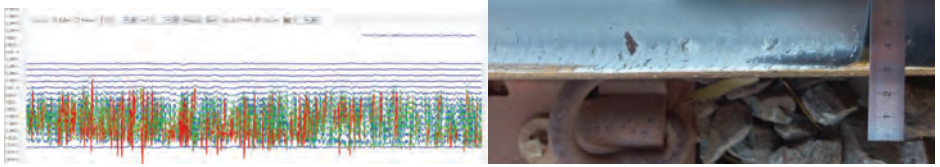

Squats

Rail Technology International

SurfaceMap Detection Capabilities

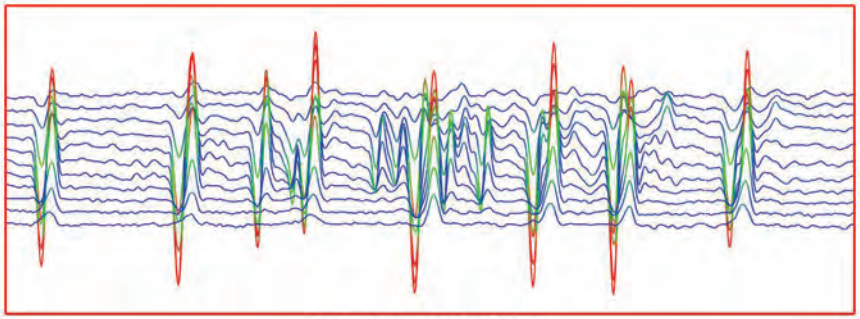

Squats as seen in EddyView

Squats as seen in field on the rail

Engine burns

SurfaceMap Detection Capabilities

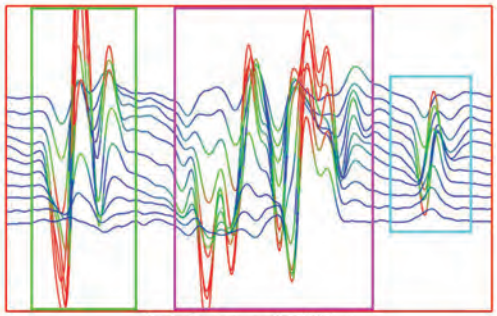

Engine burn as seen in EddyView

Engine burn as seen in field

Repeatability

SurfaceMap Detection Capabilities

Data tested from two different runs (Sample is an Engine Burn)

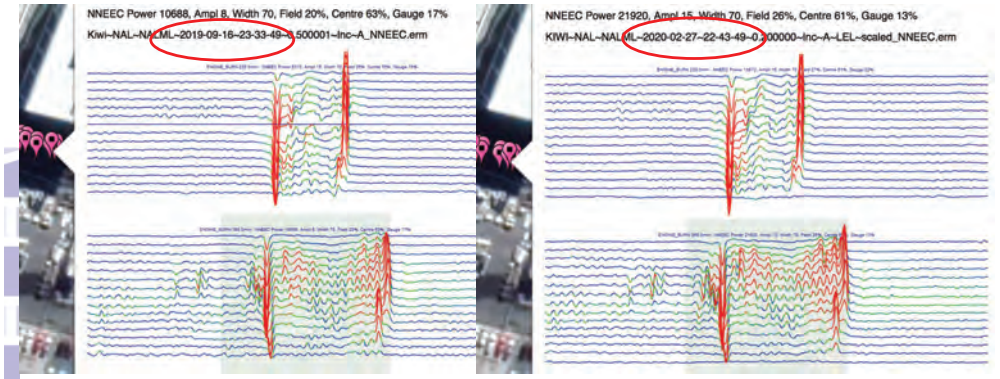

3D image

- Scanning Camara view

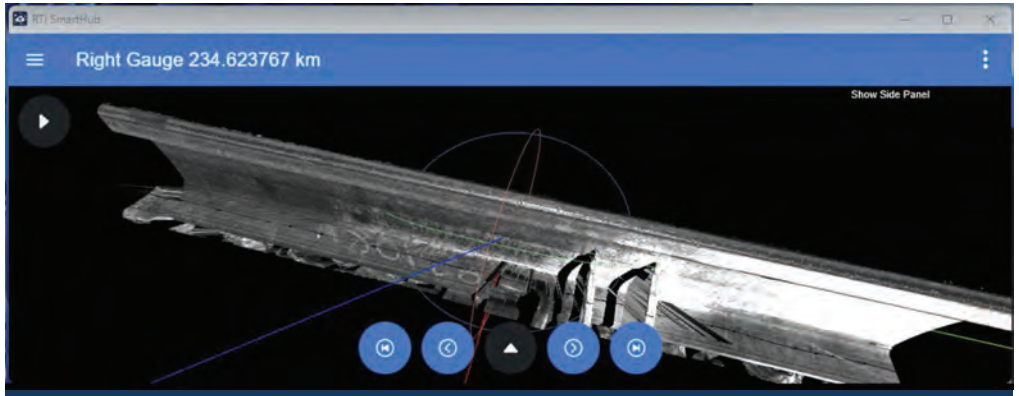

Other Track Info

- Map and Previous Defect info

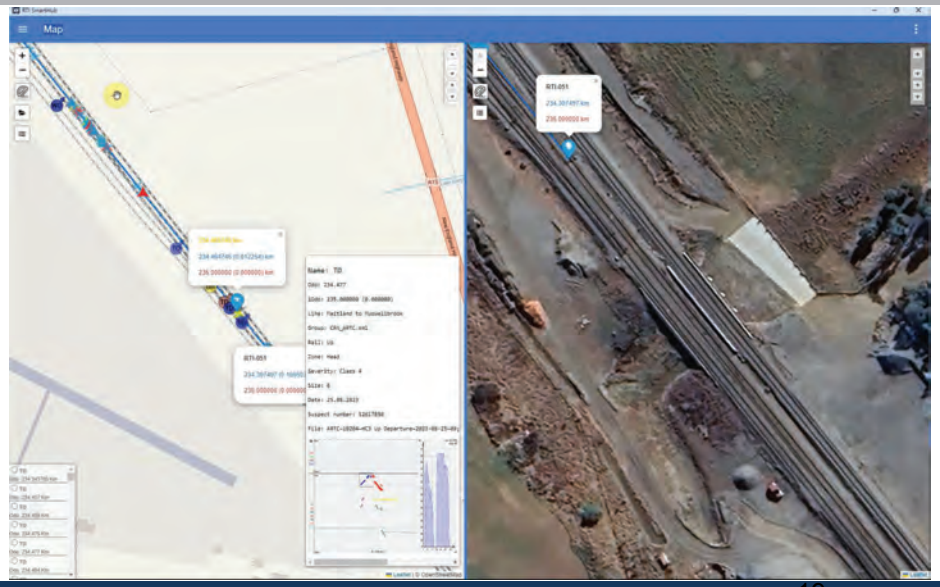

System health info

- System Health Status

Shift reporting

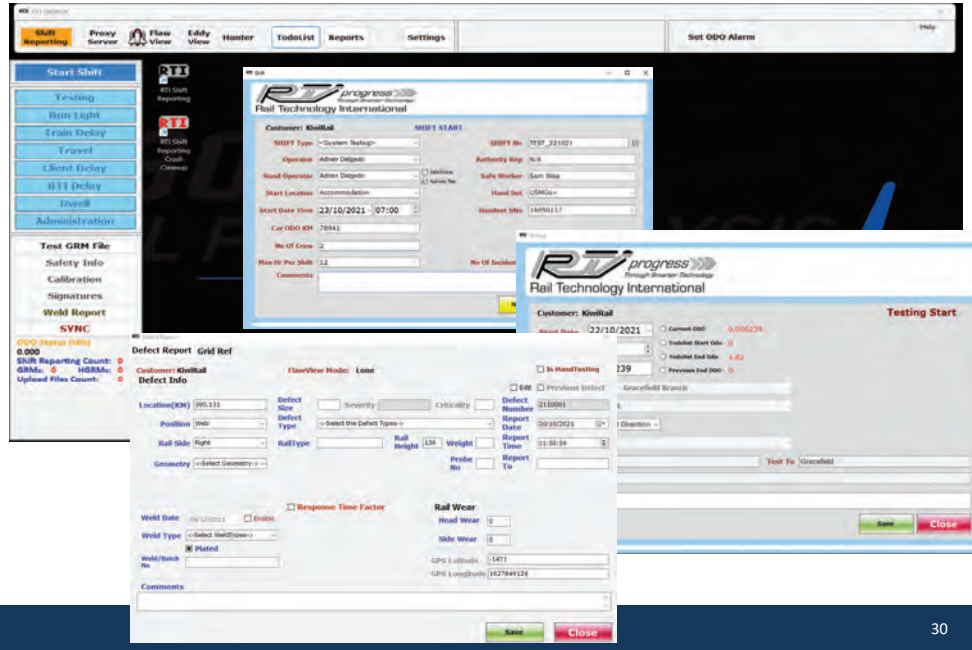

Integrated view

The GUI that the operator views

RTI Vehicles

Rail Road vehicles

Case Study

ThaiRung HiRail 1000mm Gauge Rail Flaw Detection Vehicle – 2020-2021

ARMTECH

progress Through Smarter Technology
Rail Technology International

Scope

progress Through Smarter Technology
Rail Technology International

- RFD system built onto customer supplied vehicle

Vehicle information:
ThaiRung Transformer

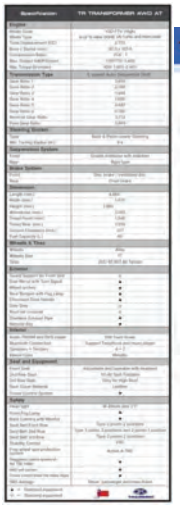

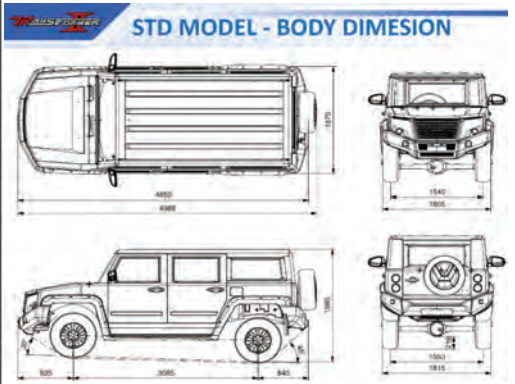

Cooperation plan (before the commencement)

progress Through Smarter Technology
Rail Technology International

8800 RFD electronics and auxiliary control system

Antennas fitted over the roof

Test carriage and lifting mechanism

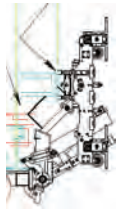

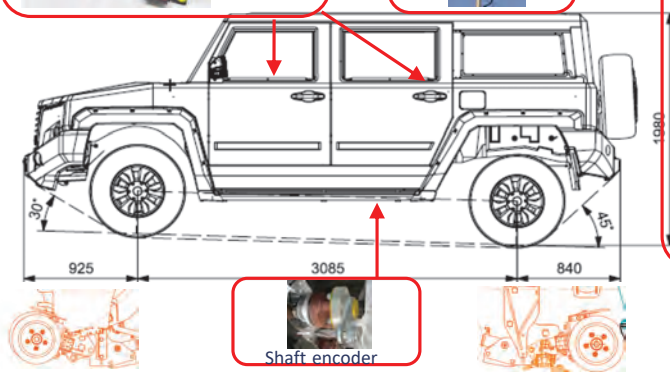

Supplied by

* Water (couplant) Tank is to be placed both side of the vehicle at door step

Hi-Rail vehicle supplied by customer

progress Through Smarter Technology
Rail Technology International

The major vehicle modification RTI expect ArmTech to do associated with the 1000mm gauge track Hi Rail application

- Rear axle modification

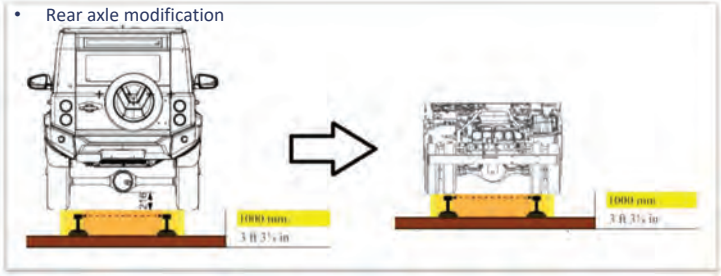

- A front axle locking system designed fabricated and installed. This feature is to ensure the front rubber wheels are clear from the rail height, which is to avoid the wheels be touching any infrastructure at the rail height level, e.g. level crossing.
- Modification made by Armtech shall be in compliance to Thailand regulations for both Rail and Road use.

Progress

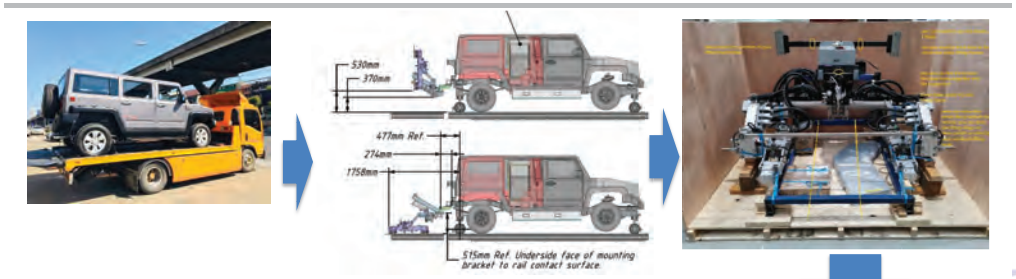

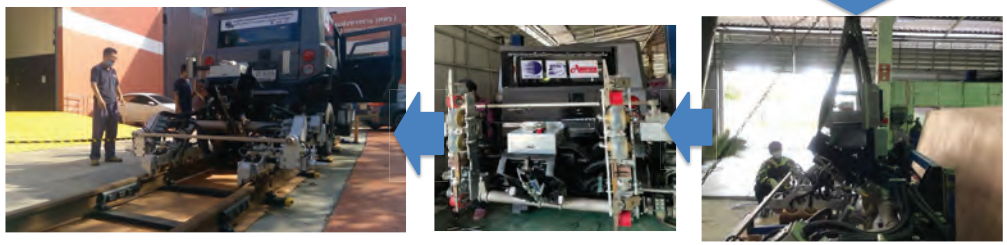

Completed in end of 2021

joonhwan.lee@wipco.co.kr

Vehicle operation

“When safety is paramount”

www.rti-group.com

Monitoring inspection system by Dr. Hafnee Lateh

ศูนย์ทดสอบมาตรฐานระบบขนส่งทางราง (ศทร.)
Railway Transportation System Testing Center (RTTC)

Inspection and Monitoring System

Present by Dr.Hafnee Lateh

ศูนย์ทดสอบมาตรฐานระบบขนส่งทางราง (ศทร.)
Railway Transportation System Testing Center (RTTC)

Introduction

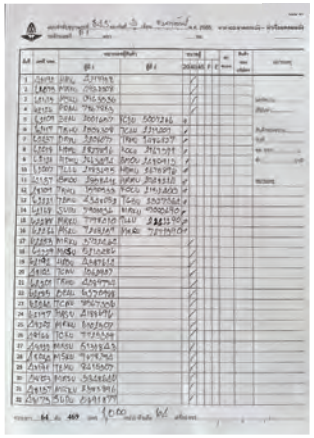

Manual Record

OVERLOAD

ศูนย์ทดสอบมาตรฐานระบบขนส่งทางราง (ศทร.)
Railway Transportation System Testing Center (RTTC)

Inspection and Monitoring System

ศูนย์ทดสอบมาตรฐานระบบขนส่งทางราง (ศทร.)
Railway Transportation System Testing Center (RTTC)

IDENT and RAWLOC systems installation

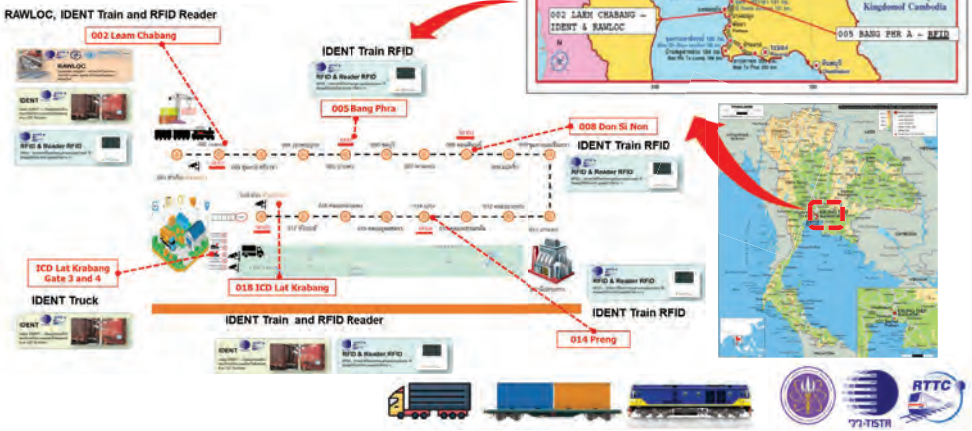

Overview of the systems and functions

The installation consists of the listed systems and the following functions:

I.	RAWLOC	In motion weighing of the wheel loads system installed to the line by welding.
II.	IDENT Thai number recognition	Pictures for wagon number.
III.	IDENT RFID	Locomotive number by RFID tag (2 tags per loc.) by side reader.
IV.	IDENT BIC	Pictures and container number. (single stacked, two container per wagon).
I.	IDENT Inspection	Pictures of wagons/trucks for inspection (left/right side)

ศูนย์ทดสอบมาตรฐานระบบขนส่งทางราง (ศทร.)
Railway Transportation System Testing Center (RTTC)

RAWLOC and IDENT at 002 Laem Chabang Station




- These systems refer to the combined system RAWLOC and IDENT – In Motion Weighing and Wagon/Container Identification system – installed in Leam Chabang, Thailand.
- The system consist of a pair of measurement rails, cameras, LED lightings, RFID-Readers and Wheel sensors which are installed in or near a railway line and used to monitoring the passing trains

ศูนย์ทดสอบมาตรฐานระบบขนส่งทางราง (ศทร.)
Railway Transportation System Testing Center (RTTC)

RAWLOC and IDENT at 002 Laem Chabang Station : Installation

ศูนย์ทดสอบมาตรฐานระบบขนส่งทางราง (ศทร.)
Railway Transportation System Testing Center (RTTC)

RAWLOC : Railway Wheel Load Control

- Dynamic train monitoring to detect unbalanced and overloaded rail cars and wheels impact and imperfection.
- The train monitoring system consists basically of two measuring rails.
- Each rail with four weighing sensors and one temperature sensor.
- The system includes a HBM measuring amplifier and an evaluation PC on which the software rawloc.exe runs.
- The two measuring rails with a length of 11.4 m (± 3 mm) correspond to different rails profiles.
- The measuring rails are primed with color. The rails are welded into the existing track.

IDENT - Wagon identification by UIC/Thai Number Recognition

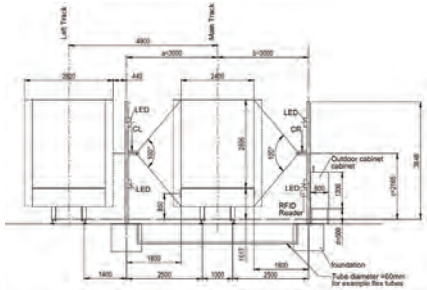

System components IDENT BIC/Thai Wagon number IDENT RFID and IDENT inspection

1 High sensitive fast daylight camera for UIC number detection an inspection left/right
2 LED flash illumination for night process
3 Electric cabinet
4 Wheel sensor for train recognition
5 Radar sensor for system wake-up
6 RFID Reader

- The train's passage is recorded by illuminated cameras from both sides. The recorded pictures are processed by a sophisticated software.
- The train is detected in all its parts and the wagons are separated.
- The UIC numbers of each one are detected and assigned, as an alternative the RFID numbers will be assigned.
- IDENT is a powerful monitoring system designed specifically for railways, logistic hubs, seaports and industries.

IDENT Train RFID at 005 Bang Phra Station, 008 Don Si Non Station and 014 Preng Station

IDENT - Wagon identification by Radio-frequency RFID

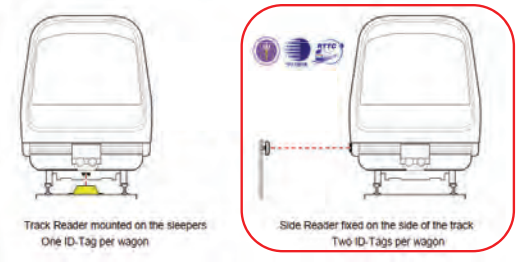

- Wagon identification by RFID to automatic ad the wagon number to the weighing data.
- Depending on the application and type of wagon, the reader is fixed on the sleepers or on the side of the track.
- The Heavy Duty ID-Tags are extremely resistant, totally encapsulated and maintenance free.

IDENT Train at 018 ICD Lad Krabang Station

IDENT Truck at 019 ICD Lad Krabang Gate 3

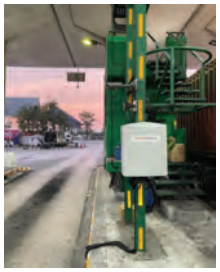

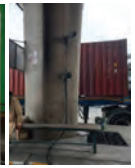

IDENT Truck at 020 ICD Lad Krabang Gate 4

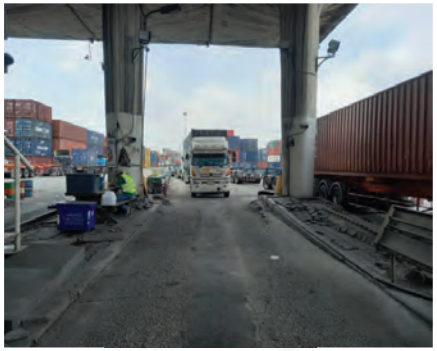

IDENT - Truck inspection station

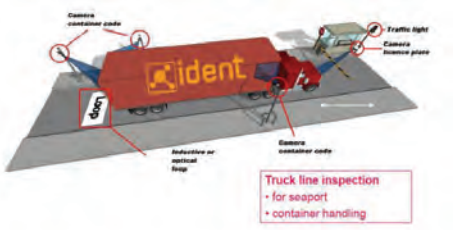

- The trucks and containers are identified and inspected at the exit/entrance of the yard, out put pictures, container number and plate number.
- The truck is recorded by illuminated cameras from both sides. The recorded pictures are processed by a sophisticated software.

- Station Overview -

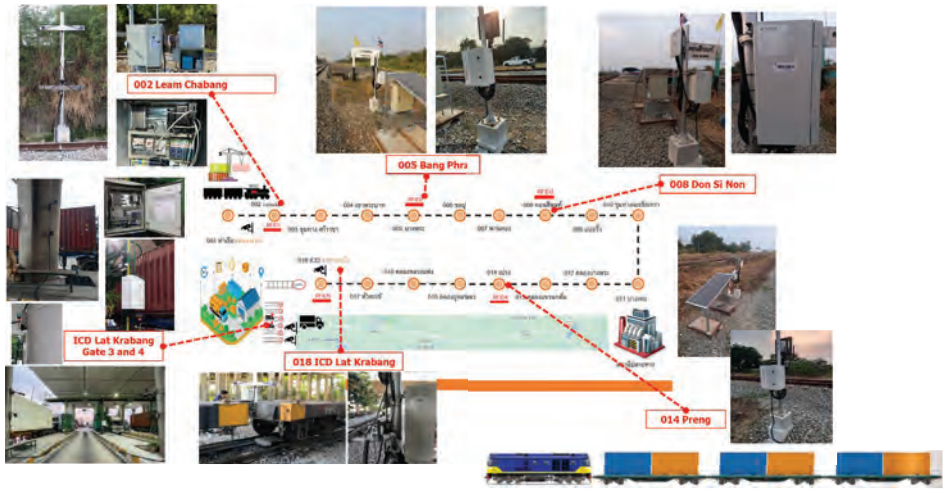

ID. No. of THAI Bogie Container Flat Wagon (B.C.F.) SYSTEM

บทค : โบกี้บรรทุกตู้สินค้า (Thai V.)
B.C.F : Bogie Container Flat Wagon (Eng. V.)

62 : Max. Load = 62 Ton
022 : No. of B.C.F

SRT: The State Railway of Thailand

Yellow Star : This train can run with max at 70 km/hr.

Yellow line: The center point of BCF

ศูนย์ทดสอบมาตรฐานระบบขนส่งทางราง (ศทร.)
Railway Transportation System Testing Center (RTTC)

The Container Numbers

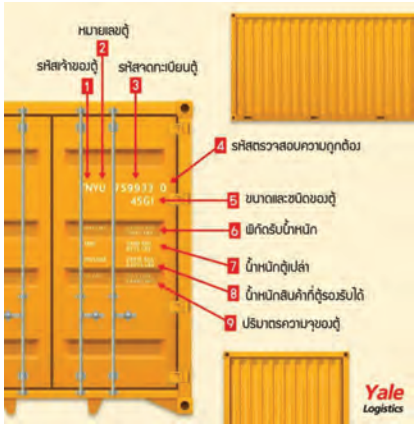

1. Owner prefix code: เป็นอักษรแทนชื่อบริษัทเจ้าของตู้ เช่น TNYU, CMAU, EGSU และ TCLU
2. Equipment Category Identifier (ECI) : จะมีเพียง 1 ตัวที่อยู่ท้ายอักษรรหัสเจ้าของตู้ จากรูปภาพคือตัวอักษร U มีความหมายคือ ตู้คอนเทนเนอร์
3. Serial Number of container: มีระบุอยู่ 6 ตัว จากตัวอย่างคือ 759933
4. Check Digit : A check digit is a single-digit number that is used to verify the authenticity of a container's identification number. The check digit can be found after the container's serial number.
5. ISO Code The container's type and dimensions. The first character of the ISO code denotes the length of the unit, and the second character indicates the height. The third and fourth characters determine the container type. Ex. 45G1
• เลข 4 ตัวแรก คือ ความยาวเท่ากับ 40 ฟุต
•เลข 5 ตัวถัด คือ ความสูงเท่ากับ 9 ฟุต 6 นิ้ว
• G1 คือ ตู้คอนเทนเนอร์ที่บรรจุสินค้าทั่วไป
6. MAX. GROSS : น้ำหนักของตู้คอนเทนเนอร์เปล่ารวมกับน้ำหนักของสินค้าที่ตู้คอนเทนเนอร์สามารถรับได้สูงสุด อาจจะแสดงข้อความ MAX. GROSS WGT., MX GR, MAX.GR. และ MAX.WT.
7. TARE : น้ำหนักของตู้เปล่า ที่ยังไม่ได้บรรจุสินค้าลงไป
8 .Net Weight: โดยอาจเขียนว่า N.W., NET WEIGHT, MAX CARGO WGT และ PAYLOAD หมายถึง น้ำหนักของสินค้าสูงสุดที่สามารถบรรจุใส่ตู้คอนเทนเนอร์นั่นได้
9. CUBE หรือ CU CAP.

https://yalelogistics.co.th/%E0%B8%8A%E0%B8%B4%E0%B8%99%E0%B8%9B%E0%B8%B4%E0%B9%89%E0%B8%A7-%E0%B9%84%E0%B8%82%E0%B8%A3%E0%B8%A8%E0%B8%B1%E0%B8%AA-%E0%B8%AA%E0%B8%A1%E0%B8%B2%E0%B8%A2%E0%B8%80%E0%B8%A5%E0%B8%82%E0%B8%95%E0%B8%89/

ศูนย์ทดสอบมาตรฐานระบบขนส่งทางราง (ศทร.)
Railway Transportation System Testing Center (RTTC)

The outputs from monitoring systems

I.	RAWLOC	In motion weighing of the wheel loads, output 5.6t, 5.4t,etc., system installed to the line by welding.
II.	IDENT Thai number recognition	Pictures for wagon number, output 62022.
III.	IDENT RFID	Locomotive number by RFID tag (2 tags per loc.) by side reader, output 006
IV.	IDENT BIC	Pictures and container number, output TCLU 759933 45G1 (single stacked, two container per wagon).
V.	IDENT Inspection	Pictures of wagons/trucks for inspection (left/right side)

ศูนย์ทดสอบมาตรฐานระบบขนส่งทางราง (ศทร.)
Railway Transportation System Testing Center (RTTC)

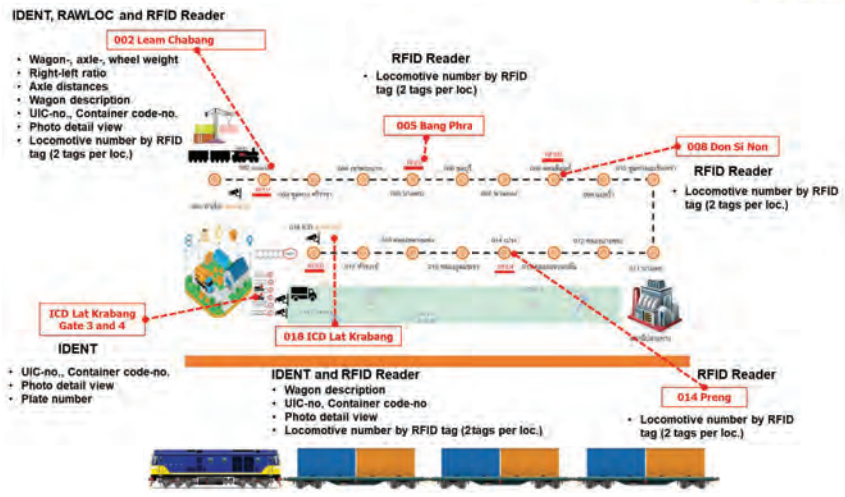

RAWLOC Software

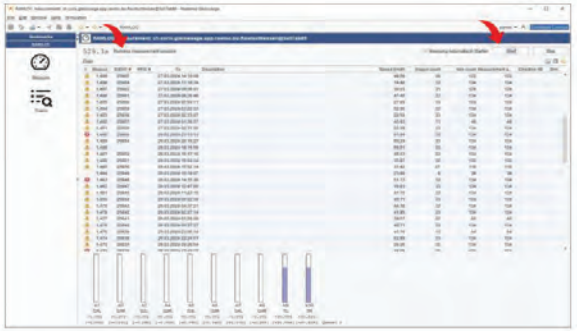

Start measurement and the time of the running session appears

RAWLOC Software

Sheet Measure: Overview of trains

1. Start/stop measurement, flag: start measurement automatically
2. Warnings/Problems Vehicle Condition
3. Measure no.
4. IDENT no.
5. Timestamp
6. Medium speed
7. Number of wagons
8. Number of axles
9. Click for measurement results
10. Measure: Overview of trains
11. Trains: Overview of trains, wagons, axles, wheels
12. Measurements sensors

RAWLOC Software

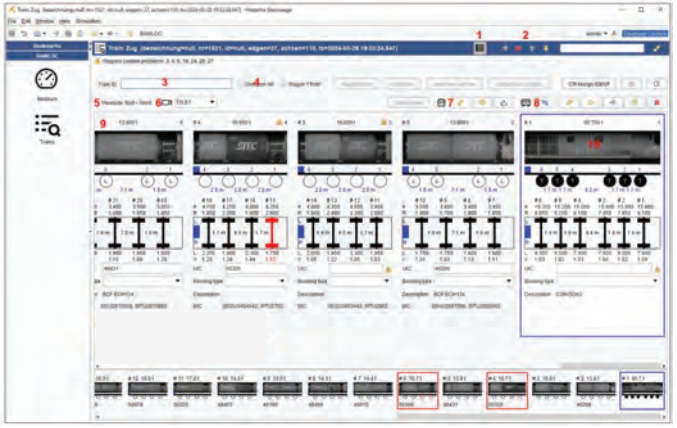

Sheet Measure: Measurement results

1. Tabular view
2. Change between measurements forward/backward, add/delete
3. Define train ID
4. Direction A⟶ B, B⟶ A
5. Point of view A-B or B-A
6. Change camera or pictogram wagon
7. Turn train, add train
8. Turn wagon, move, delete or add wagon
9. Results:
   - Wagon-, axle-, wheel weight
   - Right-left ratio
   - Axle distances
   - Measurement order
   - Wagon description
   - UIC-no., Container code-no.
10. Click on photo for details

RAWLOC Software

Sheet measure: Measurement results: Photo detail view

For full size click on the desired image:

1. Drawing wagon type
2. Photo detected UIC no. with best confidence
3. Photo detected container no. with best confidence
4. Panoramic photo left/right

RAWLOC Software

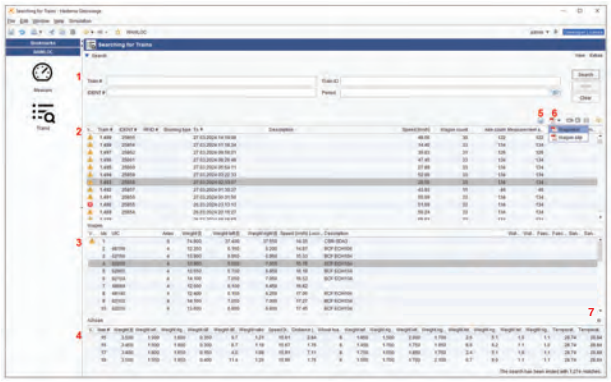

Sheet trains: Overview trains

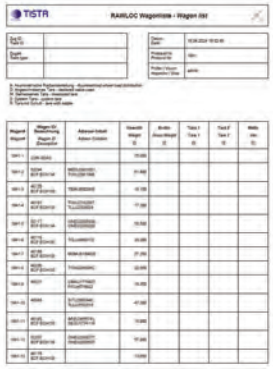

Example Wagon list

1. Search fields, 2. Train-list, 3. Wagon-list, 4. Axle-list, 5. XML-File export, 6. Print PDF wagon-list/wagon- slip and 7. Wheel analysis

IDENT Software

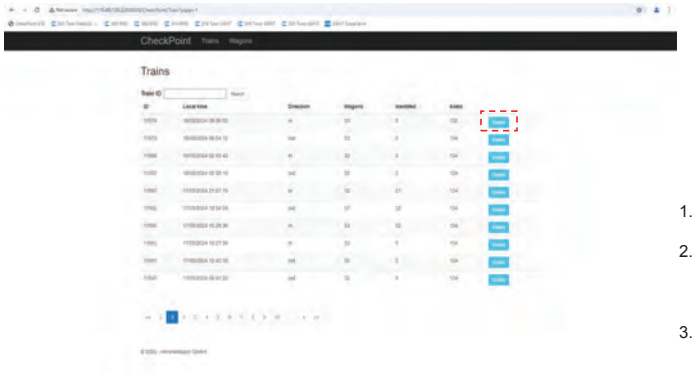

IDENT Checkpoint

The IDENT Checkpoint provides an overview in tabular form and by pictures/video of the identified recorded trains. The same data can be saved and used on a server in the cloud.

1. Select between train or wagon view.
2. Table shows ID (consecutive numbering of the cars), direction, BIC-Number, and time date of the measurement.
3. Details shows the panorama pictures and videos of the wagon

IDENT Software

IDENT Software

IDENT Video server

The Luxuriot Video Server Monitor is used to manage all the pictures and videos recorded by the IDENT cameras

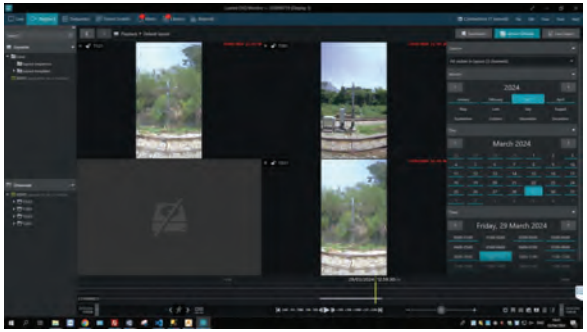

Luxuriot Video Server Monitor

1. Live/Playback view
2. Views of the different cameras, double click for zoom
3. Library of your exported data
4. Archive Calendar
5. Archive Calendar select year/month/day/time
6. Navigate in the video stream
7. Export picture/video

IDENT Software

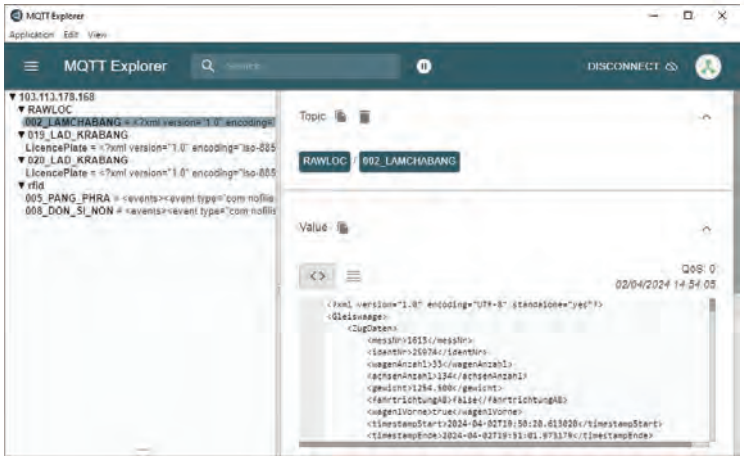

Shows XML by the MQTT Explorer

Ex: XML by the MQTT Explorer

```
<Gleiswaage>
<TrainData>
<MeasurmentNo>2156</MeasurmentNo>
<WagonCount>33</WagonCount>
<AxleCount>134</AxleCount>
<Weight>938.900</Weight>
<DirectionAB>false</DirectionAB>
<Wagon1Front>true</Wagon1Front>
<TsStart>2024-05-17T16:23:16.069614</TsStart>
<TsEnd>2024-05-17T16:24:32.803077</TsEnd>
</TrainData>
<WagonData>
<Wagon>
<WagonNo>1</WagonNo>
<Description>CSR-SDA3</Description>
<Aligment>true</Aligment>
<Locomotive>true</Locomotive>
<AxleCount>6</AxleCount>
<Weight>74.450</Weight>
<WeightLeft>36.850</WeightLeft>
<WeightRight>37.600</WeightRight>
<Speed>21.66</Speed>
</Wagon>
<Wagon>
<WagonNo>2</WagonNo>
<Description>BCF ECH134</Description>
<Aligment>true</Aligment>
<Locomotive>false</Locomotive>
<AxleCount>4</AxleCount>
<Weight>36.550</Weight>
<WeightLeft>17.550</WeightLeft>
<WeightRight>19.000</WeightRight>
<Speed>21.76</Speed>
</Wagon>
<Wagon>
<WagonNo>3</WagonNo>
<Description>BCF ECH134</Description>
<Aligment>true</Aligment>
<Locomotive>false</Locomotive>
<AxleCount>4</AxleCount>
<Weight>37.500</Weight>
<WeightLeft>18.800</WeightLeft>
<WeightRight>18.700</WeightRight>
<Speed>21.83</Speed>
```

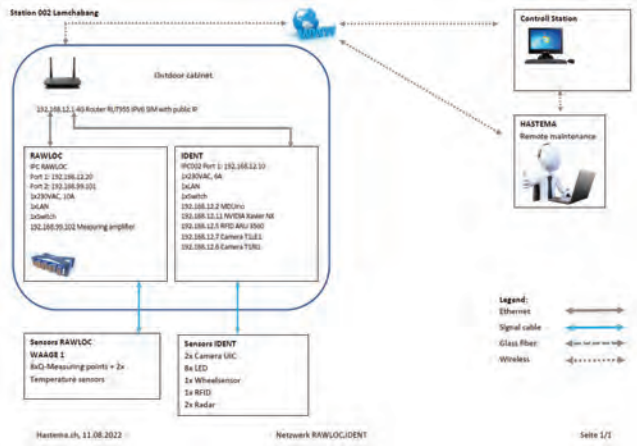

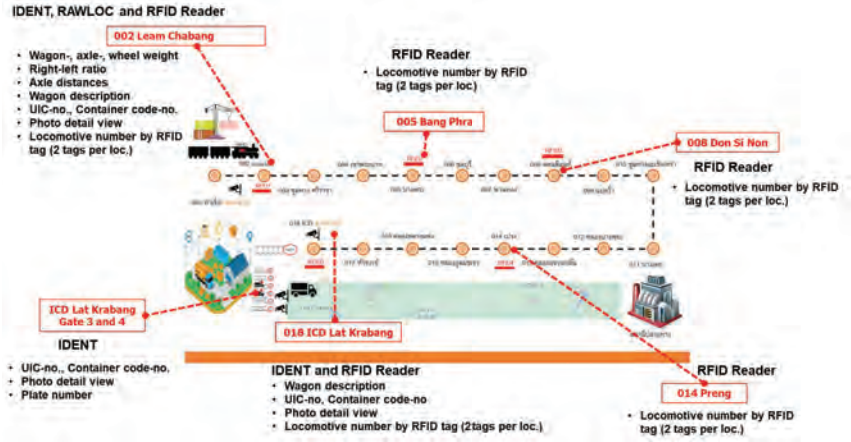

ศูนย์ทดสอบมาตรฐานระบบขนส่งทางราง (ศทร.)
Railway Transportation System Testing Center (RTTC)

Thank you for your attention

Terima Kasih

ຂອບໃຈເດີ

Implementing of metrology for safety and quality of rail transit by Dr. Sivinee Sawatdiaree

Metrology for Safety & Quality of Railway

Technical Cooperation for Research and Development and Implementation of Railway Inspection and Monitoring Technology – 10 June 2024

Sivinee Sawatdiaree, Dr. rer. nat.
National Institute of Metrology (Thailand)

Metrology in Thailand

Scientific Metrology
- National Metrology System Development Act BE 2540 (1997)
- National Institute of Metrology (Thailand), NMT
  Ministry of Higher Education, Science, Research and Innovation

Legal Metrology
- Weights and Measures Act BE 2466 (1923)
- Central Bureau of Weights and Measures
  Ministry of Commerce

National Metrology System Development Act BE 2540 (1997) & BE 2559 (2016)

- Autonomous institution under Ministry of Higher Education, Science, Research and Innovation
- Designated national highest authority in scientific metrology

Governance and Mission of NMT

- National Metrology System Development Act
- National Metrology Committee
  Chair: Minister of MHESI
  Secretary: Director of NMT
- National Metrology System Development Action Plan
  Prepared and Proposed by National Metrology Committee
  Approved by the Cabinet
- National Institute of Metrology (Thailand)

Mission of NMT

- Develop National Metrology System
  - Establish and maintain National Measurement Standards that are traceable to the SI and disseminate metrological traceability to users
  - Support and engage with calibration laboratories in building their calibration and measurement capability and network
  - Promote metrology professional
- Facilitate and cooperate with other organisations to develop the National Quality Infrastructure
- Develop metrological know-how and technology relevant to national needs

National Quality Infrastructure (NQI)

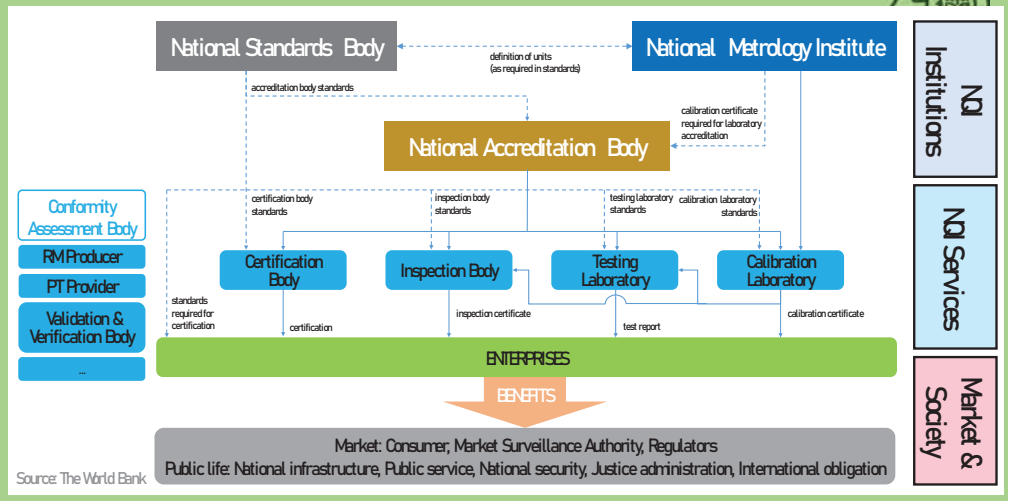

Source: The World Bank

National Institute of Metrology (Thailand)

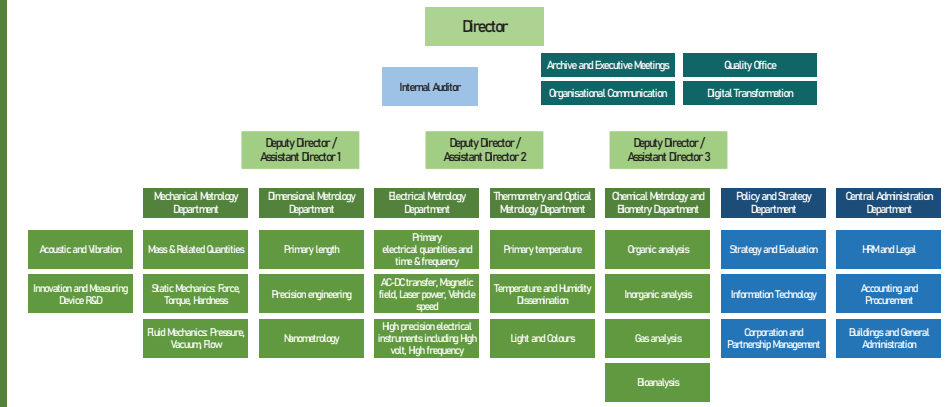

Metrological traceability

NMT Future Mobility Vision

- Metrological traceability for National Rail Infrastructure Plan
  - New facility
  - New measurement standards
- Metrological traceability for Electric Vehicle
  - Metrology roadmap: prioritised safety regulations
  - Measurement standards: supporting EVSE, parts manufacturing
- Metrological traceability for Autonomous Vehicle

Components of Railway System

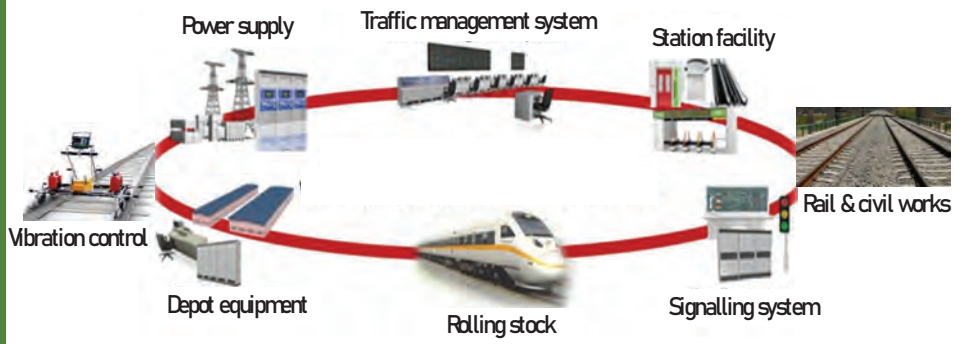

Measurement standards for Railway system

- 10 MN Force measurement standard (hydraulic)
- 40 m standard track for survey equipment
- Reference Wall for laser tracker calibration
- Very low frequency vibration measurement standard
- High frequency facility and measurement standards for 5G & EMC measurement, and antenna & electric field probe calibration
- Time dissemination system for sub microsecond accuracy

Measurement standards for Railway system

- Straightness measurement standard
- Perpendicular measurement standard
- Measurement standards for Contour Measuring Machine calibration
- Illuminance responsivity measurement standards
- Surface colour measurement standards
- Temperature and humidity measurement standards

New facility

- Force: 10 MN
- Dimension: 40 m & Reference Wall
- High frequency: EMC, 5G, E field
- Very low frequency vibration
- Time dissemination

New facility: 10 MN Force

40 m standard track and CMM

Reference wall for laser tracker calibration

Very low frequency vibration measurement system

Electrical measurement standards for railway

Navigation & Communication

- EMC & EMI and antenna
- GSM-R and Telecommunication Protocol of Railway Signalling

New facility: Hgh frequency & EMC

HF Open area test site

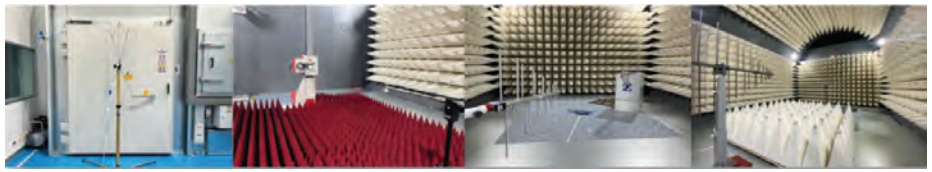

5G

5G base station and Compact Antenna Test Range (CATR)

- NTP Capacity: 17.3B sync/day
- NTP and PTP
- 1 Cs redundancy
- GPS anti-jamming systems
- NTP status via Grafana

NTP server room

Time and Frequency laboratory

Standard time UTC(NMT) dissemination: sub millisecond, sub micro second, sub nanosecond

Caesium beam atomic clock and Hydrogen Maser

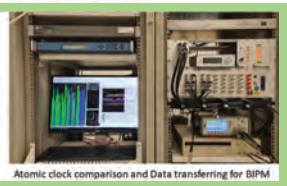

Atomic clock comparison and Data transferring for BIPM

HF EMC Frequency Summary (Typical)

• Conducted Emission	9 kHz – 30 MHz
• Power Line Disturbance	30 MHz – 300 MHz
• Radiated Emission (1 GHz/6 GHz/18 GHz/40 GHz)	30 MHz – 1 GHz
• Conducted Immunity (230 MHz)	150 kHz – 80 MHz
• Radiated Immunity (6 GHz/18 GHz/40 GHz)	80 MHz – 1 GHz

Wide Band Radio Communication Tester

- Wide Band Communication for railway systems
- Multi-RAT signalling: LTE, WCDMA, GSM, WLAN, Bluetooth
- LTE-Advanced: 8DL CC up to 4x4/8x2 MIMO fading, 2 UL CA
- WLAN11 a / b / g / n / ac / ax SISO and MIMO signalling test
- Internal server for application testing

Universal Calibration System (UCS)

On-going project

Energy storage & Power grid

- Electric power measurement standard
- Electric power quality measurement standard
- Electric energy meter calibration
- Smart grid, smart meter

Electrical Power Laboratory

Power, Energy and PQ Calibration System

Digital sampling wattmeter

Phasor Measurement Unit Calibration System

Measurand	Range	Accuracy	UUC
Phase angle	0 deg to 360 deg	± 0.001 degree	Electrical Power Source
Voltage	1 V to 520 V	± (0.002 5% to 0.005%)	
Current	1 mA to 160 A	± (0.002 5% to 0.01%)	

Require time and frequency synchronisation: GNSS is an alternative

Outlooks

- All measurements, NMT is good at, are of static nature, while, trains are moving
- Dynamic measurements are next destination
- Exchanging high accuracy static measurements with appropriate accuracy dynamic measurements, HOW?

Thank you for your attention.

National Institute of Metrology (Thailand)
Phone: +66 (0)2 577 5100
E-mail: iro@nimt.or.th

Structural Health Monitoring (SHM) technology for rail transit and high-speed train by Mr. Wang Guangjun

中国中车 CRRC

Application and Exploration of Rail Vehicle Structure Health Monitoring Technology

1

Contents

2

Part I Application background

Definition of structure health monitoring

Structural Health Monitoring (SHM): based on the service **characteristics of the structure**, adopts advanced sensor technology to **build a sensor network and monitoring system**, obtain dynamic response of the structure in real time, extract characteristic **parameters representing service status, damage degree or integrity,** analysis with **the fault diagnosis model**, to **identify the structure health status**, reliability, and durability.

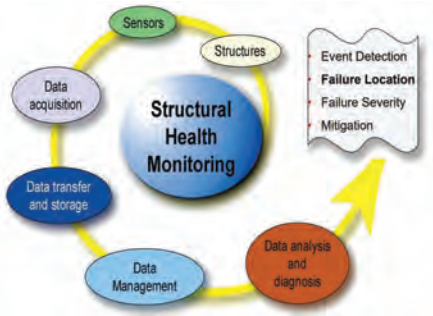

3

Part I Application background

Wide range of research and applications

At present, well-known enterprises and scientific research institutions have carried out research and layout for structural health monitoring technology, and have been widely used in aerospace, civil engineering, petrochemical, wind power and other fields.

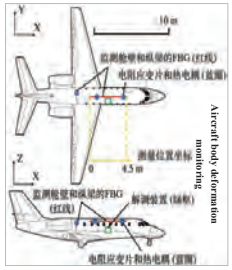

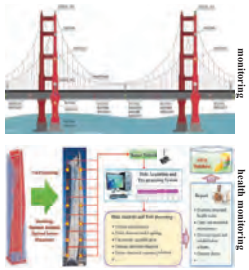

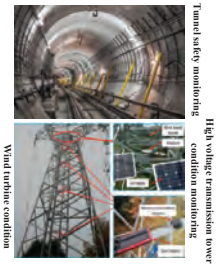

4

Part I Application background

Achievements in the development of China's high-speed rail network

High-speed rail steadily ranking first in the world

- The total operating mileage is 38,000 kilometers, accounting for more than 60% of the world;
- Online high-speed EMUs exceed 3,800 standard units, and the number of EMUs accounts for more than 60% of the world's total.
- Cover 94.7% of cities with a population of over one million

Comprehensive improvement in integrated transportation capacity

- In 2019, the total number of 3.66 billion passengers were dispatched
- In 2020, the total number of 2.17 billion passengers were dispatched
- From 2009 to 2020, the cumulative number of passengers by high speed trains breaks through more than 27 billion

Rapid development of intercity rail transit

- By the end of 2020, 208 urban rail lines with a total length of 7,715.3km have been opened in 44 cities
- 6,434.5Km of metro lines, accounting for 83.4%
- 1,280.8km of other standard lines, accounting for 16.6%

Transformation of people's travel modes

The public transportation is comfortable and convenient, changing travel concept, lifestyle and social structure.

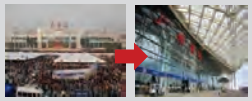

Part I Application background

New challenges brought due to service environment, system coupling, and speed improvement

Due to the complex and changeable service environment, the coupling effect of large system and the increase of design speed, it brings great challenges to train safety service, so it is necessary to improve its safety and reliability under vibration, fatigue, corrosion, sand, snow and ice.

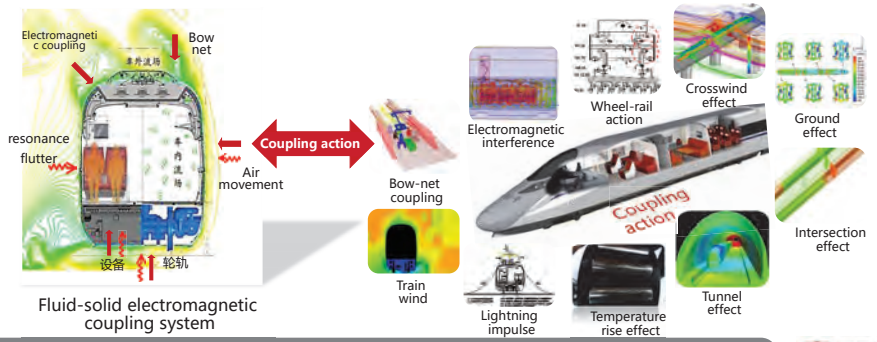

Part I Application background

Research and application significance of structural health monitoring

Develop rail vehicle structure health monitoring technology, carry out intelligent state perception, structural integrity assessment, service life prediction research, it is of great significance to ensure the safe operation of trains and improve the intelligent level of operation and maintenance.

- **New development situation**: Ensure the operation safety of lightweight train, and meet the requirements of Carbon Peak and Carbon Neutrality for environmental protection;
- **New market demand**: Improve the intelligent maintenance level of vehicle structure, promote the transition to Condition-based Repair, reduce maintenance, and enhance availability;
- **New safety challenges**: Improve the safety and reliability of trains under factors such as vibration, fatigue, corrosion, wind and sand, snow and ice;
- **New cross disciplinary technologies**: Applications such as AI can improve the accuracy of structural life prediction and safety assessment.

Contents

Part II Research status

Technical system

SHM is a technology that integrates **materials, dynamics, signal processing, embedded software and hardware**, and other disciplines to monitor and evaluate engineering structures, whose technical system includes **structural analysis**, **intelligent perception**, **data mining** and **engineering application**.

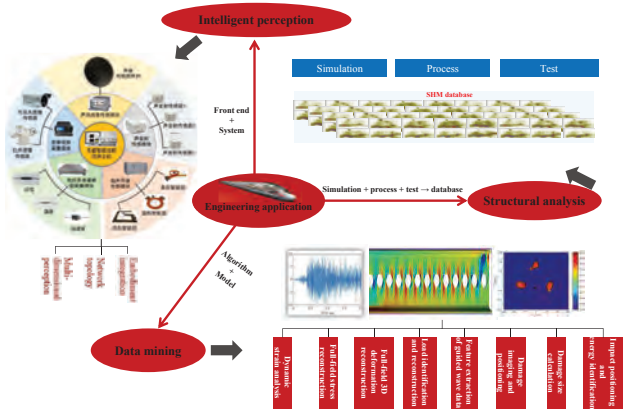

Part II Research status

Structural Aanalysis

Structural analysis is to study the failure mechanism and service evolution law through simulation, process and test methods, establish a complete SHM fault sample database, and guide the design of intelligent sensing network and the development of data mining model.

- The co-simulation ability of structural damage and sensing is studied to determine the optimal sensing method and layout design of different damage forms.
- Study the typical damage and evolutionary simulation ability of composite materials, and further improve the sample database of composite component-level structural faults;
- The evaluation and optimization method of the sensing performance and damage resistance of the embedded sensor is studied, and the internal damage state of the composite is accurately identified through the embedded sensor.

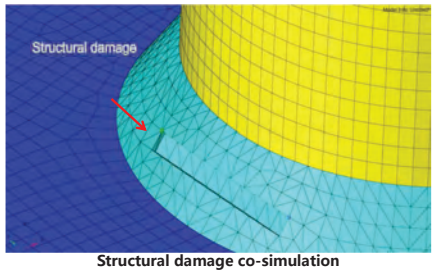

Structural damage co-simulation

Part II Research status

Intelligent Perception

Intelligent perception, establish the front multi-source perception network and on-board monitoring system, obtain the basic data that can characterize the service status of the structure, such as stress, temperature and PZT wave data.

- The embedded sensor network design method is studied to realize the effective integration with the composite structure.
- Research board card, modular SHM vehicle monitoring hardware and software, improve the level of miniaturization and integration, adapt to vehicle PHM host, and support artificial intelligence model deployment;
- New sensing technologies such as digitalization and wireless transmission are studied to improve the stability of signal transmission.

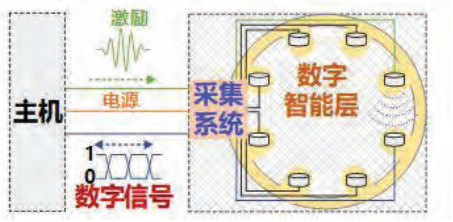

Digital Sensor (Intelligent Layer))

Part II Research status

Data Mining

Data mining is to extract the features of the basic data of perception, and identify the health state of the structure through the damage diagnosis and safety assessment model, such as whether there is damage, the size of damage, and the remaining life. After we obtain these status, we will feed this data back to the vehicle operations control center for further guidance on maintenance.

- Research the guided wave data analysis method based on deep learning to solve the complex structure signal feature extraction, temperature influence and other problems;
- The quantitative damage diagnosis model is studied, and the crack size calculation, expansion analysis and impact energy analysis are realized.
- The failure evaluation criterion and residual life prediction method of composite structure are studied to form safety evaluation capability.

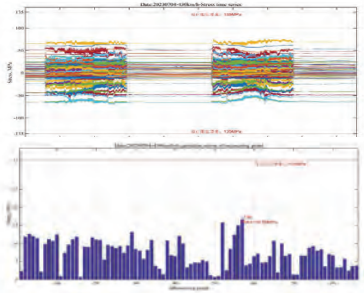

Part II Research status

Intelligent sensor

We have developed high-precision and flexible sensing network, developed an optimal design method, and realized the sensing of stress/strain, vibration acceleration, damage evolution and other data.

Fiber Grating

- **Basic principle**: Taking advantage of the photosensitivity of optical fiber materials, **when subjected to strain and temperature effects, the central wavelength of the reflected wave changes linearly with the variations of strain and temperature**.
- **Sensor**: Grating with flexible substrate protection, **the diameter of exposed grating fiber is 0.15mm**, and the grating area can be customized to 2/3/5/10mm.
- **Advantages**: **One optical fiber in series connection with multiple measuring points**; **anti-electromagnetic interference**, high stability, and adaptability to harsh environment; **good integration with structure**, etc.

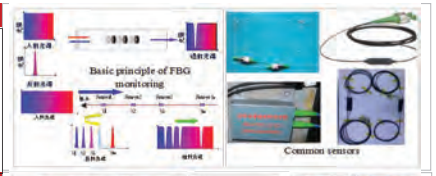

Piezoelectric intelligent layer

- **Basic principle**: Stimulate and receive guided waves in elastomer, causing waveform changes due to damage. **Detect, locate, and assess damage** through **comparison of health and damage signals**;
- **Sensor**: **the layout of the piezoelectric ceramic array and the shape of the intelligent layer shall be designed**;
- **Advantages**: Suitable for **regional monitoring**; **Lightweight and soft**, integrated with the structure **like a layer of skin.**

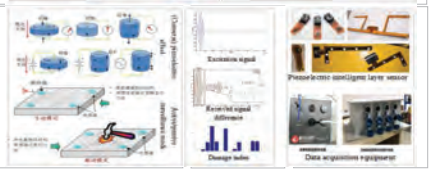

Part II Research status

System Integration

By integrating multi-source sensor network, vehicle intelligent monitoring equipment and remote data center, we established a structural health monitoring system with the function of "perception - transmission - diagnosis - early warning".

- Multi-parameter sensor network: Customized design according to the structural characteristics and service environment of rail vehicles;
- On-board intelligent monitoring equipment: Development of low-power, miniaturized, modular on-board intelligent equipment;
- Remote data center: Development and deployment of fault diagnosis model, processing of massive monitoring data, and real-time display platform for train health status.

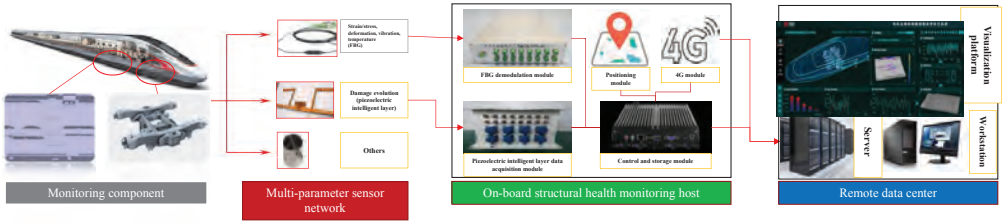

Part II Research status

Technical validation

For the structural health monitoring system, we have completed routine tests of high and low temperature, vibration and shock and protection grade. In addition, a series of tests have been carried out on the company's test bench to verify its function of monitoring multi-dimensional states such as stress, damage and temperature, as well as its application reliability in the service environment of rail vehicles.

High and low temperature test

- Carry out the test according to GB/T 2423.2-2008 Environmental testing for electric and electronic products - Part 2: Test methods - Tests A: Dry heat and cold
- Storage temperature range: -25℃~60℃
- Operating temperature range: 10℃~55℃

Shock and vibration test

- Carry out the test according to GB/T 21563-2008 Railway applications -- Rolling stock equipment -- Shock and vibration tests and other standards
- Frequency range: 5-150Hz
- Three-direction acceleration: 0.75m/S², 0.37m/S², m/S²

Damp heat test

- Carry out the test according to GB/T 2423.2-2008 Environmental testing for electric and electronic products - Part 2: Test methods - Tests Db: Damp heat, cyclic (12h + 12h cycle)
- Temperature: 55℃, Relative humidity: 95%
- Test time: 24h

Protection degree test

- Carry out the protection degree test for the host and intelligent layer according to GB 4208-2017 Degrees of protection provide by enclosure (IP code)
- Intelligent layer protection level: IP48
- Host protection level: IP43

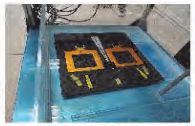

Part II Research status

Loading application - EMU body monitoring

By using optical fiber and piezoelectric intelligent layer sensing technology, we set up a tracking and monitoring system of the vehicle body, and evaluated the fatigue life of the structure.

Structural health monitoring architecture for high speed EMUs

- Monitoring parts: Underframe draft sill, bolster, transom, etc.
- Number of measuring points: 67

Construction scheme for on-board structural monitoring system

- FBG sensor network and structural integration
- High-speed data acquisition by demodulator
- Automatic acquisition program control and data save by industrial computer
- System status display and data change trend monitoring by remote monitoring software

Fatigue safety and reliability assessment of critical structures

- The maximum cumulative damage of the weld seam in one year is 2.57e-4, and that of base metal is 1.04e-6, which is relatively low;
- The inferred value of fatigue cumulative damage after 30 years of operation of EMU is less than 1e-2, satisfying the safety and reliability requirements.

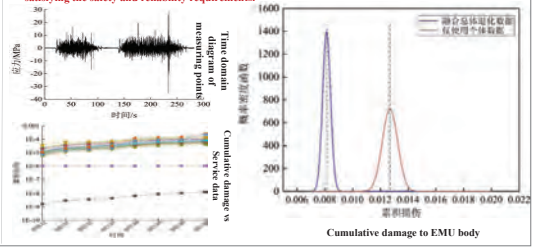

Part II Research status

Loading application - Safety assessment of overload structure of metro vehicles

Our Beijing Metro Line 4 has been operating under overload conditions for a long time, so we set up a monitoring system for the bogies to obtain structural stress data and evaluate the cumulative fatigue damage.

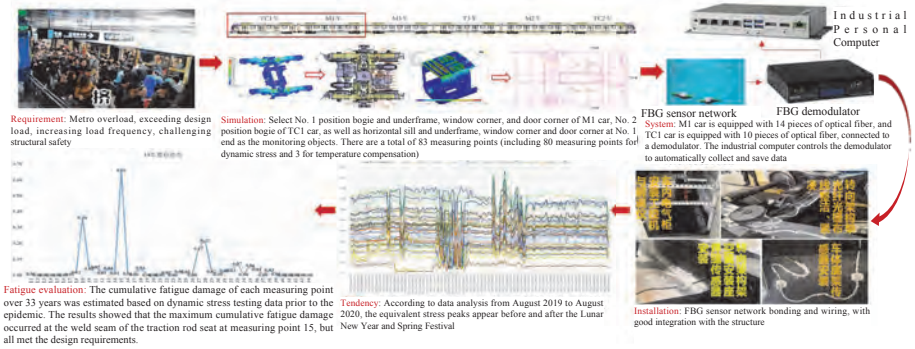

Requirement: Metro overload, exceeding design load, increasing load frequency, challenging structural safety

Simulation: Select No. 1 position bogie and underframe, window corner, and door corner of M1 car, No. 2 position bogie of TC1 car, as well as horizontal sill and underframe, window corner and door corner at No. 1 end as the monitoring objects. There are a total of 83 measuring points (including 80 measuring points for dynamic stress and 3 for temperature compensation)

System: M1 car is equipped with 14 pieces of optical fiber, and TC1 car is equipped with 10 pieces of optical fiber, connected to a demodulator. The industrial computer controls the demodulator to automatically collect and save data

Fatigue evaluation: The cumulative fatigue damage of each measuring point over 33 years was estimated based on dynamic stress testing data prior to the epidemic. The results showed that the maximum cumulative fatigue damage occurred at the weld seam of the traction rod seat at measuring point 15, but all met the design requirements.

Tendency: According to data analysis from August 2019 to August 2020, the equivalent stress peaks appear before and after the Lunar New Year and Spring Festival

Installation: FBG sensor network bonding and wiring, with good integration with the structure

Contents

Part III Future prospect

New sensor technology

Develop new sensor technologies that are lightweight, flexible, and wireless, to reduce the impact on structures and improve monitoring accuracy and detection efficiency.

- **Status monitoring and structural evaluation based on graphics/images**

Obtain the three position displacement of each component of the pantograph by binocular camera
Displacement used as a boundary condition for finite element calculation to calculate stress
Evaluate the instantaneous impact stress and fatigue accumulation of each component

- **Abnormal noise monitoring based on sound sensor array**

Reference sound signal acquisition and feature analysis
Current sound signal acquisition and feature analysis
No
Out of reference
Yes
Abnormal signal positioning and fault severity analysis

- **Structural surface damage monitoring based on smart covering**

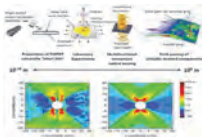

Brush a layer of carbon nanofilm on the surface of the structure
When receiving laser irradiation, it will emit fluorescence
Different strains result in different fluorescence wavelengths
Determine surface strain by analyzing wavelength

- **Structural health monitoring based on piezoelectric-laser scanning**

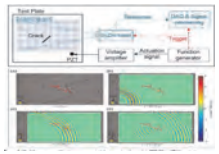

- A high-resolution spatiotemporal Lamb wave field excited by a piezoelectric ceramic driver was obtained using a scanning laser doppler vibrometer
- Transform the recorded wave field into the frequency-wavenumber domain through two-dimensional Fourier transformation
- Determine whether damage occurs and the location of damage based on changes in the frequency-wavenumber domain

Part III Future prospect

AI technology

Promote research on the application of intelligent technologies such as AI, and use deep learning technology to solve the difficult problems of structural health monitoring data mining and safety assessment.

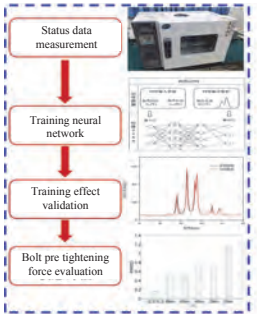

Evaluation of bolt pre tightening force based on generalized regression neural network

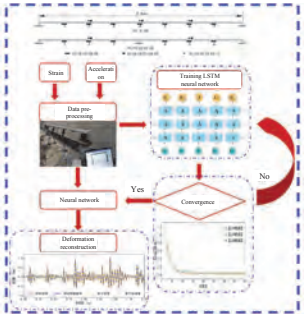

Multi-source data fusion bridge deformation reconstruction based on LSTM neural network

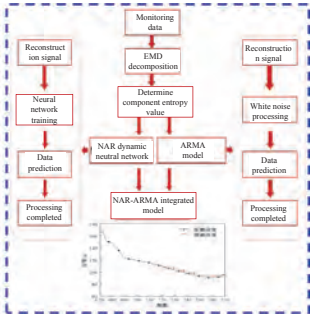

Structural strain prediction based on NAR dynamic neural network

Part III Future prospect

Structural Digital Twin technology

Develop the structure "Digital Twin" technology, based on on-line intelligent perception, ground operation and maintenance, and other multi-source data to establish the perfect mapping between **vehicle entity** and **physical model**, and realize the structural integrity evaluation, remaining life prediction, life cycle health management.

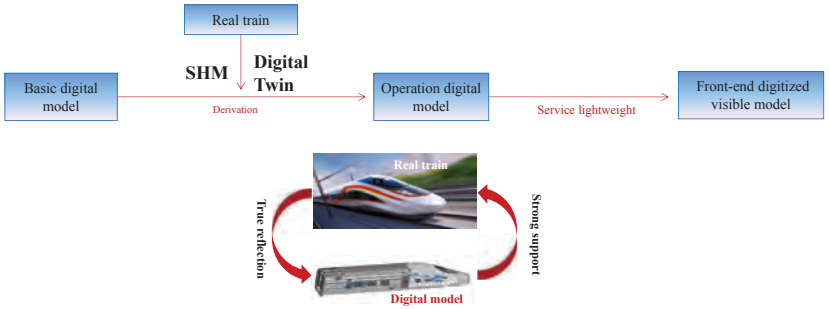

Part III Future prospect

Collaborative and win-win ecosystem

We hope to establish a win-win ecosystem, combined the domestic and foreign companies, universities and institutions, conduct research in cutting-edge technologies, promote sustainable transport development around the world.

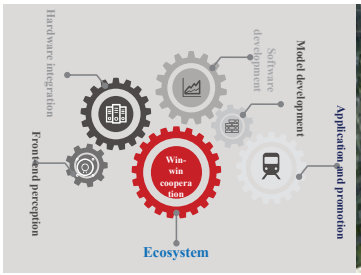

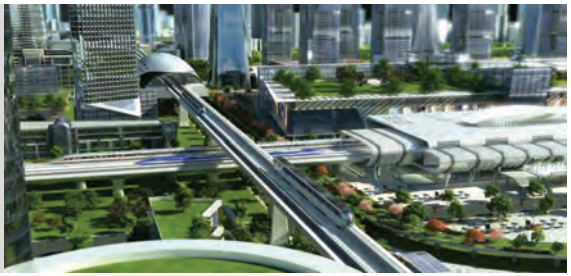

中国中车 CRRC

The development of local technology for Train Weight Devices (TWD) in Thailand by Mr.Phanasindh Paitekul

www.tistr.or.th/rttc
anat@tistr.or.th
patcharee_a@tistr.or.th

ศูนย์ทดสอบมาตรฐานระบบขนส่งทางราง (ศทร)
Railway Transportation System Testing Center (RTTC)

The development of local technology for Train Weight Device (TWD) in Thailand

สถาบันวิจัยวิทยาศาสตร์และเทคโนโลยีแห่งประเทศไทย (วว)
Thailand Institute of Scientific and Technological Research (TISTR)

Content

Background and motivation

Railway Transportation System Testing Center (RTTC) www.facebook.com/RTTC.TISTR

- Rapid expansion of global railway network
- Effective and optimum maintenance strategy (Predictive/RSHM)
- Permission of private sector to operate the train fleet

Commercial Wheel Load Detector

Railway Transportation System Testing Center (RTTC) www.facebook.com/RTTC.TISTR

Vehicle side	Wayside

System architecture and working principle

Railway Transportation System
Testing Center (RTTC)
www.facebook.com/RTTC.TISTR

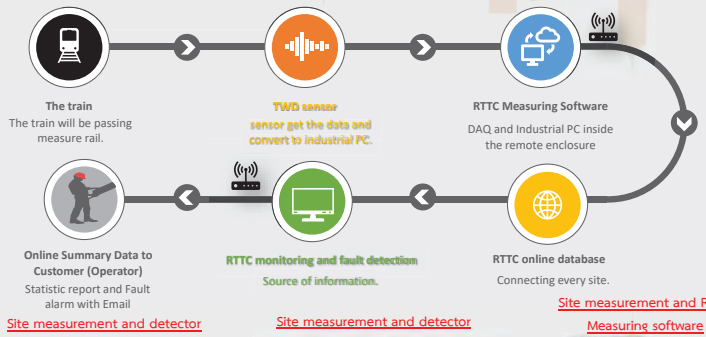

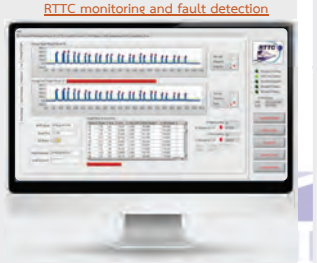

Site measurement and detector

Site measurement and detector

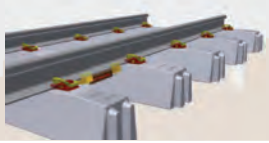

Site measurement and RTTC Measuring software

RTTC monitoring and fault detection

Overview of TWD Development

Railway Transportation System
Testing Center (RTTC)
www.facebook.com/RTTC.TISTR

Conceptual Design

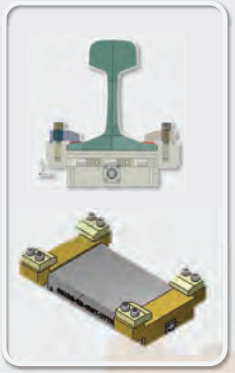

Concept Validation

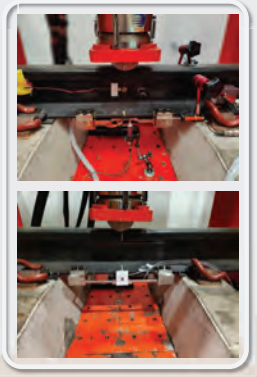

On site Calibration

On site validation

What is strain gauge and how it works?

Railway Transportation System
Testing Center (RTTC)
www.facebook.com/RTTC.TISTR

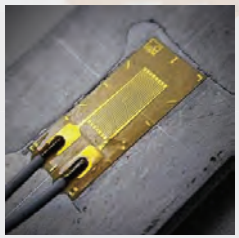

$$\frac{\Delta R}{R} = K \cdot \varepsilon$$

Resistance = R(Ω)
Changed resistance = △R(Ω)
Strain = ε
Gage factor = K

$$\frac{V_{out}}{V_{supply}} = \frac{GF * N * \varepsilon}{4}$$

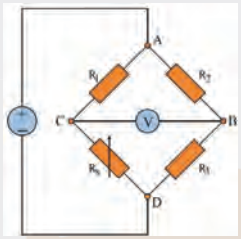

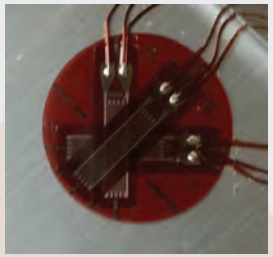

RTTC's Applications of SG in rail sector

Railway Transportation System
Testing Center (RTTC)
www.facebook.com/RTTC.TISTR

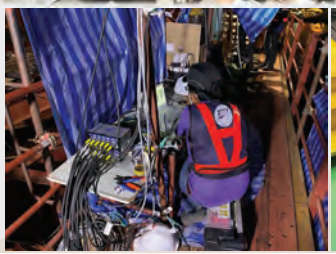

What happens to the rail under wheel load

Railway Transportation System
Testing Center (RTTC)
www.facebook.com/RTTC.TISTR

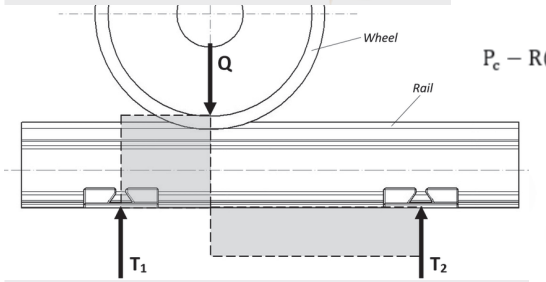

$$P_c - R(\text{Crib} = 0) = \frac{EIt}{2Q(1+v)}[(\gamma_a + \gamma_c) - (\gamma_b + \gamma_d)]$$

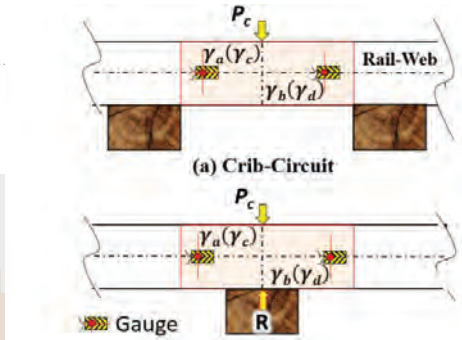

On site calibration and running test result

Railway Transportation System
Testing Center (RTTC)
www.facebook.com/RTTC.TISTR

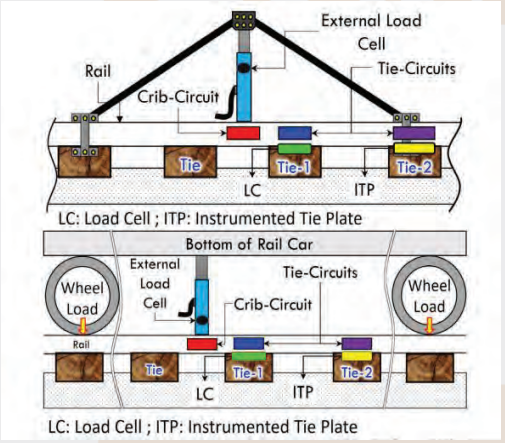

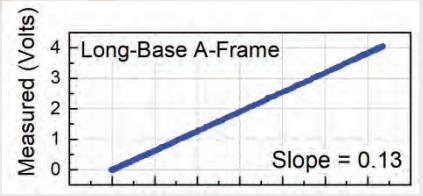

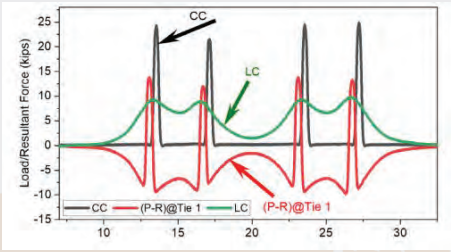

Examples of Wheel load measurement with SG

Railway Transportation System
Testing Center (RTTC)
www.facebook.com/RTTC.TISTR

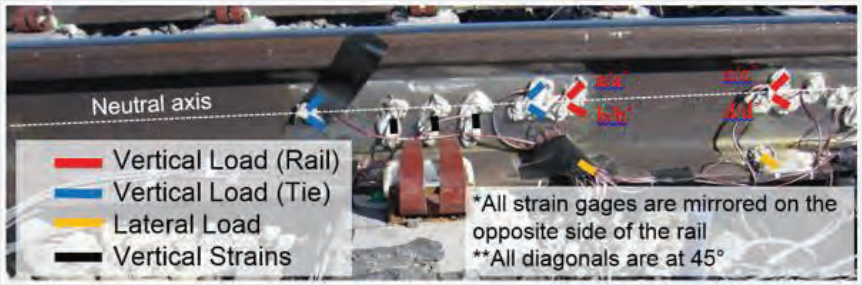

Simulation assisted design

Railway Transportation System
Testing Center (RTTC)
www.facebook.com/RTTC.TISTR

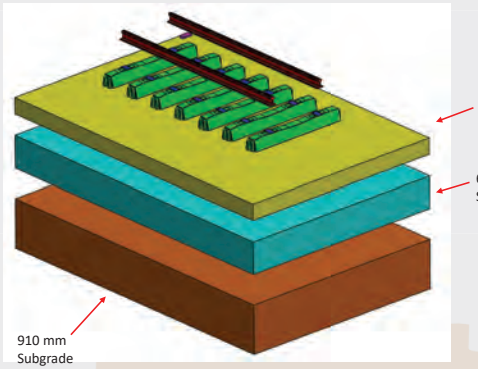

Static = 10 Ton

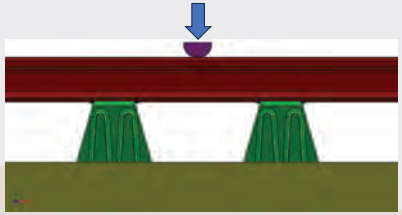

Coupling between element

Railway Transportation System
Testing Center (RTTC)
www.facebook.com/RTTC.TISTR

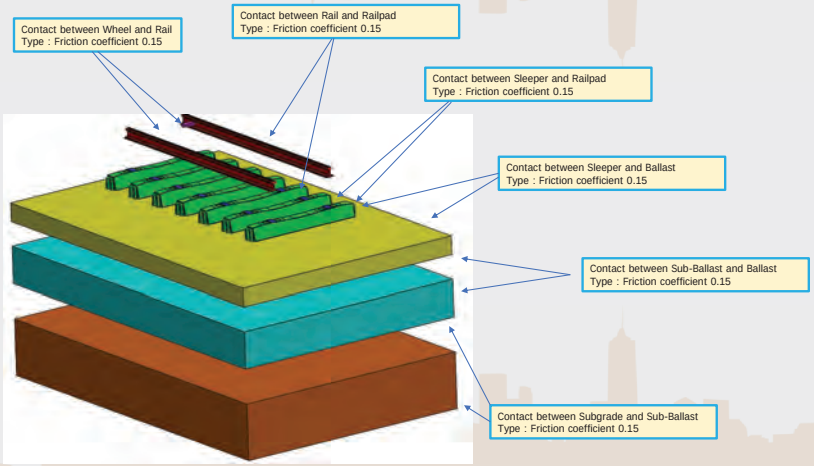

Load and Boundary conditions

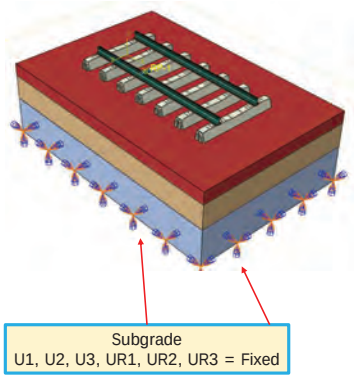

Subgrade
U1, U2, U3, UR1, UR2, UR3 = Fixed

Wheel
-U2 = Load 10 ton
U1, U3, UR2, UR3 = Fixed

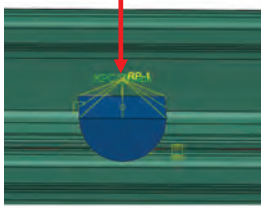

Direction
U1 = X
U2 = Y
U3 = Z
UR1 = Rotation X
UR2 = Rotation Y
UR3 = Rotation Z

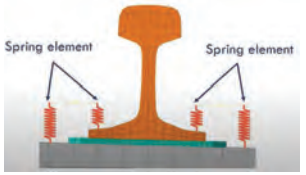

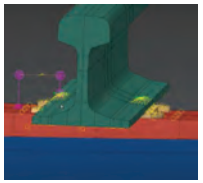

Mesh and Elements

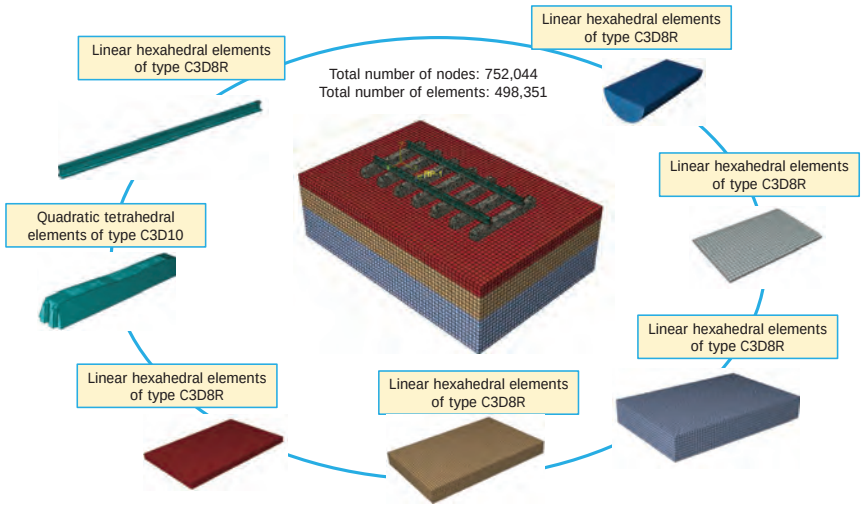

Simulation results

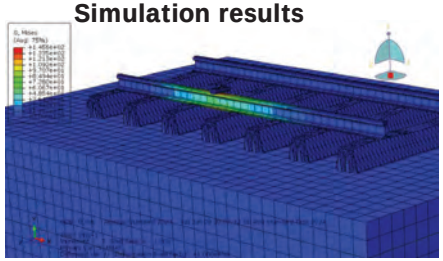

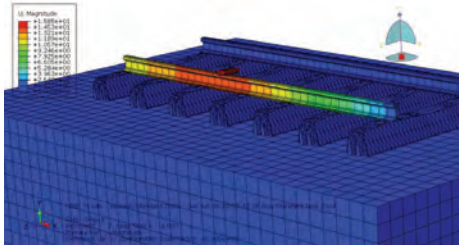

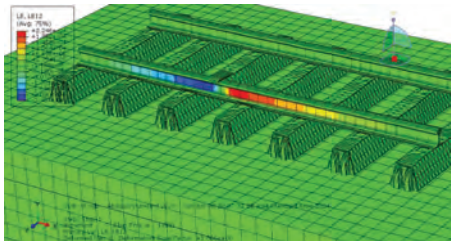

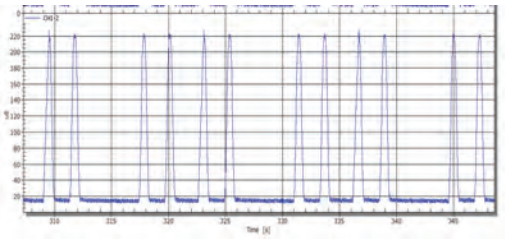

1 System overview

Railway Transportation System
Testing Center (RTTC)
www.facebook.com/RTTC.TISTR

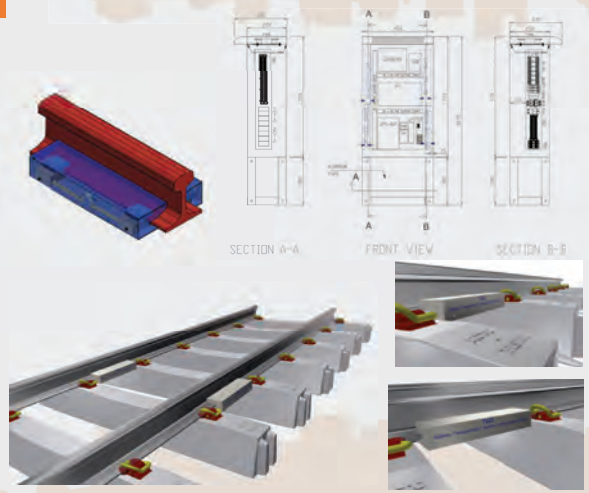

Train Weight Device (TWD)

- The TWD can be fast installation in existing railway infrastructure, without removing sleeper and without modification of the railway roadbed.
- Weighing the train made it easy.
- Information from TWD can help to know gross weight, weight balance and speed measurement in the measure zone for train passing.
- Real-time data monitoring.
- Able to identify every train when it passed and check suspicious trains and fast fault alarm with email.

1 System overview

Railway Transportation System
Testing Center (RTTC)
www.facebook.com/RTTC.TISTR

Installation of Train Weight Device (TWD)

TWD install on the track

TWD sensor

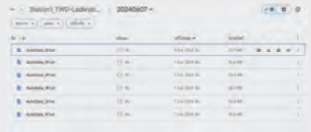

Data base

Remote enclosure

RTTC monitoring and fault detection software

2 System architecture and working principle

Railway Transportation System
Testing Center (RTTC)
www.facebook.com/RTTC.TISTR

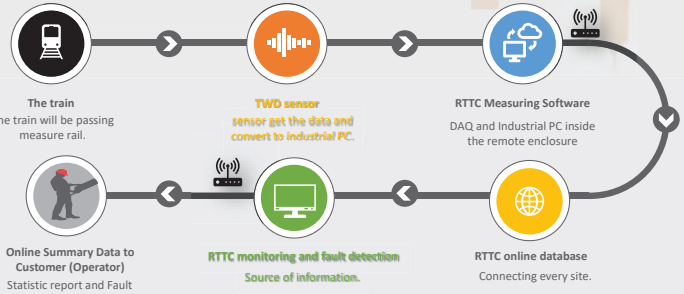

RTTC monitoring and fault detection

Site measurement and detector

Site measurement and detector

Remote enclosure and RTTC Measuring software

RTTC monitoring and fault detection

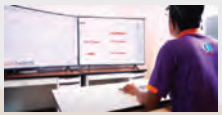

www.tistr.or.th/rttc
anat@tistr.or.th
patcharee_a@tistr.or.th

ศูนย์ทดสอบมาตรฐานระบบขนส่งทางราง (ศทร)
Railway Transportation System Testing Center (RTTC)

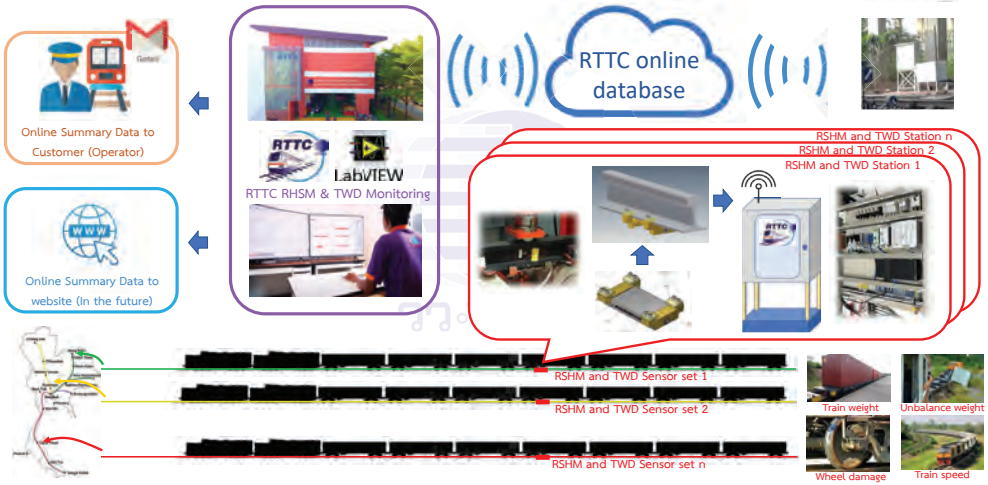

3 RTTC MONITORING SOFTYWARE

Railway Transportation System
Testing Center (RTTC)
www.facebook.com/RTTC.TISTR

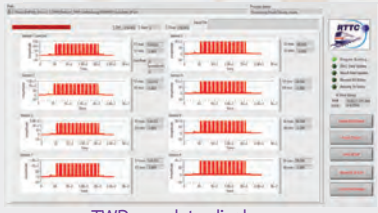
TWD raw data display


Data set of the train


Summary data in case normal

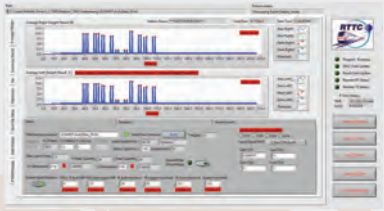
Data processing and fault setup

RTTC MONITORING SOFTYWARE (continue)

Railway Transportation System
Testing Center (RTTC)
www.facebook.com/RTTC.TISTR


Summary data in case fault


Statistical data and fault logger


Email sender setup

4 TWD validation at RTTC laboratory

Railway Transportation System
Testing Center (RTTC)
www.facebook.com/RTTC.TISTR

A. Static validation
B. Dynamic validation
C. Train wheel load simulation
D. Experimental track test

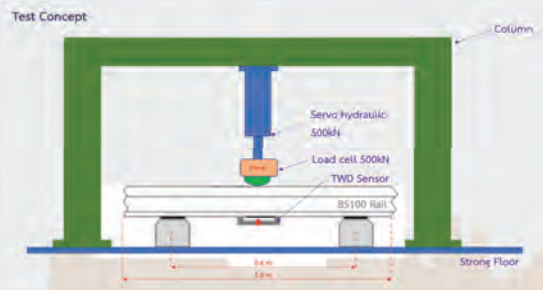

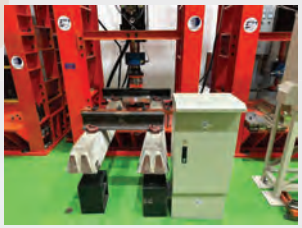

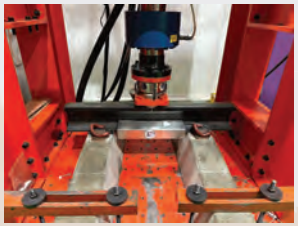

www.tistr.or.th/rttc
anat@tistr.or.th
patcharee_a@tistr.or.th

ศูนย์ทดสอบมาตรฐานระบบขนส่งทางราง (ศทร)
Railway Transportation System Testing Center (RTTC)

A. Static validation result of TWD

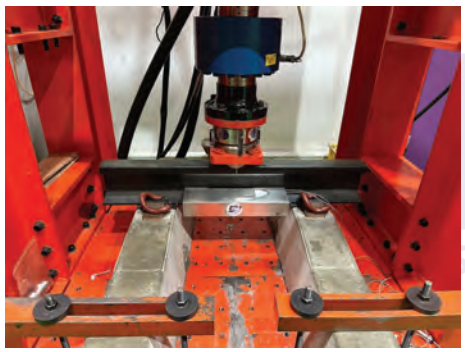
Static test setup

Noise floor = ± 3uε

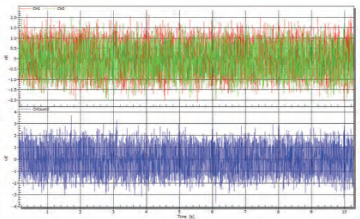
Output strain of each sensor

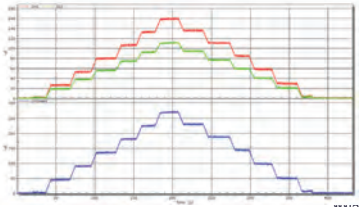

www.tistr.or.th/rttc
anat@tistr.or.th
patcharee_a@tistr.or.th

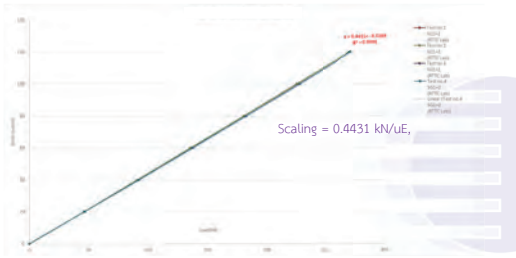

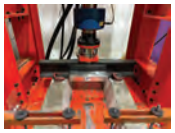

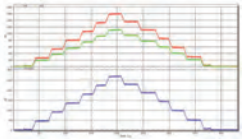

Standard force(kN)	Measuring Force (kN)			
	Test no.1 SG1+2 (RTTC Lab)	Test no.2 SG1+2 (RTTC Lab)	Test no.3 SG1+2 (RTTC Lab)	Test no.4 SG1+2 (RTTC Lab)
0	0	0	0	0
20	19.86	19.86	19.93	20.02
40	39.71	39.75	40.33	40.32
60	59.60	59.60	60.25	60.42
80	79.46	79.55	80.29	80.28
100	99.11	99.31	100.21	100.05
120	118.84	118.78	119.52	119.46
File Date	16022024			

Standard force(kN)	%Error			
	Test no.1 SG1+2 (RTTC Lab)	Test no.2 SG1+2 (RTTC Lab)	Test no.3 SG1+2 (RTTC Lab)	Test no.4 SG1+2 (RTTC Lab)
0	0.00%	0.00%	0.00%	0.00%
20	0.69%	0.71%	0.37%	-0.09%
40	0.73%	0.63%	-0.82%	-0.81%
60	0.66%	0.66%	-0.41%	-0.70%
80	0.67%	0.56%	-0.36%	-0.35%
100	0.89%	0.69%	-0.21%	-0.05%
120	0.97%	1.02%	0.40%	0.45%
Minimum Error	0.66%	0.56%	-0.82%	-0.81%
Maximum Error	0.97%	1.02%	0.40%	0.45%

www.tistr.or.th/rttc
anat@tistr.or.th
patcharee_a@tistr.or.th

ศูนย์ทดสอบมาตรฐานระบบขนส่งทางราง (ศทร)
Railway Transportation System Testing Center (RTTC)

Static calculating force result

Max. error = 1.02%

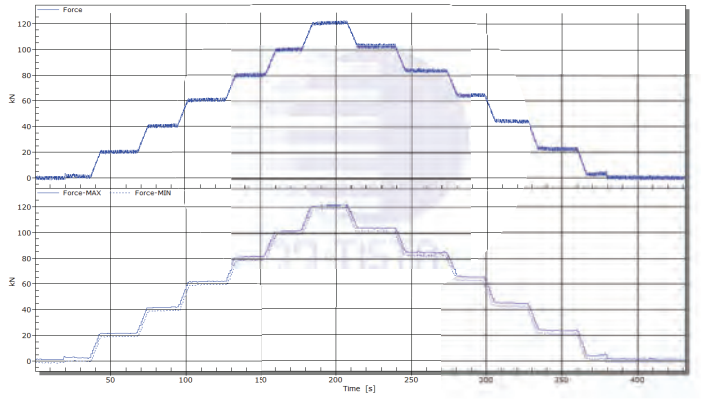

www.tistr.or.th/rttc
anat@tistr.or.th
patcharee_a@tistr.or.th

ศูนย์ทดสอบมาตรฐานระบบขนส่งทางราง (ศทร)
Railway Transportation System Testing Center (RTTC)

B. Dynamic validation result of TWD

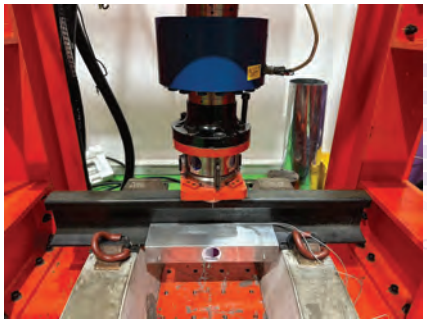

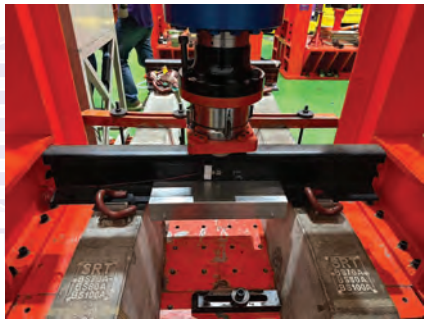

www.tistr.or.th/rttc
anat@tistr.or.th
patcharee_a@tistr.or.th

ศูนย์ทดสอบมาตรฐานระบบขนส่งทางราง (ศทร)
Railway Transportation System Testing Center (RTTC)

Dynamic result

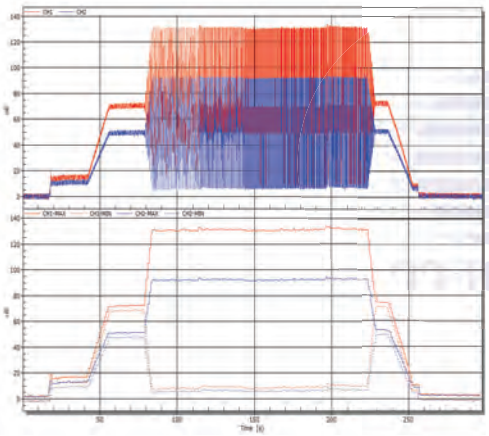

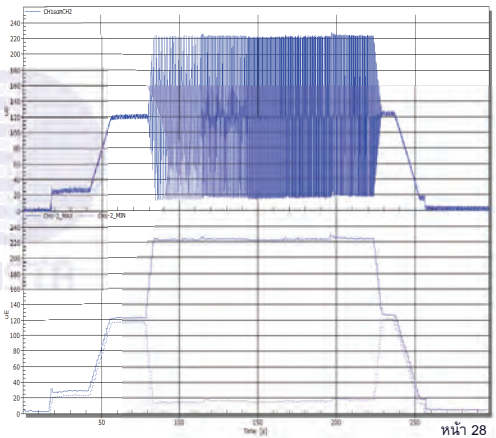

www.tistr.or.th/rttc
anat@tistr.or.th
patcharee_a@tistr.or.th
ศูนย์ทดสอบมาตรฐานระบบขนส่งทางราง (ศทร)
Railway Transportation System Testing Center (RTTC)

Dynamic calculating force result

Max. error = 0.48%

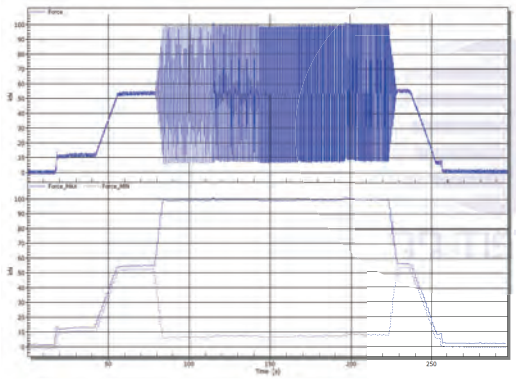

Close up the dynamic force @ 5Hz

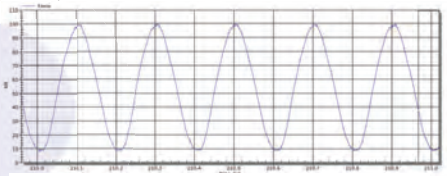

Noise floor of dynamic force

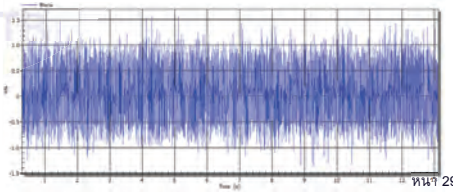

www.tistr.or.th/rttc
anat@tistr.or.th
patcharee_a@tistr.or.th
ศูนย์ทดสอบมาตรฐานระบบขนส่งทางราง (ศทร)
Railway Transportation System Testing Center (RTTC)

Dynamic force result in each frequency

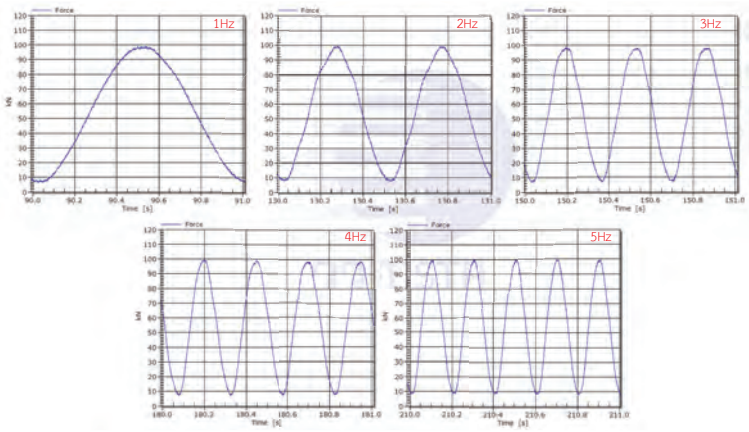

www.tistr.or.th/rttc
anat@tistr.or.th
patcharee_a@tistr.or.th
ศูนย์ทดสอบมาตรฐานระบบขนส่งทางราง (ศทร)
Railway Transportation System Testing Center (RTTC)

C. Train wheel load simulation result of TWD

Force Setpoint
Force Min = 5kN
Force Max = 100kN
Ramp up time = 500ms
Ramp down time = 500ms

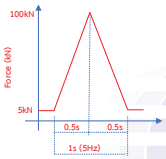

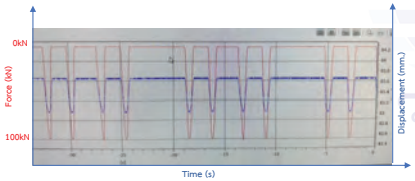

Servo actuator

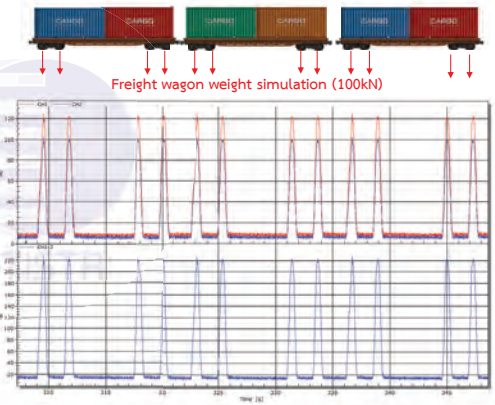

TWD Reading

www.tistr.or.th/rttc
anat@tistr.or.th
patcharee_a@tistr.or.th
ศูนย์ทดสอบมาตรฐานระบบขนส่งทางราง (ศทร)
Railway Transportation System Testing Center (RTTC)

Train weight simulation result

Max. error = 1.3%

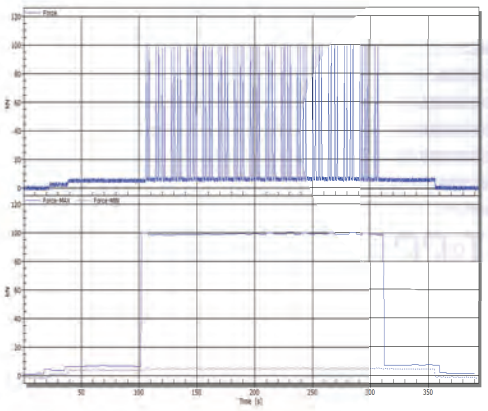

Close up the dynamic force

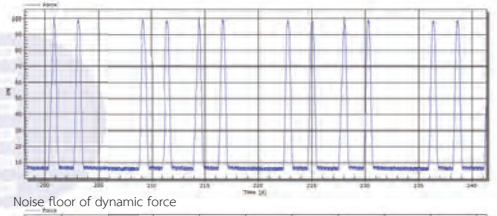

Noise floor of dynamic force

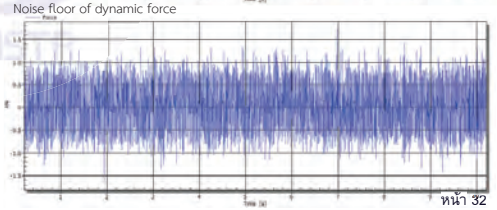

www.tistr.or.th/rttc
anat@tistr.or.th
patcharee_a@tistr.or.th

D. Experimental Track Test

TWD sensor installed on experimental track

Testing video

5 On-site calibration tool for TWD

A-Frame for TWD validation on the track

Master loadcell and hydraulic jack

6 Water proof of enclosure test

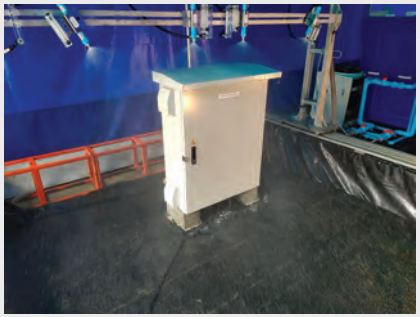

Water proof test

Water proof inspection

7 Summary Result

1. SNR calculation : $SNR = 20\log(\frac{a_{x,signal,rms}}{a_{x,noise,rms}})$

Test case	Noise Floor (μm/m)	Strain RMS measurement (μm/m)		SNR (dB)	
		Min.	Max.	Min.	Max.
Static Test	3	5.61	119.52	5.44	32.01
Dynamic test		7.34	99.52	7.78	30.42
Train wheel load simulation		5.53	98.70	5.31	30.34

2. Calibration result :

Test case	Maximum Error (%)
Static Test	1.02 %
Dynamic test	0.48 %
Train wheel load simulation	1.30%

3. TWD Ready to install on the track

3.1 The SNR value are more than 5dB that enough for train weight measurement.
3.2 The TWD have a low error with maximum error equal 1.3% in case the train wheel load simulation.
3.3 The TWD was tested water proof of enclosure that suitable for outdoor installation.
3.4 The TWD can validation with portable tool on site.
3.5 The TWD can be fast installation in existing railway and without modification of the railway roadbed.
3.6 The TWD system using remote control method for Real-time data monitoring and storing data automatically.


Thank you
www.tistr.or.th/rttc
anat@tistr.or.th
patcharee_a@tistr.or.th
(Tel) (+66)02-5779270, 025779272
081-424 4221
ศูนย์ทดสอบมาตรฐานระบบขนส่งทางราง (ศทร)
Railway Transportation System Testing Center (RTTC)
สถาบันวิจัยวิทยาศาสตร์และเทคโนโลยีแห่งประเทศไทย (วว)
Thailand Institute of Scientific and Technological Research (TISTR)
"Professional in Railway and Transportation Tests and Solutions"
Page37

The development of railway inspection by Assoc. Prof. Dr. Wichai Siwakosit

Wheel Rail Contact Inspection at Switch Points

By
Wichai Siwakosit and Thanawat Chaleekarn
Kasetsart University Rail Engineering Center

Wheel Rail Contact Inspection at Switch Points

- Introduction
- Methodology
- Application to SRT Vidura Wheel Contour and SRT Switch Points
- Tests and Evaluations
- Conclusion

Introduction

- This presentation will focus on applications of wheel contour gauges on inspection and investigation of derailment risk at switch points for the State Railway of Thailand (SRT).
- From SRT data from B.E.2557 to B.E.2561, the derailments at sidings happened more frequently than those of main lines. Inspection of switch points by SRT could be improved to lower such risk.
- Inspections were carried out as routine work, problems found were usually taken care of by repairs without getting into the root causes. If inspections were utilized to the full extents, the corrections of problems could be much more economical and result in safer railway operations.

Introduction

https://www.sanook.com/news/8205610/

Very Worn Switch Tongue (Delaware)

Introduction

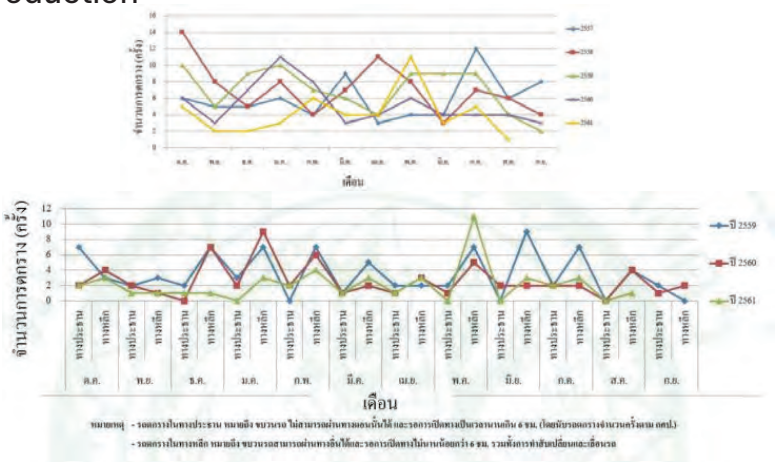

Methodology

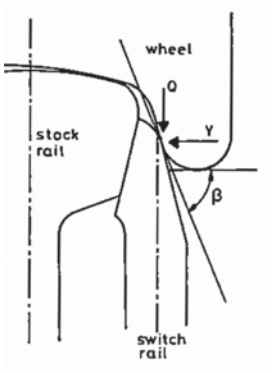

"OK" (Profilidis)

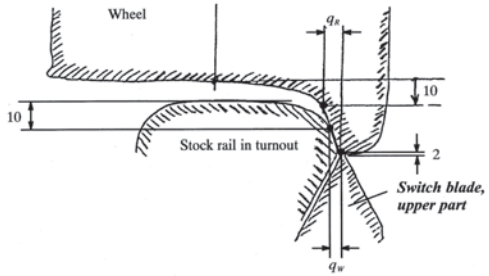

"Not OK, Flange Climbing Risk" (KTH)

Methodology

- SRT Condemn Limits for Switch
  - Top of Rail Wear
    - Main: 11 mm for BS100, 8 mm for BS80, 6 mm for BS 70
    - Siding: 12 mm for BS100, 9 mm for BS80, 7 mm for BS 70
  - Gauge Face Wear
    - Main and Siding: Track Gauge must be between 1,006 mm and 997 mm
  - Chipped Switch Tongue
    - Main and Siding: Thickness of a chipped switch tongue must be less than 5 mm

NOTE: There is no wheel profile involved! These limits will not reflect derailment risk from wheel and rail contact conditions.

Methodology

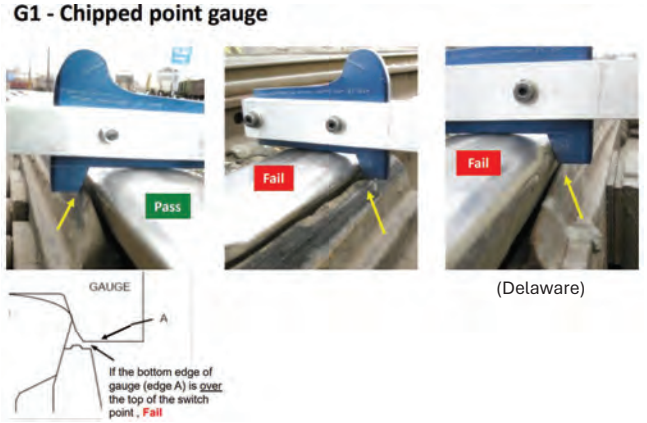

(Delaware)

Methodology

G2 - AAR 1B wheel contact gauge

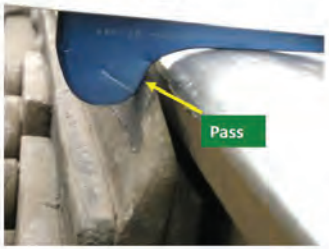

Apply this gauge where the point is worn or broken. If contact with the switch point is...

- above the 60° mark, **Pass**
- below the 60° mark, **Fail**

(Delaware)

Methodology

3. Severely worn wheel profile gauge

Apply this gauge to the first inch of the point, where head-on contact with a worn flange is most likely. Start with the 70° slider on top of the stock rail, then slowly shift the slider until it slides off the stock rail.

- If the slider slides down the gage face of the switch point, **pass**
- If the corner of the slider lands on top of the switch point, **fail**

This gauge can be used to identify gapping points, broken points and points that are exposed due to a worn stock rail.

(Delaware)

Methodology

4.Wear Angle Gauge

If the switch point's gage-face angle is...

- Less than 32° (>58°), **pass**
- Greater than 32° (<58°), **fail**

This gauge protects against a wheel climbing the gage face of the point.

(Delaware)

Application to SRT Vidura Wheel Contour and SRT Switch Points

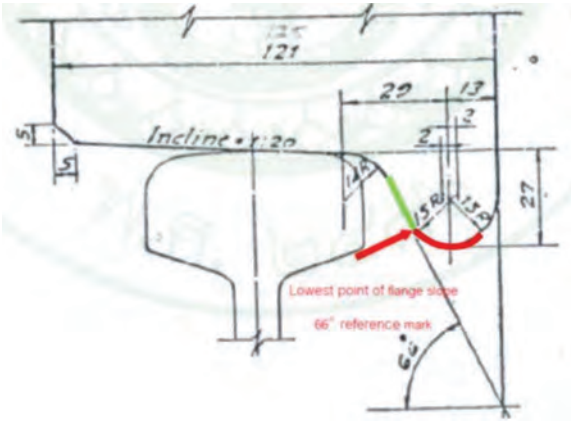

SRT Vidura Wheel Contour with 66 Deg Flange Angle

Application to SRT Vidura Wheel Contour and SRT Switch Points

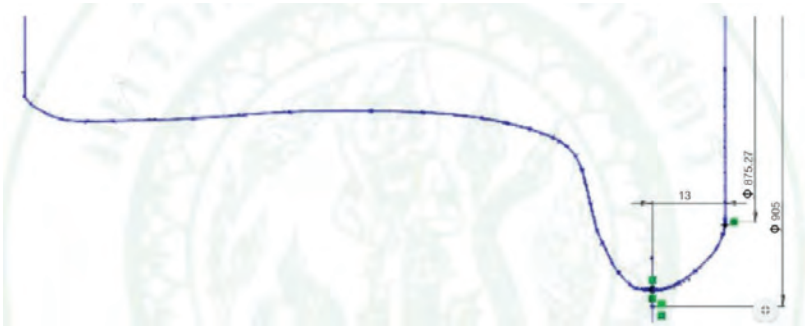

SRT Worn Vidura Wheel Contour

Application to SRT Vidura Wheel Contour and SRT Switch Points

Vidura Contour Contact Gauge, No.1

Application to SRT Vidura Wheel Contour and SRT Switch Points

Worn Vidura Contour Contact Gauge, No.2

Application to SRT Vidura Wheel Contour and SRT Switch Points

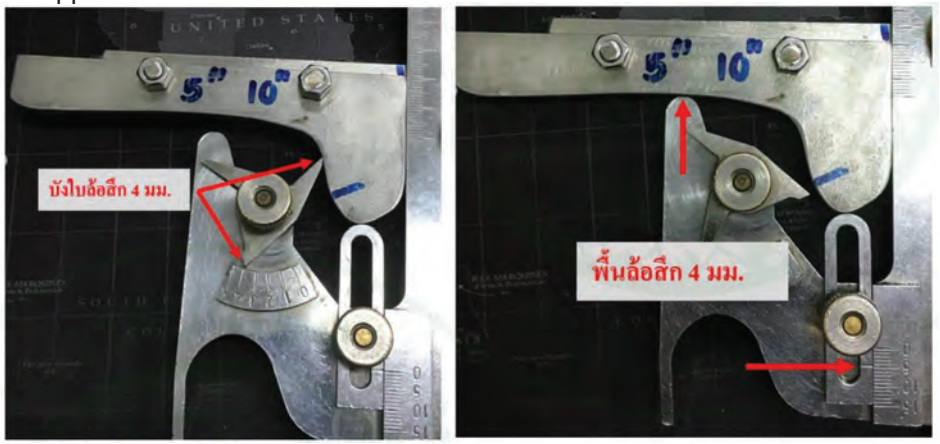

Worn Vidura Contour Contact Gauge

Application to SRT Vidura Wheel Contour and SRT Switch Points

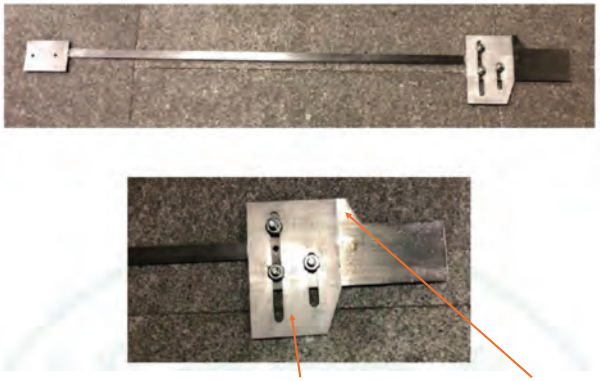

Severely Worn Profile Gauge, No.3, and Wear Angle Gauge, No.4

Tests and Evaluations

Test at Bangsue Locomotive Depot

Tests and Evaluations

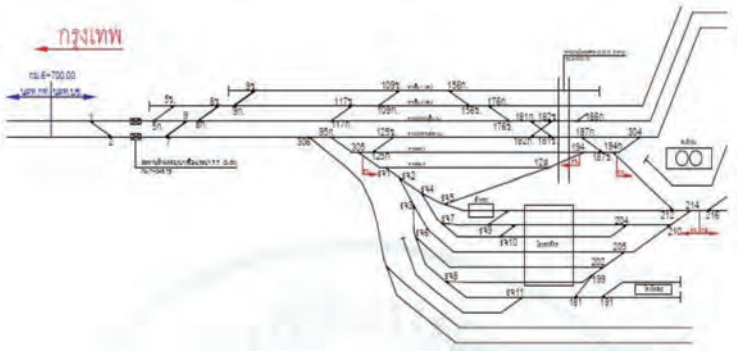

Test at Bangsue Locomotive Depot

Tests and Evaluations

Test at Bangsue Locomotive Depot, Switch No.9B "ราง9"

Tests and Evaluations

Gauge No.1, Switch No. 214, 5 in from the tongue's end
Test at Bangsue Locomotive Depot

Tests and Evaluations

Gauge No.2, Switch No. 214, 10 in from the tongue's end
Test at Bangsue Locomotive Depot

Tests and Evaluations

Gauge No.3, Switch No. 214, 2 in from the tongue's end
Test at Bangsue Locomotive Depot

Tests and Evaluations

Gauge No.4, Switch No. 214, 20 in from the tongue's end
Test at Bangsue Locomotive Depot

Tests and Evaluations

หมายเลขประแจ	วันที่ทดสอบ	ชนิดของเครื่องมือวัด 1 (5นิ้ว)	1 (10นิ้ว)	2 (5นิ้ว)	2 (10นิ้ว)	3 (2นิ้ว)	4 (10นิ้ว)	4 (20นิ้ว)
214	14/4/62	P	P	P	P	P	P	P
210	14/4/62	P	P	P	P	P	P	P
205	14/4/62	P	P	P	P	P	P	P
181	14/4/62	P	P	P	P	P	P	P
รจ9	14/4/62	P	P	P	P	P	P	P

Test at Bangsue Locomotive Depot

หมายเหตุ P = Pass (ผ่านเกณฑ์), F = Fail (ไม่ผ่านเกณฑ์)

ที่มา: การทดสอบที่โรงซ่อมรถจักรดีเซลบางซื่อ พฤษภาคม 2562

Tests and Evaluations

Gauge No.1, Switch No. 2, 5 in from the tongue's end, PASS or FAIL???

Test at Makkasan Work Shop

Tests and Evaluations

Gauge No.2, Switch No. 2, 5 in from the tongue's end, PASS or FAIL???

Test at Makkasan Work Shop

Tests and Evaluations

Gauge No.3, Switch No. 2, 2 in from the tongue's end, PASS or FAIL???

Test at Makkasan Work Shop

Tests and Evaluations

Gauge No.4, Switch No. 2, 20 in from the tongue's end, PASS or FAIL???

Test at Makkasan Work Shop

Tests and Evaluations

ตำแหน่งที่	วันที่ทดสอบ	ชนิดของเครื่องมือวัด 1 (5นิ้ว)	1 (10นิ้ว)	2 (5นิ้ว)	2 (10นิ้ว)	3 (2นิ้ว)	4 (10นิ้ว)	4 (20นิ้ว)
1	14/4/62	P	P	P	P	F	P	P
2	14/4/62	F	P	F	F	P	P	P
3	14/4/62	P	P	P	P	P	P	P
4	14/4/62	F	P	F	F	F	P	P

Test at Makkasan Work Shop

หมายเหตุ P = Pass (ผ่านเกณฑ์), F = Fail (ไม่ผ่านเกณฑ์)

Tests and Evaluations

- Pass and Fail is good
- But it could be better if there were a grading system to show relative risks
- A way to show risk levels from inspection is proposed

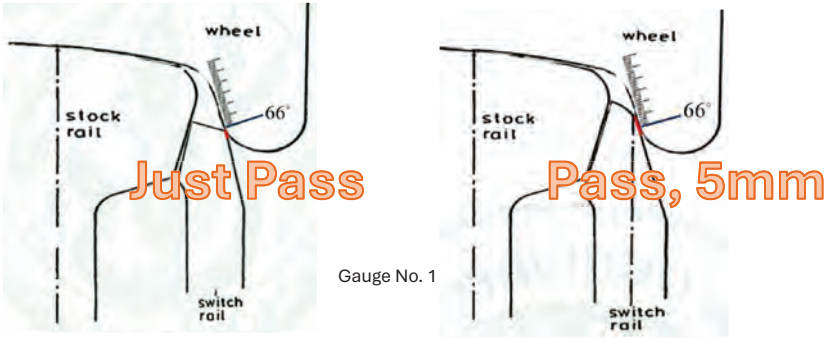

Gauge No. 1

Tests and Evaluations

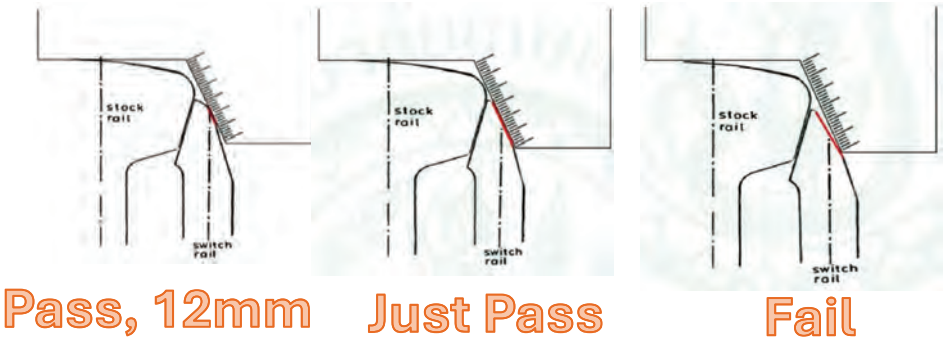

Gauge No. 4

Tests and Evaluations

Tests and Evaluations

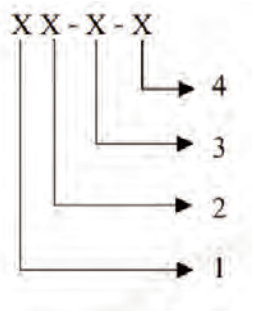

Last Contact Position on the Gauge Scale in mm

First Contact Position on the Gauge Scale in mm

Max-Min Values from measurement

1=Gauge No.1, 2=Gauge No.2, 3=Gauge No.3, 4=Gauge No.4

P=Pass, F=Fail, n/a=Unable to Judge

Tests and Evaluations

หมายเลขประแจ	วันที่ทดสอบ	ชนิดของเครื่องมือวัด 1 (5นิ้ว)	1 (10นิ้ว)	2 (5นิ้ว)	2 (10นิ้ว)	3 (5นิ้ว)	4 (10นิ้ว)	4 (20นิ้ว)
1	15/4/62	P1-9-11	P1-11-12	P	P	P	P4-14-15	P4-12-13
2	15/4/62	n/a 1-0-0	P1-0-5	P	P	P	n/a 4-0-0	P4-17-20
7	15/4/62	P1-5-13	P1-10-13	P	P	P	P4-11-13	P4-10-11
8ก	15/4/62	P1-8-11	P1-8-12	P	P	P	P4-11-13	P4- 8- 11
9	15/4/62	n/a 1-0-0	P1-4-9.5	P	P	P	P4-14-16	P4-12-14
117ก	15/4/62	P1-5-9	P1-2-6	P	P	P	P4-13-14	P4-11-12
181ก	15/4/62	n/a 1-0-0	n/a 1-0-0	P	P	P	P4-13-14	P4-10-11
181ข	15/4/62	P1-7-12	P1-6-14	P	P	P	P4-12-13	P4 -8 -9
182ก	15/4/62	P1-12-14	P1-12-14	P	P	P	P4 -10-11	P4 -8 -9
182ข	15/4/62	P1-10-12.5	P1-8-12.5	P	P	P	P4-11-12	P4-9-10

ที่มา: การทดสอบที่ย่านสถานีรถไฟชุมทางบางซื่อ เมษายน 2562

Tests and Evaluations

ตารางที่ 9 เกณฑ์ประเมินค่าความเสี่ยงต่อการปีนรางของล้อรถไฟสำหรับอุปกรณ์ที่ 1

ระยะช่วงที่อุปกรณ์สัมผัสกับลิ้นประแจ (มม.)	ระดับประเมิน	เกณฑ์ความเสี่ยงต่อการปีนราง
อุปกรณ์ไม่สัมผัสลิ้นประแจ	0	ไม่สามารถประเมินได้
13 - 15	1	น้อยมาก
10 - 12	2	น้อย
7 - 9	3	ปานกลาง
4 - 6	4	สูง
0 - 3	5	สูงมาก

Tests and Evaluations

ตารางที่ 10 เกณฑ์ประเมินค่าความเสี่ยงต่อการปีนรางของล้อรถไฟสำหรับอุปกรณ์ที่ 4

ระยะช่วงที่อุปกรณ์สัมผัสกับลิ้นประแจ (มม.)	ระดับประเมิน	เกณฑ์ความเสี่ยงต่อการปีนราง
อุปกรณ์ไม่สัมผัสลิ้นประแจ	0	ไม่สามารถประเมินได้
1 - 7	1	น้อยมาก
8 - 14	2	น้อย
15 - 21	3	ปานกลาง
22 - 28	4	สูง
มากกว่า 28	5	สูงมาก

Conclusion

- Wheel Rail Contact Inspection at Switch Points is proposed for SRT for the first time
- Methodology is based on Delaware and Norfork Southern, and applied to SRT Vidura Contour
- 4 Contact Gauges are developed for SRT
- Tests were done at Switch Points at Bangsue Locomotive Depot and Makkasan Work Shop
- Derailment Risk Levels are proposed basing on contact distance from Gauge No.1 and Gauge No.4 and test results

References

- Delaware: Zarembski, A. M. (2017). Switch Point Inspection Gauges to prevent Wheel Climb Derailments. University of Delaware. Technical Report.
- Profilidis: V.A.Profillidis. (1995). Railway Engineering : Derailment protection on switches and crossings. Democritus Thrace University, 193.
- KTH: Andersson, E., Berg, M., & Stichel, S. (2014). Rail Vehicle Dynamics : 9.2Flange Climbing - Derailment. Royal Institute of Technology.
- SRT, in Thai: ฝ่ายการช่างโยธา. (2559). คู่มือบำรุงทาง : ประแจ. การรถไฟแห่งประเทศไทย.

Appendix 2: Presentation slides of seminar and publication of the research project results

Project overview and introduction to railway inspection technology by Dr. Anat Hasap

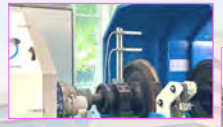

RTTC-TISTR
ISO/IEC 17025
Accreditation No.
Testing 0507

RTTC to promote rail industry and enhance Local Content Manufacturing


ISO/IEC 17025 accredited test services for rail components
Active rail projects : Thailand, Malaysia, Singapore, Indonesia, Philippine, Vietnam, Myanmar, Australia, etc.
Material test (Metal, non-metal, steel, concrete, rubber, GFRP, etc.
Sleeper and bearers (Wooden, Concrete, Composite, steel, etc)
Rail and Rail welding (FBW, ATW)
Fastening system
Insulated Rail Joint : IRJ


Accident and incident in transport require investigation, analysis, testing etc.
key test facilities in RTTC-TISTR
Universal Testing Machine 250, 500, 1,000, 2000, 5,000 kN
Material Fatigue test machine up to 10, 25, 250, 500 kN. 0.01 – 100Hz
Component Test-Line Multi-axial system (Hydraulic, pneumatic, electric) up to 20 axis, 500kN, 1200kN
4 Post tester for passenger car, light truck, EV, Etc. (100Hz, weight up to 5,000 kg)
Vibration test (ED-shaker) up to 2,800 Hz, payload 5,000 kgf
Bogie frame fatigue test, 13 axis, 100-500kn and Bogie Brake test, 1/2Axle, Full axle, max. 400 kph
Isolated strong floor, Test bed, Fixtures. (Customized to requirement)
Measurement instrument static and dynamic, Shock (16, 32, > 300 channels)
Sensors(Force, SG, LVDT, Accelerometer, etc)
Environment chamber, corrosion chamber
Portable Arm CMM (3.0m volume), Laser scanner
Non-destructive test (NDT)
3D Print (Metal and Composite, 1x1x0.6m, Etc.,
CAD, CAE, Simulation Softwares: Solidworks, Ansys, Abaqus, Simpack, LS-Dyna, MATLAB, Labview, Flexsim, Ect.


PROGRAM for Service life extension of rolling stock
บชส. Bogie Cement Hopper Wagon (Pressure Discharge) (BCP), บทธ. Bogie Container Flat Wagon (BCF.)
ASSOCIATION OF AMERICAN RAILROADS
EUROPEAN STANDARDS
Refer to relating standards, Technical requirement.
Prepare Proposal and items and method to be assessed.
Survey, assess and sampling of wagons
Running test, Data record and FEA of Key Elements
Lab. Testing (Remaining strength, Dynamic, Fatigue, Performance, etc.)
Report of assessment and propose for service life extension


Successful development of railway test infrastructures
(ISO/IEC 17025 accredited)
Example test VDO
Railway track components
Bending test of Rail welded joint

Example test VDO of RTTC-TISTR in track work components

Example test VDO of RTTC-TISTR in track work components

Example test VDO of RTTC-TISTR in rolling stock components

Background of the research project

- TISTR proposed a research project proposal titled Technical Cooperation for Research and Development and Implementation of Railway Inspection and Monitoring Technology to PGTF for South-South Cooperation in April 2021.
- TISTR was rewarded a grant From PGTF for South-South Cooperation and TICA in Nov 2021. The research contract (2022 – 2024) was signed between TISTR, UNDP and TICA.
- The objectives of the research project are :

1) To promote cooperation in railway technology transfer in ASEAN region.

2) To enhance the safety level of railway operations by developing local railway technologies and implementation in ASEAN countries.

3) To develop railway research network and implementation in ASEAN countries through the sharing of knowledge and infrastructures, co-research, and promoting self-reliant railway technologies.

4) To enhance regional connectivity for sustainable development.

- TISTR conducted the project in Thailand and cooperated with Partners in Malaysia, Indonesia and Laos PDR.

THE GROUP OF 77
Executive Secretariat
New York

PEREZ-GUERRERO TRUST FUND FOR SOUTH-SOUTH COOPERATION,
MEMBERS OF THE GROUP OF 77
GOVERNMENT OF THAILAND

Type of project:	Inter-Regional
Title:	INT/22/K08 – Technical Cooperation for Research and Development and Implementation of Railway Inspection and Monitoring Technology
Sector:	Transportation
Beneficiaries:	Railway Sectors in Thailand, Malaysia, and Indonesia
Duration of project:	August 2022 – June 2024

ASEAN's railway investment plans are crucial for enhancing regional connectivity, promoting economic growth, and ensuring sustainable development. These projects reflect the region's commitment to building a more integrated and prosperous future, with continued support from international partners and a focus on sustainable practices being key to their success.

Some the major railway investment plans in ASEAN region:

1. Trans-Asian Railway Network
- ❑ to connect Southeast Asia with South Asia, Central Asia, and Europe through an integrated rail network.
- ❑ Significant portions are under development, such as the China-Laos Railway (opened in Dec. 2021) and aims to enhance connectivity from Laos to other ASEAN countries and China.

2. China-Laos Railway
- ❑ Part of BRI. It has boosted trade, transported millions of passengers and tons of cargo, and promoted regional economic integration.

3. Malaysia 's Railway Projects: some of the major ongoing railway projects:
- ❑ East Coast Rail Link (ECRL) 665-kilometer standard gauge double-track, 2024-2027.
- ❑ Kuala Lumpur-Singapore High-Speed Rail (HSR) 335-kilometer currently suspended for reviewed
- ❑ Rapid Transit System (RTS) Link utilize a Light Rail Transit (LRT) system 2021-2026.

4. Indonesia's Jakarta-Bandung High-Speed Railway
- ❑ aims to cut travel time between Jakarta and Bandung, enhancing urban connectivity and economic activity.
- ❑ Collaboration between Indonesia and China, with a focus on modernizing Indonesia's rail infrastructure.

5. Philippines' North-South Commuter Railway (NSCR)
- ❑ The NSCR aims to connect Metro Manila to Clark International Airport, improving urban mobility and accessibility to economic zones.
- ❑ Expected to start partial operations by 2027 and full operations by 2029.

6. Thailand's Railway Upgrades
- ❑ Multiple railway projects, including the Bangkok-Nong Khai high-speed rail, to connect to the China-Laos railway, enhancing connectivity between Thailand, Laos, and China.
- ❑ Significant investments from both domestic sources and international loans.

7. Vietnam's North-South Express Railway
- ❑ The high-speed rail line connecting Hanoi and Ho Chi Minh City, aiming to reduce travel time and boost economic activities along the route.
- ❑ The project is expected to attract international investments and loans, with ongoing feasibility studies and planning.

Challenges and Funding

Large-scale infrastructure projects requires substantial financial resources. ASEAN countries are addressing these needs through a mix of domestic financing, foreign direct investment, and international loans. However, challenges such as debt sustainability and environmental impacts need to be managed carefully.

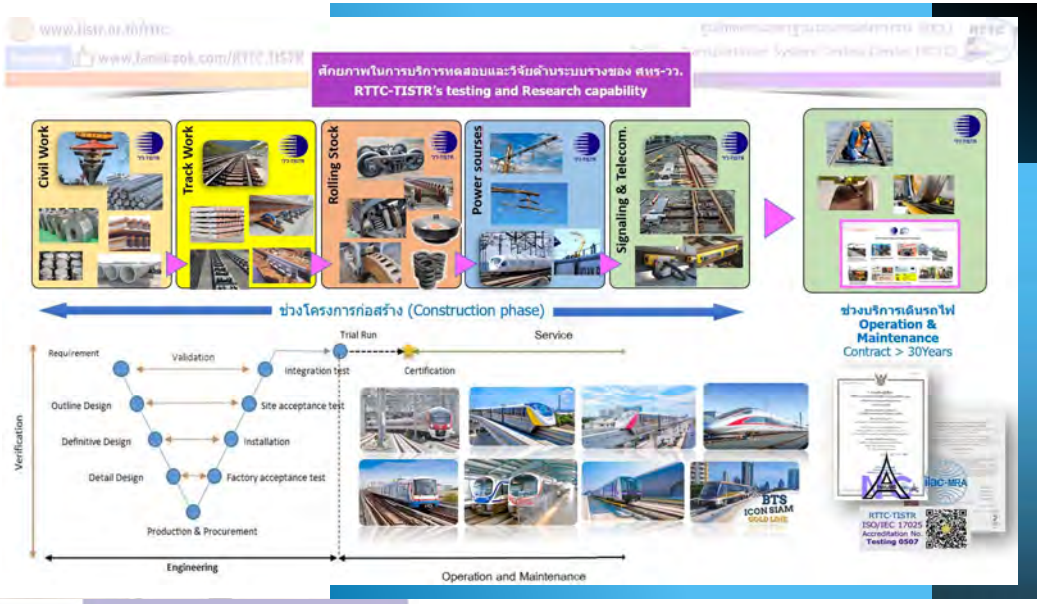

Primary failure modes of railway tracks leading to derailment

1. Rail Cracks and Fractures
- ❑ Cause: High stress, material fatigue, manufacturing defects, or corrosion
- ❑ Effect: Can lead to sudden rail breaks, posing significant derailment risks.
- ❑ Mitigation: Regular ultrasonic testing, rail grinding, and timely replacement of damaged rails.

2. Track Misalignment (Track Geometry Defects)
- ❑ Cause: Soil settlement, thermal expansion and contraction, poor construction, or maintenance practices.
- ❑ Effect: Results in uneven track, leading to poor ride quality and increased derailment risk.
- ❑ Mitigation**: Routine track inspection and maintenance, including tamping and realignment.

3. Wear
- ❑ Cause: Continuous wheel-rail contact, particularly on curves, leading to plastic deformation and wear.
- ❑ Effect: Can cause rail profile changes, affecting the stability of trains.
- ❑ Mitigation: Regular rail grinding and replacing worn-out rails.

4. Ballast Fouling
- ❑ Cause: Contamination by fines, wear particles, or biological materials.
- ❑ Effect: Reduces drainage and track stability, leading to uneven settlement.
- ❑ Mitigation: Periodic ballast cleaning or replacement, proper drainage maintenance.

5. Sleeper (Tie) Failure
- ❑ Cause: Material degradation, mechanical damage, or excessive loading.
- ❑ Effect: Results in reduced support for the rails, leading to gauge widening and instability.
- ❑ Mitigation: Regular inspection and replacement of damaged sleepers.

6. Fastener Failure
- ❑ Cause: Corrosion, mechanical wear, or inadequate fastening systems.
- ❑ Effect: Leads to loose rails, gauge widening, and track instability.
- ❑ Mitigation: Regular inspection and replacement of fasteners, use of corrosion-resistant materials.

7. Buckling
- ❑ Cause: Extreme heat causing thermal expansion, combined with inadequate rail anchoring.
- ❑ Effect: Sudden lateral displacement of the track, leading to derailments.
- ❑ Mitigation: Using rail expansion joints, stressing rails properly during installation, and monitoring track temperature.

8. Subgrade Failure
- ❑ Cause: Poor soil conditions, water infiltration, or inadequate compaction.
- ❑ Effect: Leads to uneven settlement and loss of track support.
- ❑ Mitigation: Proper subgrade preparation, use of geotechnical solutions, and maintaining effective drainage systems.

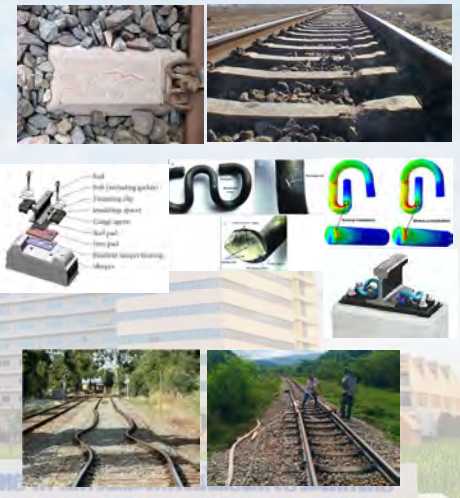

How to avoid the track failure
- ❑ Effective track maintenance and regular inspections are crucial to identify and mitigate these failures.
- ❑ Utilizing advanced technologies such as ultrasonic testing, track geometry monitoring, and real-time sensor data to enhance track safety and reliability can prevent accidents and extend the lifespan of railway infrastructure.

Primary failure modes for rolling stock and railway vehicles:

1. Wheel and Axle Failures
- Cause: Fatigue crack, excessive wear, thermal stress, and impacts.
- Effect: lead to derailments, loss of stability, and increased maintenance costs.
- Mitigation: Regular ultrasonic and magnetic particle inspections, lubrication, timely replacement of worn parts.

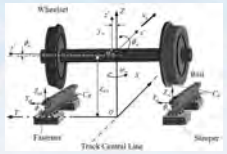


2. Brake System Failures
- Cause: Wear and tear of brake components, hydraulic or pneumatic system leaks, and electronic control failures.
- Effect: Reduced braking efficiency, longer stopping distances, and potential collisions.
- Mitigation: Frequent inspections and maintenance of brake systems, monitoring of pad and disc, ensuring proper fluid levels.

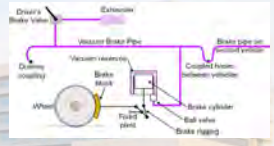


3. Suspension System Failures
- Cause: Fatigue of suspension springs, dampers, and bushings, as well as mechanical damage.
- Effect: Poor ride quality, increased wear on other components, and potential derailments.
- Mitigation: Regular inspections and replacement of worn suspension parts, and monitoring for signs of mechanical fatigue.

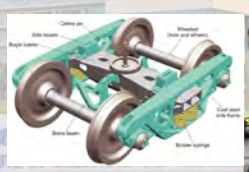

4. Electrical System Failures
- Cause: Short circuits, component overheating, battery failures, and wiring issues.
- Effect: Loss of critical functions, such as lighting, control systems, and safety mechanisms.
- Mitigation: Routine electrical system inspections, using high-quality components, and ensuring proper insulation and cooling.

5. Structural Failures
- Cause: Metal fatigue, corrosion, and impacts.
- Effect: loss of structural integrity leading to collapses or failures during operation.
- Mitigation: Regular structural inspections, using corrosion-resistant materials, and applying protective coatings.

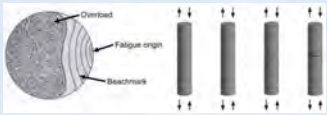

6. Coupling Failures
- Cause: Mechanical wear, misalignment, and impact damage.
- Effect: Separation of train cars, leading to potential accidents and operational disruptions.
- Mitigation: Frequent inspection and maintenance of couplings, ensuring proper alignment and fitment .


7. Bearing Failures
- Cause: Insufficient lubrication, contamination, and excessive load.
- Effect: Increased friction, overheating, and potential axle failures.
- Mitigation: Regular lubrication, using high-quality bearings, and monitoring for signs of wear and contamination.


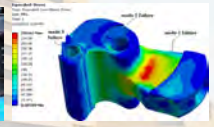

8. Door System Failures
- Cause: Mechanical wear, electronic control issues, and physical obstructions.
- Effect: Doors not open or close properly, leading to safety hazards for passengers.
- Mitigation: Regular maintenance of door mechanisms, checking electronic control systems, and ensuring clear pathways for door operation.



How to avoid the rolling stock failure
- Realizing their failure modes through proactive inspection.
- Implementing stringent maintenance schedules, use of advanced diagnostic tools, employing modern technologies for real-time monitoring can significantly reduce the risk of failures and improve overall operational efficiency.

Modern inspection technologies in the railway industry

Modern inspection tech. have advanced significantly, leveraging AI, IoT, and other innovations to enhance Safety, Efficiency, and Reliability.

1. **Ultrasonic Inspection and Eddy current**: allow daily long-distance inspection identifying surface and internal Flaws. It can significantly speeds up the inspection process and increases the accuracy of defect detection.
2. **Predictive Maintenance**: use AI and machine learning to forecast equipment failures. For example using wireless IoT sensors for real-time safety monitoring and prediction of wheel and bearing failures, thus reducing maintenance costs and preventing potential failures.
3. **AI and Machine Vision**: use high pixel cameras to capture ultra-high-resolution images, and AI algorithms to analyse these images to detect defects, allowing for proactive maintenance and enhanced safety.
4. **Autonomous Inspection**: use sensors and algorithms to measure in real-time, such as track geometry and rail wear, offering comprehensive assessments of track conditions. No manual inspection is needed, thus increasing efficiency and reducing operational disruptions.
5. **Internet of Trains (IoT):** play crucial role in modern rail inspections by enabling condition-based monitoring. It helps prevent delays caused by track and train part failures by optimizing maintenance schedules and improving overall reliability. It provides railway operators with data-driven insights to enhance fleet control and operational efficiency.

These technologies collectively enhance the safety, efficiency, and reliability of railway operations by enabling more accurate, real-time inspections and maintenance planning.


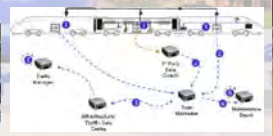
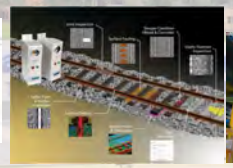


RTTC's Modern Inspection and Mmonitoring technologies


เทคโนโลยีตรวจสอบเฝ้าระวังน้ำหนักบรรทุกรถไฟ (RAWLOC)


เทคโนโลยีตรวจวัดน้ำหนักรถไฟพลวัตร (IWS)


เทคโนโลยีตรวจสอบความบกพร่องของทางรถไฟ (RFD)


เทคโนโลยีตรวจวิเคราะห์การใช้งานระบบรถไฟ (RSM)

เทคโนโลยีตรวจวิเคราะห์การขนส่งหลายรูปแบบ (IDENT)


RTTC 4 Post for full-scale test for **Battery Vehicle**

www.tistr.or.th/rttc
anat@tistr.or.th
patcharee_a@tistr.or.th

ศูนย์ทดสอบมาตรฐานระบบขนส่งทางราง (ศทร)
Railway Transportation System Testing Center (RTTC)

RTTC-TISTR research project funded by UNDP (PGTF) and TICA

Research project : Technical Cooperation for Research and Development and Implementation of Railway Inspection and Monitoring Technology

Installation and field demonstration on track in Thailand, Indonesia and Malaysia

Pérez-Guerrero Trust Fund for South-South Cooperation (PGTF)

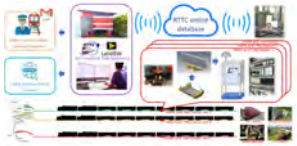

Page25

Train Weight Device (TWD)

Invented by RTTC-TISTR under UNDP-TICA fund.

- The TWD can quickly be installed in existing railway infrastructure, without removing the sleeper and modifying the railway track.
- Weighing the train without stop the train.
- Information from TWD can be used to accurately determine the gross weight of goods in rail transport, weight balance of every single bogie, early-stage symptoms of train abnormality and re-check of train speed.
- Real-time data monitoring and cloud data collection.

Technical specification

Item	specification
1. TWD controller cabinet	
1.1 Power input	Single phase 220V, 16A, 50Hz or Battery 24V (45Ah)
1.2 Nominal power consumption	Normal 150W (1,200W max. in case restart)
1.3 Data interface	Cellular router 4G/3G
1.4 Enclosure dimension	W450mm x D330mm x H1070mm. (appx. 37kg.)
1.5 Enclosure installation method	On ground fixed to RC block
1.6 Operation temperature	0°c to 50°c
1.7 Degree of protection	Waterproof enclosure IP66
2. TWD Sensor	
2.1 Rail section	BS100A, EN54E1, UIC60 (Adjustable to any size)
2.2 Sensor installation method	Mechanical fixed
2.3 Number of installation point	4 points sensor (2 on left and 2 on right)
2.4 Sensor installation span	600mm. – 1200mm.
2.5 Sensor dimension	W400mm x D245mm x H66mm. (appx. 9kg./sensor)
2.6 Signal cable	2 x signal cables/sensor (Total 8 cable)
2.7 Maximum voltage resistance	50V
2.8 Degree of protection	Waterproof sensor

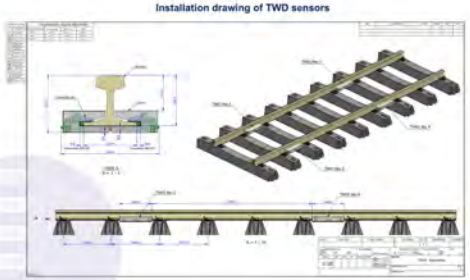

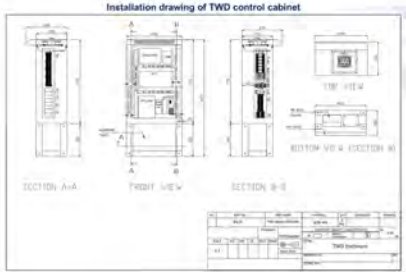

Inspection and Monitoring of large structures
ศทร-วว. พัฒนางานตรวจสอบและเฝ้าระวังโครงสร้าง

- Inspect/monitor road bridge & railway bridge ตรวจสอบ/เฝ้าระวังสะพานทางหลวง สะพานรถไฟ
- Inspect/monitor safety and reliability of track and large structure ตรวจสอบ/เฝ้าระวัง ความมั่นคงปลอดภัยของโครงสร้างโยธาขนาดใหญ่ อื่นๆ

Rama VI Bridge
Location: Bangkok
Age: 97 years
Distance: 442 m.

Technology to be implemented

- Structural model and simulation
- Structural measurement and analysis
- Inspection and maintenance
- Monitoring (online, long-term)
- Failure/life prediction

Krung Thon bridge
(Sang Hee)
Location: Bangkok
Age: 66 years
Distance: 648.9 m.

Phra Phuttha Yodfa Bridge,
(Memorial Bridge)
Location: Bangkok
Age: 92 years
Distance: 229.76 m.

สรุปบัญชีสะพานทางหลวงชนบท ประจำปีงบประมาณ 2568

ลำดับที่	หน่วยงาน	สะพานคอนกรีต		สะพานเหล็ก		สะพานไม้		สะพานข้ามแม่น้ำลำคลอง	
		จำนวน (แห่ง)	ความยาว (ม.)	จำนวน (แห่ง)	ความยาว (ม.)	จำนวน (แห่ง)	ความยาว (ม.)	จำนวน (แห่ง)	ความยาว (ม.)
1	สำนักงานทางหลวงชนบทที่ 1 (ปทุมธานี)	53	6,286.00	398	16,017.24	-	-	-	-
2	สำนักงานทางหลวงชนบทที่ 2 (สระบุรี)	73	9,171.00	302	10,803.60	2	865.00	-	-
3	สำนักงานทางหลวงชนบทที่ 3 (ระยอง)	45	4,833.50	414	15,687.70	13	6,547.00	-	-
4	สำนักงานทางหลวงชนบทที่ 4 (เพชรบุรี)	90	10,449.70	880	28,288.30	11	4,214.00	-	-
5	สำนักงานทางหลวงชนบทที่ 5 (นครราชสีมา)	107	12,744.50	495	17,083.80	8	4,542.98	-	-
6	สำนักงานทางหลวงชนบทที่ 6 (ขอนแก่น)	111	12,832.00	518	16,033.90	1	810.00	-	-
7	สำนักงานทางหลวงชนบทที่ 7 (อุบลราชธานี)	78	11,527.00	673	23,240.00	2	705.00	-	-
8	สำนักงานทางหลวงชนบทที่ 8 (นครสวรรค์)	115	14,255.00	417	15,658.00	2	729.00	-	-
9	สำนักงานทางหลวงชนบทที่ 9 (อุดรธานี)	159	15,176.93	380	13,458.80	2	394.00	-	-
10	สำนักงานทางหลวงชนบทที่ 10 (เชียงใหม่)	119	13,222.00	476	17,050.60	12	4,826.30	-	-
11	สำนักงานทางหลวงชนบทที่ 11 (สุราษฎร์ธานี)	103	10,535.00	639	26,372.82	4	2,725.50	-	-
12	สำนักงานทางหลวงชนบทที่ 12 (สงขลา)	59	7,243.40	757	23,907.40	1	72.00	-	-
13	สำนักงานทางหลวงชนบทที่ 13 (นครปฐม)	131	9,438.14	462	20,722.35	10	3,739.14	-	-
14	สำนักงานทางหลวงชนบทที่ 14 (กรมรี)	69	8,133.50	477	19,669.50	3	1,690.00	-	-
15	สำนักงานทางหลวงชนบทที่ 15 (อุดรธานี)	73	6,115.60	461	12,634.73	1	292.33	-	-
16	สำนักงานทางหลวงชนบทที่ 16 (กาฬสินธุ์)	70	10,484.00	711	23,003.10	1	2,040.00	-	-
17	สำนักงานทางหลวงชนบทที่ 17 (เชียงราย)	94	12,724.00	537	21,133.00	7	3,989.00	-	-
18	สำนักงานทางหลวงชนบทที่ 18 (สุพรรณบุรี)	97	10,593.00	362	10,855.60	3	993.00	-	-
19	สำนักบำรุงทาง	-	-	29	2,095.00	72	51,055.40	13	7,676.00
	รวม	1,626	185,762.27	9,388	333,715.44	155.00	90,229.65	13	7,676.00
	รวมทั้งสิ้น	11,182							





THANK YOU

Dr.Anat Hasap
Director of RTTC-TISTR
081-4244221
anat@tistr.or.th

TWD technology the development implementation and future application by Dr. Worawat Songkitti and Mr. Sarawut Saengvichien

www.tistr.or.th/rttc
sarawut@tistr.or.th
worawat_son@tistr.or.th

ศูนย์ทดสอบมาตรฐานระบบขนส่งทางราง (ศทร)
Railway Transportation System Testing Center (RTTC)

The development of local technology for Train Weight Device (TWD)

สถาบันวิจัยวิทยาศาสตร์และเทคโนโลยีแห่งประเทศไทย (วว)
Thailand Institute of Scientific and Technological Research (TISTR)

Content

1 Background and motivation

Railway Transportation System Testing Center (RTTC)
www.facebook.com/RTTC.TISTR

- Rapid expansion of the global railway network
- Effective and optimum maintenance strategy (Predictive/RSHM)
- Permission of the private sector to operate the train fleet

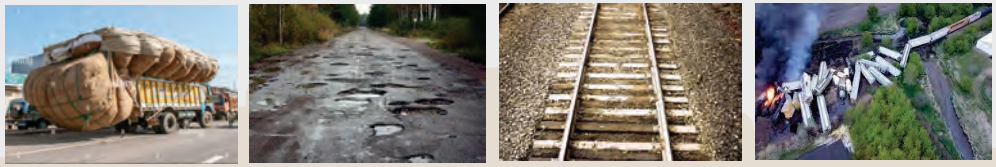

Commercial Wheel Load Detector

Railway Transportation System Testing Center (RTTC)
www.facebook.com/RTTC.TISTR

Vehicle side	Wayside

2 System architecture and working principle

Railway Transportation System
Testing Center (RTTC)
www.facebook.com/RTTC.TISTR

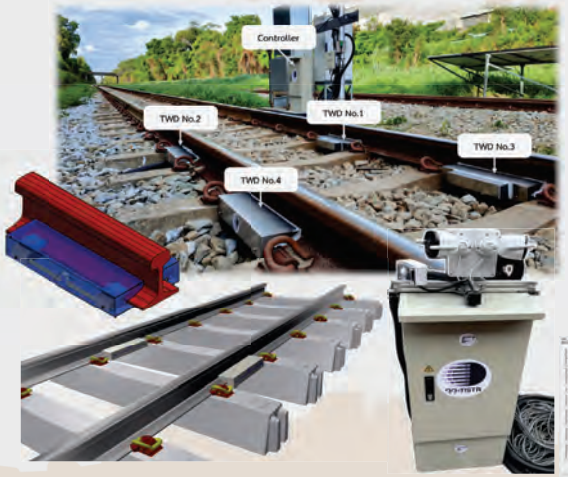

Train Weight Device (TWD)

- The TWD can be quickly installed in existing railway infrastructure, without removing the sleeper and without modification of the railway roadbed.
- Weighing the train made it easy.
- Information from TWD can help to know the gross weight, weight balance, and speed measurement in the measuring zone for train passing.
- Real-time data monitoring.
- Able to identify every train when it passed and check suspicious trains and fast fault alarms with email.

System overview
Train Weight Device (TWD)

Railway Transportation System
Testing Center (RTTC)
www.facebook.com/RTTC.TISTR


RTTC remote software

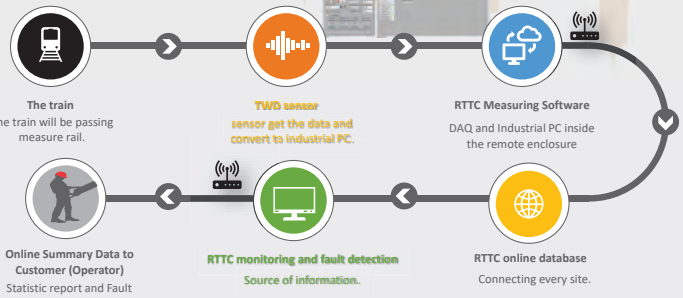


RTTC monitoring and fault detection software

Site measurement and detector

Site measurement and detector

RTTC remote enclosure (instument)

RTTC monitoring and fault detection

System overview
Installation of Train Weight Device (TWD)

Railway Transportation System
Testing Center (RTTC)
www.facebook.com/RTTC.TISTR


TWD install on the track

TWD sensor

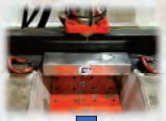


RTTC remote software


Remote enclosure

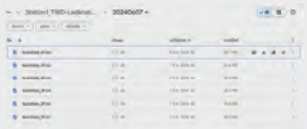
Data base


RTTC monitoring and fault detection software

System overview
Train Weight Device (TWD)

Railway Transportation System
Testing Center (RTTC)
www.facebook.com/RTTC.TISTR


Online Summary Data to Customer (Operator)


Online Summary Data to website (In the future)

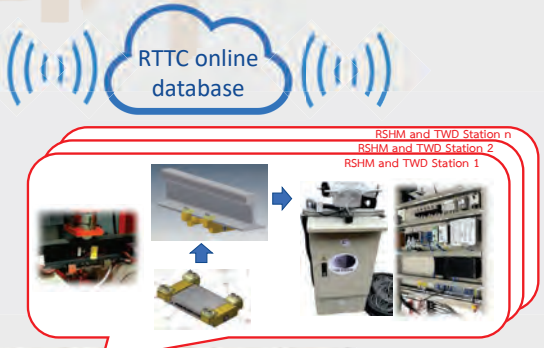

3 Overview of TWD Development

Railway Transportation System
Testing Center (RTTC)
www.facebook.com/RTTC.TISTR

Conceptual Design | Concept Validation | On site Calibration | On site validation

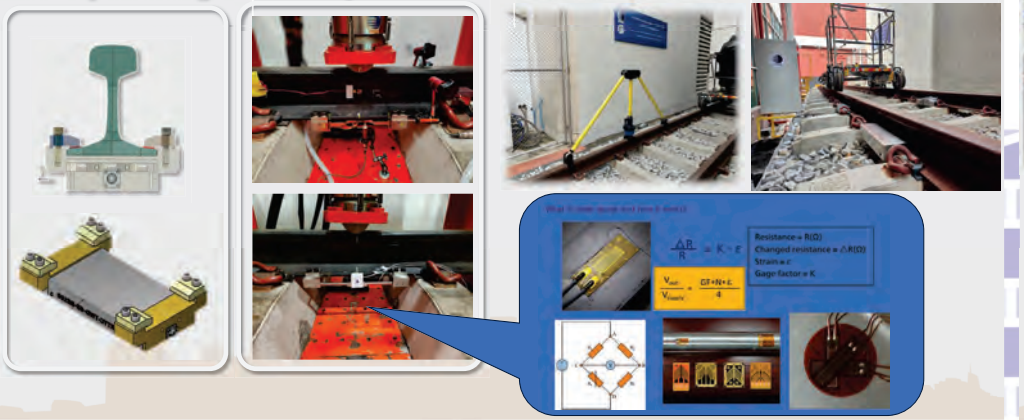

RTTC's Applications of SG in rail sector

Railway Transportation System
Testing Center (RTTC)
www.facebook.com/RTTC.TISTR

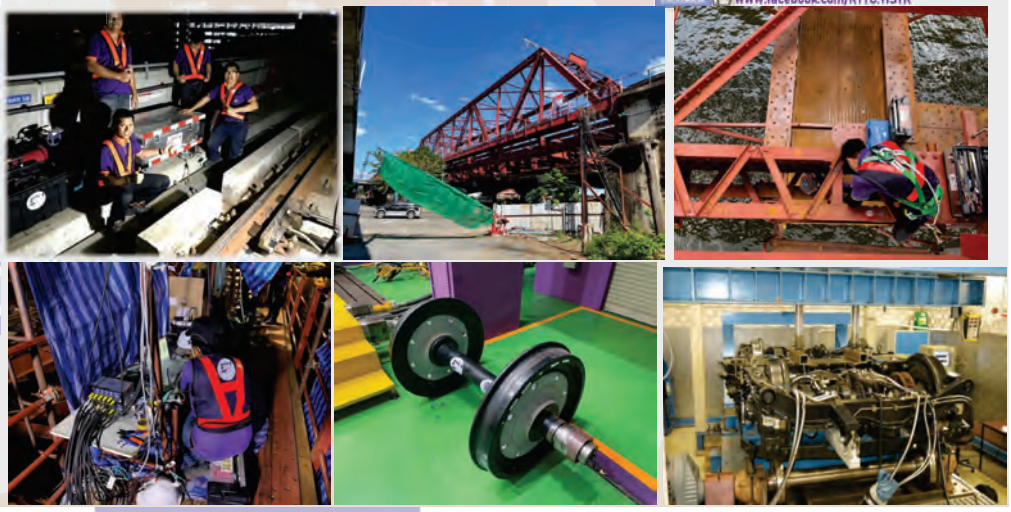

Simulation of TWD with FEA

Railway Transportation System
Testing Center (RTTC)
www.facebook.com/RTTC.TISTR

Simulation assisted design

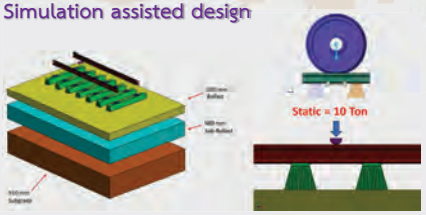

Coupling between element

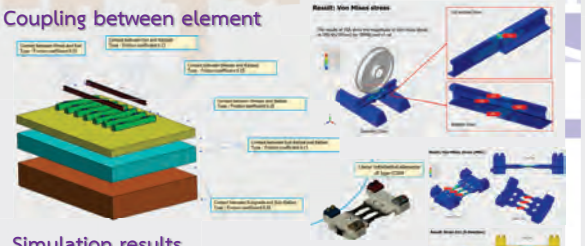

Load and Boundary conditions

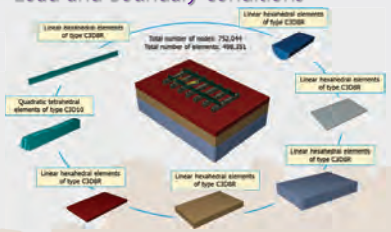

Simulation results

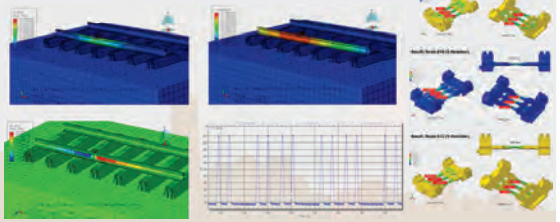

On site calibration and running test result

Railway Transportation System
Testing Center (RTTC)
www.facebook.com/RTTC.TISTR

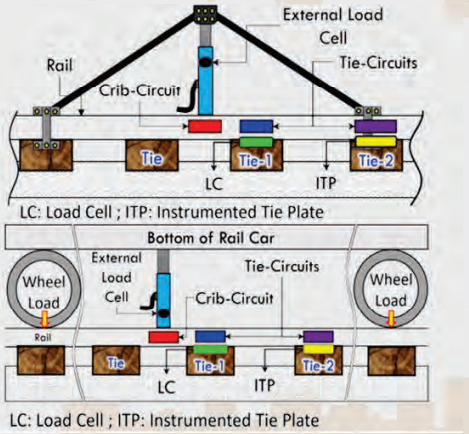

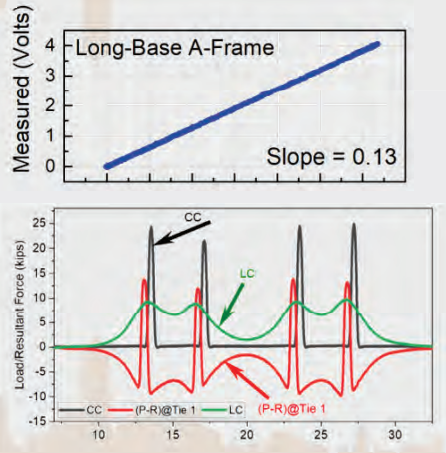

4 RTTC MONITORING SOFTYWARE

Railway Transportation System
Testing Center (RTTC)
www.facebook.com/RTTC.TISTR

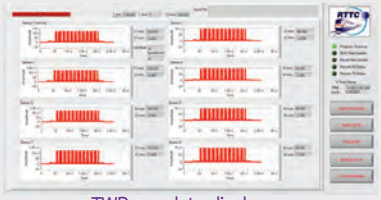
TWD raw data display


Data set of the train

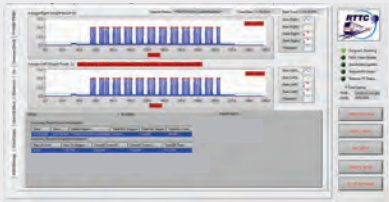
Summary data in case normal

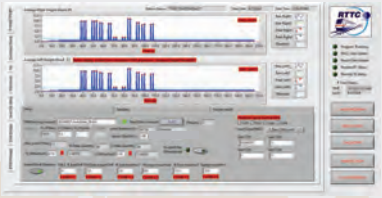
Data processing and fault setup

RTTC MONITORING SOFTYWARE (continue)

Railway Transportation System
Testing Center (RTTC)
www.facebook.com/RTTC.TISTR


Summary data in case fault

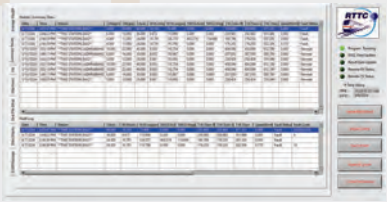
Statistical data and fault logger


Email sender setup

5 TWD validation at RTTC laboratory

Railway Transportation System
Testing Center (RTTC)
www.facebook.com/RTTC.TISTR

A. Static validation
B. Dynamic validation
C. Train wheel load simulation
D. Experimental track test

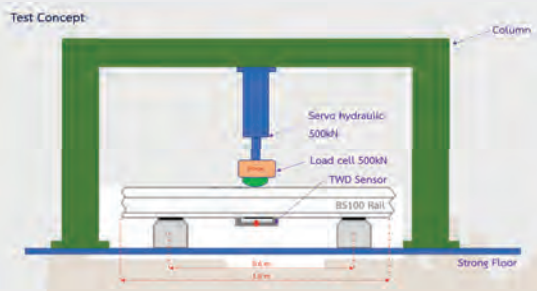

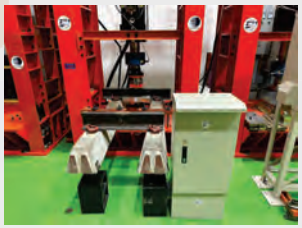

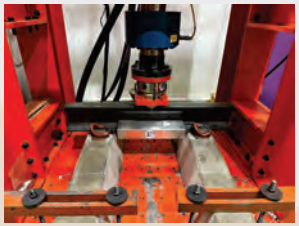

www.tistr.or.th/rttc
sarawut@tistr.or.th
worawat_son@tistr.or.th

ศูนย์ทดสอบมาตรฐานระบบขนส่งทางราง (ศทร)
Railway Transportation System Testing Center (RTTC)

A. Static validation result of TWD

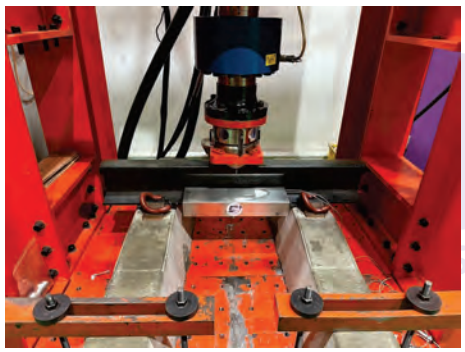
Static test setup

Noise floor = ± 3uε

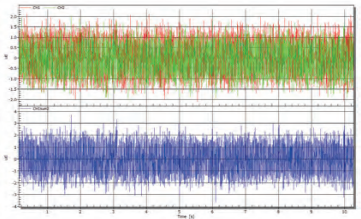
Output strain of each sensor

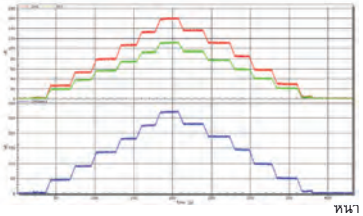

หน้า 16

www.tistr.or.th/rttc
sarawut@tistr.or.th
worawat_son@tistr.or.th

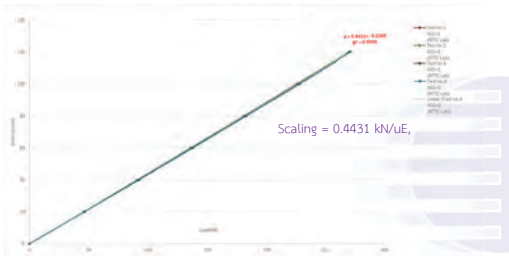

Standard force(kN)	Measuring Force (kN)			
	Test no.1 SG1+2 (RTTC Lab)	Test no.2 SG1+2 (RTTC Lab)	Test no.3 SG1+2 (RTTC Lab)	Test no.4 SG1+2 (RTTC Lab)
0	0	0	0	0
20	19.86	19.86	19.93	20.02
40	39.71	39.75	40.33	40.32
60	59.60	59.60	60.25	60.42
80	79.46	79.55	80.29	80.28
100	99.11	99.31	100.21	100.05
120	118.84	118.78	119.52	119.46
File Date	16022024			

Standard force(kN)	%Error			
	Test no.1 SG1+2 (RTTC Lab)	Test no.2 SG1+2 (RTTC Lab)	Test no.3 SG1+2 (RTTC Lab)	Test no.4 SG1+2 (RTTC Lab)
0	0.00%	0.00%	0.00%	0.00%
20	0.69%	0.71%	0.37%	-0.09%
40	0.73%	0.63%	-0.82%	-0.81%
60	0.66%	0.66%	-0.41%	-0.70%
80	0.67%	0.56%	-0.36%	-0.35%
100	0.89%	0.69%	-0.21%	-0.05%
120	0.97%	1.02%	0.40%	0.45%
Minimum Error	0.66%	0.56%	-0.82%	-0.81%
Maximum Error	0.97%	1.02%	0.40%	0.45%

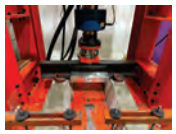

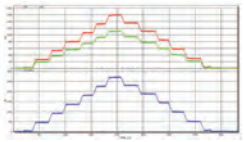

www.tistr.or.th/rttc
sarawut@tistr.or.th
worawat_son@tistr.or.th

ศูนย์ทดสอบมาตรฐานระบบขนส่งทางราง (ศทร)
Railway Transportation System Testing Center (RTTC)

Static calculating force result

Max. error = 1.02%

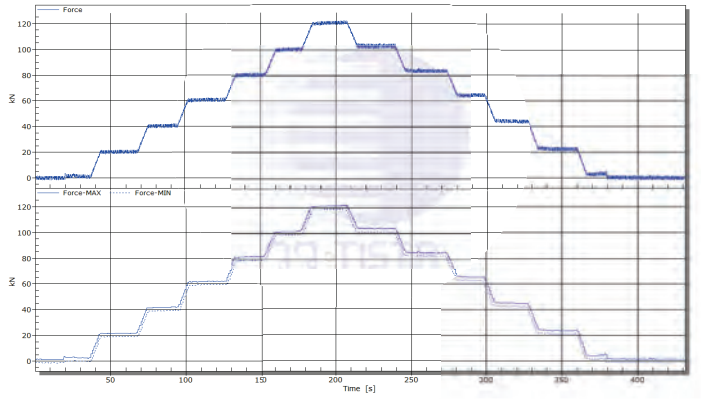

www.tistr.or.th/rttc
sarawut@tistr.or.th
worawat_son@tistr.or.th

ศูนย์ทดสอบมาตรฐานระบบขนส่งทางราง (ศทร)
Railway Transportation System Testing Center (RTTC)

B. Dynamic validation result of TWD

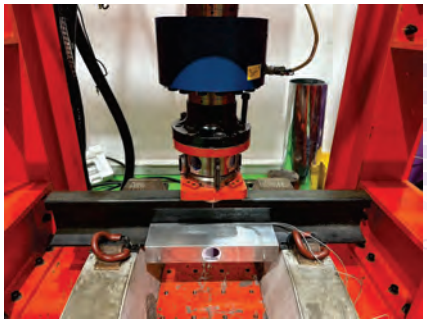

Dynamic test setup

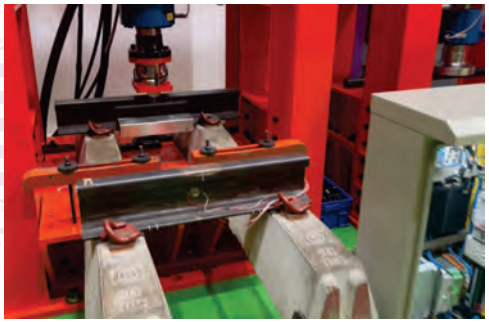

Dynamic testing VDO

www.tistr.or.th/rttc
sarawut@tistr.or.th
worawat_son@tistr.or.th

ศูนย์ทดสอบมาตรฐานระบบขนส่งทางราง (ศทร)
Railway Transportation System Testing Center (RTTC)

Dynamic result

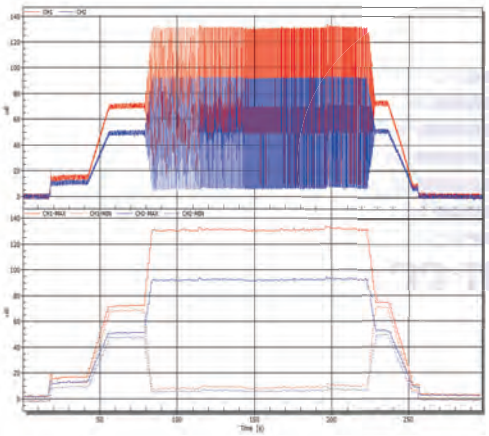

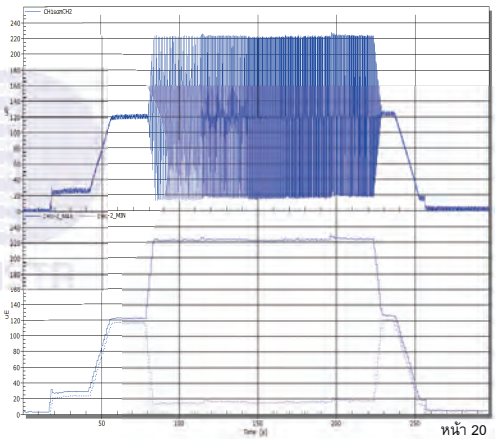

www.tistr.or.th/rttc
sarawut@tistr.or.th
worawat_son@tistr.or.th

Dynamic calculating force result

Max. error = 0.48%

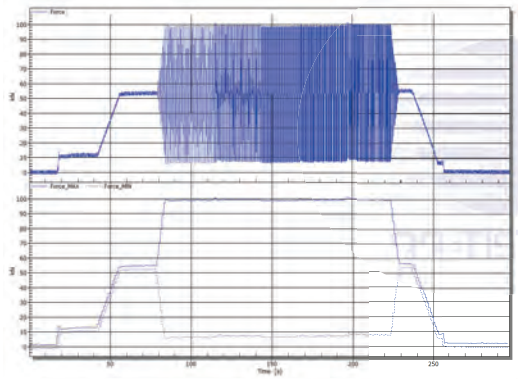

Close up the dynamic force @ 5Hz

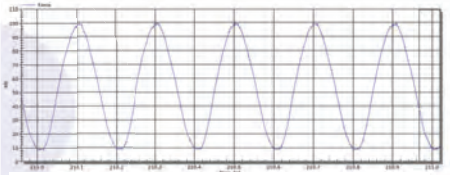

Noise floor of dynamic force

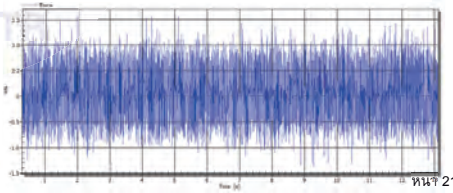

www.tistr.or.th/rttc
sarawut@tistr.or.th
worawat_son@tistr.or.th

ศูนย์ทดสอบมาตรฐานระบบขนส่งทางราง (ศทร)
Railway Transportation System Testing Center (RTTC)

Dynamic force result in each frequency

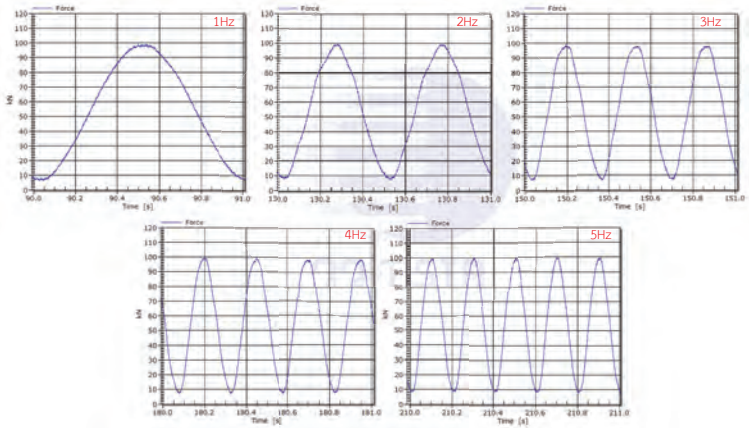

www.tistr.or.th/rttc
sarawut@tistr.or.th
worawat_son@tistr.or.th

ศูนย์ทดสอบมาตรฐานระบบขนส่งทางราง (ศทร)
Railway Transportation System Testing Center (RTTC)

C. Train wheel load simulation result of TWD

Force Setpoint
Force Min = 5kN
Force Max = 100kN
Ramp up time = 500ms
Ramp down time = 500ms

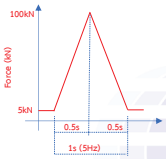

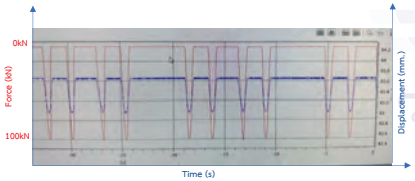

Servo actuator

Freight wagon weight simulation (100kN)

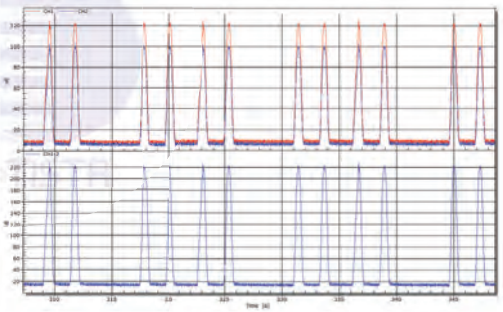

TWD Reading

www.tistr.or.th/rttc
sarawut@tistr.or.th
worawat_son@tistr.or.th

ศูนย์ทดสอบมาตรฐานระบบขนส่งทางราง (ศทร)
Railway Transportation System Testing Center (RTTC)

Train weight simulation result

Max. error = 1.3%

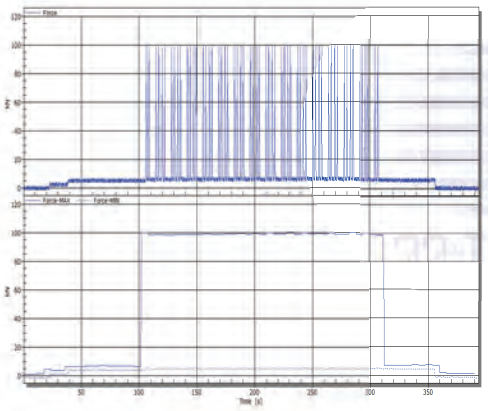

Close up the dynamic force

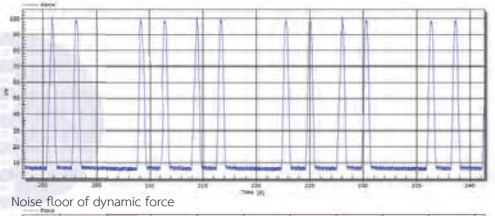

Noise floor of dynamic force

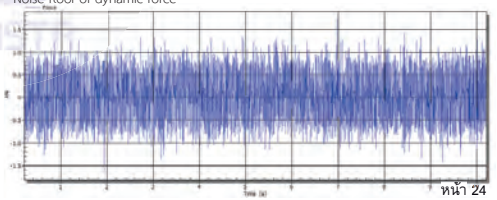

www.tistr.or.th/rttc
sarawut@tistr.or.th
worawat_son@tistr.or.th
ศูนย์ทดสอบมาตรฐานระบบขนส่งทางราง (ศทร)
Railway Transportation System Testing Center (RTTC)

D. Experimental Track Test

Testing video

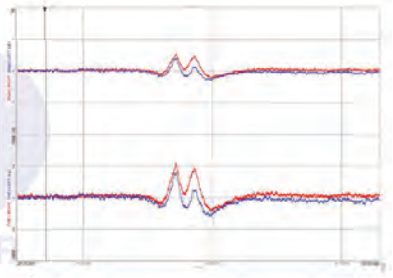

TWD Reading

www.tistr.or.th/rttc
sarawut@tistr.or.th
worawat_son@tistr.or.th
ศูนย์ทดสอบมาตรฐานระบบขนส่งทางราง (ศทร)
Railway Transportation System Testing Center (RTTC)

Data processing test

Raw data processing with our algorithm

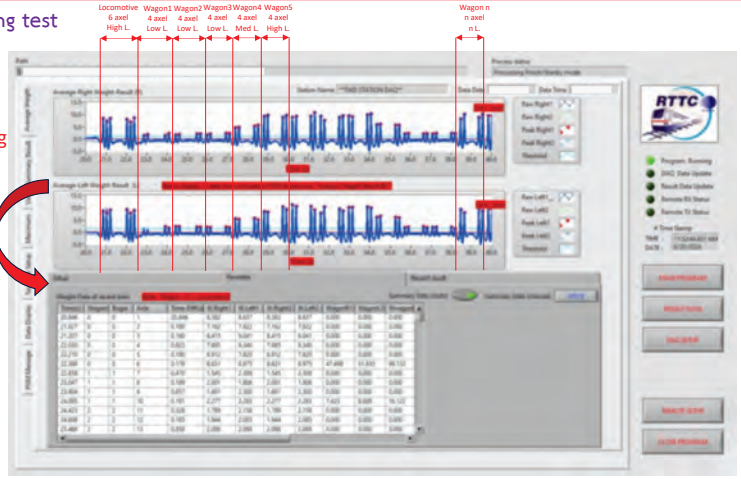

6 On-site calibration tool for TWD

Railway Transportation System Testing Center (RTTC) www.facebook.com/RTTC.TISTR

A-Frame for TWD validation on the track

Master loadcell and hydraulic jack

7 Water proof of enclosure test

Railway Transportation System Testing Center (RTTC) www.facebook.com/RTTC.TISTR

Water proof test video

Water proof inspection

8 TWD installation in Thailand

at SRT Laem Chabang station

Railway Transportation System
Testing Center (RTTC)
www.facebook.com/RTTC.TISTR

A. Installation Detail

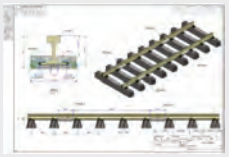

TWD installation drawing

TWD installation on field site

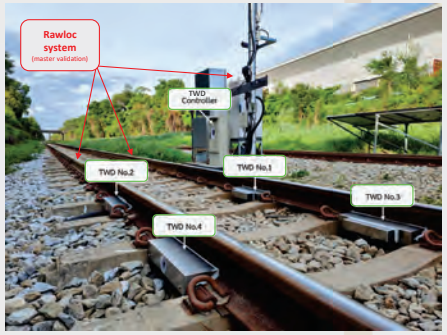

The RAWLOC system connect to TWD system on field site

Train passing TWD video

Weight result from TWD

8 TWD installation in Thailand

at SRT Laem Chabang station

Railway Transportation System
Testing Center (RTTC)
www.facebook.com/RTTC.TISTR

The train are passing measure station

The TWD are measuring weight of the train.

- TWD measured data = 13 trainset
- TWD validation = 3 trainset (1 day)
- Master validation data = From Rawloc system
- TWD recorded data = 13 trainset (3 day)
- TWD software = Good transferring and processing data
- TWD setup and communication = Easy and Stable
- TWD Accuracy= Good accuracy for dynamic

9 TWD installation in Overseas

Railway Transportation System
Testing Center (RTTC)
www.facebook.com/RTTC.TISTR

Onsite TWD installation.

TWD Software monitoring.

TWD enclosure.

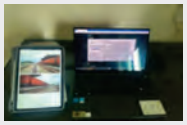

Remote monitoring.

The train are passing measure station video

- TWD measured data = 4 trainset (1 day)
- TWD validation = 1 trainset
- Master validation data = From operator
- TWD recorded data = 4 trainset
- TWD rail type = Difference from Thailand
- TWD software = Good transferring and processing data
- Internet Network = Difference from Thailand
- TWD setup and communication = Easy and Stable
- TWD Accuracy= Good accuracy for dynamic

10 TWD Demonstrate and Seminar

Railway Transportation System
Testing Center (RTTC)
www.facebook.com/RTTC.TISTR

Onsite demonstration at KAI Medan and organizing a training seminar at Universitas Sumatera Utara (USU)

11 Summary of Research Project

Railway Transportation System
Testing Center (RTTC)
www.facebook.com/RTTC.TISTR

1. The TWD system can easily install and fast measure of dynamic weight for reduced time to measure and easy to access data everywhere.
2. The TWD system can accurately measure dynamic weight and validate weight and speed.
3. The TWD result can indicate a fault of wheel and wagon following limitation or standard.
4. The Statistical data of the TWD database can be using to analyze and fix problems.
5. The TWD can record image and VDO of the train to fulfill information in the database and can develop the image processing system for identify each wagon.
6. The TWD can develop a smart and predictive maintenance concept and increase high accuracy with extending measuring points in the future.

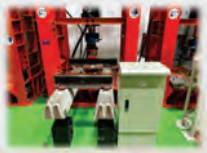

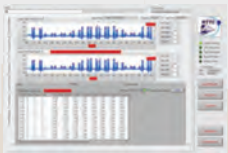


Thank you

www.tistr.or.th/rttc
sarawut@tistr.or.th
worawat_son@tistr.or.th
(Tel) (+66)02-577-9063

ศูนย์ทดสอบมาตรฐานระบบขนส่งทางราง (ศทร)

Railway Transportation System Testing Center (RTTC)

สถาบันวิจัยวิทยาศาสตร์และเทคโนโลยีแห่งประเทศไทย (วว)

Thailand Institute of Scientific and Technological Research (TISTR)

"Professional in Railway and Transportation Tests and Solutions"

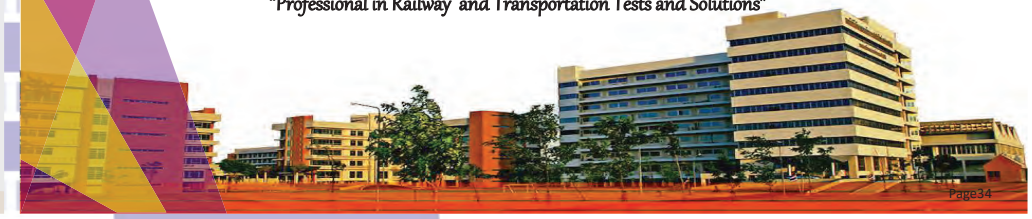

The Inspection and Monitoring Research in Earthquake in China by Prof. Dr. Zhong Tao

Introduction of recently research and practice on energy dissipation, base-isolated structures design

Research Representative: **Tao Zhong, PhD/Professor/PhD Supervisor**

Tel:13888932718
Email:tsy0410km@126.com

Faculty of Civil Engineering and Mechanics, Kunming University of Science and Technology
Kunming University of Science and Technology Design and Research Institute Co., Ltd.
Yunnan Engineering Earthquake Resistance Technology Research Center

Outline

- *The reinforced concrete frame structure, strengthened with buckling-resistance braces, underwent a shaking table test*
- *Equivalent linearization design method and application of base-isolated structure*
- *Overturning failure mechanism and experimental study of isolated step-terrace Structure*
- *Research on pilot project of new technology application of friction pendulum bearing*
- *Passive vibration control theory and engineering application for primary-attached structural system*
- *Experimental and theoretical research on traditional Chuan-dou type timber structure*

- *Thanks*

The reinforced concrete frame structure, strengthened with buckling-resistance braces, underwent a shaking table test

Tel: 13529366815
Email: Wukc@kmu.edu.cn

An overview of the vibration table test

Overview of the structure

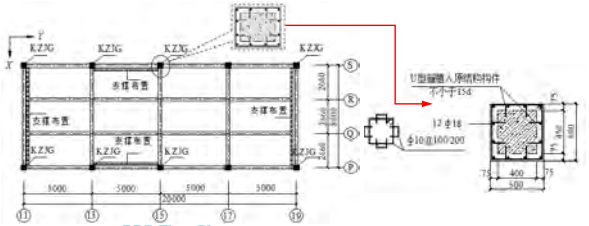

The teaching building was built in 1990s. The design intensity increase from 7 degrees (0.1 g) to 8 degrees (0.2 g). The structural system is a single-span frame structure with 3 floors and a floor height of 3.6 m. The site category is Class II, the earthquake group is Group II, and the seismic resistance level of the frame has increased from Level III to Level I.

The reinforced concrete frame structure, strengthened with buckling-resistance braces, underwent a shaking table test. 1-2

An overview of the vibration table test

Structure design and production

物理量	相似关系	相似系数	物理量	相似关系	相似系数
长度 L	S_L	0.200	集中力 F	$S_\sigma S_L^2$	0.016
弹性模量 E	S_σ	0.400	周期 T	$\sqrt{S_L / S_a}$	0.421
水平加速度 a	S_a	1.130	频率 f	$\sqrt{S_a / S_L}$	2.377
重力加速度 g	S_g	1.000	质量 m	$S_\rho S_L^3$	0.014
质量密度 ρ	$S_E / (S_a S_L)$	1.769	刚度 k	$S_\rho S_a S_L^2$	0.080
应变 ε	S_ε	1.000	阻尼比 ζ	S_ζ	1.000

The constraint equation determines three basic controllable parameters. The hoisting capacity and the vibration table bearing capacity constrain the mass density similarity ratio, and we should comprehensively consider its relationship with the acceleration similarity ratio.

- ✓ Micro-concrete replaces original concrete
- ✓ Galvanized iron wire replaces longitudinal reinforcement and stirrups for beams and columns
- ✓ Galvanized wire mesh replaces floor reinforcement
- ✓ Scaled BRB is made of Q235 steel

The reinforced concrete frame structure, strengthened with buckling-resistance braces, underwent a shaking table test. 1-3

Design and performance testing of a scaled BRB

Structure design and production

构件类型	支撑编号	支撑长度 l/mm	外套筒尺寸 /mm	屈服强度 f_y/Mpa	屈服承载力 F_y/kN	刚度比 α	屈服位移 Δ_y/mm	极限位移 Δ_u/mm
足尺 BRB	BRB 1	4200	□150×150×4	235	650	0.02	4.69	75.64
	BRB 2	3300	□100×100×4	235	250	0.02	3.92	57.59
	BRB 3	3300	□100×100×4	235	200	0.02	3.92	57.59
	BRB 4	4200	□150×150×4	235	300	0.02	4.97	75.64
缩尺 BRB	BRB 1m	840	□40×40×2	242	10.4	0.03	0.94	15.81
	BRB 2m	660	□40×40×2	242	4.0	0.03	0.76	12.42
	BRB 3m	660	□40×40×2	242	3.2	0.03	0.76	12.42
	BRB 4m	840	□40×40×2	242	4.8	0.03	0.94	15.81

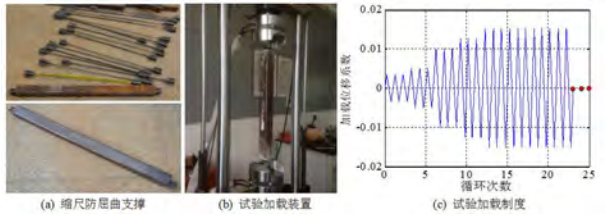

(a) 缩尺防屈曲支撑 (b) 试验加载装置 (c) 试验加载制度

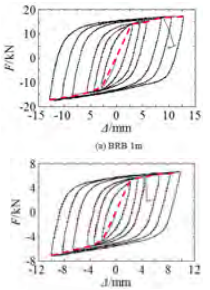

The design of the scaled BRB is based on the yield bearing capacity and yield displacement of the original BRB.

$$A^m = \frac{S_E F_y^p l^m}{S_L E^m u^p}$$

The reinforced concrete frame structure, strengthened with buckling-resistance braces, underwent a shaking table test. 1-4

Design of a vibration table test

Test conditions and measurement point arrangement

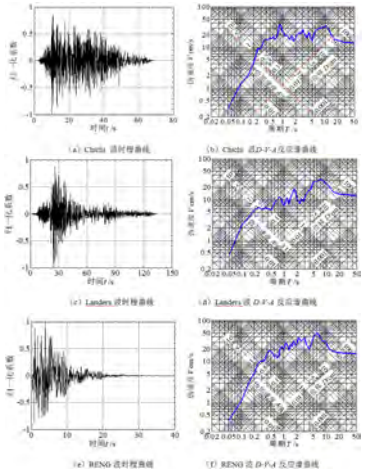

结构	输入方向	加速度峰值 a_{pg}/g	时程输入顺序
无控结构	X/Y	0.07(白噪声)，0.079，0.226，0.452	Landers→ChiChi→RenG
有控结构	X/Y	0.07(白噪声)，0.079，0.226，0.452，0.701	Landers→ChiChi→RenG

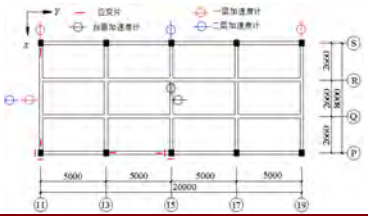

The test loading was carried out in the order of 8-degree small earthquake, medium earthquake, and large earthquake, and white noise (0.07 g) was used for frequency sweep before and after loading. The sensors mainly used accelerometers and strain gauges.

The reinforced concrete frame structure, strengthened with buckling-resistance braces, underwent a shaking table test. 1-5

Test results and analysis

Experimental phenomenon

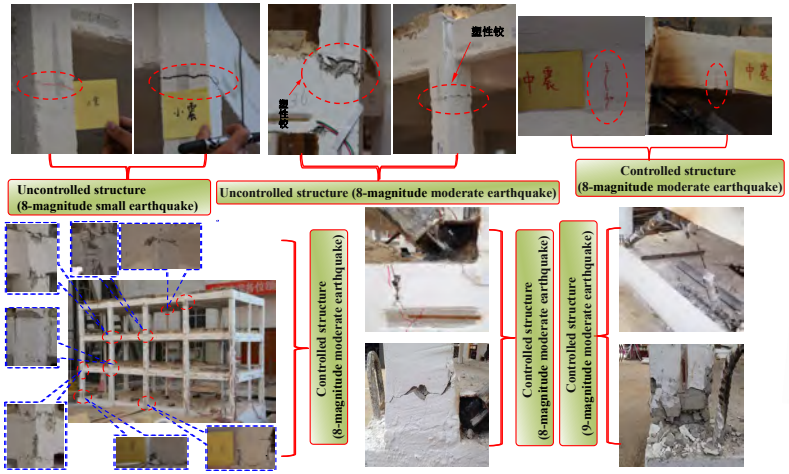

Comparison of failure modes:
- ✓BRBF - "Strong Columns Weak Beams"
- ✓CF-"Strong Beams and Weak The frame yield mechanism has changed, and the BRB has a significant energy dissipation and shock absorption effect.

The reinforced concrete frame structure, strengthened with buckling-resistance braces, underwent a shaking table test. 1-6

Test results and analysis

Model structure displacement response

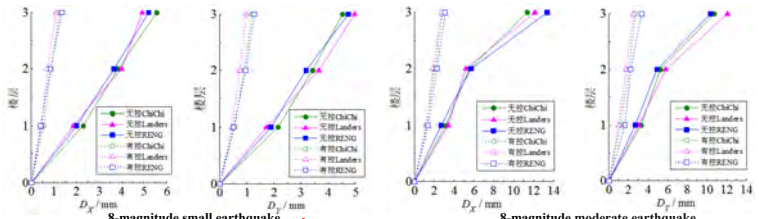

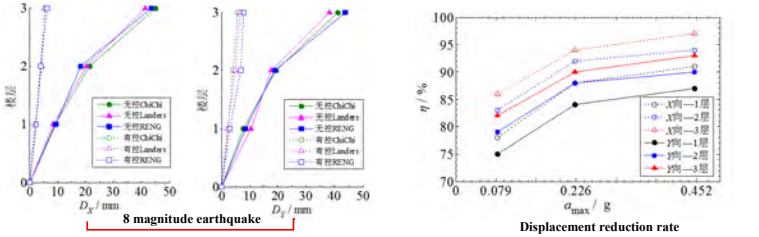

Displacement reduction rate

The BRB has a big impact on how the structure moves. For example, the top layer of the structure moves 89% less during small earthquakes, 92% less during medium earthquakes, and 96% less during large earthquakes of 8 degrees.

Test results and analysis

Model structural shear response

楼层	工况	地震波	无控结构 楼层剪力 V/kN X向	无控结构 楼层剪力 V/kN Y向	有控结构 楼层剪力 V/kN X向	有控结构 楼层剪力 V/kN Y向
1层	8度小震	ChiChi	8.3	8.9	17.3	15.8
		Landers	7.2	8.1	18.1	17.7
		RENG	8.5	9.4	15.6	14.9
	8度中震	ChiChi	25.4	28.3	42.4	40.0
		Landers	21.8	25.7	48.5	45.4
		RENG	27.1	32.6	46.9	43.8
	8度大震	ChiChi	41.5	47.5	85.9	81.3
		Landers	48.6	50.9	93.1	89.6
		RENG	51.7	58.4	89.6	83.7
2层	8度小震	ChiChi	6.6	7.5	13.8	11.7
		Landers	6.0	7.1	14.2	12.4
		RENG	6.5	8.3	12.2	11.5
	8度中震	ChiChi	20.0	22.6	33.9	30.5
		Landers	17.9	20.3	37.7	34.7
		RENG	22.1	25.8	34.4	31.6
	8度大震	ChiChi	33.5	37.4	67.4	64.9
		Landers	39.6	41.0	71.3	68.7
		RENG	41.8	45.9	68.8	62.3
3层	8度小震	ChiChi	3.9	4.3	7.5	6.4
		Landers	3.6	4.2	8.1	6.9
		RENG	4.1	5.1	6.9	6.0
	8度中震	ChiChi	8.9	9.5	19.2	18.2
		Landers	8.1	8.7	22.4	19.4
		RENG	9.3	11.4	20.5	16.7
	8度大震	ChiChi	9.4	8.6	39.2	36.2
		Landers	10.5	10.7	43.7	39.8
		RENG	8.8	11.3	37.5	34.3

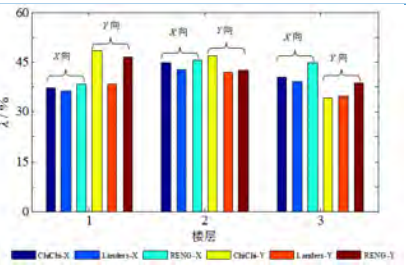

BRB shear distribution rate

BRB has almost no seismic control effect on the structural shear response, and its maximum shear sharing rate is 49%. The residual seismic shear is only about 8%~19% higher than the uncontrolled structure.

Test results and analysis

BRB energy consumption analysis

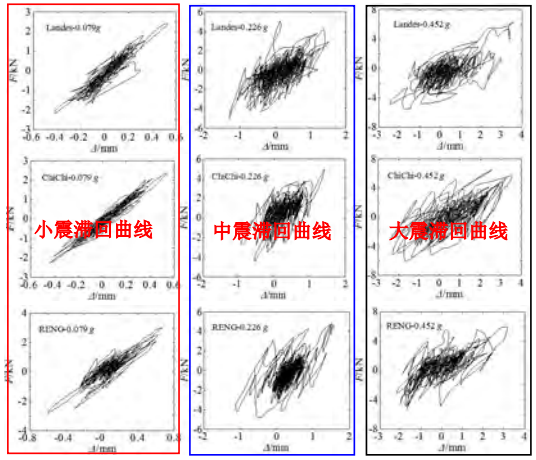

- ✓ Under small earthquakes, the BRB maintains elasticity and increases the structure's lateral stiffness.
- ✓ Under moderate and large earthquakes, BRB yields and dissipates energy, reducing the structure's seismic response.

Test results and analysis

Earthquake input energy and distribution

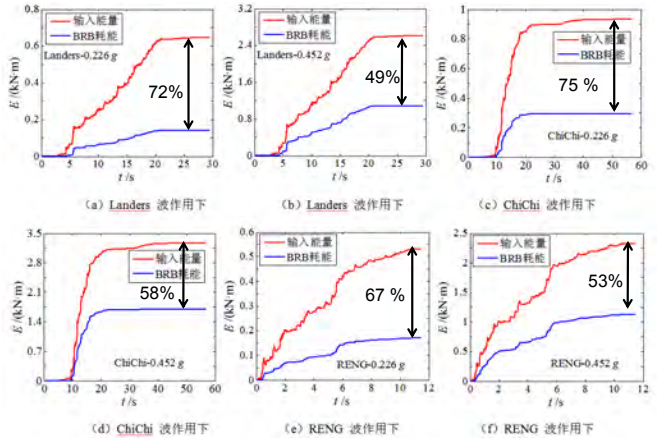

BRBs dissipate significant energy under moderate and large earthquakes.

Performance evaluation of BRB after earthquake

昆明理工大学 Kunming University of Science and Technology

Performance comparison analysis

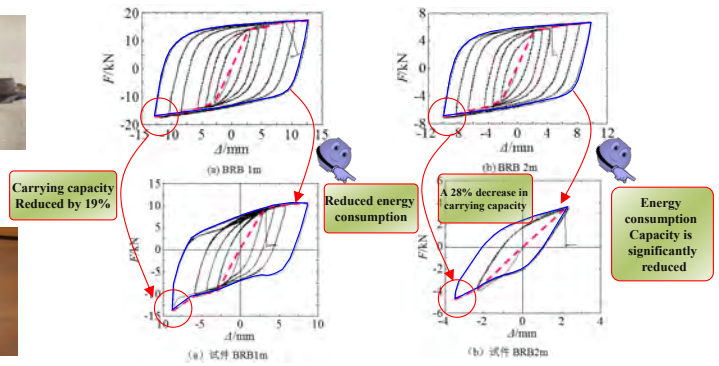

The reinforced concrete frame structure, strengthened with buckling-resistance braces, underwent a shaking table test. 1-11

Failure form and mechanism of BRB structure system

昆明理工大学 Kunming University of Science and Technology

Failure mechanism

Under the action of extremely rare earthquakes, some BRBs began to break, the structural "fuse" failed, and the structure transformed from a frame support system to a pure frame. The beams and columns primarily carried the earthquake action, transforming the frame into the primary lateral force-resisting system. The connection of the beams and columns to the BRB resulted in a plastic hinge failure, which ultimately led to the collapse of the entire structure.

The reinforced concrete frame structure, strengthened with buckling-resistance braces, underwent a shaking table test. 1-12

昆明理工大学 Kunming University of Science and Technology

Innovation Coordination Green Open Sharing

Equivalent linearization design method and application of base-isolated structure

The topic's importance and background

昆明理工大学 Kunming University of Science and Technology

Background

1. At present, there are differences (vibration modes) between the theoretical analysis model of seismic isolation design and the actual stress model.

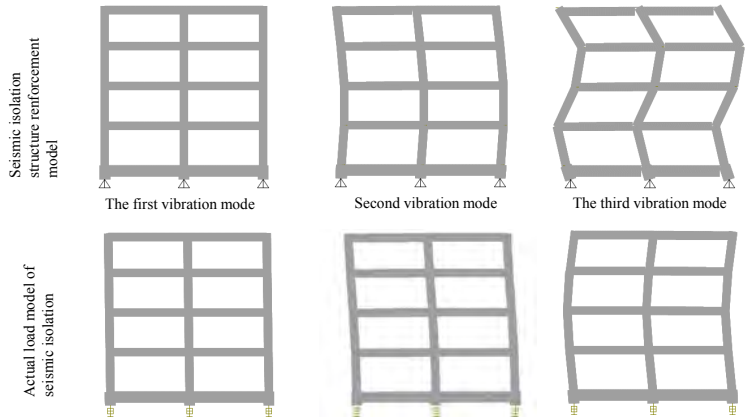

The topic's importance and background

Background

1. At present, there is a difference between the theoretical analysis model of seismic isolation design and the actual force model (shear force).

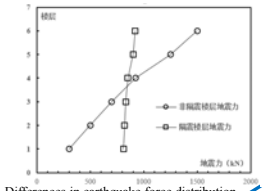

Differences in earthquake force distribution

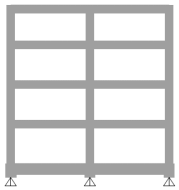

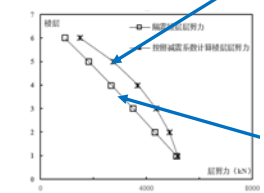

Difference in shear force distribution between floors

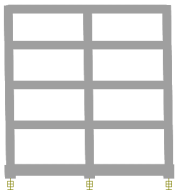

When designing according to a shock absorption coefficient, the upper floors of the structure generally have excess reinforcement.

The topic's importance and background

Background

1. At present, there are differences between the theoretical analysis model for seismic isolation design and the actual stress model.

Under the same inter-story displacement angle (such as 1/50), the hinged model's reinforcement arrangement results in evenly distributed plastic hinges, whereas the isolation model's plastic hinges concentrate in the lower part, which is not conducive to earthquake resistance.

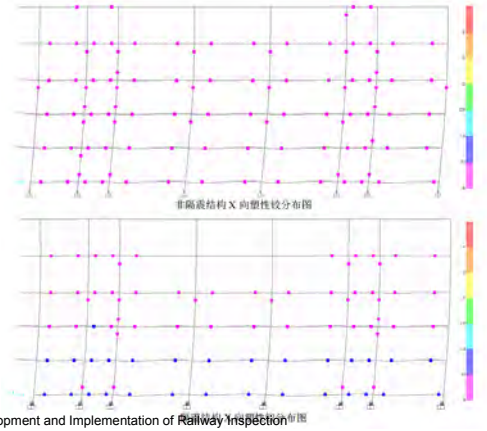

The topic's importance and background

Background

2. The results of the time history analysis are discrete. Different earthquake waves have different degrees of structural damage.）

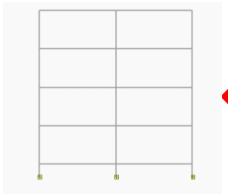

The same seismic isolation model

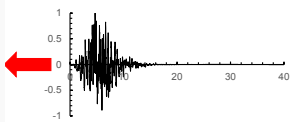

Same peak acceleration

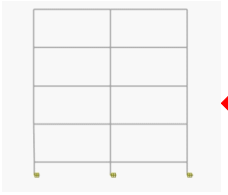

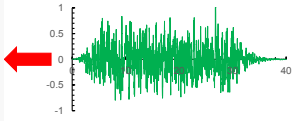

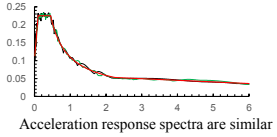

Acceleration response spectra are similar

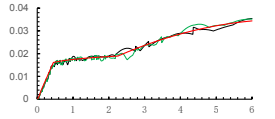

Similar velocity response spectra

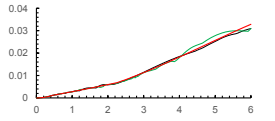

Displacement response spectra are similar

The topic's importance and background

Background

1. Consider the isolation bearing's nonlinear characteristics.

2. Avoid the discreteness of time course analysis results.

It is recommended to use: Equivalent linearization design method!

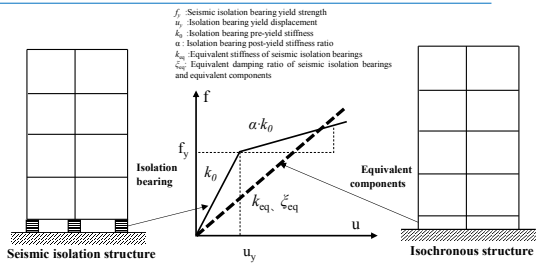

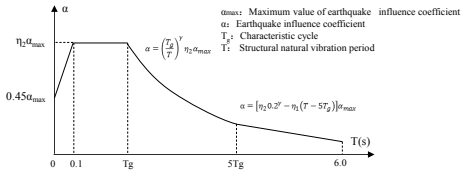

Key Question 1: Standard Analysis Results

Recommended values for Determine the duration of earthquake motion artificial wave intensity envelope parameters

Recommended values for artificial wave intensity envelope parameters

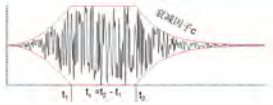

Seismic design intensity	Parameter Type		Frequent earthquakes			Fortification earthquakes			Rare earthquake		
	Earthquake Grouping		Group 1	Group 2	Group 3	Group 1	Group 2	Group 3	Group 1	Group 2	Group 3
6	Acceleration value			18			50			125	
	Strength envelope parameters	t1	2.42	2.49	0.39	3.32	4.55	6.02	4.63	7.05	10.23
		ts	3.33	3.59	0.30	4.04	5.78	7.92	6.70	11.25	17.74
		c	4.44	4.99	0.24	0.27	0.21	0.17	0.19	0.13	0.10
7 0.10 g	Acceleration value			35			100			220	
	Strength envelope parameters	t1	2.01	2.78	3.77	2.83	3.88	5.55	4.07	6.26	9.35
		ts	2.18	3.17	4.48	3.66	5.24	8.06	6.38	10.86	17.78
		c	0.42	0.32	0.26	0.29	0.22	0.17	0.19	0.13	0.09
7 0.15 g	Acceleration value			55			150			310	
	Strength envelope parameters	t1	1.81	2.52	3.33	2.56	3.50	5.04	3.83	5.92	8.14
		ts	2.04	2.98	4.10	3.45	4.94	7.70	6.37	10.96	16.24
		c	0.43	0.33	0.27	0.30	0.23	0.17	0.19	0.13	0.10
8 0.20 g	Acceleration value			70			200			400	
	Strength envelope parameters	t1	1.63	2.33	2.94	2.36	3.42	4.68	3.73	6.06	6.80
		ts	1.86	2.82	3.67	3.28	5.04	7.44	6.57	12.01	13.90
		c	0.46	0.35	0.29	0.30	0.23	0.17	0.18	0.12	0.11
8 0.30g	Acceleration value			110			300			510	
	Strength envelope parameters	t1	1.43	1.98	2.47	2.09	3.03	4.13	3.21	5.07	5.63
		ts	1.69	2.48	3.18	3.03	4.71	6.96	5.83	10.32	11.79
		c	0.49	0.37	0.32	0.32	0.23	0.18	0.20	0.13	0.12
9	Acceleration value			140			400			620	
	Strength envelope parameters	t1	1.23	1.67	2.06	1.89	2.74	3.69	2.96	4.50	4.74
		ts	1.47	2.10	2.67	2.83	4.45	6.48	5.58	9.48	10.16
		c	0.53	0.42	0.35	0.33	0.24	0.18	0.20	0.14	0.13

Key issue 2: Improve analysis accuracy

Ideas for improving accuracy 1: Comparison of accuracy of methods in various countries

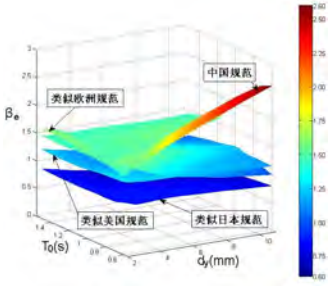

100 single-degree-of-freedom LRB isolation model

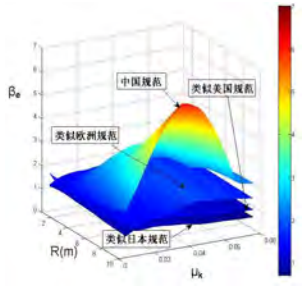

100 single-degree-of-freedom FPS isolation models

The equivalent linearization analysis methods in Japan, the United States, and Europe all have a certain degree of accuracy. The accuracy of equivalent linearization analysis in China is very low!

One of the reasons: the calculation method of equivalent stiffness and equivalent damping ratio does not match the standard response spectrum!

Key issue 2: Improve analysis accuracy

Improving Accuracy Approach 2: Propose New Equivalent Parameters

$$T_{eq}=\begin{cases} T_0\sqrt{\dfrac{\mu}{1+(\mu-1)\alpha}} & \mu\le 2 \\ T_0\dfrac{1.0}{1+P_{T1}\cdot(1-\alpha)^{P_{T2}}\cdot\ln\left[P_{T3}\cdot(\mu-2)+1\right]}\sqrt{\dfrac{\mu}{1+(\mu-1)\alpha}} & 2<\mu\le 18 \\ T_0\dfrac{\mu^{P_{T5}\alpha-P_{T5}}}{\mu^{P_{T5}\alpha-P_{T5}}+P_{T1}\cdot(1-\alpha)^{P_{T2}}\cdot\ln\left[P_{T3}\cdot(18-2)+1\right]\cdot 18^{P_{T5}\alpha-P_{T5}}}\sqrt{\dfrac{\mu}{1+(\mu-1)\alpha}} & \mu>18 \end{cases}$$

$$\xi_{eq}=\begin{cases} \left(P_{\xi1}-\dfrac{P_{\xi2}\times 2}{P_{\xi3}+\ln(2-1)}\right)\cdot(\mu-1)\sqrt{\dfrac{T_{eq}}{T_0}-1}+\xi_0 & \mu\le 2 \\ \left(P_{\xi1}-\dfrac{P_{\xi2}\mu}{P_{\xi3}+\ln(\mu-1)}\right)\sqrt{\dfrac{T_{eq}}{T_0}-1}+\xi_0 & 2<\mu\le 18 \\ \left(P_{\xi1}-\dfrac{P_{\xi2}\times 18}{P_{\xi3}+\ln(18-1)}\right)\dfrac{18^{P_{\xi5}}+P_{\xi4}}{18^2}\dfrac{\mu^2}{\mu^{P_{\xi5}}+P_{\xi4}}\sqrt{\dfrac{T_{eq}}{T_0}-1}+\xi_0 & \mu>18 \end{cases}$$

LRB seismic isolation system				FPS seismic isolation system			
Equivalent cycle T_{eq}		Equivalent damping ratio ξ_{eq}		Equivalent cycle T_{eq}		Equivalent damping ratio ξ_{eq}	
Parameter	Numeric	Parameter	Numeric	Parameter	Numeric	Parameter	Numeric
P_{T1}	0.19	$P_{\xi1}$	0.32	P_{T1}	0.19	$P_{\xi1}$	0.16
P_{T2}	4.67	$P_{\xi2}$	0.03	P_{T2}	4.67	$P_{\xi2}$	0.03
P_{T3}	3.90	$P_{\xi3}$	0.90	P_{T3}	3.90	$P_{\xi3}$	100
P_{T4}	4.06	$P_{\xi4}$	1.00	P_{T4}	4.06	$P_{\xi4}$	40.0
P_{T5}	-0.16	$P_{\xi5}$	2.10	P_{T5}	-0.16	$P_{\xi5}$	2.10

Equivalent parameter calculation formula suitable for "Code for Seismic Design of Buildings"!

Key Issue 2: Improving Analytical Precision

Idea 2 to improve accuracy: New method accuracy

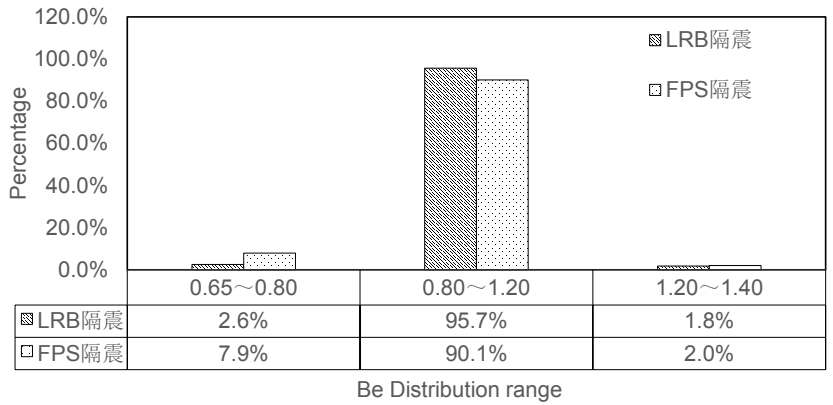

	0.65～0.80	0.80～1.20	1.20～1.40
LRB隔震	2.6%	95.7%	1.8%
FPS隔震	7.9%	90.1%	2.0%

The new method can ensure that the error between more than 90% of the analysis results and the time-course analysis results is within 20%!

Applied Research

Application theory-verification model introduction

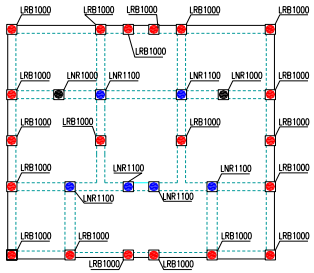

Seismic isolation bearing arrangement

Shaking table test model

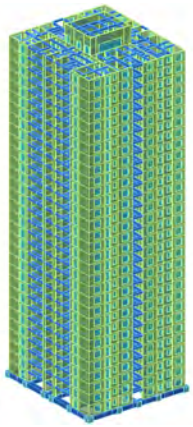

Computational analysis model

High-rise shear wall rubber isolation structure!

Applied Research

Application theory - comparison results of floor displacement

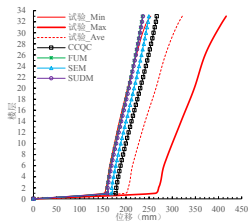

Fortification

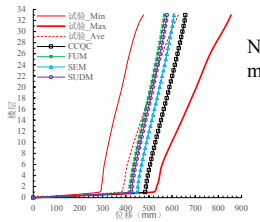

New method

Rare Encounter

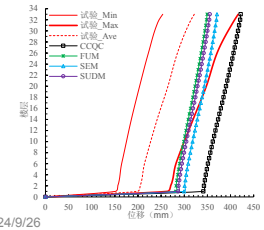

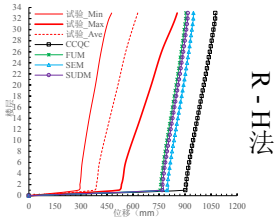

R - H法

The analysis results of the new method are close to the experimental results.
The analysis results of the original method were far greater than the experimental results!

Conclusion

- **Theoretical and applied research is carried out to improve the current theory and methods of seismic isolation structure design and analysis in my country. The research has important academic value and engineering application value for improving the current theory and methods of seismic isolation structure design and analysis in my country.**
- **Based on a review of seismic isolation technologies, seismic isolation design theories, and methods at home and abroad, the limitations and main problems of seismic isolation design methods at this stage are proposed.**
- **According to the theory of earthquake attenuation and design earthquake grouping in my country, a set of strength envelope model parameters for generating artificial earthquake motion based on peak earthquake acceleration and design earthquake grouping was proposed. Through a large number of trial calculations, quantitative suggestions for using strength envelope model parameters to generate artificial waves for seismic isolation time-history analysis with reasonable control of analysis accuracy and calculation cost were given.**
- **A new equivalent parameter equivalent linearization analysis method based on my country's acceleration response spectrum and damping adjustment coefficient is explained and proposed to improve the overall design of my country's equivalent linearization seismic isolation structure at this stage, and it is verified through examples.**

Overturning failure mechanism and experimental study of isolated step-terrace Structure

Artificial wave 8 magnitude earthquake resistance

Artificial wave 8 magnitude seismic isolation

Research background and significance

Seismic Isolation Technology + Mountain Building → Mountain seismic isolation building

Seismic Isolation Technology

Yunnan Province

- Rationally develop terraces and slopes to alleviate the pressure on construction land.
- It is beneficial to protecting the ecological environment and achieving harmonious coexistence between man and nature.
- Avoid large-scale excavation and filling work and reduce the risks of environmental, geological, and traffic disasters.
- Improve the seismic safety of mountain buildings and resist earthquake disasters.

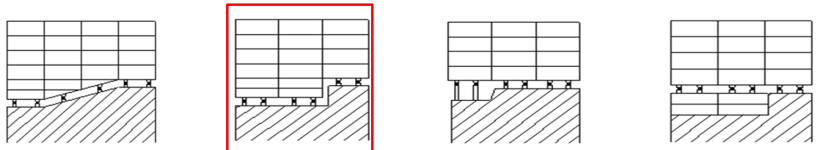

（a）斜板式　（b）掉层式　（c）吊脚式　（d）层间式

Critical conditions for overturning failure of seismic isolation foundation on flat ground

Whether the vertical tensile and compressive stiffness of the isolation layer is consistent or not has a great influence on the vertical force distribution law of the isolation layer of the flat ground foundation isolation and the mountain drop-story isolation structure, and it must be considered in the process of deriving the overturning failure mechanism theory.

Tensile discrimination condition

$$\begin{cases} \varphi^2 = \dfrac{1}{\gamma} - \dfrac{2}{\dfrac{3}{2}k\gamma\cdot\dfrac{H}{b} + \dfrac{\gamma}{1+\varphi} + \dfrac{\gamma}{2}} \\ \dfrac{3}{2}k\left(1+\dfrac{1}{\varphi}\right)\cdot\dfrac{H}{b} - \dfrac{1}{2\varphi} - \dfrac{3}{2} = \dfrac{1}{\sigma_0} \end{cases}$$

$$\begin{cases} \varphi^2 = \dfrac{1}{\gamma} - \dfrac{2}{\dfrac{3}{2}k\gamma\cdot\dfrac{H}{b} + \dfrac{\gamma}{1+\varphi} + \dfrac{\gamma}{2}} \\ \dfrac{3}{2}k(1+\varphi)\cdot\dfrac{H}{b} + \dfrac{\varphi}{2} + \dfrac{3}{2} = \dfrac{30}{\sigma_0} \end{cases}$$

Pressure judgment conditions

$\gamma = \dfrac{K_{V1}}{K_{Vp}}$ Vertical tensile compressive stiffness ratio of the isolation layer

$\varphi = \dfrac{l_1}{l_2}$ Ratio of the length of the tension zone to the compression zone

$\sigma_0 = \dfrac{G}{b}$ Vertical compressive stress of seismic isolation layer under deadweight

$k = \dfrac{a_0}{g}$ Seismic force coefficient

σ_0 Value

Building Type	Class A Building	乙Class B Building	Class C building
Compressive stress limit(MPa)	10	12	15

γ *advisable1/10*

Critical conditions for failure of seismic isolation overturning in mountainous areas due to layer loss—downslope

When the center of rotation is located on the upper ground plane

When the center of rotation is located at the lower ground layer

$\gamma = \dfrac{K_{V1}}{K_{Vp}}$　$\sigma_0 = \dfrac{G}{b}$　$\varphi = \dfrac{l_1}{b - l_1}$

$\alpha = \dfrac{h}{H}$　$\beta = \dfrac{a}{b}$

α: Height Ratio
β: Width Ratio
φ: Ratio of the length of the tension zone to the length of the compression zone
γ: Vertical tensile and compressive stiffness ratio of seismic isolation layer
η: Horizontal stiffness ratio of upper and lower ground layers
σ_0: Surface pressure of rubber bearing under gravity

Positive overturning　Negative overturning

Envelope design method for seismic isolation structure with falling floors in mountainous areas

The floor acceleration ratio is used as the improved horizontal phase damping coefficient of the mountainous floor-falling structure, and then the improved horizontal damping coefficient is used to simplify the model's partial reinforcement design. The elastic time-history analysis method is then used to design the reinforcement of the actual seismic isolation finite element model. The reinforcement of the two models is then enveloped, and the envelope design results are used as the final reinforcement of the mountainous floor-falling isolation structure.

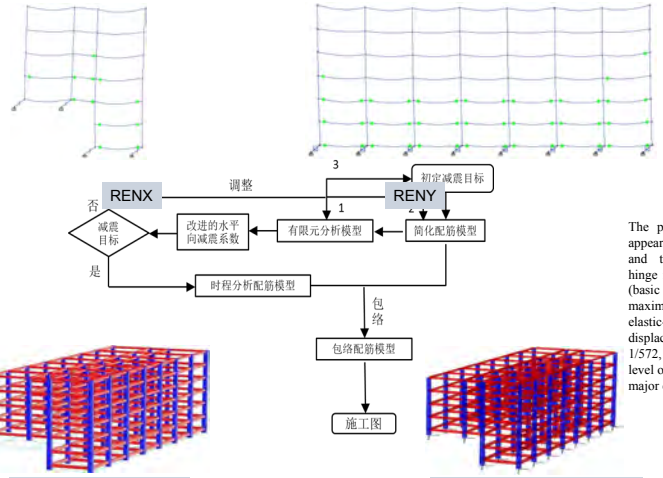

YJK Simplified reinforcement model　ETABS Time-history reinforcement model

The plastic hinge first appears in the D1 layer, and the final plastic hinge is in the IO stage (basic operation). The maximum value of the elastic-plastic interlayer displacement angle is 1/572, reaching the level of "no damage in a major earthquake."

Seismic isolation and earthquake-resistant structure model for mountainous areas

Based on the model geometry, vibration table bearing capacity, model making experience, and gantry truck load, the model length similarity coefficient is determined to be 0.1, the stress similarity coefficient is 0.25, the acceleration similarity coefficient is 1, and the other similarity coefficients are solved by the principle of π. C30 concrete is replaced by micro concrete with strength grade M7.5, steel bars are replaced by galvanized iron wire, and the moment bearing capacity and shear bearing capacity of the model component reinforcement are determined on the principle of equivalence.

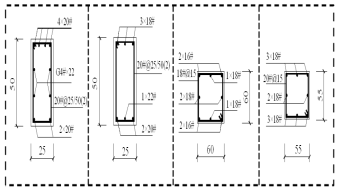

(a) D1 层边梁配筋　(b) D1 层拉梁配筋　(c) D2 层柱配筋　(d) 1 层柱配筋

Based on the same stiffness center, same mass center, equivalent overturning moment, and equivalent torsional torque, the seismic isolation layer is equivalent to 8 LRB100s, and the vertical and horizontal mechanical properties are tested.

Yield KN	Equivalent horizontal stiffness KN/mm	Post-yield stiffness KN/mm	Stiffness before yield KN/mm
0.55	0.152	0.10	1.02

Shaking table test ground vibration and working conditions

The grounding layer of the mountainous seismic isolation building is not unique, and the model contains rubber seismic isolation bearings with strong nonlinearity, so the base shear force comparison is very difficult. Therefore, the test selected the artificial wave of the third group of Class II sites, the pulse-type Ludian wave representative of Yunnan, and the Taft wave suitable for Class II sites as the test input.

地震波	发生时间	记录台站	方向	PGA cm/s²
人工波	—	—	—	100
塔夫特波	1952年7月21日	TAFT LINCOLN SCHOOL TUNNEL	N21E	949.1
鲁甸波	2014年08月03日	龙头山镇台站	EW	152.7

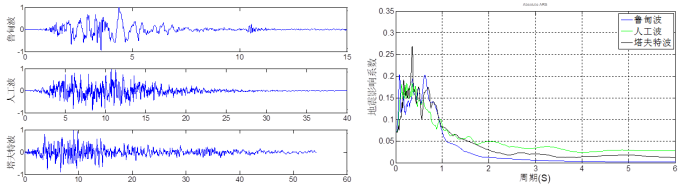

The test was loaded in the order of 8-magnitude frequent earthquake, 8-magnitude fortification earthquake, 8-magnitude rare earthquake, 8.5-magnitude rare earthquake and 9-magnitude rare earthquake. White noise was used to scan before and after the test and between the earthquake actions at each level, for a total of 34 effective loading conditions.

Horizontal slope direction

b_0=4.2m
H=1.8m
γ=0.26
σ_0=2.3Mpa

Substitution

$$\begin{cases} \varphi^2=\dfrac{1}{\gamma}-\dfrac{2}{\dfrac{3}{2}k\gamma\cdot\dfrac{H}{b_0}+\dfrac{\gamma}{1+\varphi}+\dfrac{\gamma}{2}} \\ \dfrac{3}{2}k\left(1+\dfrac{1}{\varphi}\right)\cdot\dfrac{H}{b_0}-\dfrac{1}{2\varphi}-\dfrac{3}{2}=\dfrac{1}{\sigma_0} \end{cases}$$

$$\begin{cases} \varphi^2=\dfrac{1}{\gamma}-\dfrac{2}{\dfrac{3}{2}k\gamma\cdot\dfrac{H}{b_0}+\dfrac{\gamma}{1+\varphi}+\dfrac{\gamma}{2}} \\ \dfrac{3}{2}k(1+\varphi)\cdot\dfrac{H}{b_0}+\dfrac{\varphi}{2}+\dfrac{3}{2}=\dfrac{30}{\sigma_0} \end{cases}$$

$$\begin{cases} \dfrac{H}{b_0}=\dfrac{2}{3}\cdot\dfrac{0.987}{k} & \text{受拉失效} \\ \dfrac{H}{b_0}=\dfrac{2}{3}\cdot\dfrac{4.253}{k} & \text{受压失效} \end{cases}$$

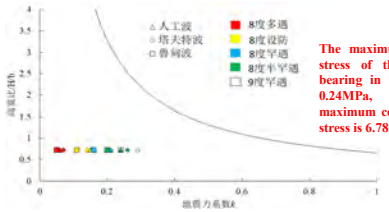

Tensile failure

The maximum tensile stress of the rubber bearing in the test is 0.24MPa, and the maximum compressive stress is 6.78MPa

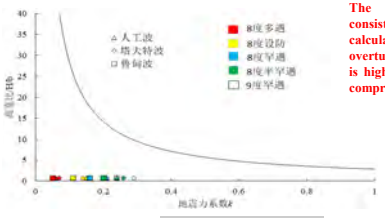

Compressive failure

Test results and theoretical values

The test results are consistent with theoretical calculations. The risk of overturning under tension is higher than that under compression.

Along the slope

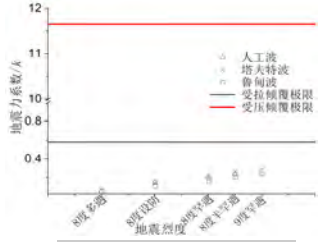

The upper ground layer is tensile and causes overturning failure

The maximum tensile stress of the rubber bearing in the test is 0.89 MPa, and the maximum compressive stress is 13.00 MPa.

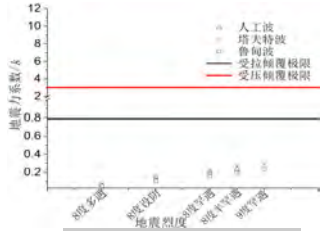

The lower ground layer is tensile and causes overturning failure

In the test, the seismic force coefficients of artificial waves, Taft waves, and Ludian waves did not exceed the tensile and compressive overturning limits along the slope under earthquakes of magnitude 8, frequent, magnitude 8, rare, magnitude 8.5, and rare.

Theoretical calculations are consistent with test results. The risk of overturning under tension is higher than under compression.

Acceleration attenuation coefficient

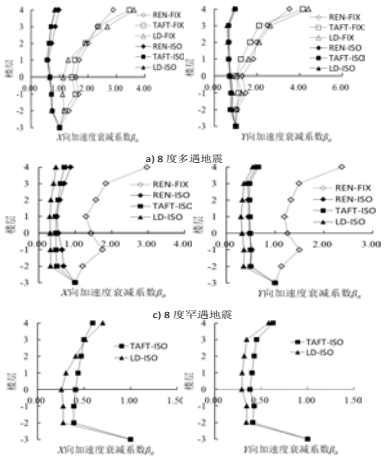

The acceleration attenuation coefficients of the bottom-level isolation model are all less than 1, which shows acceleration attenuation, while the acceleration attenuation coefficients of the falling-story seismic model are all greater than 1, and the floor acceleration shows amplification, which can reach a maximum of 4 times. The isolation structure is still elastic after experiencing a 9-magnitude earthquake, while the seismic-resistant structure has cracks under an 8-magnitude small earthquake, is severely damaged under an 8-magnitude moderate earthquake, and is severely destroyed under an 8-magnitude large earthquake, with plastic hinges generated in many columns.

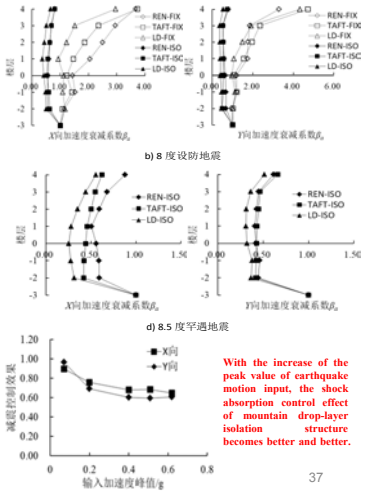

With the increase of the peak value of earthquake motion input, the shock absorption control effect of mountain drop-layer isolation structure becomes better and better.

Mechanical properties test of guide rail tensile rubber bearing

LNR600 parameter

参数	取值
支座高度 H/mm	203
单层橡胶层厚度/mm	6.22
橡胶层数 n_1	18
橡胶层总厚度 T_r/mm	112
单层钢板厚度/mm	3
钢板层数 n_2	17
钢板总厚度/mm	51
支座中孔直径 d/mm	100
第一形状系数 S_1	23.44
第二形状系数 S_2	5.35

Guide rail type tensile rubber bearing structure

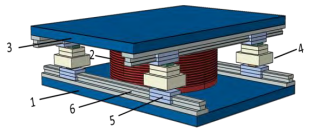

Note: 1—lower connecting plate, 2—rubber support, 3—upper connecting plate, 4—tension box, 5—fastener, 6—guide rail

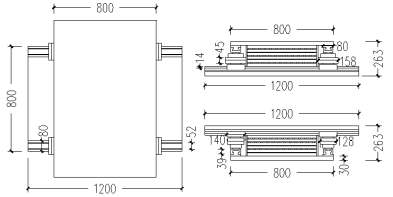

Mechanical properties test of guide rail tensile rubber bearing

试验编号	试验对象	加载角度	加载方案
T1	LNR600	/	竖向预加压应力 15MPa，水平向剪应变 γ=100%加载，循环 3 次，加载频率 f=0.02Hz
T2	RTD&LNR600	45°	
T3	RTD&LNR600	0°	
T4	LNR600	/	竖向单轴单调拉伸 5.2mm
T5	RTD&LNR600	/	

When the loading angle is 45° and 0°, the equivalent horizontal stiffness increase rate of RTD&LNR600 is 4.0% and 3.9%, respectively.

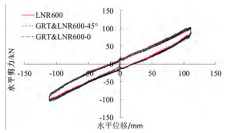

RTD&LNR600-45° RTD&LNR600-0° LNR600

Horizontal compression shear test

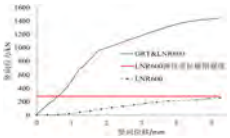

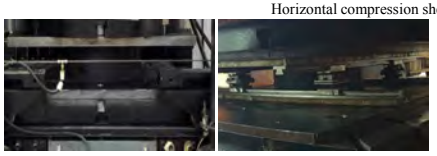

LNR600 RTD&LNR600

Uniaxial vertical tensile test

Within the elastic range, the load-displacement relationship of the vertical uniaxial tension of LNR600 is approximately linear, and the stiffness is about 50kN/mm, while the load-displacement relationship of the uniaxial tension of RTD&LNR600 is bilinear, and the tensile bearing capacity is increased by 3.6 times.

Finite element numerical simulation of guide rail tensile rubber bearing

	LNR600	RTD&LNR600-45°	RTD&LNR600-0°
试验(kN/mm)	0.891	0.927	0.926
有限元(kN/mm)	0.913	0.957	0.945
误差(%)	2.5	3.2	2.1

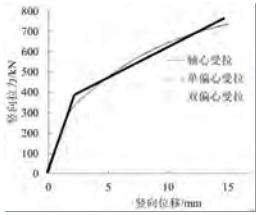

Single RTD Finite Element Model

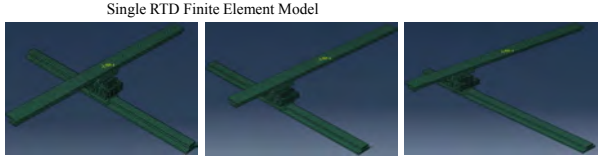

（a）轴心受拉 （b）单偏心受拉 （c）双偏心受拉

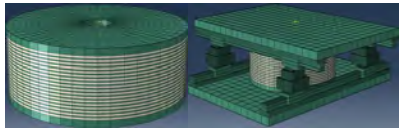

LNR600 有限元模型 RTD&LNR600 有限元模型

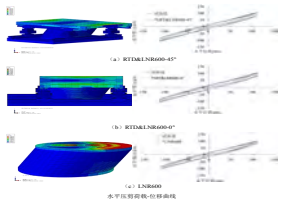

试验编号	试验对象	输入角度	加载方案
T6	RTD&LNR600	0°	竖向预加拉应力 1.0、1.5、2.0、2.5、3.5MPa，水平向剪应变 γ=100%加载，循
T7	RTD&LNR600	45°	环 3 次，加载频率 f=0.02Hz

Conclusion

- Based on a review of the current research status of mountain earthquake resistance and flat ground seismic isolation at home and abroad, the research content and main technical routes for improving the seismic safety of mountain buildings by using mountain seismic isolation technology are proposed.
- By introducing the inconsistency of vertical tensile and compressive stiffness of the isolation layer, the parameterized judgment conditions for controlling the overturning failure of the isolation structure with falling floors in mountainous areas are derived and proposed.
- Aiming at the fact that the existing seismic isolation design method on flat ground is not fully applicable to the actual requirements of seismic isolation design in mountainous areas, an envelope design method suitable for seismic isolation structures with falling floors in mountainous areas is proposed on the basis of improving the original calculation method of horizontal damping coefficient.
- The shaking table test verified the correctness of the overturning failure theory of mountainous floor-drop isolation structures and the effectiveness of the envelope design method. It also directly proved that the seismic performance of mountainous floor-drop isolation structures is much higher than that of floor-drop seismic-resistant structures, and its seismic performance has reached the level of "not being damaged in a major earthquake".
- The shear force of the upper ground layer columns of the mountain drop-story seismic isolation structure is reduced by more than 72.8% compared with the drop-story seismic resistance, which greatly improves the seismic safety performance of the upper ground layer columns and structures.
- In response to the need to resist overturning hazards of mountain floor-falling seismic isolation structures, a rail-type tensile rubber seismic isolation bearing was developed. The rail-type tensile rubber bearing has a tensile performance that is more than three times higher than that of ordinary rubber bearings of the same specification without changing the horizontal performance of ordinary rubber bearings, thereby improving the anti-overturning ability of mountain floor-falling structures.

Research on pilot project of new technology application of friction pendulum bearing

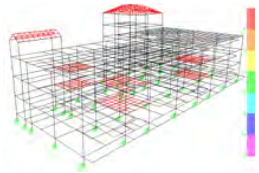

1 研究背景 RESEARCH BACKGROUNDS

Topic SOURCE

Phase 2

In September 2013, an earthquake simulation shaking table experiment was conducted on a three-story steel frame structure equipped with a friction slip pendulum.

Phase 4

In January 2016, the detection scheme of the friction sliding pendulum bearing was explored and studied, and in May of the same year, the bearing performance detection test was carried out on the friction sliding pendulum bearing used in the pilot project.

1 2 3

Phase 1

The research team launched a project in 2013 to study the friction pendulum isolation technology. The research team conducted theoretical exploration and research on the friction sliding pendulum support.

Phase 3

In 2015, we explored and studied the seismic isolation analysis method for the Tuanshan New Town Kindergarten pilot project, and conducted two expert demonstrations on the pilot project.

Phase 5

Experts reviewed the seismic isolation analysis report for the third time in February 2017 after recalculating the analysis model based on the bearing performance test results.

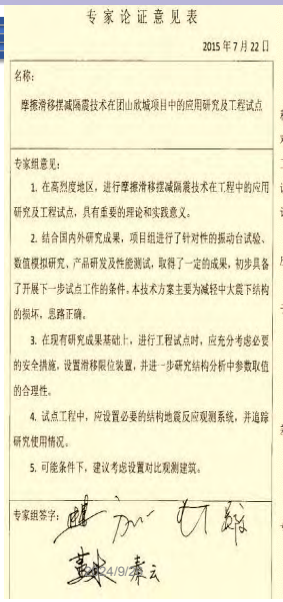

专家论证意见表

2015年7月22日

名称：

摩擦滑移摆减隔震技术在团山底城项目中的应用研究及工程试点

专家组意见：

1. 在高烈度地区，进行摩擦滑移摆减隔震技术在工程中的应用研究及工程试点，具有重要的理论和实践意义。

2. 结合国内外研究成果，项目组进行了针对性的振动台试验、数值模拟研究、产品研发及性能测试，取得了一定的成果，初步具备了开展下一步试点工作的条件，本技术方案主要为减轻中大震下结构的损坏，思路正确。

3. 在现有研究成果基础上，进行工程试点时，应充分考虑必要的安全措施，设置滑移限位装置，并进一步研究结构分析中参数取值的合理性。

4. 试点工程中，应设置必要的结构地震反应观测系统，并追踪研究使用情况。

5. 可能条件下，建议考虑设置对比观测建筑。

专家组签字：

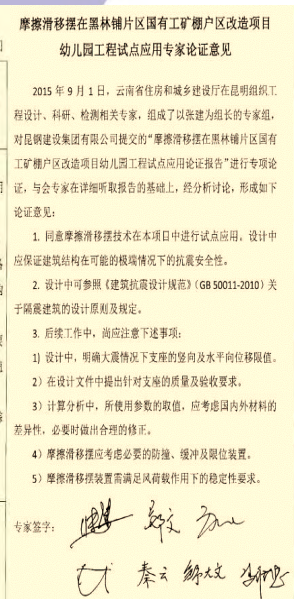

摩擦滑移摆在黑林铺片区国有工矿棚户区改造项目幼儿园工程试点应用专家论证意见

2015年9月1日，云南省住房和城乡建设厅在昆明组织工程设计、科研、检测相关专家，组成了以张建为组长的专家组，对昆钢建设集团有限公司提交的"摩擦滑移摆在黑林铺片区国有工矿棚户区改造项目幼儿园工程试点应用论证报告"进行专项论证，与会专家在详细听取报告的基础上，经分析讨论，形成如下论证意见：

1. 同意摩擦滑移摆技术在本项目中进行试点应用，设计中应保证建筑结构在可能的极端情况下的抗震安全性。

2. 设计中可参照《建筑抗震设计规范》(GB 50011-2010)关于隔震建筑的设计原则及规定。

3. 后续工作中，尚应注意下述事项：

1）设计中，明确大震情况下支座的竖向及水平向位移限值。

2）在设计文件中提出针对支座的质量及验收要求。

3）计算分析中，所使用参数的取值，应考虑国内外材料的差异性，必要时做出合理的修正。

4）摩擦滑移摆应考虑必要的防撞、缓冲及限位装置。

5）摩擦滑移摆装置需满足风荷载作用下的稳定性要求。

专家签字：

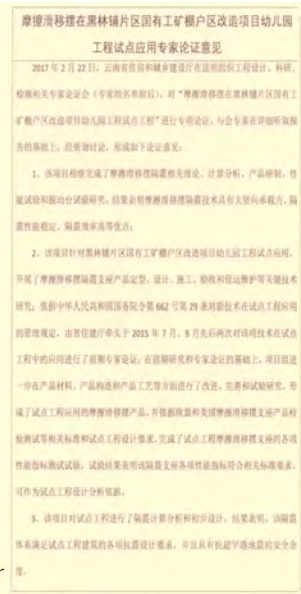

摩擦滑移摆在黑林铺片区国有工矿棚户区改造项目幼儿园工程试点应用专家论证意见

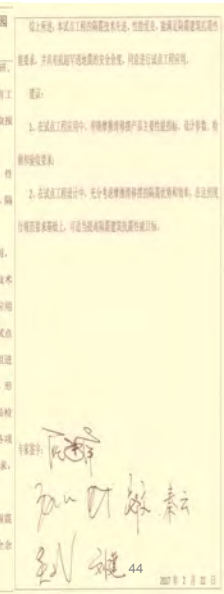

Topic Background

Heilinpu District State-owned Industrial and Mining Shantytown Reconstruction Project Tuanshan Xincheng Kindergarten Pilot Project

Yunnan Kunming Steel Structure Co., Ltd. collaborated on the project, implementing a new isolator, the friction sliding pendulum isolation bearing, in the kindergarten. The construction project in Yunnan Province utilized this isolation technology for the first time, making it a pilot project. In order to promote and apply this technology to actual projects, the research team went through a long period of research and development, conducting in-depth exploration and research in theoretical research, product design, product testing, and computational analysis.

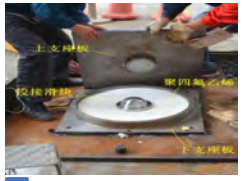

First generation product (2013)

The upper and lower support plates are made of cast steel, the slider is made of stainless steel, and the wear-resistant plate is made of polytetrafluoroethylene plate, which is embedded in the sliding surface and the rotating surface, respectively.

Second generation product (2015)

The upper support plate and the lower support plate are made of cast steel, while the slider is made of stainless steel. The sliding surface and the slider, respectively, are sprayed with wear-resistant material and polytetrafluoroethylene.

Third generation product (2016)

The upper support plate and the lower support plate are made of cast steel, the slider is made of stainless steel, the wear-resistant material is MTF plate, which is embedded in the slider, and silicone grease is applied on the rotating surface to increase lubrication.

Discussion on wear-resistant materials

The friction surface of the friction sliding pendulum isolation bearing is mainly composed of non-metallic wear-resistant materials and stainless steel. The effective performance of the isolation efficiency of the friction sliding pendulum bearing is directly related to how much weight it can hold and how resistant it is to wear. Therefore, it is crucial to select suitable and reliable wear-resistant materials:

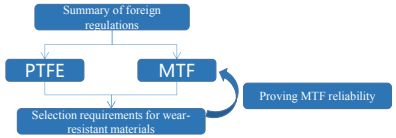

Research on detection methods

China doesn't have any specific testing standards for friction sliding pendulum isolation bearings used in buildings. So, this paper combines the European standard "EN15129," the American Highway and Transportation Association's "Seismic Isolation Design Manual," and the Chinese standard "GB/T 20688.1 Rubber Bearings Part 1: Test Scheme for Seismic Isolation Rubber Bearings," among others, to come up with useful ways to check finished bearings.

Research Content

Exploration of seismic isolation analysis methods

There aren't any design guidelines or specifications for friction sliding pendulum seismic isolation in China yet. This paper uses the "Anti-seismic Code" rules for rubber bearings and the properties of the friction sliding pendulum to come up with a way to analyze this kind of seismic isolation bearing.

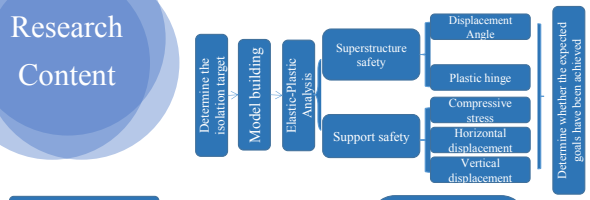

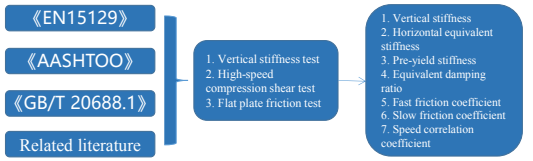

2 耐磨材料的选择及使用
Selection and application of wear resistant material

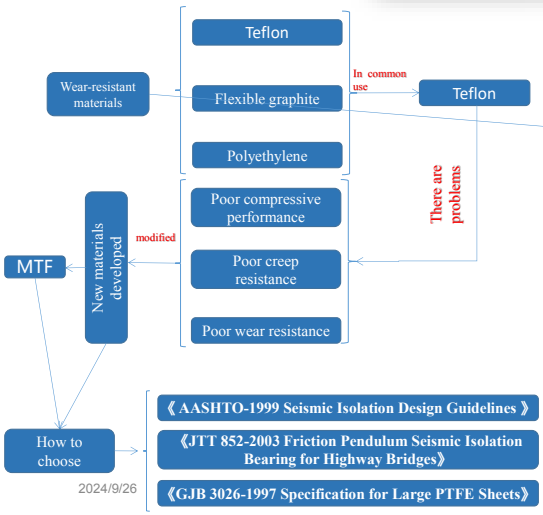

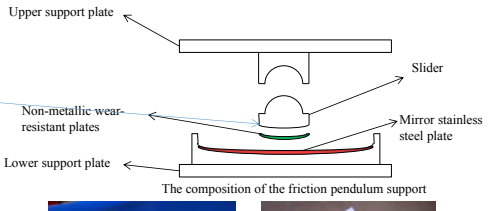

The composition of the friction pendulum support

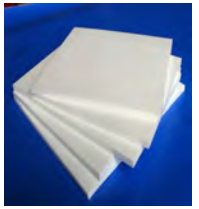

PTFE plate

MTF plate

2 耐磨材料的选择及使用 Selection and application of wear resistant material

Comparison of physical, chemical and mechanical properties between PTFE and MTF

物理及化学性能对比

项目	单位	MTF 参数	PTFE 参数	规范对耐磨材料要求
密度	g/cm³	2.2	1.44	JTT 852-2003 公路桥梁摩擦摆式减隔震支座中 5.2.3.4 条规定耐磨材料密度≥0.98g/cm3
介电强度	kV/mm	20	18~20	GJB 3026-1997 中 3.3.2 条规定≥10kV/mm
适用温度	°C	-20~115	-200~250	无规范要求

机械性能对比

球压痕硬度	MPa	160	23~30	JTT 852-2003 公路桥梁摩擦摆式减隔震支座中 5.2.3.4 条规定不小于 33MPa。
竖压屈服应力	MPa	270	12~25MPa	AASHTO(美标)中 16.4.1 规定非地震设计荷载下支座的压应力≤34MPa，地震荷载下平均应力≤41MPa。
弹性模量	MPa	2600	280	JTT 852-2003 公路桥梁摩擦摆式减隔震支座中 5.2.3.4 条规定弹性模量不低于 850（1±20%）MPa

Friction performance comparison

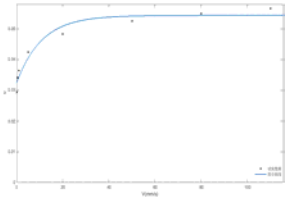

PTFE friction coefficient and velocity variation curve

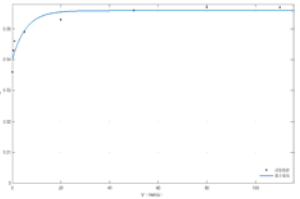

Friction coefficient and velocity variation curve of MTF

Fitting formula for u-v curve of PTFE:

$$\mu_{PTFE} = 0.0544 - 0.022e^{-9.17v}$$

MTF U-V curve fitting formula:

$$\mu_{MTF} = 0.05571 - 0.01635e^{-23.42v}$$

Comparison of Friction Performance between PTFE and MTF

项目	PTFE 材料	MTF 材料
快摩擦系数 f_{max}	0.0544	0.05571
慢摩擦系数 f_{min}	0.0324	0.03936
速度相关系数 a	9.17s/m	23.42s/m
动摩擦系数变化范围	0.022	0.01635

3 力学性能检测试验研究 Study on the test of mechanical properties

3 力学性能检测试验研究 Study on the test of mechanical properties

Support design for testing (third generation product)

◆ **Slider**

A wear-resistant plate mounting groove with a diameter of Φ140mm and a depth of 5mm is machined on the lower spherical surface of the slider.

◆ **Wear Plate**

Use an MTF plate to process a wear-resistant plate with a diameter of approximately 140mm and a thickness of 8mm, then install it in the wear-resistant plate groove of the slider during assembly.

◆ **Lower support plate**

The processing volume for the three sets of lower support plates is consistent. After processing, the spherical surface is polished, and the roughness is within Ra0.4

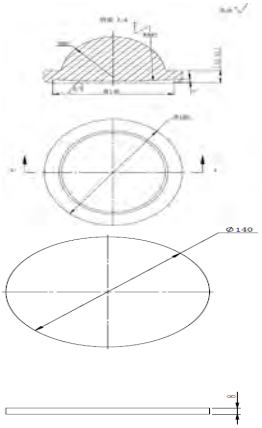

Table 1 Design parameters of friction pendulum support

Support design parameters	Numeric	Unit
Equivalent period of friction pendulum T	2	s
Equivalent radius R of friction pendulum	1000	mm
Non-seismic design bearing capacity N_{sd}	530	kN
Design displacement D	± 150	mm
Design speed V_m	200	mm/s

3 力学性能检测试验研究 Study on the test of mechanical properties

竖向刚度试验 The vertical stiffness test

Purpose of the test

The vertical stiffness value of the support is obtained through the vertical stiffness test and used as the indicator basis for calculation and analysis, so as to be used in SAP2000 modal analysis and nonlinear analysis.

Reference standards and literature

◆American Association of State Highway and Transportation Officials

"AASHTO-1999 Seismic Isolation Design Guidelines"

◆National Standards

GB/T 20688.1-2007, Rubber Bearings Part 1, describes the test methods for seismic isolation rubber bearings.

Loading scheme

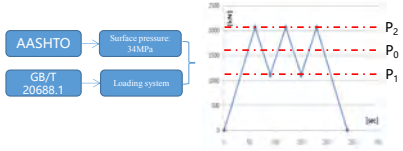

Loading curve

3 力学性能检测试验研究 Study on the test of mechanical properties

Original specification:

According to 0-P0-P2-P0-P1 (first loading), P1-P0-P2-P0-P1 (second loading), and P1-P0-P2-P0-P1 (third loading), the design pressure is P0.The vertical force control system first applies a vertical load of 2066 kN to the support group in accordance with the above specifications, then reduces the actuator's load to 1113 kN To complete the vertical stiffness test.

The vertical compression stiffness KV is calculated as follows:

$$K_v = \frac{P_2 - P_1}{Y_2 - Y_1}$$

Where:

P1-----Less pressure during three cycles

P2-----The maximum pressure during three cycles

Y1-----Minimum displacement during three cycles

Y2-----Minimum displacement during three cycles

Test results

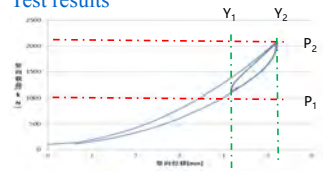

Vertical force and vertical displacement curve

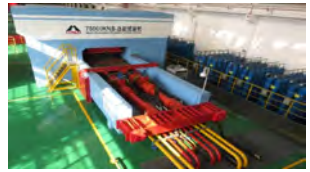

Multifunctional testing machine

Vertical stiffness test results

Vertical load	2066kN	1113kN
Vertical displacement	5.20mm	4.18mm
Vertical compression stiffness	934.30kN/mm	

3 力学性能检测试验研究 Study on the test of mechanical properties

High-speed compression shear test → Shear and press test of high speed

Purpose of the test

The equivalent stiffness, pre-yield stiffness, post-yield stiffness, and equivalent damping ratio of the support are obtained through high-speed compression and shear tests.

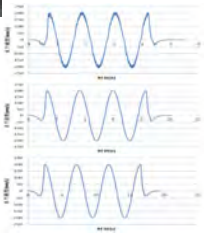

AASHTO → 面压：34MPa

EN15129 → 加载制度

d(t)=37.5sin(5.33t)

d(t)=75.0sin(2.66t)

d(t)=150sin(1.33t)

Loading curve

项目	团山欣城幼儿园摩擦滑移摆隔震支座性能检测试验研究								样品数量：3
试验样品	摩擦滑移摆支座								
试验类型	力学性能试验								
Test No.	Test Case	MainDof.	Vert. Load[kN]	Ampl.[mm]	Max Vel.[mm/s]	Freq.[Hz]	LoadShape	Cycles	SampingFreq.	Remark
1	高速剪切试验速度	Ilor	1589	37.5	200	0.849	Sine	3	400	动态1
		Hor	1589	75. 0	200	0.424	Sine	3	200	动态2
		Ilor	1589	150. 0	200	0.212	Sine	3	100	动态3

Test results

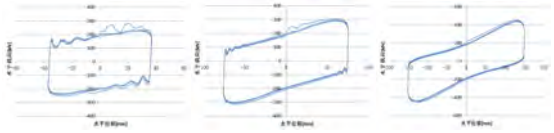

200mm/s dynamic 1 hysteresis curve　200mm/s dynamic 2 hysteresis curve　200mm/s dynamic 3 hysteresis curve

Friction sliding pendulum bearing performance parameters

Peak speed	Peak displacement	Equivalent stiffness	Stiffness before yield	Post-yield stiffness	Equivalent damping ratio
200mm/s	37.5mm	2.093kN/mm	23.26kN/mm	0.50kN/mm	0.55
	75.0mm	1.363kN/mm	26.22kN/mm	0.63kN/mm	0.46
	150mm	1.007kN/mm	24.4kN/mm	0.57kN/mm	0.339

3 力学性能检测试验研究 Study on the test of mechanical properties

Plate friction test → Shear and press test of high speed

Purpose of the test

By testing the friction coefficient between the MTF plate and the stainless steel plate at different sliding speeds, the slow friction coefficient, fast friction coefficient, and speed correlation coefficient of the contact surface between the MTF plate and the stainless steel plate were obtained.

Reference standards and literature

◆The American Association of State Highway and Transportation Officials "AASHTO-1999 Seismic Isolation Design Guidelines"

◆Literature

Work《Performance of Seimic Islation Hardware under Service and Seismic Loading》

Loading scheme

AASHTO → Surface pressure : 34MPa

literature → Loading system

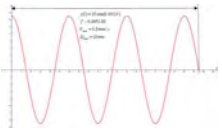

Loading curve

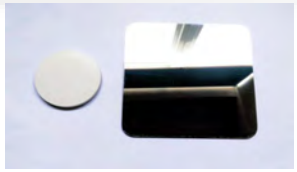

Wear-resistant material MTF and stainless steel plate

Plate friction test specimen parameters

编号	材料	尺寸	数量
SJ-1	MTF	直径：100mm，厚度：8mm	8
SJ-2	不锈钢板	直径：100mm，厚度：3mm	8

In order to obtain the relationship curve between the friction coefficient and the sliding speed, 8 groups of friction tests were carried out at different speeds, namely 0.1 mm/s, 0.5 mm/s, 1 mm/s, 5 mm/s, 20 mm/s, 50 mm/s, 80 mm/s, and 110 mm/s. The required curve was fitted through the test results to obtain the slow friction coefficient, fast friction coefficient, and speed correlation coefficient between MTF and stainless steel.

Test results

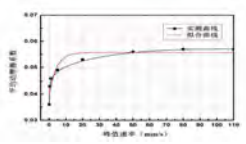

Friction performance parameters between MTF and stainless steel

参数	拟合值	标准误差
f_{max}	0.05571	0.00145
f_{min}	0.03936	0.0022
a	23.42s/m	0.12519
拟合相似度		0.85997

The fitting formula obtained according to the fitting results is:

$$\mu = 0.05571 - (0.05571 - 0.03936)e^{-23.42v}$$

4 隔震效应分析 Base isolation effect analysis

4 隔震效应分析 Base isolation effect analysis

The earthquake had a magnitude of 8 (0.2 g), belonged to the third group in the design earthquake group, was located at a type II site, and had a site characteristic period of 0.45s

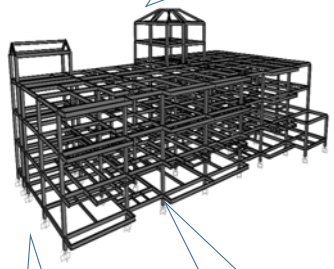

Located in Heilinpu, Wuhua District, Kunming

With a height-to-width ratio of 0.73 and dimensions of 25.7 m wide by 18.7 m high, the three-story steel frame structure falls under the key defense category.

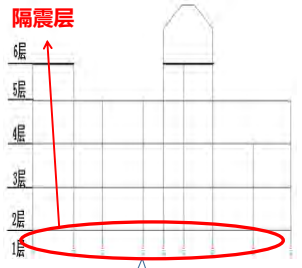

On the upper part of the structure, the middle tower is two stories and the edge tower is one story, with the first floor as the seismic isolation layer. The seismic isolation bearings are friction sliding pendulum bearings, with a total of 41 sets.

PK模型与SAP2000模型对比

Model cycle comparison

振型	SATWE(s)	sap2000(s)	差值(%)
1	0.987	1.006	1.932
2	0.980	1.000	2.015
3	0.840	0.859	2.256

Layer shear force comparison

层数	SATWE (KN)		SAP2000 (KN)		差值(%)	
	X	Y	X	Y	X	Y
6	225	240	216	224	-4.21	-6.70
5	437	451	413	426	-5.57	-5.62
4	1494	1490	1434	1417	-4.04	-4.86
3	2285	2255	2185	2154	-4.35	-4.49
2	2748	2723	2634	2608	-4.14	-4.24
1	3585	3469	3470	3363	-3.20	-3.05

Model quality comparison

SATWE(Ton)	sap2000(Ton)	差值(%)
5521.8	5521.2	-0.01

$$差值 = \frac{|SAP2000 - SATWE|}{SATWE} \times 100\%$$

According to SAP2000, the pressure value of each seismic isolation bearing under normal use is calculated, and the seismic isolation bearing model is preliminarily selected. According to the calculated bearing reaction force, FRB-36-700 bearings with large reaction force are arranged, and FRB-28-600 bearings with small reaction force are arranged. Finally, the seismic isolation bearing model and quantity are determined according to the subsequent time history analysis results (maximum and minimum surface pressure, structural torsion, etc.). The seismic isolation bearing arrangement of this project is as follows:

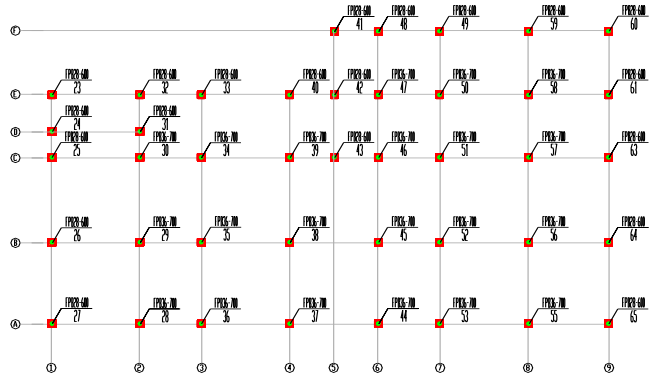

Isolation bearing parameters

类别		FRB-28-600	FRB-36-700
使用数量		20	21
竖向刚度	kN/mm	934.3	934.3
等效水平刚度	kN/mm	1.006	1.006
摩擦系数	慢	0.03936	0.03936
	快	0.05571	0.05571
速度相关系数	s/m	23.42	23.42
曲率半径	m	1	1

支座编号	屈服前刚度 (kN/m)	支座编号	屈服前刚度 (kN/m)
23	9782	44	24446
24	11184	45	29095
25	15349	46	26244
26	19391	47	25221
27	17451	48	17012
28	25647	49	18979
29	23517	50	28225
30	19796	51	30617
31	13959	52	29934
32	15974	53	24450
33	17867	55	26885
34	28646	56	23245
35	32138	57	33713
36	24773	58	19963
37	29889	59	18393
38	21921	60	10449
39	25823	61	15877
40	17867	63	18863
41	11220	64	19796
42	18567	65	12942
43	15957		

The combination of 1.0D+0.5L is used for bearing compressive stress verification under non-seismic design loads. Table 8 displays the long-term compressive stress of each bearing. The table reveals that each bearing has a small long-term compressive stress, all under 34 MPa. The maximum compressive stress of the bearing occurs at bearing No. 57 experiences the highest compressive stress, with a value of 21.0 MPa. All bearings have sufficient safety reserves.

Compressive stress of each support under normal use

支座编号	支座型号	1.0D+0.5L P (kN)	长期极大压应力 (Mpa)
23	FPB28-600	621	10.1
24	FPB28-600	710	11.5
25	FPB28-600	974	15.8
26	FPB28-600	1230	20.0
27	FPB28-600	1107	18.0
28	FPB36-700	1627	16.0
29	FPB36-700	1492	14.7
30	FPB36-700	1256	12.3
31	FPB28-600	886	14.4
32	FPB28-600	1014	16.5
33	FPB28-600	1134	18.4
34	FPB36-700	1818	17.9
35	FPB36-700	2039	20.0
36	FPB36-700	1572	15.5
37	FPB36-700	1897	18.6
38	FPB36-700	1391	13.7
39	FPB36-700	1639	16.1
40	FPB28-600	1134	18.4
41	FPB28-600	712	11.6
42	FPB28-600	1178	19.1
43	FPB28-600	1012	16.5
44	FPB36-700	1551	15.2
45	FPB36-700	1846	18.1
46	FPB36-700	1665	16.4
47	FPB36-700	1600	15.7
48	FPB28-600	1079	17.5
49	FPB28-600	1204	19.6
50	FPB36-700	1791	17.6
51	FPB36-700	1943	19.1
52	FPB36-700	1899	18.7
53	FPB36-700	1551	15.2
55	FPB36-700	1706	16.8
56	FPB36-700	1475	14.5
57	FPB36-700	2139	21.0
58	FPB36-700	1267	12.5
59	FPB28-600	1167	19.0
60	FPB28-600	663	10.8
61	FPB28-600	1007	16.4
63	FPB28-600	1197	19.4
64	FPB28-600	1256	20.4
65	FPB28-600	821	13.3

The maximum compressive stress meets the design requirements

Comparison of isolation and non-isolation model cycles

振型号	周期 非隔震 (s)	周期 隔震 (s)	两方向差值 (%)
1	1.00	2.47	1.25
2	0.99	2.44	
3	0.85	2.23	

The addition of the friction sliding pendulum bearing significantly extends the natural seismic period of the upper structure, resulting in an isolation period that is nearly 2.5 times larger than the non-isolation period. The first-order vibration mode is mainly X-direction vibration; the second-order vibration mode is mainly Y-direction vibration; and the third-order vibration mode is mainly torsion.

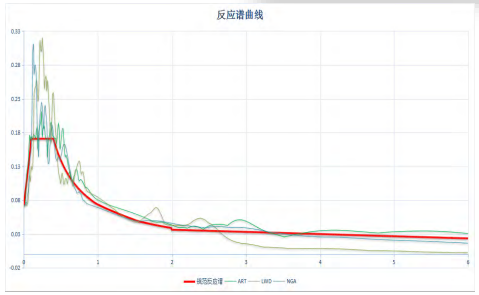

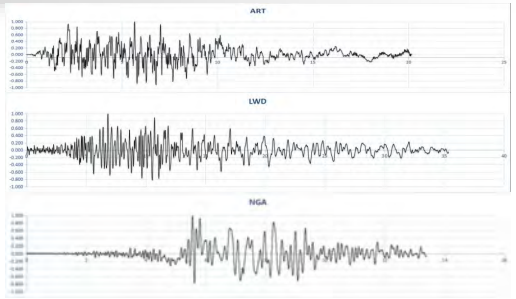

Comparison of time-history response spectrum and standard response spectrum curves

Time course curve

Base shear of non-isolated structure (moderate earthquake)

工况		反应谱	ART	LWD	NGA	时程平均
剪力 (kN)	X	7557	8057	8009	6770	7612
	Y	7260	7985	7935	6766	7562
比例 (%)	X	100	107	106	90	101
	Y	100	110	109	93	104

3 time-course response spectrum duration table

时程名称	第一次达到该时程曲线最大峰值10%对应的时刻 (S)	最后一次达到该时程曲线最大峰值10%对应的时刻 (S)	有效持续时间 (S)	结构基本周期 (S)	比值
ART	0.68	20.4	19.72	2.473	7.974
LWD	0.02	33.62	33.6	2.473	13.344
NGA	2.3	18.73	16.43	2.473	6.644

Comparison table of 3 time-history response spectra and standard response spectrum curves

振型号	非隔震周期 (s)	规范反应谱影响系数 (α)	时程平均影响系数 (α)	差值 (%)
1	1.00	0.074	0.078	5.94
2	0.99	0.07440	0.07957	6.94
3	0.85	0.086	0.089	4.50
振型号	隔震周期 (s)	规范反应谱影响系数 (α)	时程平均影响系数 (α)	差值 (%)
1	2.47	0.038	0.043	12.72
2	2.44	0.038	0.043	12.33
3	2.23	0.039	0.042	7.53

The structural seismic response of non-isolated structures and seismic isolation structures under different seismic waves is obtained through time history analysis. The input seismic fortification intensity of the structure is 8 degrees (the peak input acceleration during the fortification earthquake is PGA = 200 cm/s²), which is used to calculate the horizontal damping coefficient of the seismic isolation structure.

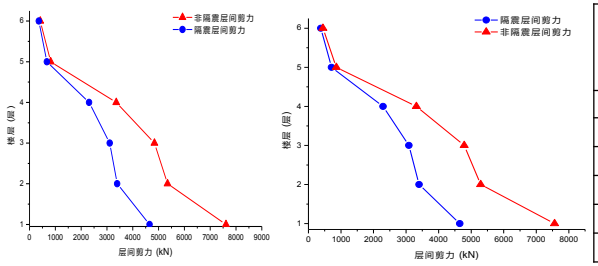

Comparison of interlayer shear force between seismic isolation and non-seismic isolation in moderate earthquakes

楼层	层间剪力比 X向 ART	X向 LWD	X向 NGA	X向包络值	Y向 ART	Y向 LWD	Y向 NGA	Y向包络值	X、Y向最大值
6	0.85	0.78	0.97	0.97	0.82	0.79	0.96	0.96	0.97
5	0.81	0.75	0.90	0.90	0.80	0.77	0.94	0.94	0.94
4	0.69	0.61	0.77	0.77	0.69	0.63	0.76	0.76	0.77
3	0.63	0.57	0.73	0.73	0.63	0.58	0.73	0.73	0.73
2	0.63	0.62	0.66	0.66	0.64	0.62	0.68	0.68	0.68
1	0.66	0.53	0.65	0.66	0.66	0.53	0.65	0.66	0.66

The maximum value of the interlayer shear force ratio of each layer in the X and Y directions is 0.97 (excluding the isolation layer), that is, the horizontal shock absorption coefficient is 0.97.

According to Article 12.2.5 of the Anti-Seismic Code, the maximum value of the horizontal earthquake influence coefficient after seismic isolation is determined as:

$$\alpha_{max\,1} = \beta \times \alpha_{max\,1} = 0.97 \times 0.16 = 0.1552$$

The highest value of the horizontal seismic influence coefficient is set at 0.16 because the project's superstructure is based on the idea that seismic action and seismic structural measures will not be decreased.

Floor displacement angle under earthquake protection

Floor	X向			Y向			Maximum
	ART	LWD	NGA	ART	LWD	NGA	
6	1/337	1/312	1/344	1/341	1/305	1/291	1/291
5	1/303	1/274	1/315	1/305	1/281	1/274	1/274
4	1/265	1/266	1/263	1/271	1/270	1/267	1/263
3	1/252	1/255	1/258	1/260	1/256	1/250	1/252
2	1/316	1/345	1/354	1/301	1/333	1/354	1/301
隔震层	1/632	1/664	1/696	1/745	1/794	1/852	1/632

There is no plastic hinge in the upper structure under the earthquake protection, and the structure remains elastic

The left figure shows that, under the design earthquake, the seismic isolation structure has reached performance level 2, while the non-seismic isolation structure is at level 3. The seismic isolation structure has improved one performance level compared to the non-seismic isolation structure.

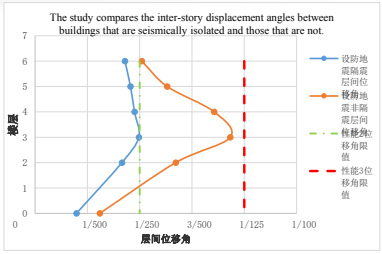

The maximum surface pressure of the friction sliding bearing under earthquake protection is

Support number	Support model	Maximum axial force of support (kN)	Surface pressure (MPa)
47	FPB36-700	-2225	36

Less than the maximum surface pressure of 41MPa allowed by the American Standard

Horizontal displacement of friction sliding bearings under earthquake protection

Support number	Support model	Maximum horizontal displacement of support
59	FPB28-600	30.166mm

The maximum displacement of the support is less than 160mm, and there will be no collision between the slider and the limit device.

表 M. 1. 1-2 结构构件实现抗震性能要求的层间位移参考指标示例

性能要求	多遇地震	设防地震	罕遇地震
性能 1	完好，变形远小于弹性位移限值	完好，变形小于弹性位移限值	基本完好，变形略大于弹性位移限值
性能 2	完好，变形远小于弹性位移限值	基本完好，变形略大于弹性位移限值	有轻微塑性变形，变形小于 2 倍弹性位移限值
性能 3	完好，变形明显小于弹性位移限值	轻微损坏，变形小于 2 倍弹性位移限值	有明显塑性变形，变形约 4 倍弹性位移限值
性能 4	完好，变形小于弹性位移限值	轻～中等破坏，变形小于 3 倍弹性位移限值	不严重破坏，变形不大于 0.9 倍塑性变形限值

Through time-history analysis, the structural seismic responses of non-isolated and isolated structures under different seismic waves are obtained. The structure's input seismic fortification intensity is 8 degrees (in rare earthquakes, the input acceleration peak value is PGA = 400 cm/s2).

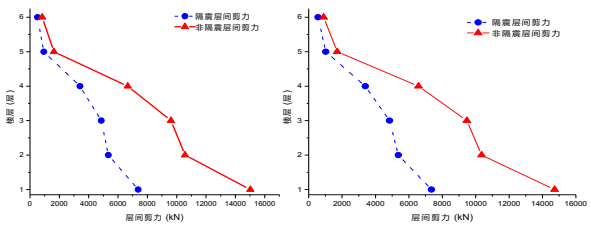

罕遇地震隔震与非隔震层间剪力对比

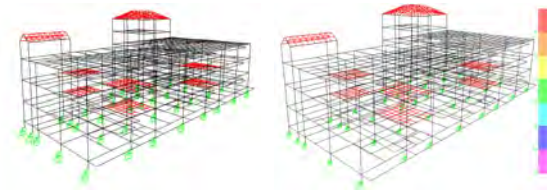

NGA-X Directional structural deformation　　NGA-Y Directional structural deformation

楼层	层间剪力比								
	X向			X向包络值	Y向			Y向包络值	X、Y向最大值
	ART	LWD	NGA		ART	LWD	NGA		
6	0.59	0.56	0.70	0.70	0.60	0.58	0.71	0.71	0.71
5	0.57	0.52	0.67	0.67	0.57	0.54	0.71	0.71	0.71
4	0.54	0.46	0.54	0.54	0.54	0.47	0.54	0.54	0.54
3	0.50	0.50	0.52	0.52	0.51	0.51	0.51	0.51	0.52
2	0.51	0.50	0.52	0.52	0.52	0.50	0.53	0.53	0.53
1	0.53	0.36	0.59	0.59	0.54	0.37	0.60	0.60	0.60

On the top floor, the maximum value of the inter-layer shear ratio occurs on the top floor, with a magnitude of 0.71. Without considering the tower, the maximum value of the inter-layer shear ratio for the main part of the structure occurs on the third floor (excluding the seismic isolation layer), with a magnitude of 0.54.

Under rare earthquakes, the maximum surface pressure of the friction sliding bearing is as follows:

Support number	Support model	Maximum axial force of support (kN)	Surface pressure (MPa)
23	FPB28-600	-2364	38

Less than the maximum surface pressure of 41MPa allowed by the American Standard

Floor displacement angle under rare earthquake

楼层	X向			Y向			最大值
	ART	LWD	NGA	ART	LWD	NGA	
6	1/190	1/178	1/181	1/239	1/209	1/198	1/178
5	1/149	1/138	1/169	1/149	1/145	1/144	1/144
4	1/137	1/138	1/137	1/144	1/143	1/140	1/137
3	1/129	1/130	1/124	1/139	1/135	1/139	1/129
2	1/152	1/161	1/193	1/143	1/160	1/174	1/143
隔震层	1/537	1/561	1/585	1/569	1/508	1/525	1/508

The left figure shows that under rare earthquakes, the seismic isolation structure has reached performance level 2, while the non-seismic isolation structure is at performance level 4. The seismic isolation structure has improved two levels of performance compared to the non-seismic isolation structure.

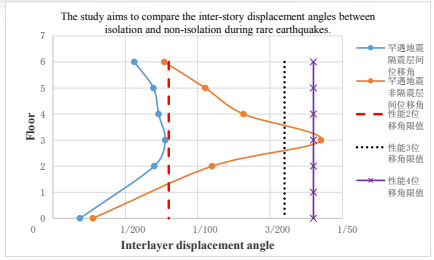

Under rare earthquakes, both the isolation structure and the non-isolation structure have maximum inter-story displacement angles on the third floor. The isolation structure's maximum interstory displacement angle is 1/129, while the non-isolation structure's maximum interstory displacement angle is 1/54.

Elastic-Plastic Analysis Results

There are five beam hinges in the ARTY condition and four in the NGAY condition, which are in the IO section. In other situations, there are no hinges.

The maximum horizontal displacement is 79mm, while the designed effective displacement is 160mm.
The maximum vertical displacement is 2.136mm, and the engagement depth is 72mm.

In rare earthquake conditions, the upper structure begins to enter plasticity but still can withstand a large earthquake.

When sliding, the friction pendulum does not collide with the limit device.

The top floor of the non-isolated structure has a maximum acceleration of 6.92 m/s2. The isolated structure has a maximum acceleration of the top floor of the isolated structure of 4.70 m/s2.

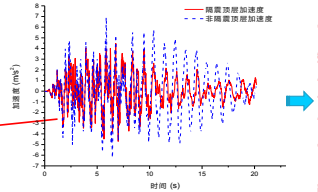

Comparison of top floor acceleration between seismically isolated and non-seismically isolated structures (rare earthquakes)

The acceleration is significantly reduced

Since the friction sliding pendulum bearing's seismic isolation performance in extremely rare earthquakes is its biggest advantage over rubber bearings, we carried out an isolation analysis of the structure with a seismic fortification intensity of 9 degrees (the peak input acceleration during extremely rare earthquakes is PGA = 620 cm/s2) to verify the friction sliding pendulum bearing's seismic isolation efficiency.

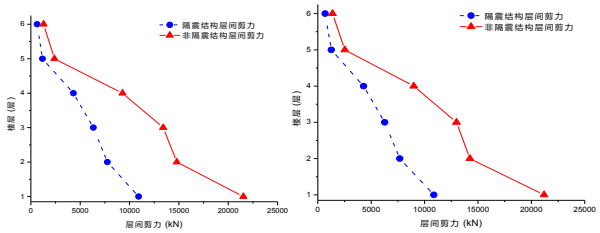

极罕遇地震隔震与非隔震层间剪力对比

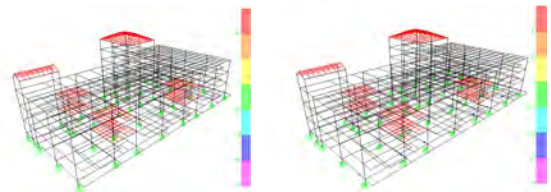

ART-X方向结构变形　　ART-Y方向结构变形

楼层	层间剪力比								
	X向			X向包络值	Y向			Y向包络值	X、Y向最大值
	ART	LWD	NGA		ART	LWD	NGA		
6	0.49	0.46	0.54	0.54	0.48	0.48	0.55	0.55	0.55
5	0.48	0.44	0.57	0.57	0.47	0.46	0.58	0.58	0.58
4	0.48	0.45	0.46	0.48	0.51	0.46	0.46	0.51	0.51
3	0.47	0.49	0.45	0.49	0.49	0.51	0.45	0.51	0.51
2	0.50	0.50	0.47	0.47	0.42	0.41	0.49	0.50	0.50
1	0.51	0.40	0.62	0.62	0.51	0.41	0.63	0.63	0.63

The maximum inter-layer shear ratio occurs in the first layer (excluding the isolation layer), which is 0.51.

The maximum surface pressure of the friction sliding bearing under rare earthquakes is:

支座编号	支座型号	支座最大轴力(kN)	面压（MPa）
42	FPB28-600	-2541	40

Less than the maximum surface pressure of 41MPa allowed by the American Standard

4 隔震效应分析 Base isolation effect analysis

Under extremely rare earthquakes, the maximum inter-story displacement angles of both the seismic isolation structure and the non-seismic isolation structure appear on the third floor. The seismic isolation structure's maximum interstory displacement angle is 1/105, while the non-seismic isolation structure's maximum interstory displacement angle is 1/52.

Displacement angle of the floor of the seismic isolation structure under extremely rare earthquakes								Displacement angle of non-isolated structures under extremely rare earthquakes						
楼层	X向			Y向			最大值	X向			Y向			最大值
	ART	LWD	NGA	ART	LWD	NGA		ART	LWD	NGA	ART	LWD	NGA	
6	1/202	1/191	1/188	1/198	1/168	1/165	1/165	1/142	1/120	1/158	1/151	1/134	1/152	1/120
5	1/159	1/140	1/176	1/144	1/140	1/144	1/140	1/109	1/92	1/120	1/114	1/100	1/129	1/92
4	1/122	1/116	1/124	1/122	1/120	1/132	1/116	1/82	1/74	1/83	1/81	1/80	1/88	1/74
3	1/110	1/106	1/118	1/105	1/108	1/117	1/105	1/72	1/71	1/78	1/52	1/71	1/78	1/52
2	1/142	1/155	1/150	1/130	1/152	1/134	1/130	1/100	1/108	1/126	1/94	1/101	1/124	1/94
上支墩	1/532	1/525	1/522	1/394	1/383	1/392	1/383	1/353	1/392	1/377	1/291	1/441	1/292	1/291

Elastic-Plastic Analysis Results

- ARTX, ARTY, LWDY, NGAX, and NGAY conditions rarely encounter earthquakes on the first and second floors, but no column hinges appear. Most beam hinges are in the IO stage, and some have progressed to the LS stage.
- The maximum horizontal displacement is 152mm, while the design effective displacement is 160mm. The maximum vertical displacement is 2.33mm, and the engagement depth is 72mm.

- In rare earthquake conditions, the upper structure has a large plasticity, but it still meets the requirements for strong earthquake resistance.
- When sliding, the friction pendulum does not collide with the limit device.

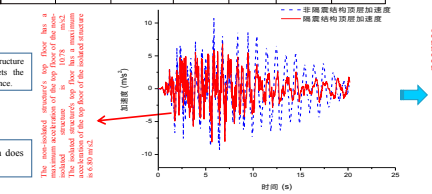

The non-isolated structure's top floor has a maximum acceleration of the top floor of the non-isolated structure is 0.51 m/s2. The isolated structure's top floor has a maximum acceleration of the top floor of the isolated structure is 0.09 m/s2

The acceleration is significantly reduced

Comparison of top floor acceleration between seismically isolated and non-seismically isolated structures (in extremely rare earthquakes)

Conclusion

- Pilot projects proposed the parameter index of wear-resistant materials for friction sliding isolation bearings, and experiments verified the reliability of new wear-resistant materials.
- Combining the testing standards of similar products at home and abroad, a set of performance testing methods and standards for friction sliding pendulum isolation bearings has been developed.
- A friction-sliding isolation design and analysis method suitable for pilot projects is proposed.
- The pilot project was subjected to seismic isolation calculation and analysis, and the results showed that the seismic performance was improved by one level under the design earthquake and by two levels under the rare earthquake.
- The technical route and system plan for seismic isolation observation and monitoring of the pilot project were proposed and demonstrated.

Passive vibration control theory and engineering application for primary-attached structural system

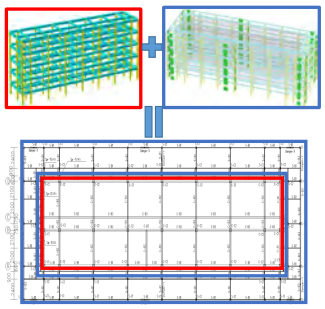

The topic's importance and background

Structural system

Initial concept

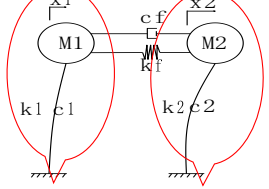

Main structure: "What should we do if an earthquake comes?"

Attached structure: "Uncoordinated deformation provides reaction force and dissipates part of the earthquake energy."

Integrated building functions; Simultaneous shock control;

FUC, AUC, FC: "The AC model has the worst control effect on the main structure."

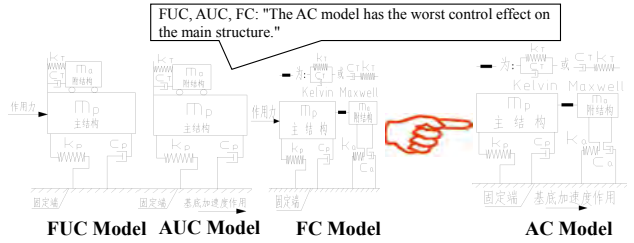

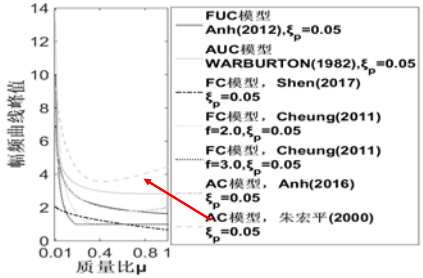

除相邻结构连接之外，AC模型可作为主-附体系的模型代表，最有可能实现建筑功能和结构抗震性能的同时提升

The equations for motion in two-degree-of-freedom systems and amplitude-frequency curves are presented.

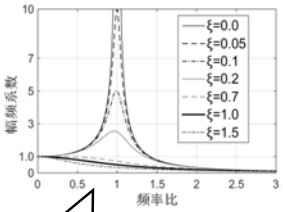

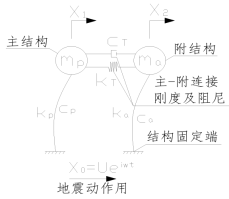

$$m_p\ddot{x}_1 + (c_p + c_T)\dot{x}_1 + (k_p + k_T)x_1 - (c_T\dot{x}_2 + k_Tx_2) = -m_p\ddot{x}_0$$
$$m_a\ddot{x}_2 + (c_a + c_T)\dot{x}_2 + (k_a + k_T)x_2 - (c_T\dot{x}_1 + k_Tx_1) = -m_a\ddot{x}_0$$

Shock absorption: add damping or avoid resonance; reduce the peak value of the amplitude-frequency curve.

$$\gamma_{mp} = \sqrt{\frac{(g^2 - \beta^2 - (1+\mu)f^2)^2 + 4g^2(\xi_a\beta + (1+\mu)\xi_T f)^2}{d_1^2 + d_2^2}} \quad \text{主} \quad \gamma_{mp} = \frac{1}{\sqrt{(1-g^2)^2 + (2\xi_p g)^2}}$$

$$\gamma_{ma} = \beta^2\sqrt{\frac{(g^2 - 1 - (1+\mu)f^2)^2 + 4g^2(\xi_p\beta + (1+\mu)\xi_T f)^2}{d_1^2 + d_2^2}} \quad \text{附} \quad \gamma_{ma} = \frac{1}{\sqrt{(1-(g/\beta)^2)^2 + (2\xi_a(g/\beta))^2}}$$

$\mu = m_a/m_p$， Represents the mass ratio of the structure； $\omega_p = \sqrt{k_p/m_p}$， Indicates the main structural circle frequency； $\xi_p = c_p/2m_p\omega_p$， The damping ratio of the main structure； $\omega_{Ta} = \sqrt{k_T/m_a}$， Indicates the coupling frequency； $\xi_T = c_T/2m_a\omega_{Ta}$， The coupling damping ratio； $\omega_a = \sqrt{k_a/m_a}$， Indicates the circular frequency of the attached structure； $\xi_a = c_a/2m_a\omega_a$， Indicates the damping ratio of the attached structure； $g = \omega/\omega_p$， $f = \omega_{Ta}/\omega_p$， $\beta = \omega_a/\omega_p$ Define for different frequency ratios， ω is the frequency of external load .

Two-degree-of-freedom system: main structure control

Undamped main structure control

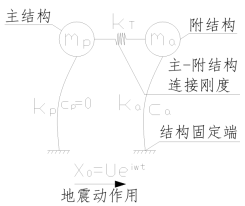

$(\xi_T = 0, \xi_a \neq 0)$

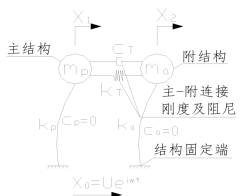

$(\xi_a = 0, \xi_T \neq 0)$

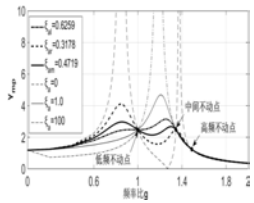

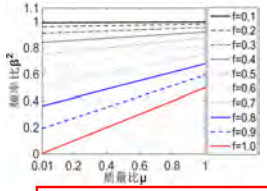

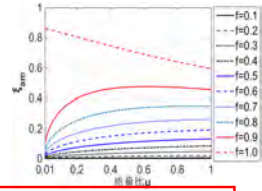

The frequency control equation and damping calculation formula are derived from the fixed point theory.

$$\beta^2 = 1 + (0.5\mu - 1)f^2 \qquad \xi_{am} = \xi_{am}(\mu, f)$$
$$\beta^2 = \frac{2f^2(1+\mu)^2}{\mu - 2} + 1 \qquad \xi_{Tm} = \xi_{Tm}(\mu, f)$$

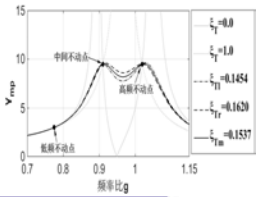

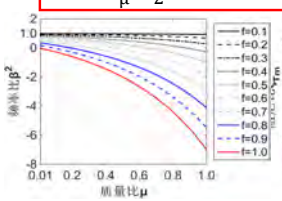

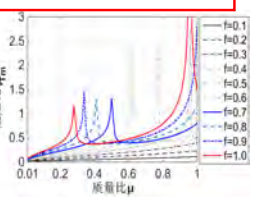

Two-degree-of-freedom system: main structure control

Damped main structure control

Equivalent Linearization Method

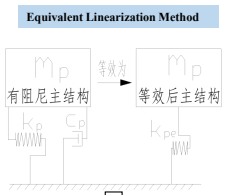

$$\omega_{pe\_wei} = \mathrm{ELF} \cdot \omega_p$$

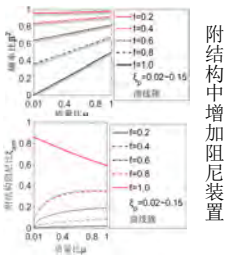

附结构中增加阻尼装置

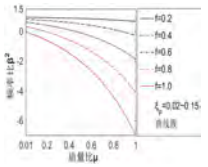

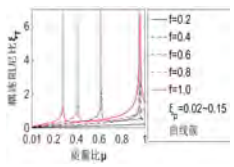

The damping device connects the main and auxiliary structures.

Adjustment factor method

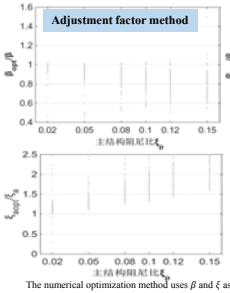

主、附结构间连接阻尼装置

β_{opt} *is smaller than that of the main structure without damping*

ξ_{opt} *is larger than that of the main structure without damping*

The numerical optimization method uses β and ξ as variables to obtain a double-peaked amplitude-frequency curve with equal height.

$$\beta\_opt = frequency\ ratio\ adjustment\ factor * \beta, \xi\_opt = damping\ "adjustment"\ factor * \xi$$

When the main structure's damping is low (less than 0.05), the equivalent linearization method or the damping adjustment coefficient method can effectively reduce the main structure's amplitude-frequency peak.
When the damping of the main structure is high (greater than 0.05), it is recommended to use the numerical optimization method.

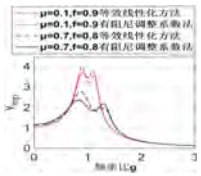

Two-degree-of-freedom system: main structure control

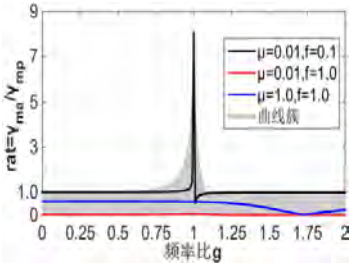

After a multi-parameter combination, the numerical simulation revealed that in some parameter combinations, the attached structure's dynamic amplification response sharply amplifies at the main structure's resonant frequency, while in other parameter combinations, the attached structure's amplitude-frequency amplification coefficient can be smaller than the main structure's across the entire frequency domain.

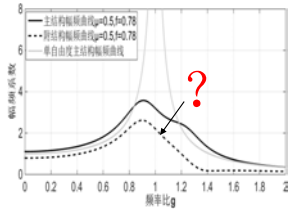

约束方程

$$\gamma_{ma}/\gamma_{mp} \leq 1.0$$

$$Ag^4 - (2Ab + 2B + C)g^2 + Ab^2 + 2bB \leq 0$$

When the constraint equation is satisfied, the attached structure's dynamic amplification effect is smaller than that of the main structure in the full frequency domain.

Add damping devices to the attached structure.

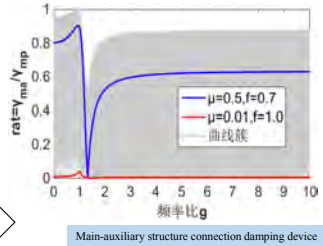

Main-auxiliary structure connection damping device

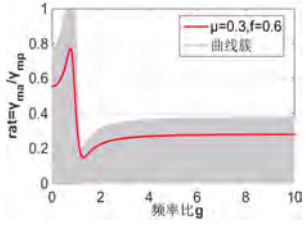

The two-degree-of-freedom system represents the passive vibration reduction design theory of the main-accessory structure.

Critical curve graph

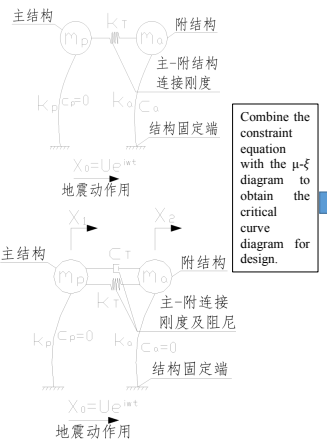

Combine the constraint equation with the μ-ξ diagram to obtain the critical curve diagram for design.

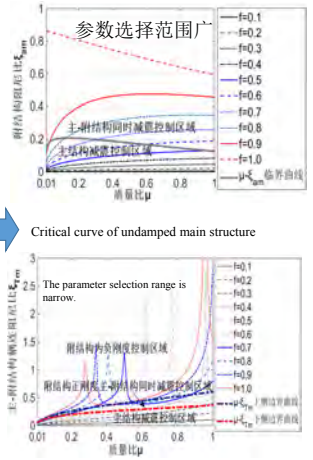

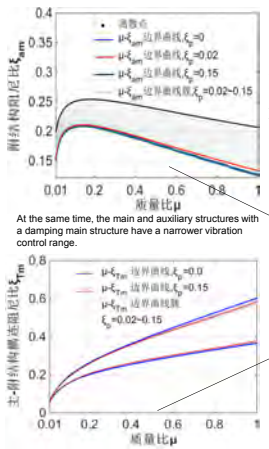

√The main attachment system with damping devices added to the attachment structure is preferred.

Convenient for design
– ξ curve
– f curveFitting critical cu

and use

The main accessory system uses passive vibration control with multiple degrees of freedom.

Equation, frequency modulation conditions

$$\begin{cases} \boldsymbol{M_a} = \mu.\times \boldsymbol{M_p} \\ \boldsymbol{K_a} = \alpha.\times \boldsymbol{K_p} \\ \boldsymbol{K_T} = Factor.\times \boldsymbol{M_a} \end{cases}$$

$$\left|\boldsymbol{K_p} - \omega_{pi}^2 \boldsymbol{M_p}\right| = 0 \qquad \left[\mathbf{K_p} - \omega_{\mathbf{pi}}^2 \mathbf{M_p}\right]\boldsymbol{\varphi_{pi}} = 0$$

$$\alpha\left|\boldsymbol{K_p} - \frac{\mu}{\alpha}\omega_{ai}^2 \boldsymbol{M_p}\right| = 0 \qquad \left[\mathbf{K_a} - \omega_{\mathbf{ai}}^2 \mathbf{M_a}\right]\boldsymbol{\varphi_{ai}} = 0$$

$$\omega_{\mathrm{pi}}^2 = \frac{\mu}{\alpha}\omega_{\mathrm{ai}}^2 \qquad \left[\boldsymbol{K_p} - \omega_{pi}^2 \boldsymbol{M_p}\right]\boldsymbol{\varphi_{pi}} = 0$$

$$\alpha\left[\mathbf{K_p} - \omega_{\mathbf{pi}}^2 \mathbf{M_p}\right]\boldsymbol{\varphi_{ai}} = 0$$

$$\boldsymbol{\Phi_p} = \boldsymbol{\Phi_a}$$

The main and auxiliary structures' modal frequencies are in the same proportion, and the vibration modes fit into the same matrix.

$$\begin{bmatrix} \boldsymbol{M_p} & \mathbf{0} \\ \mathbf{0} & \mathbf{M_a} \end{bmatrix}\begin{bmatrix} \ddot{\mathbf{X}}_\mathbf{p} \\ \ddot{\mathbf{X}}_\mathbf{a} \end{bmatrix} + \begin{bmatrix} \mathbf{C_{pT}} & -\mathbf{C_T} \\ -\mathbf{C_T} & \mathbf{C_{aT}} \end{bmatrix}\begin{bmatrix} \dot{\mathbf{X}}_\mathbf{p} \\ \dot{\mathbf{X}}_\mathbf{a} \end{bmatrix} + \begin{bmatrix} \mathbf{K_p} + \mathbf{K_T} & -\mathbf{K_T} \\ -\mathbf{K_T} & \mathbf{K_a} + \mathbf{K_T} \end{bmatrix}\begin{bmatrix} \mathbf{X_p} \\ \mathbf{X_a} \end{bmatrix} = \begin{bmatrix} \mathbf{M_p} & \mathbf{0} \\ \mathbf{0} & \mathbf{M_a} \end{bmatrix}\mathbf{E}\ddot{\mathbf{X}}_\mathbf{0}$$

$$\mathbf{X_p} = \boldsymbol{\Phi_p}\boldsymbol{q_1},\ \boldsymbol{X_a} = \boldsymbol{\Phi_a}\boldsymbol{q_2}$$

$$\begin{bmatrix} \boldsymbol{M_{pm}} & \mathbf{0} \\ \mathbf{0} & \boldsymbol{M_{am}} \end{bmatrix}\begin{bmatrix} \ddot{\boldsymbol{q}}_1 \\ \ddot{\boldsymbol{q}}_2 \end{bmatrix} + \begin{bmatrix} \boldsymbol{C_{pTm}} & -\boldsymbol{C_{Tm}} \\ -\boldsymbol{C_{Tm}^T} & \boldsymbol{C_{aTm}} \end{bmatrix}\begin{bmatrix} \dot{\boldsymbol{q}}_1 \\ \dot{\boldsymbol{q}}_2 \end{bmatrix} + \begin{bmatrix} \boldsymbol{K_{pTm}} & -\boldsymbol{K_{Tm}} \\ -\boldsymbol{K_{Tm}^T} & \boldsymbol{K_{aTm}} \end{bmatrix}\begin{bmatrix} \boldsymbol{q_1} \\ \boldsymbol{q_2} \end{bmatrix} = \begin{bmatrix} \boldsymbol{\Phi_p^T M_p} & \mathbf{0} \\ \mathbf{0} & \boldsymbol{\Phi_a^T M_a} \end{bmatrix}\mathbf{E}\ddot{\mathbf{X}}_\mathbf{0}$$

$$\boldsymbol{K_{Tm}} = \boldsymbol{K_{Tm}^T}$$

M_pm, ***K_pTm***, etc. are all diagonal matrices, so the modes of different orders between the main and auxiliary structures are decoupled. That is, only the first-order mode of the auxiliary structure controls the first-order mode of the main structure without controlling other modes.

The study focuses on the numerical simulation analysis of a main-accessory system with multiple degrees of freedom.

Equal degrees of freedom analysis object

Structural parameters: μ=0.3, ka/kp=0.15
Main and auxiliary structures simultaneously control the area

Structural parameters:
Critical curve edge

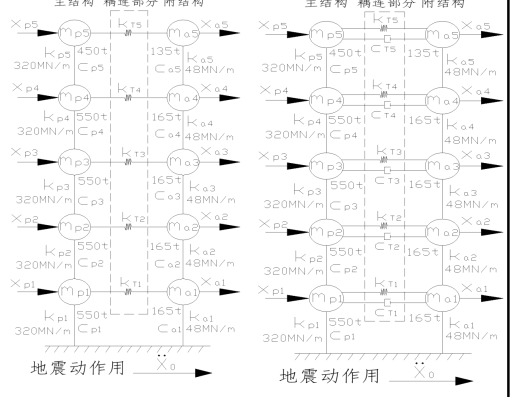

Unequal degrees of freedom analysis objects

Structural parameters:
Main and auxiliary structures simultaneously control the area

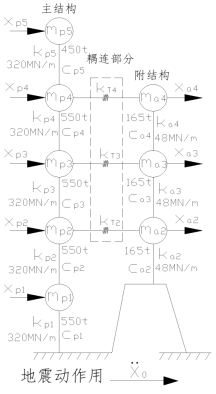

Structural parameters:
Critical curve edge

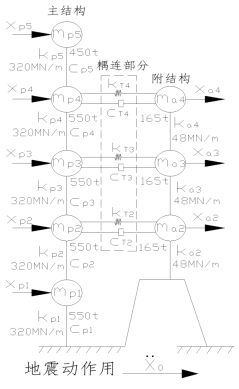

The study focuses on the numerical simulation analysis of a main-accessory system with multiple degrees of freedom.

The numerical analysis involves adding a damping device to the main supplementary structure.

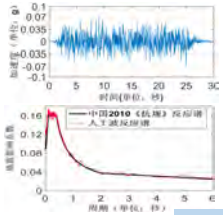

NEWMARK-β法

Comparison: The main structure exists independently, while the main and auxiliary structures are rigidly connected.

- **Forced semi-decoupling method**
- **According to the first-order mode equivalent**
- **Equivalent to the position of the maximum modal amplitude**
- **Weighted Control Multimodality**
- **Controlling the first mode**

Unequal degrees of freedom results

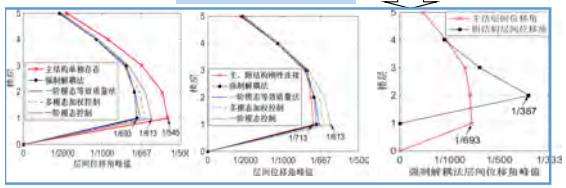

The control effect is not as good as the rigid connection between the main and auxiliary structures; the layer displacement angle ratio is greater than 0.5, and there is still a control effect on the auxiliary structure.

Equal degrees of freedom results

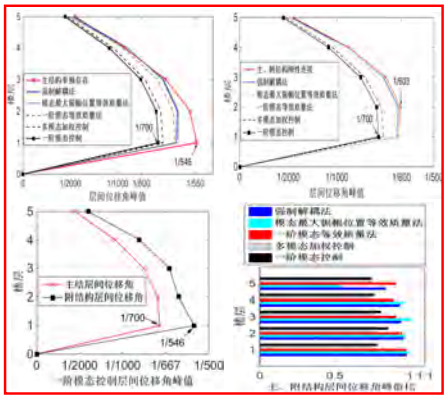

The shock absorption effect is significant, and the main structure control with equal degrees of freedom is better than the main structure existing alone, as is the rigid connection between the main and attached structures. The layer displacement angle ratio is greater than 0.5, which has a controlling effect on the attached structure.

Main-auxiliary system engineering application

Overview of existing concrete structures

There are 5 floors in total; each floor is 3.0 m high, and the total height of the structure is 15.0 m. The building's basic seismic fortification intensity is 8 degrees; the basic earthquake acceleration is 0.2 g; the design earthquake group is the third group; the site category is Class II; and the construction time is June 2003.

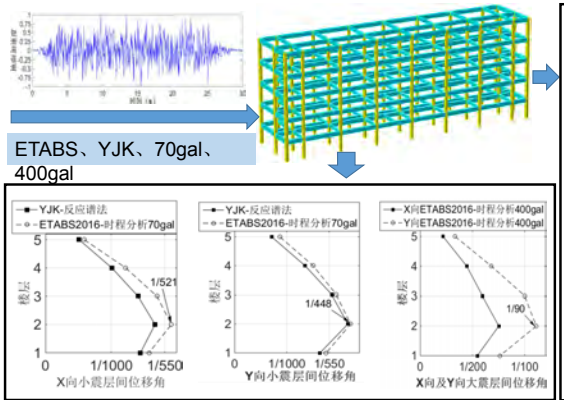

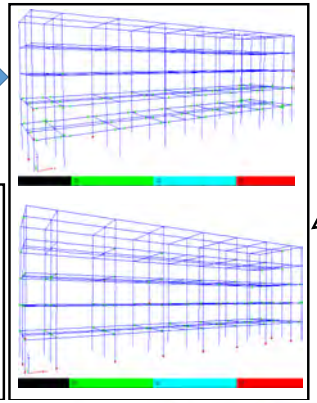

The original structure is damaged by "strong beams and weak columns":
☆Weak lateral stiffness
☆High risk of collapse in rare earthquakes

Want to expand the office building area and improve the seismic performance of the structure

Main-auxiliary system engineering application

Reinforcement plan: We connect the steel structure, which has dampers added to the outer shell, to the original concrete frame using elastic floor slabs.

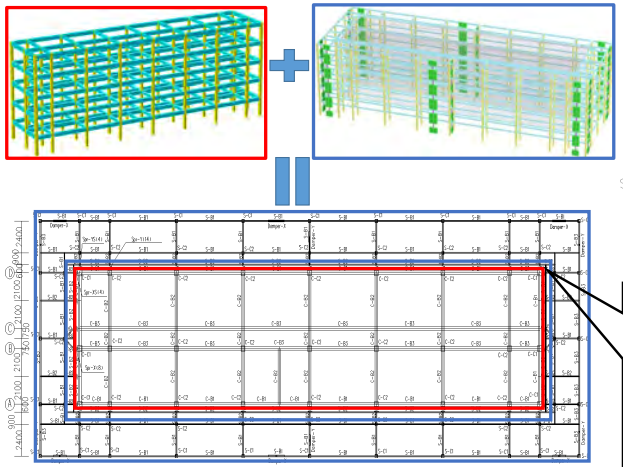

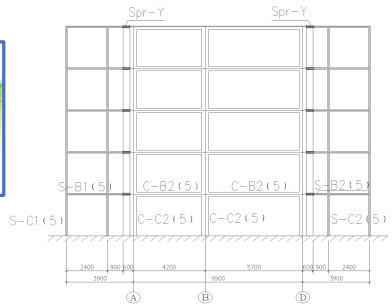

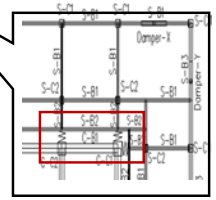

This image provides an enlarged view of the steel spring connection in the main accessory system.

Main-auxiliary system engineering application

Analyze the results

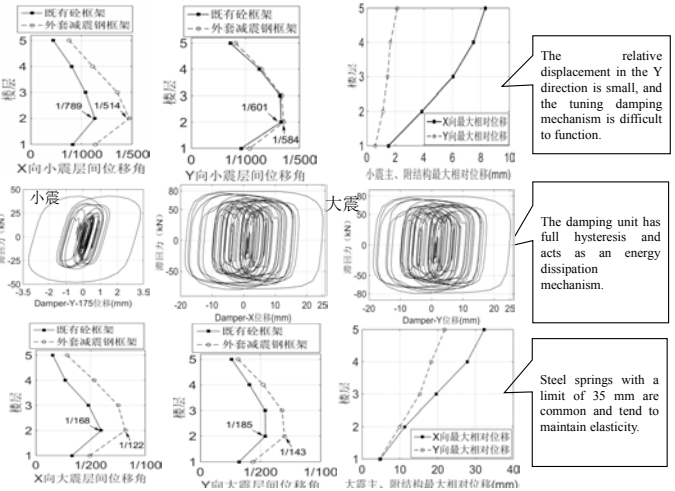

The relative displacement in the Y direction is small, and the tuning damping mechanism is difficult to function.

The damping unit has full hysteresis and acts as an energy dissipation mechanism.

Steel springs with a limit of 35 mm are common and tend to maintain elasticity.

Steel springs at floor position: Steel springs with a limit of 35mm are common and simple to maintain elasticity.

Damper: 80kN, 25mm limit dampers are more common.

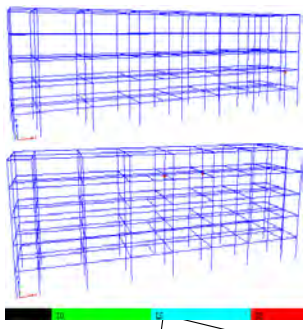

Plastic hinge distribution has significantly improved, and recoverability is robust.

Conclusion

- The basic control equations and constraint equations of passive vibration reduction design parameters of the two-degree-of-freedom main-accessory system with no damping main structure are obtained, and they are extended to the main-accessory system with damping main structure. The basic relationship that each structural parameter should follow in the design of the main-accessory system is explained.
- The passive damping design theory of the main-accessory structure is proposed; that is, the critical curve diagram is used to identify the parameter combination area where the main and auxiliary structures are simultaneously damped, which provides a theoretical basis for the engineering design of the main-accessory system. The main accessory system with a damping device added to the auxiliary structure has a wider range of parameters for simultaneous damping control of the main and auxiliary structures, so it is the first choice for the design of the main accessory system.
- The main accessory structure design theory is extended from a two-degree-of-freedom system to a multi-degree-of-freedom system and is applicable to a wide range of structural types. Numerical analysis and software simulation have proven the effectiveness of the main-accessory structure's seismic control.

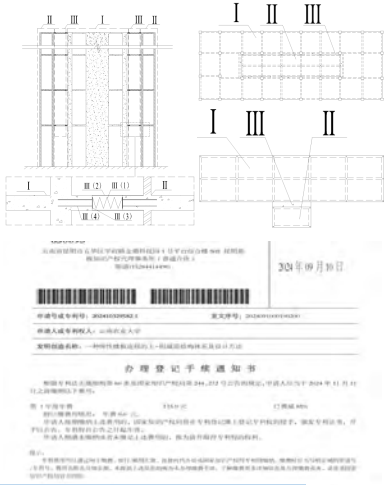

The latest authorized Chinese patents are available in both the main and subsidiary systems.

Experimental and theoretical research on traditional Chuan-dou type timber structure

Significance and background of the topic

Background

The protection of ancient wooden structures with important cultural relics, religious values, or historical and cultural research values is necessary.

In many rural areas, traditional residential buildings serve as residences, necessitating the protection of life and property.

"Create guidelines for enhancing the appearance of villages, taking into account local, regional, and ethnic characteristics... Implement demonstration of concentrated protection and utilization of traditional villages, establish and improve systems for traditional village investigation and identification, pre-merger review, and disaster prevention."
"Support the renovation of dilapidated houses and earthquake-resistant renovations in rural areas."

The CPC Central Committee and the State Council have expressed their opinions on the comprehensive promotion of key tasks for rural revitalization in 2023.

Significance and background of the topic

Background

It benefits the preservation of ancient wooden structures as well as the construction and reinforcement of traditional wooden residential buildings.

Developing the seismic resistance theory of traditional wooden structures and improving their ability to withstand earthquakes have important theoretical value and urgent practical significance.

It is also very important to learn about, pass on, and explore the unique earthquake-resistant structural knowledge that is contained in the construction technology of traditional wooden structures. We should also recreate and improve the cultural and structural earthquake-resistant technical value of our traditional wooden structures and support the growth of modern building structure earthquake-resistant theory and ideas.

"Wood Classics", "Construction Methods" and "Engineering Practice Rules"

Sliding Friction Pendulum Technology ⟷ Flat swing and floating support of column base

Self-centering semi-rigid joint ⟷ Semi rigid mortise and tenon joint

Significance and background of the topic

Background

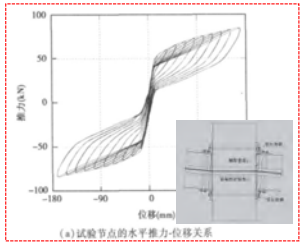

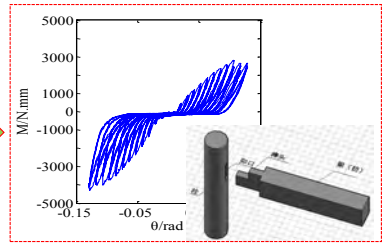

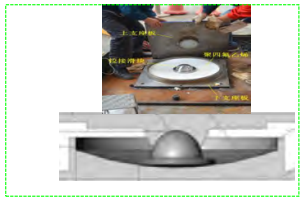

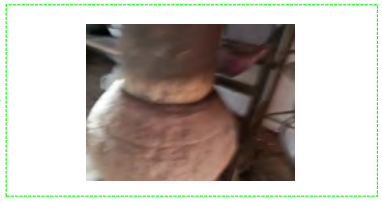

Research question 1: An experimental study on the seismic performance of mortise and tenon joints based on friction mechanism characteristics

Experimental model design

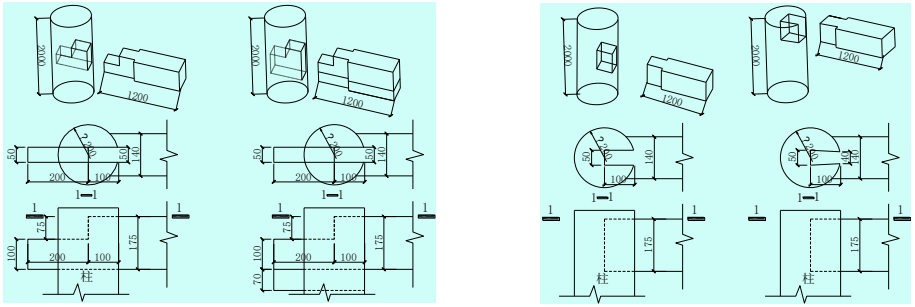

(a) Step tenon joint | (b) There is a beam joint under the beam | (c) Half tenon joint | (d) Dovetail node

Method: "Yingzaofashi" and "Yunnan Yikeyin";
Friction control: Control the friction coefficient by applying oil or not applying oil between the mortise and tenon joints.

Research question 1: An experimental study on the seismic performance of mortise and tenon joints based on friction mechanism characteristics

Test model loading

Determination of mechanical properties and friction coefficient of wood

木材力学性能

材料测定方向	抗压弹性模量 E/MPa	剪切模量 G/MPa	泊松比μ
顺纹	11580	920	0.37
径向	890	680	0.49
弦向	493	220	0.43

The material is fir, density: 0.506g/cm3, moisture content: 12.2%

$$\mu_{dyn} = \frac{F_{dyn}}{N} = \frac{F_{dyn}}{G_1 + G_2}$$

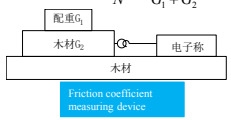

Friction coefficient measuring device

The average value of the 32 test results was taken, and the friction coefficient of the unoiled specimen was 0.38, and that of the oiled specimen was 0.20.

Loading scheme

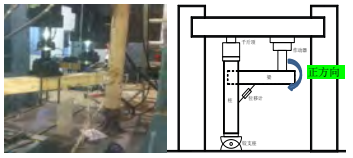

Loading device schematic

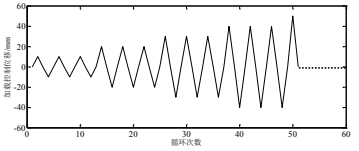

Loading system

Research question 1: An experimental study on the seismic performance of mortise and tenon joints based on friction mechanism characteristics

Analysis of seismic performance of test model

Energy consumption analysis

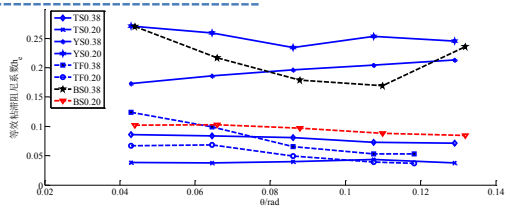

Relationship between equivalent viscous damping coefficient and rotation angle θ

Friction plays an important role in the seismic energy dissipation of step-through-tenon joints, step-through-tenon joints with beams under beams, and half-tenon joints. Friction has a significant influence on the speed at which the dovetail tenon joint model exerts its energy dissipation capacity. The node model with a friction coefficient of 0.20 exerts its energy dissipation capacity faster, while the node model with a friction coefficient of 0.38 has the opposite change trend.

Ductility Analysis

Whether the friction coefficient changes or not, the maximum rotation angle of the node model with beam under beam reaches 0.118 rad, while the other two models reach 0.129 rad. The friction coefficient's size will not affect the node's ductility.

Research question 2: Conduct an experimental study on the seismic performance of mortise and tenon joints with varying side tightness.

Experimental model design

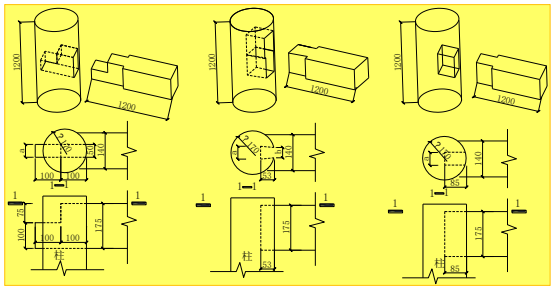

(a) Step tenon joint | (b) Half tenon joint | (c) Dovetail node

Method: "Yingzaofashi" and "Yunnan Yikeyin"; By keeping the width of the mortise unchanged and changing the width of the tenon, three models are made for each type of node: tight, moderate, and loose. Draw a 5mm*5mm square grid at the stress-bearing part of the tenon.

Component Name	Cross-section	Section size/mm	Length/mm
Column	Round	170	1200
Beam	Rectangle	140×175	1200

Research question 2: Conduct an experimental study on the seismic performance of mortise and tenon joints with varying side tightness.

Analysis of seismic performance of test model

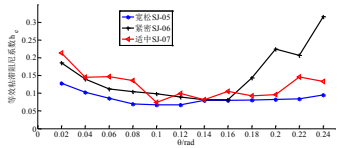

(a) Step tenon skeleton curve

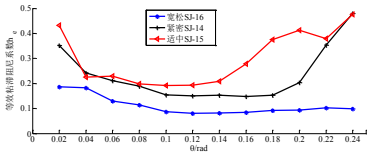

(b) Half-tenon joint skeleton curve

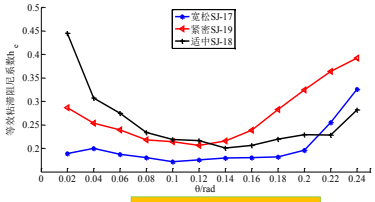

(c) Dovetail joint skeleton curve

It is not possible for stepped tenon, half tenon, and dovetail tenon joints to lose energy with a loose or tight model, especially when it comes to the early nodes.

Research Question 3: M-θ Curve Model of Mortise and Tenon Joints Based on Wood Friction Mechanism and Embedding Characteristics

Theory of Wood Compression Yield

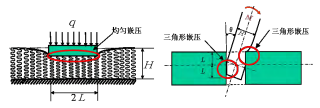

Schematic diagram of uniform and triangular wood embedding pressure

Mechanical assumptions of triangle embedding theory:

1. Elastic range and stress-strain obey Hooke's law;
2. Elastic range: Under compression deformation, the wood's compression pit volume V is proportional to the load P.
3. The indirect load action area's deformation curve is an exponential function:

$$z = \theta x_p e^{-\alpha_0 x}$$

Winkler foundation model

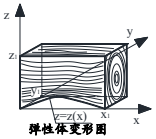

弹性体变形图

嵌压力P

$$\sigma(x) = \varepsilon(x)E = \frac{z(x)}{z_1}E$$

$$P = y_1 E_{90}\int_0^{x_0}\frac{z(x)}{z_1}dx = \frac{E_{90}}{z_1}V$$

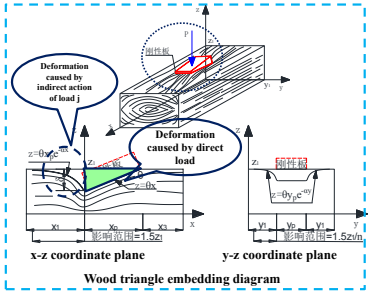

Basic assumptions for deriving the M-θ relationship of mortise and tenon joints

1. Ignore the effect of the circular column mortise on the tenon's uneven force;
2. Ignore the mortar's pressure on the grain;
3. Ignore the initial defects of the wood and the stratification characteristics of the spring and autumn wood.
4. The theoretical model does not consider the complex process of large deformation.

Research Question 3: M-θ Curve Model of Mortise and Tenon Joints Based on Wood Friction Mechanism and Embedding Characteristics

M-θ curve model of straight tenon joint

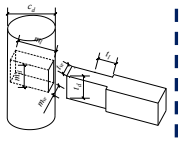

Straight tenon joint structure diagram

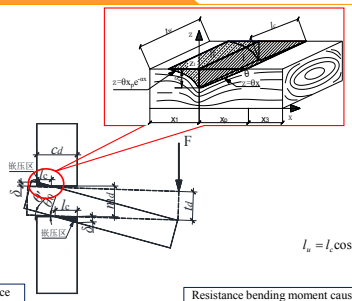

Schematic diagram of straight tenon deformation

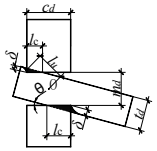

(a) Deformation geometry

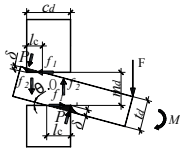

(b) Force analysis

The embedding pressure causes a resistance bending moment.

$$P_t = \frac{E_{90}}{t_d}(V_1+V_2) = \frac{E_{90}}{t_d}\left(\frac{1}{2}l_c^2 t_w + 0.6 l_c t_d t_w\right)\theta$$

$$P_b = \frac{E_{90}}{t_d}(V_1+V_2) = \frac{E_{90}}{t_d}\left(\frac{1}{2}l_c^2 t_w + 0.6 l_c t_d t_w\right)\theta$$

$$M_{em} = (P_t+P_b)l_u = \frac{2E_{90}}{t_d}\left(\frac{1}{2}l_c^2 t_w + 0.6 l_c t_d t_w\right)l_u\theta$$

Resistance bending moment caused by friction

$$F_t = \mu P_t(1+\nu_{23})$$

$$F_b = \mu P_b(1+\nu_{23})$$

$$M_{RF} = \frac{\mu(1+\nu_{23})l_d}{2}(P_t+P_b)$$

$$l_u = l_c\cos\theta + \frac{c_d/2 - l_c}{\cos\theta} + \frac{t_d}{2}\tan\theta$$

$$l_u = \frac{c_d}{2} + \frac{t_d}{2}\tan\theta$$

The relationship between the bending moment and rotation angle in the elastic stage is as follows:

$$K_R = \frac{2E_{90}}{t_d}\left(0.5 l_c^2 t_w + 0.6 l_c t_d t_w\right)l_u$$

$$K_{RF} = E_{90}\mu(1+\nu_{23})\left(0.5 l_c^2 t_w + 0.6 l_c t_d t_w\right)$$

$$M = M_{em} + M_{RF} = K_R\theta + K_{KF}\theta$$

Research Question 3: M-θ Curve Model of Mortise and Tenon Joints Based on Wood Friction Mechanism and Embedding Characteristics

M-θ curve model of straight tenon joint

Elastic-Plastic Stage

Determination of yield displacement and yield rotation

Yield displacement

$$\delta_y = \frac{2.4 f_{w,d} t_d}{E_{90}\sqrt{C_x C_y C_{90} C_{ym}}}$$

Yield Angle

$$\theta_y = \arctan\frac{\delta_y}{l_c} + \theta_0$$

$$V = V_e + V_p$$

$$V_e = \frac{1}{2}\left[\left(\frac{\delta-\delta_y}{\theta} + \frac{t_d}{1.5}\ln\frac{\delta_y}{\delta}\right) + (l_c + 1.5t_d)\right]\delta_y t_w$$

$$V_p = \frac{1}{2}\left(\frac{\delta-\delta_y}{\theta} + \frac{t_d}{1.5}\ln\frac{\delta_y}{\delta}\right)(\delta-\delta_y)$$

$$P_p = \frac{E_{90}}{t_d}V_e = \frac{E_{90}}{2t_d}\left\{\left[\left(\frac{\delta-\delta_y}{\theta} + \frac{t_d}{1.5}\ln\frac{\delta_y}{\delta}\right) + (l_c+1.5t_d)\right]\delta_y t_w\right\}$$

$$= \frac{E_{90}\delta_y t_w}{2t_d}\left[\left(\frac{\delta-\delta_y}{\theta} + \frac{t_d}{1.5}\ln\frac{\delta_y}{\delta}\right) + (l_c+1.5t_d)\right]$$

M-θ relationship in the elastic-plastic stage:

$$\begin{cases} M_p = 2P_p l_u \\ M_{PF} = \mu(1+\nu_{23})l_d P_p \end{cases}$$

$$M_p = 2P_p l_u + \mu(1+\nu_{23})l_d P_p$$

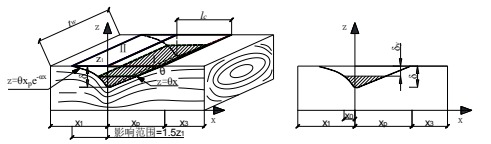

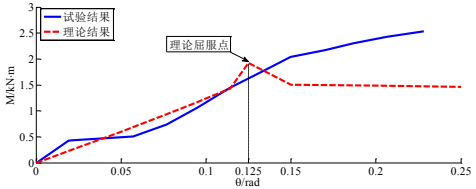

Comparison between the experimental and theoretical values of the SJ-03 straight tenon joint model

Research Question 3: M-θ Curve Model of Mortise and Tenon Joints Based on Wood Friction Mechanism and Embedding Characteristics

M-θ curve model of stepped tenon joint

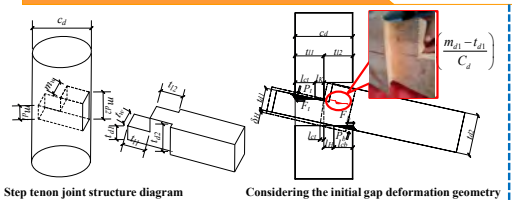

Step tenon joint structure diagram

Considering the initial gap deformation geometry

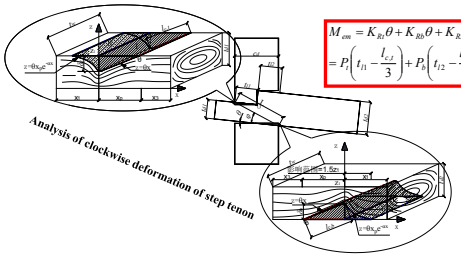

Analysis of clockwise deformation of step tenon

$$M_{em} = K_{Bi}\theta + K_{Bli}\theta + K_{BFi}\theta = P_t\left(t_{t1} - \frac{l_{c,t}}{3}\right) + P_b\left(t_{t2} - \frac{l_{c,b}}{3}\right) + F_b t_{d1}$$

Elastic phase when rotating clockwise

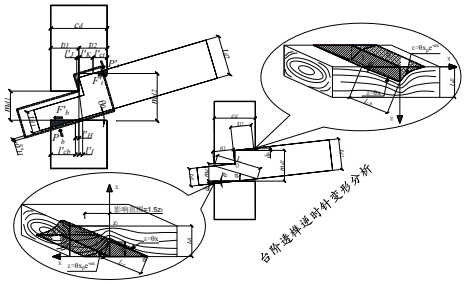

台阶透榫逆时针变形分析

$$V = P_t' - P_b'$$

$$M = P_b' t_{t1} + P_t' t_{t2} + F_b' t_{d1} + F_t'(t_{d2} - t_{d1})$$

Elastic phase when rotating counterclockwise

Research Question 3: M-θ Curve Model of Mortise and Tenon Joints Based on Wood Friction Mechanism and Embedding Characteristics

M-θ curve model of stepped tenon joint

When rotating clockwise, it enters the elastic-plastic stage: $\theta > \theta_y$

$$M_{pR} = \frac{E_{90}\delta_y t_w}{2t_{d1}}\left(\frac{\delta-\delta_y}{\theta} + \frac{t_{d1}}{1.5}\ln\frac{\delta_y}{\delta} + l_{ct} + 1.5t_{d1}\right)\left(t_{t1} - \frac{l_{ct}}{3}\right) + \frac{E_{90}\delta_y t_w}{2t_{d2}}\left(\frac{\delta-\delta_y}{\theta} + \frac{t_{d2}}{1.5}\ln\frac{\delta_y}{\delta} + l_{cb} + 1.5t_{d2}\right)\left(t_{t2} - \frac{l_{cb}}{3}\right)$$

$$M_{pRF} = \frac{E_{90}\delta_y t_w t_{d1}\mu(1+\nu_{23})}{2t_{d2}}\left(\frac{\delta-\delta_y}{\theta} + \frac{t_{d2}}{1.5}\ln\frac{\delta_y}{\delta} + l_{cb} + 1.5t_{d2}\right)$$

$$M_p = M_{pR} + M_{pRF}$$

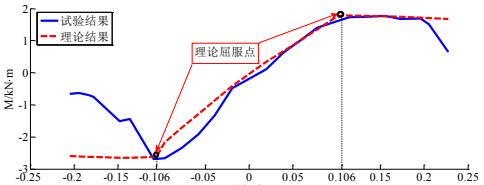

Comparison between experimental and theoretical values of SJ-07 model of through-tenon joint

When rotating counterclockwise, it enters the elastic-plastic stage : $\theta > \theta_y$

$$M'_{pR} = \frac{E_{90}\delta_y t_w}{2t_{d1}}\left(\frac{\delta-\delta_y}{\theta} + \frac{t_{d1}}{1.5}\ln\frac{\delta_y}{\delta} + l'_{cb} + 1.5t_{d1}\right)\left(t_{t1} - \frac{l'_{cb}}{3}\right) + \frac{E_{90}\delta_y t_w}{2t_{d2}}\left(\frac{\delta-\delta_y}{\theta} + \frac{t_{d2}}{1.5}\ln\frac{\delta_y}{\delta} + l'_{ct} + 1.5t_{d2}\right)\left(t_{t2} - \frac{l'_{ct}}{3}\right)$$

$$M'_{pRF} = \frac{E_{90}\delta_y t_w\mu(1+\nu_{23})}{2}\left(\frac{\delta-\delta_y}{\theta} + \frac{t_{d1}}{1.5}\ln\frac{\delta_y}{\delta} + l'_{cb} + 1.5t_{d1}\right) + \frac{E_{90}\delta_y t_w\mu(1+\nu_{23})}{2t_{d2}}\left(\frac{\delta-\delta_y}{\theta} + \frac{t_{d2}}{1.5}\ln\frac{\delta_y}{\delta} + l'_{ct} + 1.5t_{d2}\right)(t_{d2} - t_{d1})$$

$$M'_p = M'_{pR} + M'_{pRF}$$

Research Question 3: M-θ Curve Model of Mortise and Tenon Joints Based on Wood Friction Mechanism and Embedding Characteristics

M-θ curve model of half-tenon joint

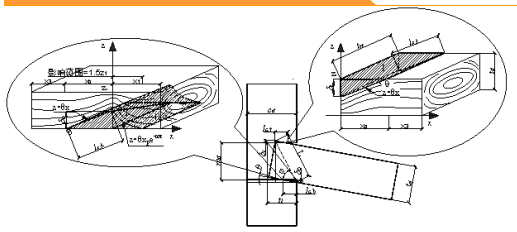

半榫节点变形分析

Elasticity stage

$$M_{em} = \frac{E_{90}}{2t_d}l_c^2 t_w l_u\theta + \frac{E_{90}}{t_d}\left(\frac{1}{2}l_c^2 t_w + 0.6l_c t_w t_d\right)l_u\theta = \frac{E_{90}}{t_d}l_u\left(l_c^2 t_w + 0.6l_c t_w t_d\right)\theta$$

$$M_{RF} = \frac{\mu(1+\nu_{23})t_d}{2}(P_t + P_b)$$

Elastic-Plastic Stage

$$\begin{cases} M_P = 2P_p l_u \\ M_{PF} = \mu(1+\nu_{23})t_d P_p \end{cases}$$

$$M_p = 2P_p l_u + \mu(1+\nu_{23})t_d P_p$$

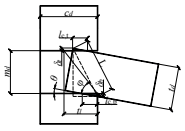

(a) Geometric relationship diagram

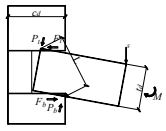

(b) Force analysis diagram

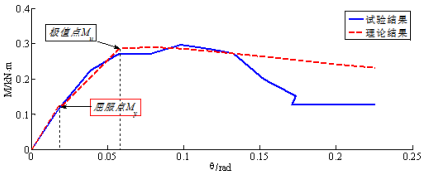

A comparison was made between the experimental and theoretical values of the SJ-15 model of the half-mortise joint.

Research Question 3: M-θ Curve Model of Mortise and Tenon Joints Based on Wood Friction Mechanism and Embedding Characteristics

M-θ curve model of dovetail joint

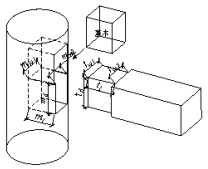

Dovetail node structure diagram

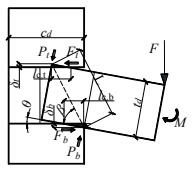

(a) The embedding pressure and friction on the upper and lower surfaces of the tenon

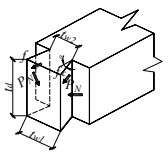

(b) Extrusion force and friction force on the side of the tenon

Force analysis of dovetail joints

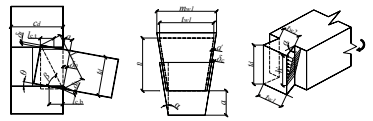

Dovetail joint geometry

$$M_{em} = \frac{E_{90}}{2t_d}l_c^2 t_w\left(\frac{t_t}{2} - \frac{l_c}{3}\right)\theta + \frac{E_{90}}{t_d}\left(\frac{1}{2}l_c^2 t_w + 0.6l_c t_w t_d\right)\left(\frac{t_t}{2} - \frac{l_c}{3}\right)\theta = \frac{E_{90}}{t_d}\left(\frac{t_t}{2} - \frac{l_c}{3}\right)\left(l_c^2 t_w + 0.6l_c t_w t_d\right)\theta$$

$$M_{RF} = \frac{\mu(1+\nu_{23})t_d}{2}(P_t + P_b)$$

$$M = M_{em} + M_{RF} + M_{RG} = K_R\theta + K_{KF}\theta + \mu P_N\left(\frac{t_d}{2} - \frac{h'}{3}\right)$$

Elasticity stage

$$\begin{cases} M_P = 2P_p l_u \\ M_{PF} = \mu(1+\nu_{23})t_d P_p \end{cases}$$

$$M = 2P_p l_u + \mu(1+\nu_{23})t_d P_p + \mu P_N\left(\frac{t_d}{2} - \frac{h'}{3}\right)$$

Elastic-Plastic Stage

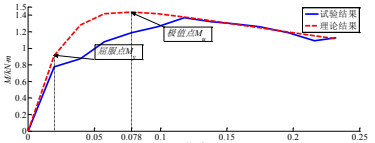

Comparison between experimental and theoretical values of dovetail joint SJ-18 model

Research Problem 4: Hysteresis Model of Dovetail Joint Based on Genetic Algorithm

Hysteretic model of dovetail joint

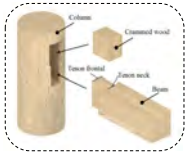

$$E=\sum_{i=1}^{m}\frac{1}{2}\left[V_r(t_i)+V_r(t_{i-1})\right]\left[x_r(t_i)-x_r(t_{i-1})\right]-\sum_{i=1}^{m}\frac{1}{2}\left[V_s(t_i)+V_s(t_{i-1})\right]\left[x_s(t_i)-x_s(t_{i-1})\right]$$

$$M=\sum_{i=1}^{m}M_r(t_i)-M_s(t_i)$$

Objective function

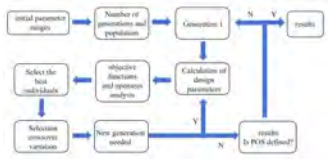

Model parameter identification process

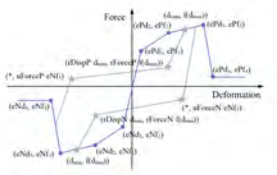

Schematic diagram of the Pinching4 material

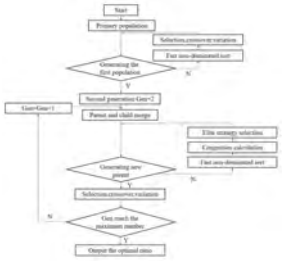

Schematic diagram of NSGA-II algorithm

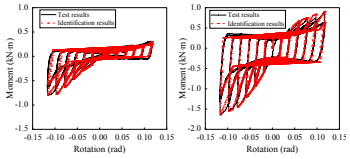

（a）model SJ-17（loose） （b）model SJ-19（tight）

Research Question 5: A Shaking Table Test Study of a Through-Beam Timber Building Model

Vibration table test and conclusion

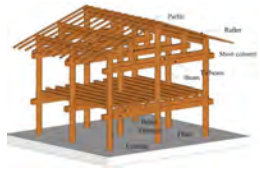

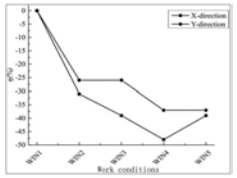

Stiffness degradation of the test model

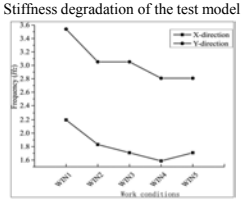

Natural frequency of test model

This structural system satisfies the requirements of China’s 9-degree seismic code. Using a similar wooden construction with this structural system in a high-intensity zone is safe and reliable.

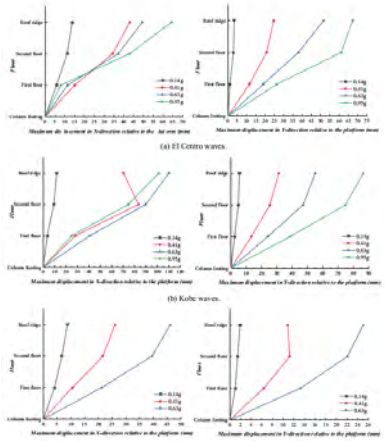

Maximum displacement relative to base under each load case

昆明理工大学 Kunming University of Science and Technology

Innovation Coordination Green Open Sharing

昆明理工大学 Kunming University of Science and Technology

Innovation Coordination Green Open Sharing

2024-9-Bangkok

Conclusion

- Conducted quasi-static test research on traditional mortise and tenon joints based on the wood's embedding and friction characteristics;
- The M-θ curve model of mortise and tenon joints based on wood friction mechanism and embedding characteristics was derived.
- The dovetail node hysteresis model was constructed based on a genetic algorithm.
- The structural system can meet the seismic safety requirements in high-intensity areas, according to a shaking table simulation study on a through-beam timber structure building model.

Posters
Other researches are undergoing now.

Dr. Bihui Dai
Join: 09-2018

Dr. Wahab Abdul Ghafar
Join: 09-2019

Dr. Lei Wu
Join: 09-2019

Dr. Yi Zhang
Join: 09-2020

Dr. Zhiqi Zhang
Join: 09-2021

Dr. Md Mehedi Hasan
Join: 09-2023

Fan-shaped Shear Dampers Strengthen Mortise-tenon Joints in Chinese Traditional Timber Structures

Bihui Dai, Yonglin Gao, Zhong Tao, Haihong Su & Hexian Su

DOI:10.1080/15583058.2021.201147

Looseness, deformation, and tenon pulled in the mortise-tenon joint constitute the primary causes of failure in traditional Chinese timber structure building. However, the introduction of the joint damper technology and installation of the fan-shaped shear damper at the mortise-tenon joints of traditional wooden structure solves these issues. Herein, we explored the strengthening effect of dovetail mortise-tenon joints with dampers. We designed six dovetail mortise-tenon joint models, three without dampers, and the other three were installed with dampers. Using the low cycle repeated loading test, we examined the hysteretic response, skeleton curve, stiffness degradation curve, and equivalent viscous damping coefficient curves of the six test models. Consequently, we established that the joint damper effectively controls the joint tenon pulled problem and enhances energy dissipation, strength, and rotational stiffness. Besides, the ultimate bearing capacity of the damper models was nearly four-fold that of models without dampers.

Experimental work

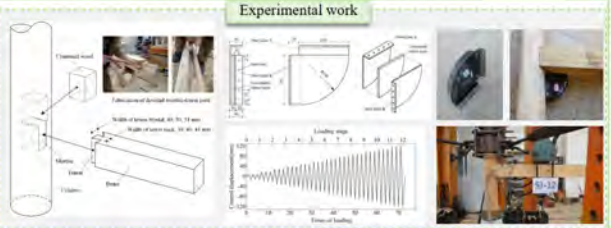

Results and discussion

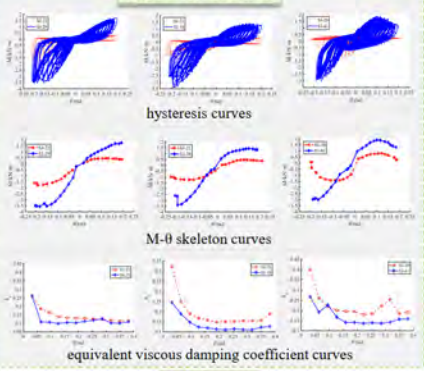

Conclusions

- Installing fan-shaped damper on the mortise-tenon joint models can effectively control the damages caused by pullout of the tenon.
- The hysteresis loop area of the model significantly increases, and the hysteresis curve becomes fuller and smoother after installing the dampers on the joint model. Moreover, the joint model exhibits better recovery ability during the unloading process.
- The installation of the damper enhances the strength and stiffness of the joint model. The ultimate bearing capacity of the joint model with damper is four times higher than that of the joint model without damper.

Dynamic simulation and seismic analysis of hillside RC buildings isolated by high-damping rubber bearings using DHI model

Wahab Abdul Ghafar[1] , and Tao Zhong[1,*]
[1], Faculty of Civil Engineering and Mechanics, Kunming University of Science and Technology, Kunming 650500, China

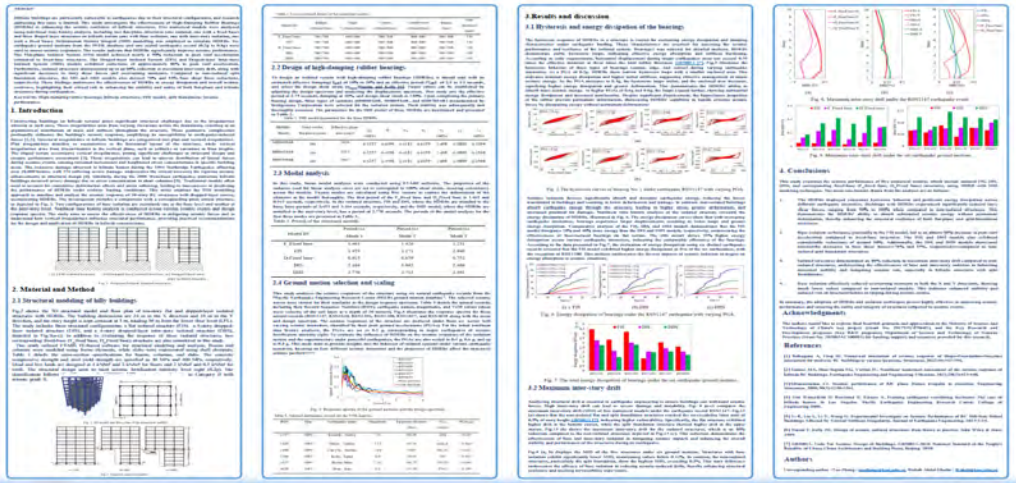

Seismic performance of retrofitted RC frame structure after column removal and retrofitted by post-tensioning tendons and RC jacketing

Abdul Ghafar Wahab, and Tao Zhong
Civil Engineering and Architecture Faculty, Kunming University of Science and Technology, Kunming 650500, China

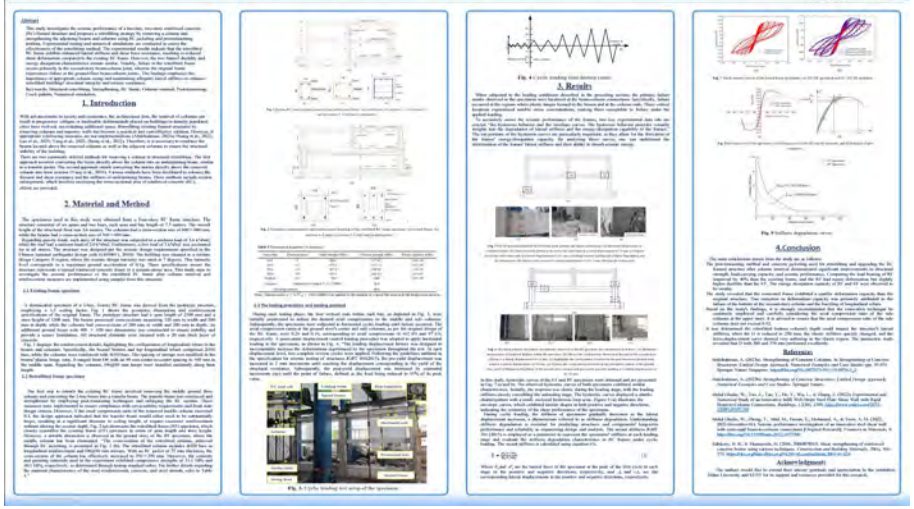

Basalt Fiber Reinforced Phosphorus Building Gypsum Composite Materials : an Analysis on its Working Performance and Mechanical Properties

Lei Wu , **Zhong Tao**, Ronggui Huang, Zhiqi Zhang, Jinjin Shen and Weijie Xu

DOI:10.3390/inorganics11060254

The preparation of fiber reinforced phosphorus building gypsum composite materials (FRPGC) is an important approach to enlarging the utilization of phosphogypsum resources. Through reinforcing phosphorus building gypsum(PBG) with basalt fiber (BF), this article probes into the effects of the length and fiber content of BF on the working performance and mechanical properties of basalt fiber reinforced phosphorus building gypsum composite materials (BRPGC) and accesses the toughness of BRPGC under bending load using residual strength. The results show that the addition of BF can significantly promote the mechanical properties of BRPGC. However, due to the adverse effect of fibers on the working performance of BRPGC, the fiber content is constrained. After adding 1.2% of 6mm BF, the bending strength and compressive strength of FRPGC reach the maximum values of 10.98 MPa and 29.83 MPa, respectively. Under bending load, BRPGC exhibits apparent ductile behavior. The P-δcurve presents five stages, with an evident phase of strength stability after cracking. Larger fiber content is conducive to the toughness of BRPGC. When 1.6% of 6mm BF is added, the residual strength of FRPGC can reach 6.77 MPa.

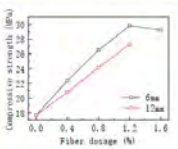

The strength of BRPGC

Raw Materials

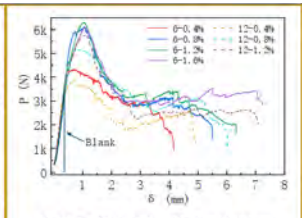

the P-δ of BRPGC in the bending test

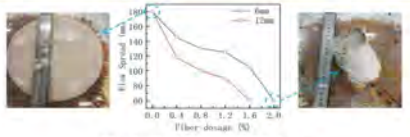

The fluidity of the BRPGC slurry.

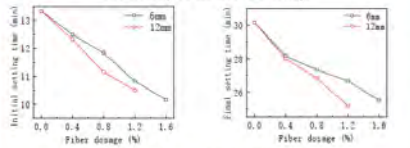

The setting time of the BRPGC slurry

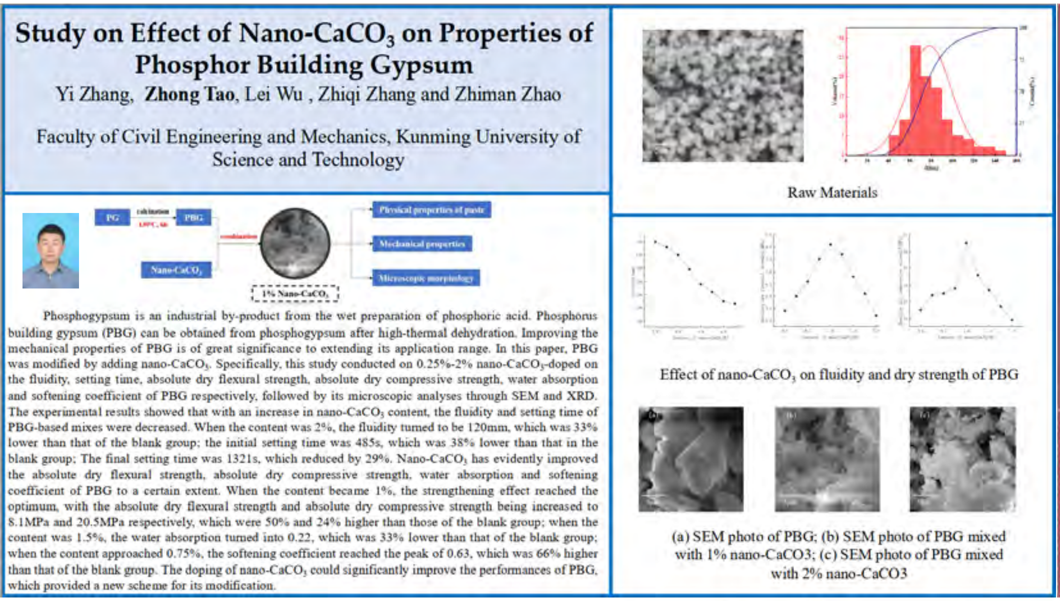
Study on Effect of Nano-CaCO3 on Properties of Phosphor Building Gypsum
Yi Zhang, Zhong Tao, Lei Wu , Zhiqi Zhang and Zhiman Zhao
Faculty of Civil Engineering and Mechanics, Kunming University of Science and Technology
PG
calcination
PBG
Nano-CaCO3
combination
1% Nano-CaCO3
Physical properties of paste
Mechanical properties
Microscopic morphology
Phosphogypsum is an industrial by-product from the wet preparation of phosphoric acid. Phosphorus building gypsum (PBG) can be obtained from phosphogypsum after high-thermal dehydration. Improving the mechanical properties of PBG is of great significance to extending its application range. In this paper, PBG was modified by adding nano-CaCO3. Specifically, this study conducted on 0.25%-2% nano-CaCO3-doped on the fluidity, setting time, absolute dry flexural strength, absolute dry compressive strength, water absorption and softening coefficient of PBG respectively, followed by its microscopic analyses through SEM and XRD. The experimental results showed that with an increase in nano-CaCO3 content, the fluidity and setting time of PBG-based mixes were decreased. When the content was 2%, the fluidity turned to be 120mm, which was 33% lower than that of the blank group; the initial setting time was 485s, which was 38% lower than that in the blank group; The final setting time was 1321s, which reduced by 29%. Nano-CaCO3 has evidently improved the absolute dry flexural strength, absolute dry compressive strength, water absorption and softening coefficient of PBG to a certain extent. When the content became 1%, the strengthening effect reached the optimum, with the absolute dry flexural strength and absolute dry compressive strength being increased to 8.1MPa and 20.5MPa respectively, which were 50% and 24% higher than those of the blank group; when the content was 1.5%, the water absorption turned into 0.22, which was 33% lower than that of the blank group; when the content approached 0.75%, the softening coefficient reached the peak of 0.63, which was 66% higher than that of the blank group. The doping of nano-CaCO3 could significantly improve the performances of PBG, which provided a new scheme for its modification.
Raw Materials
Effect of nano-CaCO3 on fluidity and dry strength of PBG
(a) SEM photo of PBG; (b) SEM photo of PBG mixed with 1% nano-CaCO3; (c) SEM photo of PBG mixed with 2% nano-CaCO3

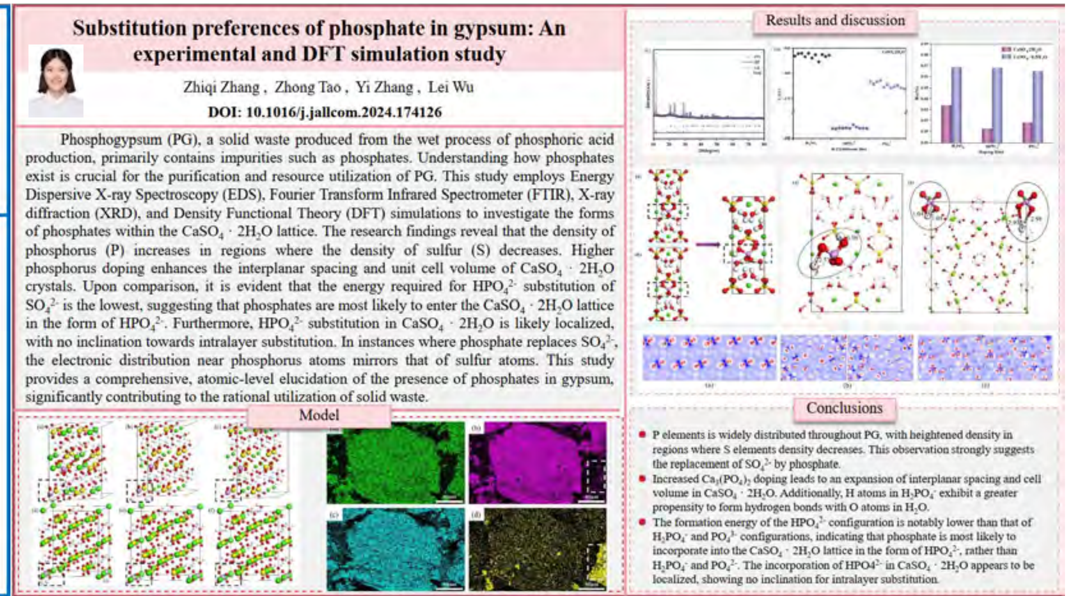
Substitution preferences of phosphate in gypsum: An experimental and DFT simulation study
Zhiqi Zhang , Zhong Tao , Yi Zhang , Lei Wu
DOI: 10.1016/j.jallcom.2024.174126
Phosphogypsum (PG), a solid waste produced from the wet process of phosphoric acid production, primarily contains impurities such as phosphates. Understanding how phosphates exist is crucial for the purification and resource utilization of PG. This study employs Energy Dispersive X-ray Spectroscopy (EDS), Fourier Transform Infrared Spectrometer (FTIR), X-ray diffraction (XRD), and Density Functional Theory (DFT) simulations to investigate the forms of phosphates within the CaSO4 · 2H2O lattice. The research findings reveal that the density of phosphorus (P) increases in regions where the density of sulfur (S) decreases. Higher phosphorus doping enhances the interplanar spacing and unit cell volume of CaSO4 · 2H2O crystals. Upon comparison, it is evident that the energy required for HPO4 2- substitution of SO4 2- is the lowest, suggesting that phosphates are most likely to enter the CaSO4 · 2H2O lattice in the form of HPO4 2-. Furthermore, HPO4 2- substitution in CaSO4 · 2H2O is likely localized, with no inclination towards intralayer substitution. In instances where phosphate replaces SO4 2-, the electronic distribution near phosphorus atoms mirrors that of sulfur atoms. This study provides a comprehensive, atomic-level elucidation of the presence of phosphates in gypsum, significantly contributing to the rational utilization of solid waste.
Model
Results and discussion
Conclusions
P elements is widely distributed throughout PG, with heightened density in regions where S elements density decreases. This observation strongly suggests the replacement of SO4 2- by phosphate.
Increased Ca3(PO4)2 doping leads to an expansion of interplanar spacing and cell volume in CaSO4 · 2H2O. Additionally, H atoms in H3PO4 exhibit a greater propensity to form hydrogen bonds with O atoms in H2O.
The formation energy of the HPO4 2- configuration is notably lower than that of H2PO4- and PO4 3- configurations, indicating that phosphate is most likely to incorporate into the CaSO4 · 2H2O lattice in the form of HPO4 2-, rather than H2PO4- and PO4 3-. The incorporation of HPO4 2- in CaSO4 · 2H2O appears to be localized, showing no inclination for intralayer substitution.

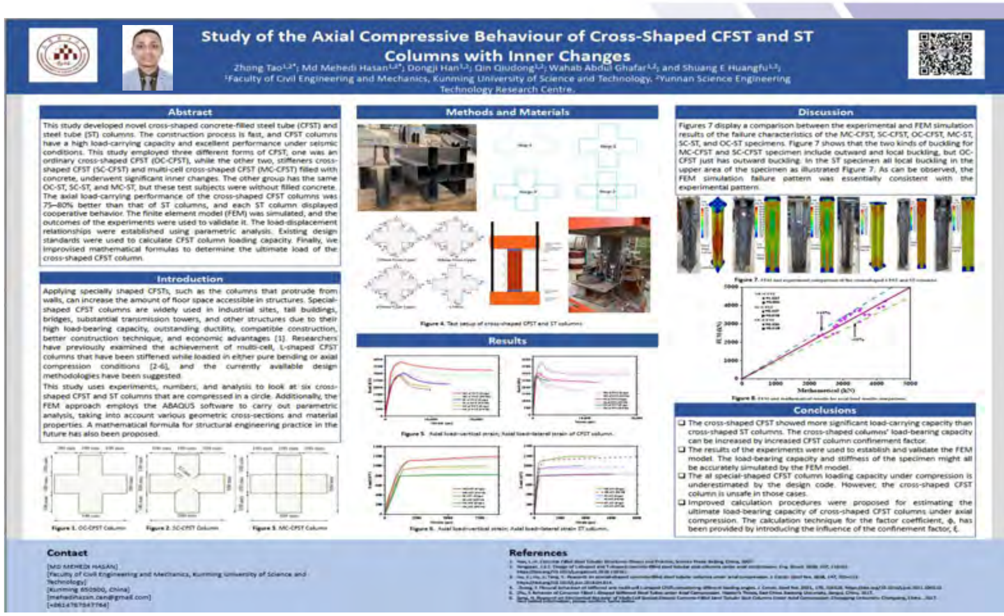
Study of the Axial Compressive Behaviour of Cross-Shaped CFST and ST Columns with Inner Changes
Abstract
Methods and Materials
Discussion
Introduction
Results
Conclusions
Contact
References

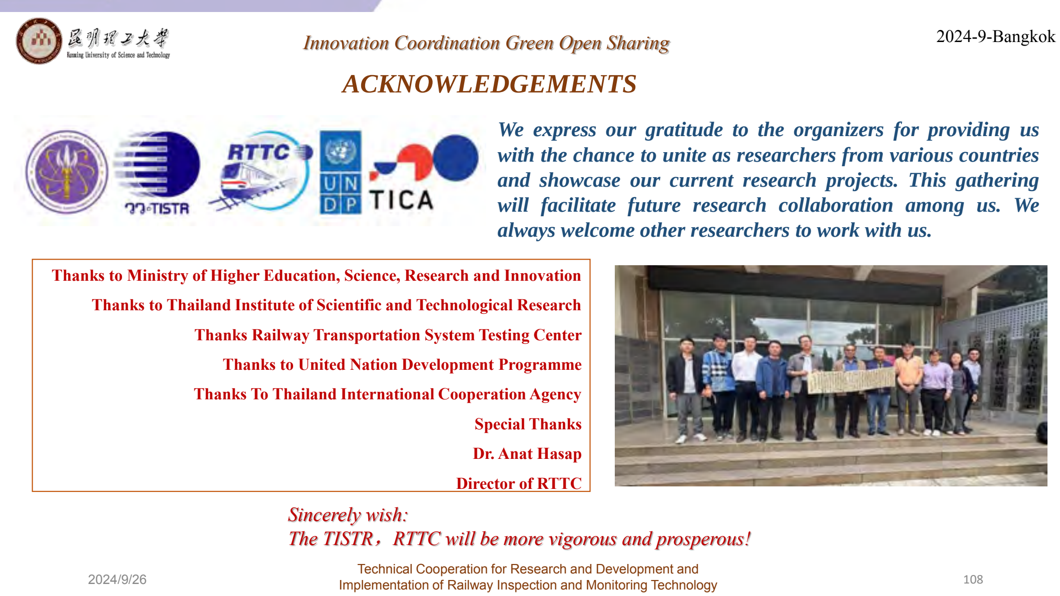
Innovation Coordination Green Open Sharing
2024-9-Bangkok
ACKNOWLEDGEMENTS
TISTR
RTTC
UNDP
TICA
We express our gratitude to the organizers for providing us with the chance to unite as researchers from various countries and showcase our current research projects. This gathering will facilitate future research collaboration among us. We always welcome other researchers to work with us.
Thanks to Ministry of Higher Education, Science, Research and Innovation
Thanks to Thailand Institute of Scientific and Technological Research
Thanks Railway Transportation System Testing Center
Thanks to United Nation Development Programme
Thanks To Thailand International Cooperation Agency
Special Thanks
Dr. Anat Hasap
Director of RTTC
Sincerely wish:
The TISTR，RTTC will be more vigorous and prosperous!
2024/9/26
Technical Cooperation for Research and Development and Implementation of Railway Inspection and Monitoring Technology
108

Rail Noise and Vibration: Mechanisms, Predictions and Controls

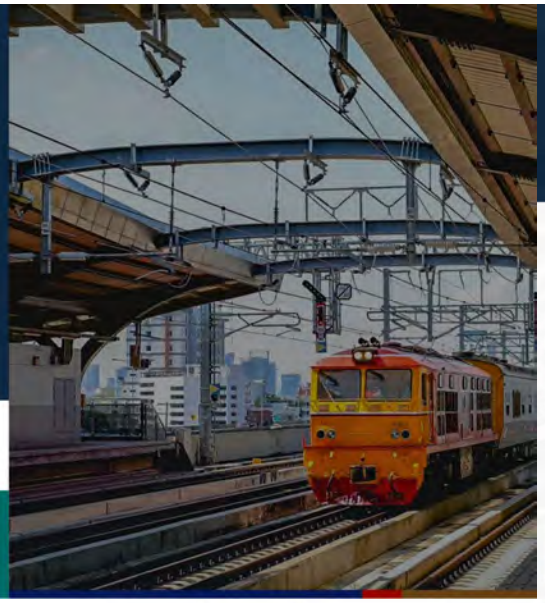

Sorawit Limthongkul, PhD
Lecturer
Kasetsart University, Bangkok
fengswl@ku.ac.th

Agenda

- Railway Noise and Vibration.
  - Why Noise and Vibration?
  - Sources of noise and vibration.
- Railway Noise Predictions.
- Controls and Mitigations.
- What is next?
- Q&A.

Railway Noise and Vibration | Why Noise and Vibration?

…Concerns in terms of vibration…

- Ride and comfort for passengers
- Integrity of the structure for wheel, track and nearby structures

Ref: https://doi.org/10.3390/su12030937

Ref: https://www.youtube.com/watch?v=CCo6AkB_s0M

Railway Noise and Vibration | Why Noise and Vibration?

… Concerns in terms of noise…

- Noise pollution, annoyance.
- Health and safety.

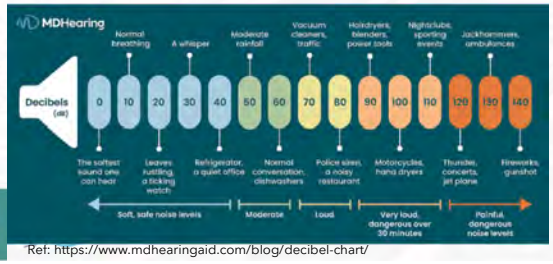

Ref: https://www.mdhearingaid.com/blog/decibel-chart/

Ref: https://www.youtube.com/watch?v=hhVf_C_qIcU

Railway Noise and Vibration | Sources of Noise and Vibration

- Railway noise is speed-dependent.

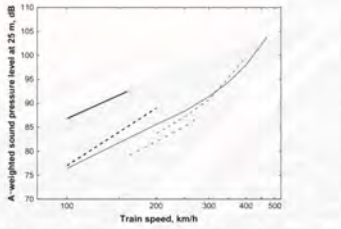

FIGURE 2-3 Rolling noise from various types of train. Tread braked vehicles: —, BR Mk II coaches; – – –, TGV-PSE. Disc-braked vehicles: - - -, BR Mk III coaches; —, TGV-A, Duplex and Thalys (from manufacturer's data); – – –, ICE/V; – – –, Talgo (drum brakes) [2.2–2.5].

Ref: Thompson, David. *Railway noise and vibration: mechanisms, modelling and means of control*. Elsevier, 2008.

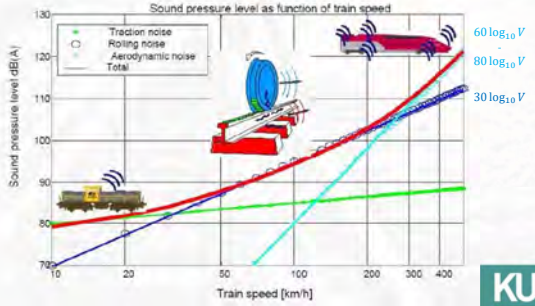

Ref: Fernandez, Pilar & Diez, Itxasne & García, José & Aspuru, Itziar. (2013). Noise barriers customized to abate non conventional noise sources.

Railway Noise and Vibration | Sources of Noise and Vibration

- Wheel/Rail interaction.
- Structure-borne and air-borne noise.

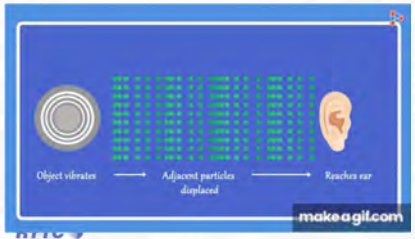

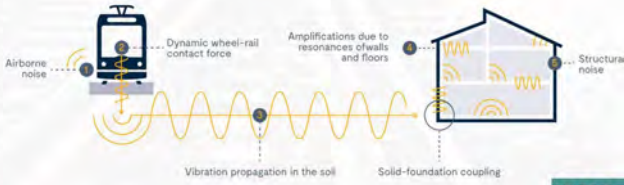

Ref: https://www.pandrol.com/insight/innovation-in-urban-integration-mitigating-noise-and-vibration-from-city-centre-railways/

Railway Noise and Vibration | Railway Noise

- Wheel/Rail Interaction
  - Rolling Noise.
  - Squeal Noise.
  - Impact Noise.
- Aerodynamics Noise.
  - Pantograph
  - Bogie, inter-coach region and etc…
- Bridge Noise.
- Ground-borne Noise.

Railway Noise and Vibration | Rolling Noise

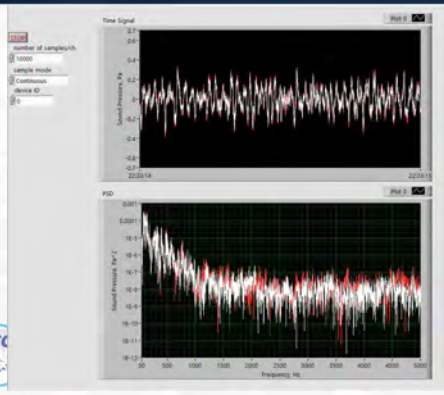

Railway Noise and Vibration | Rolling Noise

Railway Noise and Vibration | Squeal Noise

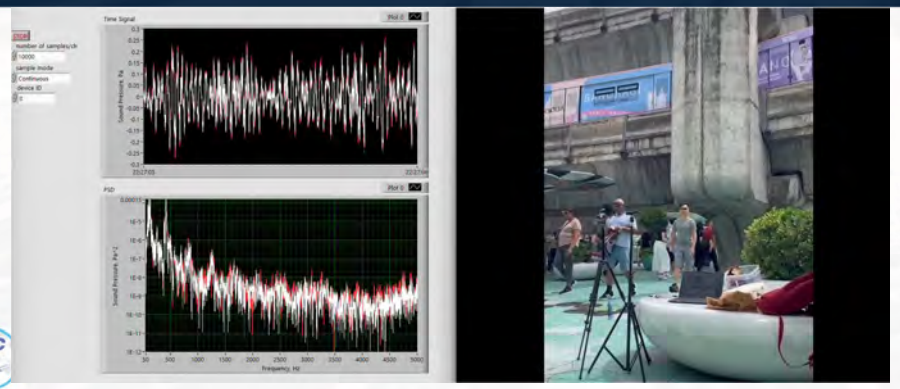

Railway Noise and Vibration | Squeal Noise

Railway Noise and Vibration | Impact Noise

Railway Noise and Vibration | Aerodynamic Noise

- Pantograph/Bogie/etc…

Fig. 7 Pantograph noise on an electric unit of the 671 series pass at 160 km/h (own research)

Ref: Zvolensky, Peter, et al. "Pantograph impact on overall external noise of a pantographed." *Transportation Research Procedia* 55 (2021): 661-666.

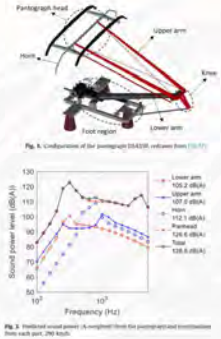

Ref: Li, Hui, et al. "The distribution of pantograph aerodynamic noise on train external surfaces and the influence of flow." *Applied Acoustics* 188 (2022): 108542.

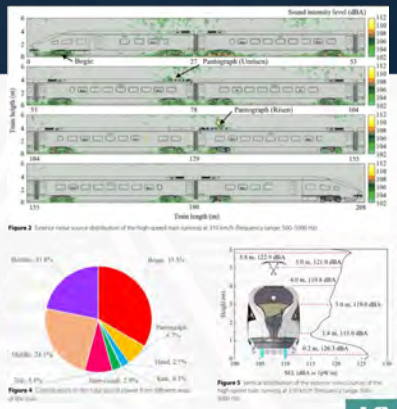

Ref: Zhang, Jie, et al. "Sound source localisation for a high-speed train and its transfer path to interior noise." *Chinese Journal of Mechanical Engineering* 32 (2019): 1-16.

Railway Noise and Vibration | Bridge Noise

- Wheel/Rail interaction (changing in track properties)
  - ➢ Impact loading
    - ➢ Rail vibration
      - ➢ Vibrating bridge components
        - ➢ Bridge noise

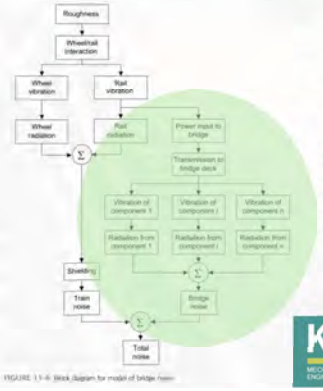

Ref: Thompson, David. *Railway noise and vibration: mechanisms, modelling and means of control*. Elsevier, 2008.

Railway Noise and Vibration | Ground-borne Noise

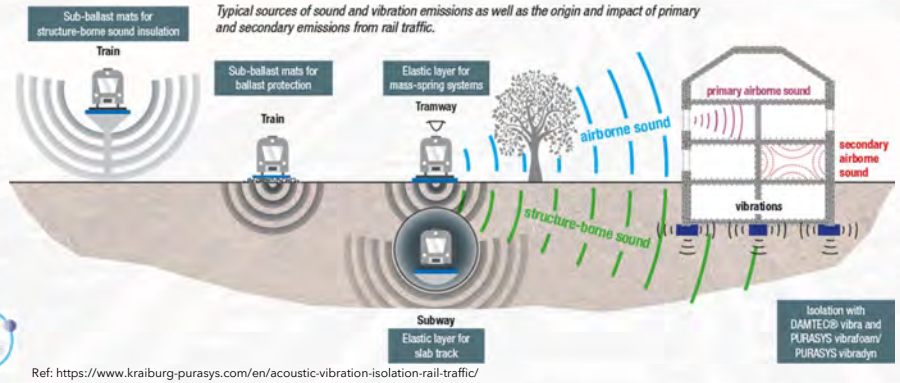

Ref: https://www.kraiburg-purasys.com/en/acoustic-vibration-isolation-rail-traffic/

Railway Noise Prediction | Wheel Vibration

- Rigid wheelset/Rail vehicle dynamics

- Flexible wheelset

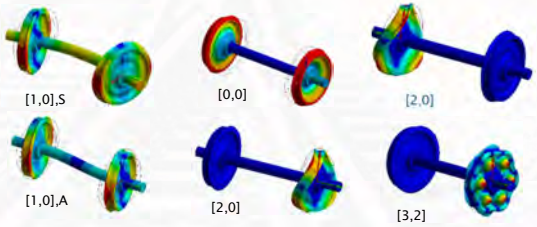

Symmetric and antisymmetric responses, n<2
Independent bending modes, n≥2

Railway Noise Prediction | Wheel Vibration

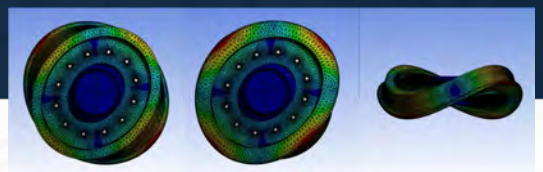

- Mode-shapes of the Disc-like structure

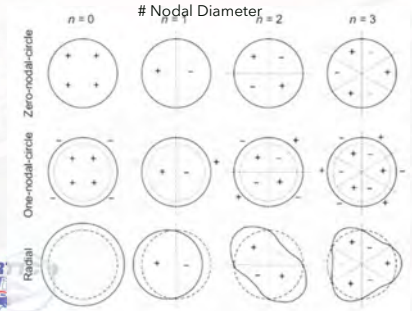

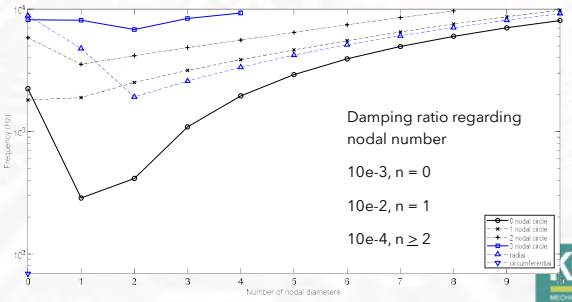

Railway Noise Prediction | Wheel Vibration

- Transfer function in form of Receptant/Mobility/Accelerance

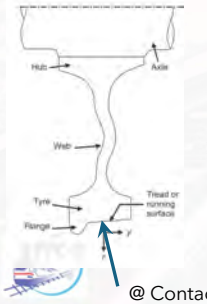

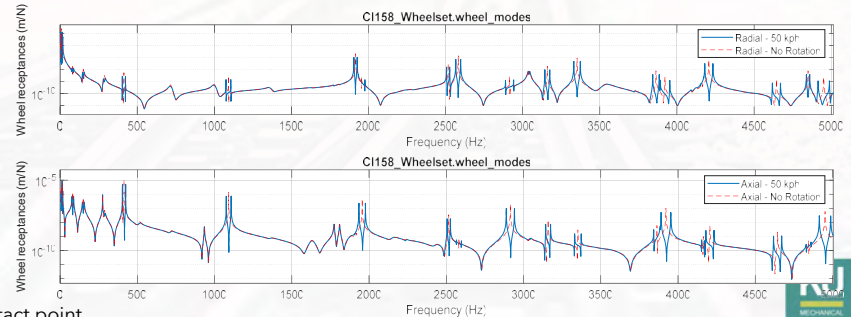

Railway Noise Prediction | Rail Vibration

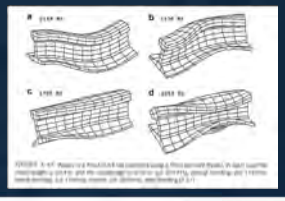

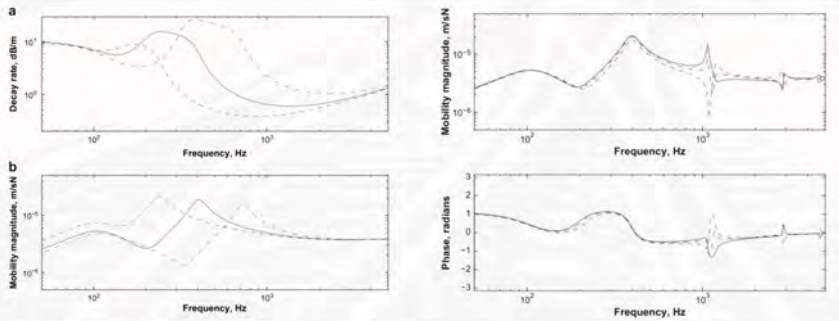

FIGURE 3-32 Results predicted for track with different rail pad stiffnesses using Timoshenko beam with $\eta_s = 0.02$. (a) Decay rates, (b) point mobilities. – – –, $S_p = 100$ MN/m²; —, $S_p = 300$ MN/m²; – · –, $S_p = 1000$ MN/m²

FIGURE 3-33 Vertical point mobility of track with discrete supports, pad stiffness 180 MN/m. —, excitation at mid-span; – – –, excitation above a sleeper; – · –, excitation at quarter span; ····, continuous support

Ref: Thompson, David. *Railway noise and vibration: mechanisms, modelling and means of control*. Elsevier, 2008.

Railway Noise Prediction | Sleeper Vibration

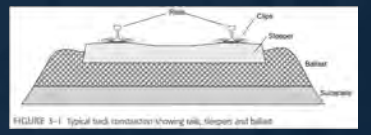

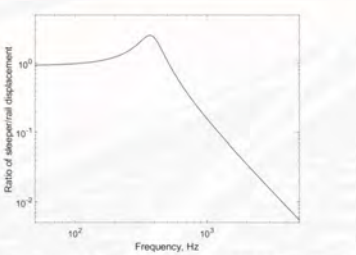

Figure 4-11: Ratio of sleeper/rail displacement corresponding to the track properties.

The sleeper vibration can be obtained from the ratio of the sleeper displacement u_s to the rail displacement u_r [1]

$$\tau = \frac{u_s}{u_r} = \frac{S_p}{(S_p + S_b - \omega^2 m_s')} \quad (4\text{-}17)$$

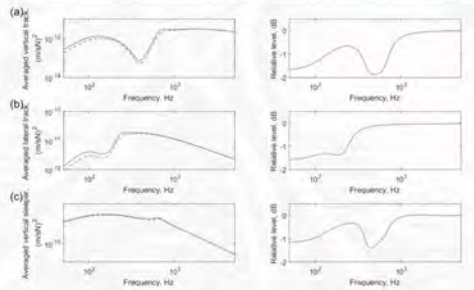

Figure 4-13: Averaged track responses ±20 m distance and relative level between coherent and incoherent combined (a) vertical rail, (b) lateral rail and (c) vertical sleeper response: ____ coherently; _ _ _ _ incoherently combined.

Railway Noise Prediction | Wheel/Rail Interaction

- Wheel/Rail Interaction prediction

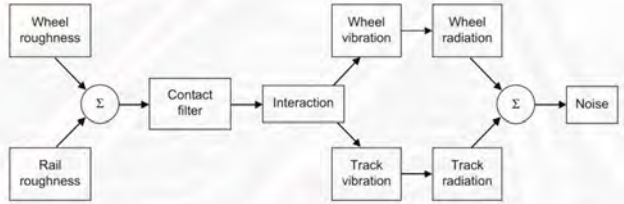

FIGURE 1-1 Model for rolling noise generation

Ref: Thompson, David. *Railway noise and vibration: mechanisms, modelling and means of control*. Elsevier, 2008.

Railway Noise Prediction | Wheel/Rail Interaction

Vibration comes from…?

- Wheel/Rail Interaction…
- Roughness excitation…

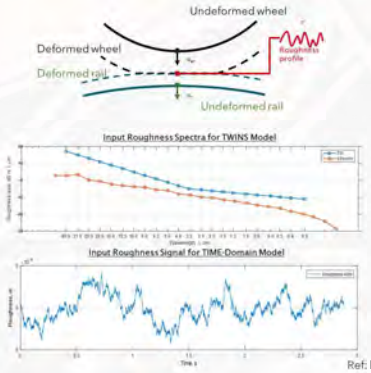

Ref: https://www.youtube.com/watch?v=yNRfrwWVIqU

Railway Noise Prediction | Rolling Noise

- Wheel/rail rolling noise prediction
  - ➢ Frequency domain model
  - ➢ Time domain model
    - ✓ Direct approach
    - ✓ Modal approaches

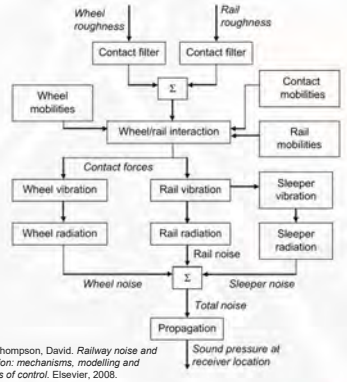

Ref: Thompson, David. *Railway noise and vibration: mechanisms, modelling and means of control*. Elsevier, 2008.

Railway Noise Prediction | Rolling Noise

- Wheel/Rail Interaction model
- Sound radiation model

Wheel/Rail Interaction model

Sound radiation model

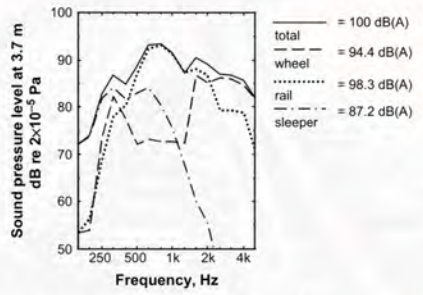

Ref: Thompson, David. *Railway noise and vibration: mechanisms, modelling and means of control*. Elsevier, 2008.

FIGURE 2-14 Results from typical prediction using TWINS model showing contributions of wheel, rail and sleeper components to total noise [2.21]

Wheel/Rail Interaction Model | Contact Model

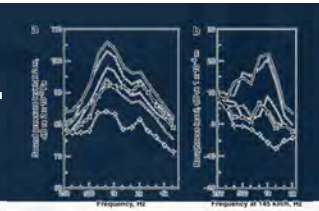

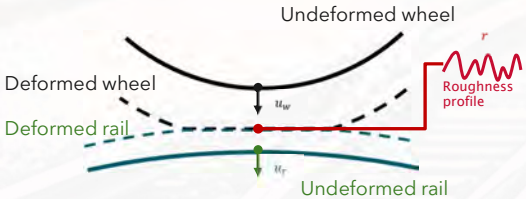

$$F_v = \begin{cases} C_H u_c^{3/2} & ;u_c = u_w - u_r + r > 0 \\ 0 & ;u_c = u_w - u_r + r \le 0 \end{cases}$$

where u_c = Contact deflection
u_w = wheel vertical response
u_r = rail vertical response
r = roughness or trajectory path

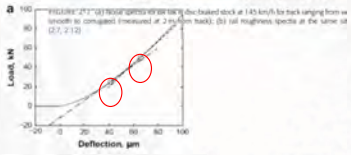

$$\frac{dF_v}{du_c} = K_H = \begin{cases} \frac{dC_H u_c^{3/2}}{du_c} = \frac{3}{2} C_H u_c^{1/2} & ;u_c > 0 \\ 0 & ;u_c \le 0 \end{cases}$$

F_l

Wheel vibration

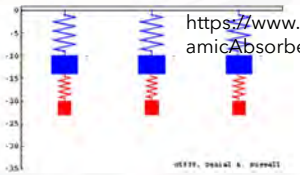

https://www.acs.psu.edu/drussell/Demos/absorber/DynamicAbsorber.html

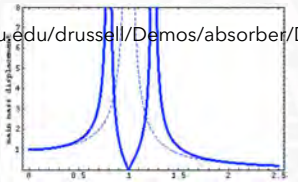

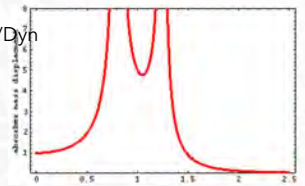

- Vertical Contact Model: Non-linear Hertzian Contact and loss of contact in vertical direction

Controls and Mitigations | Rolling Noise

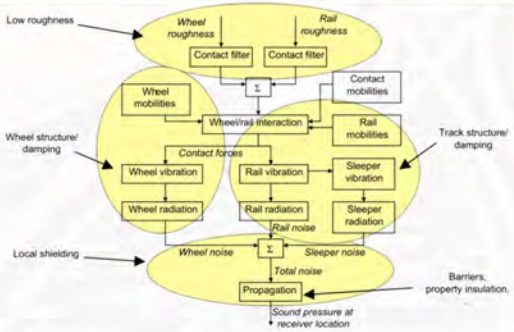

FIGURE 7-1 Schematic view of the model for rolling noise, showing the main potential means of reducing rolling noise

Ref: Thompson, David. *Railway noise and vibration: mechanisms, modelling and means of control*. Elsevier, 2008.

Controls and Mitigations | Wheel Design

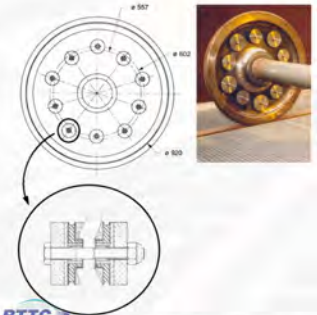

FIGURE 7-21 Friction damper developed by Lucchini in Silence project. Photo by courtesy of DB

FIGURE 7-26 Silent Freight shape-optimized 860 mm wheel with perforated web. Photo: Rick Jones, used courtesy of UIC

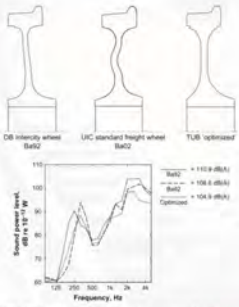

Ref: Thompson, David. *Railway noise and vibration: mechanisms, modelling and means of control*. Elsevier, 2008.

Controls and Mitigations | Noise Barrier

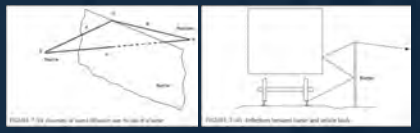

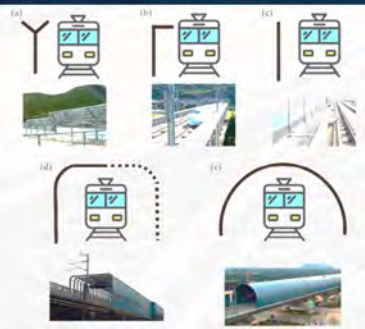

Ref: Yan, Hongyu, et al. "A review of recent research into the causes and control of noise during high-speed train movement." *Applied Sciences* 12.15 (2022): 7508.

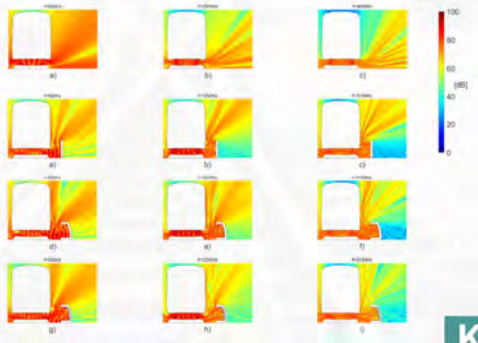

Ref: Lázaro, João, et al. "Performance of low-height railway noise barriers with porous materials." *Applied Sciences* 12.6 (2022): 2960.

Controls and Mitigations | Rail Dampers

Multi-Directional Tuned Mass Damper Isometric View

Ref: https://www.wal.hk/

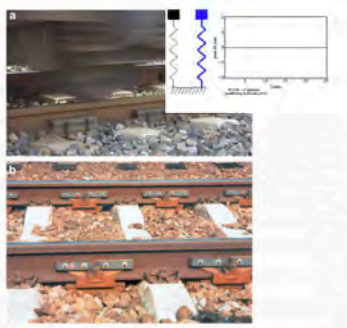

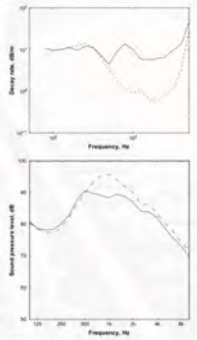

Ref: Thompson, David. Railway noise and vibration: mechanisms, modelling and means of control. Elsevier, 2008.

Controls and Mitigations | Rail Griding

https://railroadrails.com/knowlege/rail-grinding/

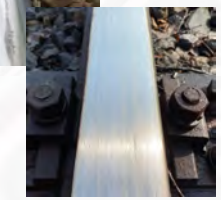

https://www.railtechnology.com/rt-st-rail-grinding-technology/

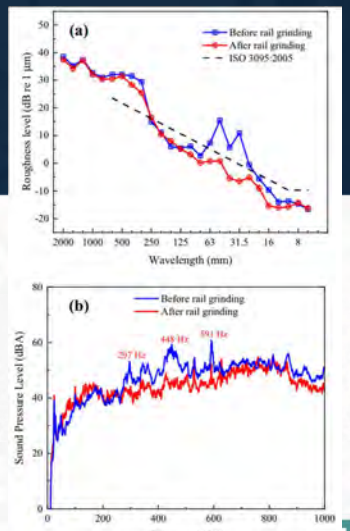

Figure 4 Effect of rail roughness: (**a**) roughness spectrum and (**b**) sound spectrum

https://doi.org/10.1186/s10033-022-00696-2

Controls and Mitigations | Resilient Rail Fasteners

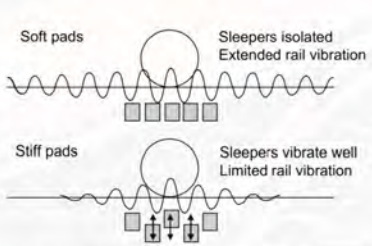

FIGURE 3-7 Illustration of the effect of the rail pad stiffness on the coupling between rail and sleeper and on the damping of waves in the rail

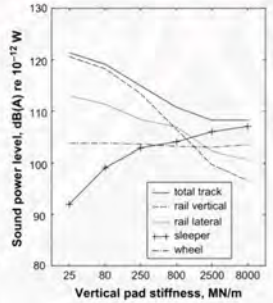

FIGURE 7-27 Example of predicted sound power due to one wheel and the associated track vibration versus high frequency rail pad stiffness. Calculations using TWINS for a standard 920 mm freight wheel at 100 km/h, with a typical tread-braked roughness

Ref: Thompson, David. Railway noise and vibration: mechanisms, modelling and means of control. Elsevier, 2008.

Controls and Mitigations | Design of the High-Speed Train

Tunnel noise reduction and other issues regarding high-speed train

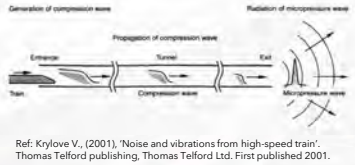

Ref: Krylove V., (2001), 'Noise and vibrations from high-speed train'. Thomas Telford publishing, Thomas Telford Ltd. First published 2001.

DOI: 10.3390/biomimetics6040056

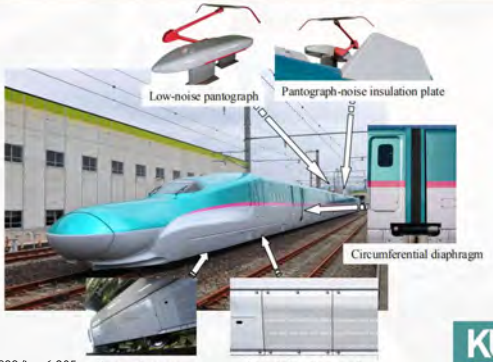

Doi: 10.1299/jee.6.805

Controls and Mitigations | Other Mitigations

- Rail-web shielding
- Absorptive slab track

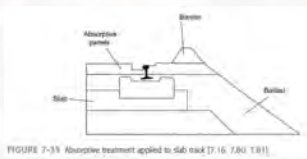

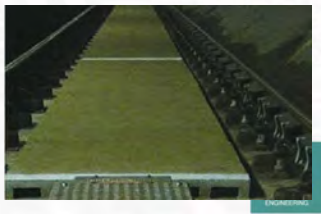

https://www.quietstone.co.uk/product/quietstone-rail-track-slab/

What is Next? | Vibration Prediction

Wheel and Track responses

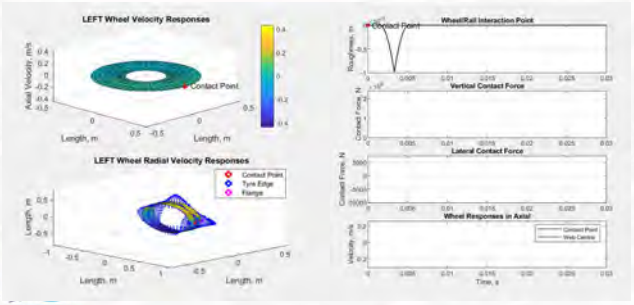

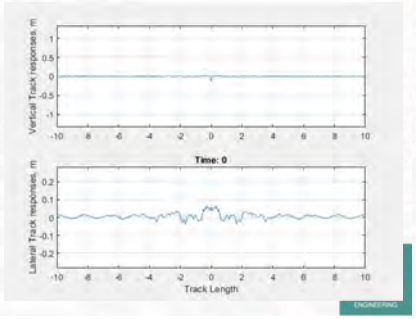

What is Next? | Contact Force Prediction

Vertical Contact Force

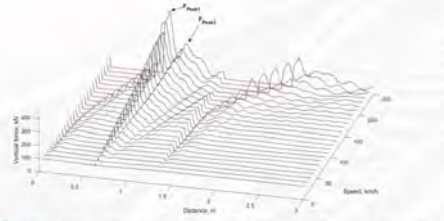

Figure 5-22: Vertical contact force in the spatial domain for travelling speeds from 10 km/h to 250 km/h with the static load of 70 kN. Noted that red marks indicate the loss of contact.

Lateral Contact Force

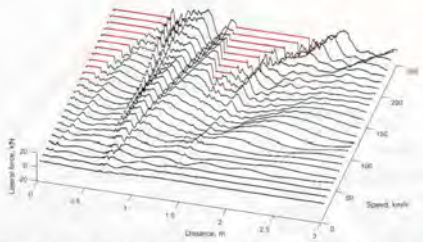

Figure 5-24: Lateral force in the spatial domain for travelling speeds from 10 km/h to 250 km/h with a static load of 70 kN. Noted that red marks indicate the loss of contact.

What is Next?
| Acoustic Prediction

Sound pressure prediction

60 km/h

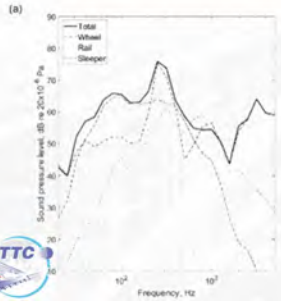

140 km/h

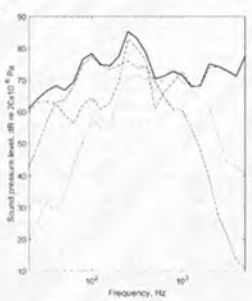

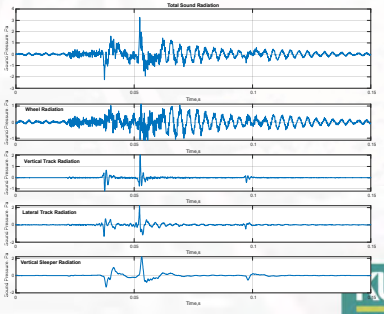

What is Next?
| Acoustic Prediction

Sound pressure prediction

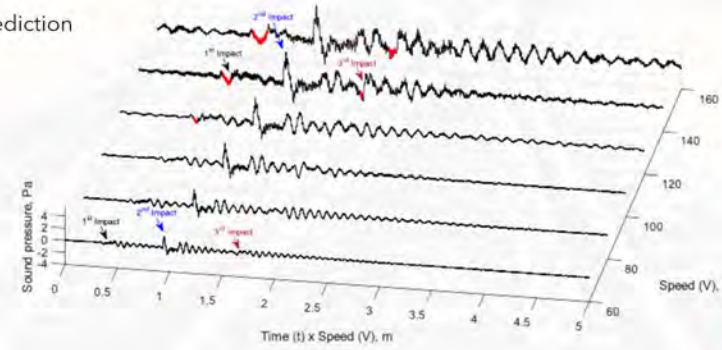

What is Next?
| Current and on going…

Prediction of railway noise through the DIGITAL TWINS…

Structure Health Monitoring aided by ….

acoustic/ acoustic emission/ vibration analysis/ ML/ AI

To observe the change in wheel/rail properties

FIGURE 4. Most frequent terms

DOI 10.1109/ACCESS.2023.3327042

Q & A

TISTR สถาบันวิจัยวิทยาศาสตร์และเทคโนโลยีแห่งประเทศไทย
THAILAND INSTITUTE OF SCIENTIFIC AND TECHNOLOGICAL RESEARCH

Monitoring and Seismic Retrofit of Reinforced Concrete Buildings to Resistance Future Earthquake for Sustainable Cities

Lecturer : Asst. Prof. Dr. Panumas Saingam

Department of Civil Engineering, School of Engineering
King Mongkut's Institute of Technology Ladkrabang (KMITL), Thailand

Seismic PGA map : The PGA with a 10% probability of exceedance in 50 years

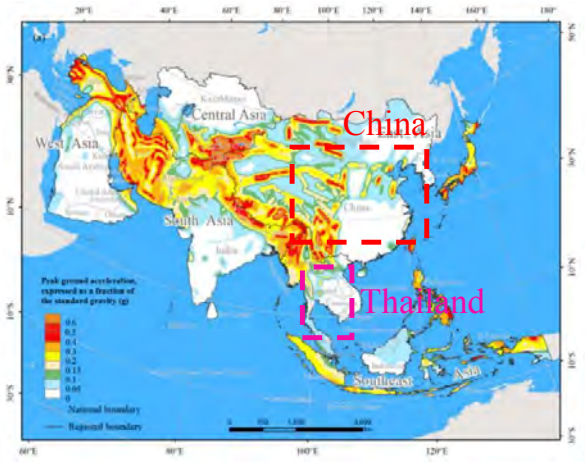

Reference: Y. Dou, Q. Huang, C. He, S. Meng and Q. Zhang. Rapid Population Growth throughout Asia's Earthquake-Prone Areas: A Multiscale Analysis. International Journal of Environmental Research and Public Health v.15(9), 2018 Sep.

Reinforcement of RC Building to resist only vertical load

Many buildings in Asia were designed to resist the only vertical load.

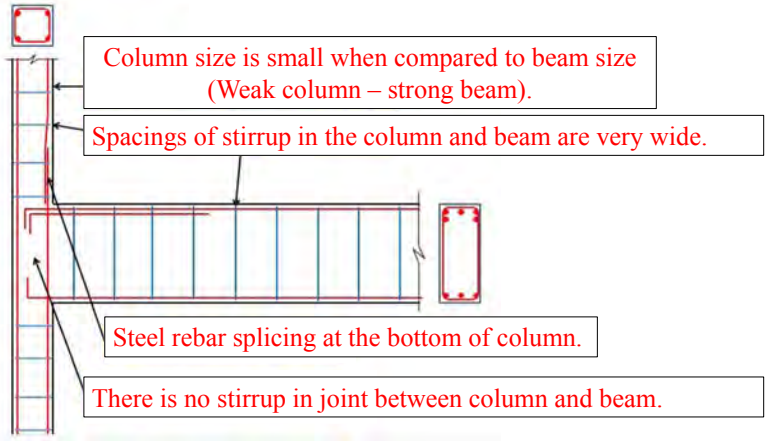

Reference: Council of Engineers, Thailand.

Effect of earthquake on structure

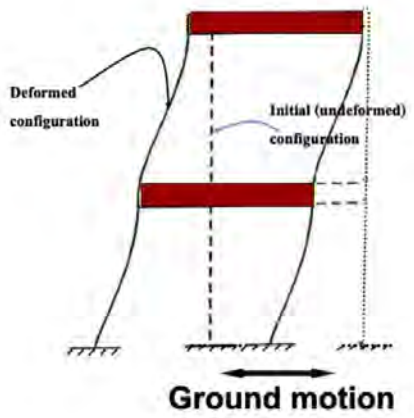

Reference: Council of Engineers, Thailand.

Bending moment of structure under lateral load

Earthquake

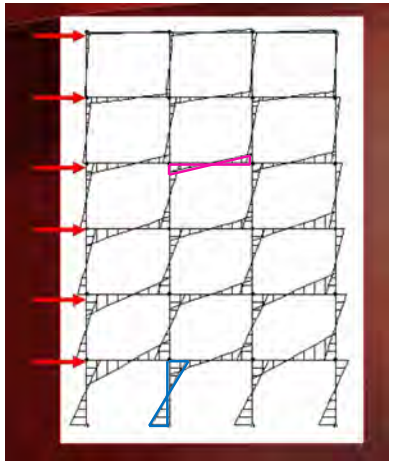

Earthquake

Beam: Maximum moment is at the end of beam.

Column: Maximum moment is at the top and bottom of column.

To prevent the damage from earthquake, the end of beam and columns should increase number of stirrup.

Damage from experiment

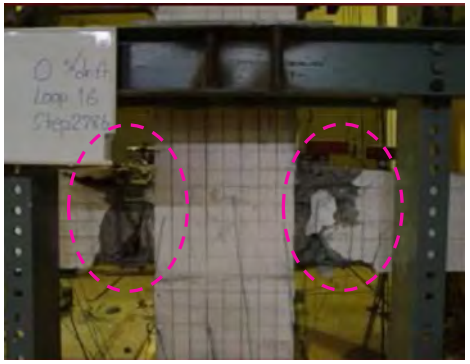

How to prevent the damage from earthquake?

Principle idea to resist the lateral load

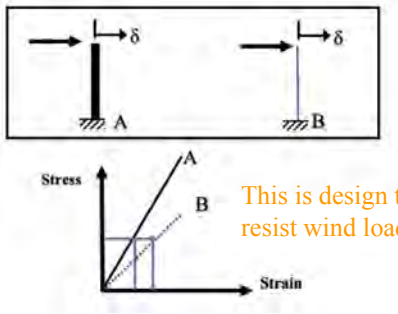

This is design to resist wind load.

Stiffness of **Column A** is higher than stiffness Column B.

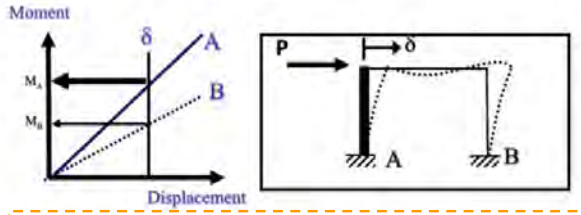

Load is distributed based on the stiffness of structures. Therefore, **Column A** is received load higher than Column B.

In this case, Column B has higher ductile than Column A. It should be noted that the ductile is important factor to prevent damage from EQ.

Prevent damage from earthquake by increasing ductile of RC beam

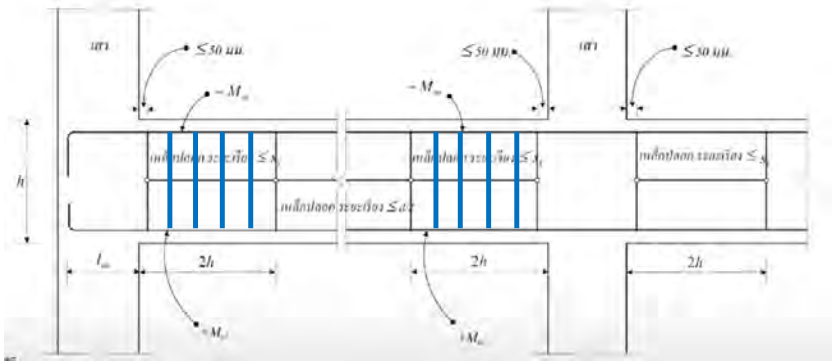

❑Increase number of stirrup.

Prevent damage from earthquake by increasing ductile of RC column

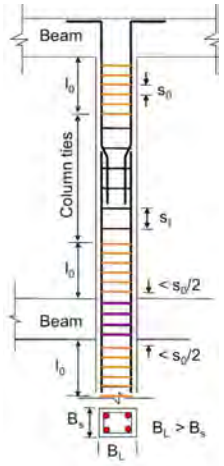

- Increase number of stirrup.
- Avoid splice steel rebar at the end of beam and column.

Prevent damage from earthquake at joint between beam and column

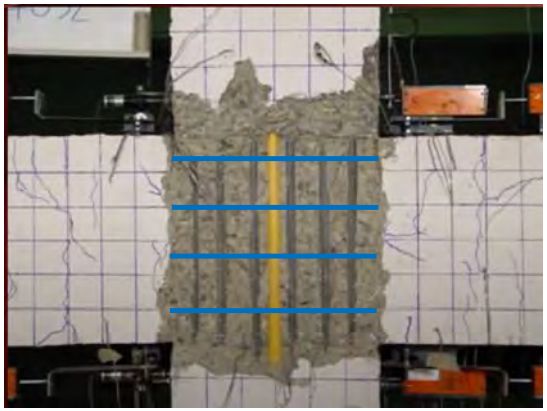

- Add stirrup at joint between beam and column.

Period of vibration

Period is the time it takes for one full cycle.

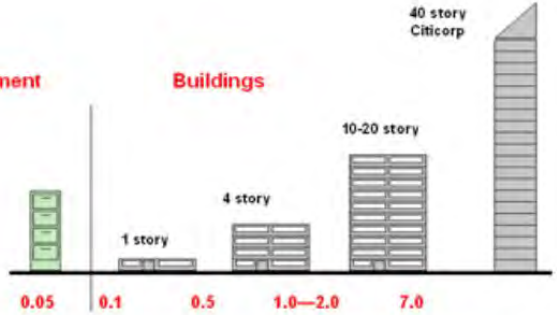

Height is the main determinant of fundamental period.
Each object has its own fundamental period at which it will vibrate.
The period is proportionate to the height of the building.

Design response acceleration spectrum

$F = ma$; when acceleration (a) increases force (F) will be increase.

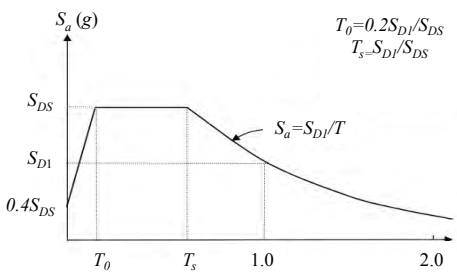

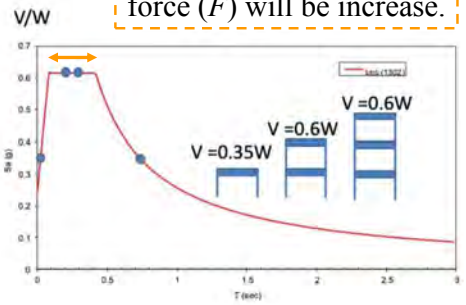

High acceleration at short vibration period.

Principle seismic design

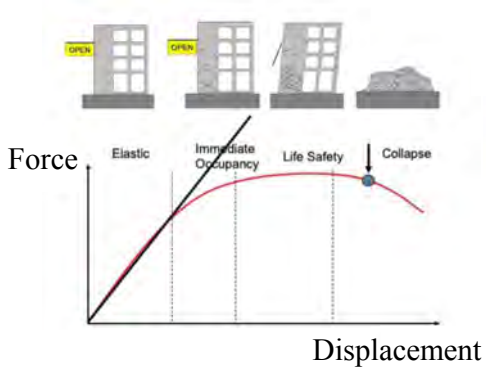

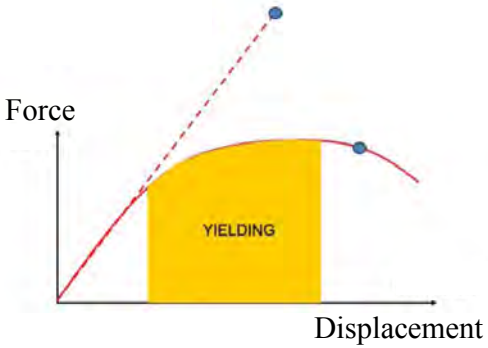

Principle seismic design

- ❑ Earthquake resistance

Damage to structure

- ❑May be occurred; however, the structure will not collapse.
- ❑Damage is ductile failure under the control and prediction of designer.

Structural Health Monitoring (SHM)

The benefits of SHM: tracking, identifying, measuring features of interest from structure responses have endless applications for saving cost, time and improving safety

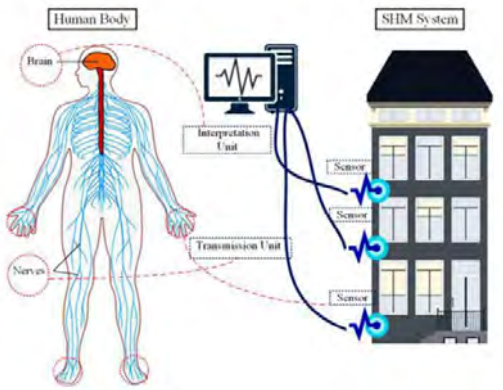

Fig. Comparison between the human body and the SHM system [13]

Reference: [13] V.R. Gharehbaghi, E. N. Farsangi, M. Noori, T. Y. Yang, S. Li, A. Nguyen, C. M. Chuquitaype, P. Gardoni and S. Mirjalili. "A Critical Review on Structural Health Monitoring: Definitions, Methods, and Perspectives" Archives of Computational Methods in Engineering (2022) 29:2209–2235

Based on research by Rytter [14], damage identification levels in SHM can be defined into 4 levels as follows:

Level 1: Identification: determining the existence of a defect on a global scale.

Level 2: Localization: determining the location and coordinates of the damage.

Level 3: Assessment: determining the intensity of damage in various components.

Level 4: Lifetime prediction: estimating the structure's remaining life.

This concept can be applied to monitor the structures for maintenance or seismic retrofit.

Reference: [14] Rytter A "Vibrational based inspection of civil engineering structures". Fract Dyn R9314(44). Ph.D.-Thesis defended publicly at the University of Aalborg, April 20, 1993

Seismic retrofit of existing RC Buildings in Asia countries

Problems from previous earthquake:

* Loss of lives.

* Damage to buildings and properties, causes economic loss, time to repair or rebuild, and opportunities loss.

Possible reason of the problems: Buildings have insufficient lateral force resisting systems or lack of seismic resistance that are sensitive to significant damage.

Solution: Improve the force resisting system and develop seismic performance of the building.

Type of valuable target buildings: Public buildings such as schools and hospitals, which play important post-disaster roles as shelters for some countries and in treating the injured people. These buildings are reinforced concrete (RC) buildings in many countries.

Reference: Lukkunaprasit et al. Performance of Structures in the Mw 6 1 Mae Lao Earthquake in Thailand on May 5 2014 and Implications for Future Construction. Journal of Earthquake Engineering 2015; 20: 219-242.

Conventional retrofit methods

Conventional retrofit methods of RC buildings

Reinforced concrete jacketing [1].

Conventional retrofit methods of RC buildings

Steel jacketing by steel plate and steel encasement.

Examples of conventional retrofit methods of RC buildings

Addition of shear wall to RC building [1].

Addition of conventional brace to RC building [1].

- Economical, strength-based design, less ductile.
- Difficult to secure immediate occupancy under severe earthquake (i.e. MCE level).
- With higher strength, excitation of acceleration, damages to surrounding frames are expected.

Innovative retrofit methods

Examples of energy-dissipation devices (EDDs) studies and applications

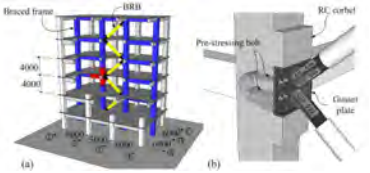

Qu, Sakata and Wada et al. introduced continuously buckling restrained braced frame (CBRBF) system to RC members.[1]

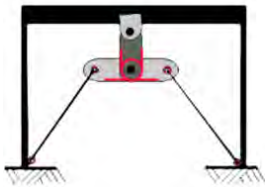

Naeem and Kim introduced rotational friction damper concept.[3]

Takeuchi and Yasuda et al. applied façade and BRB to retrofit Midorigaoka building number 1, Tokyo Institute of Technology.[2]

Yildirim et al. mentioned the rotational friction dampers to seismic retrofit of RC building.[4]

Reference: **[1]** Z. Qu, S. Kishiki, H. Sakata, A. Wada, Y. Maida. Subassemblage cyclic loading test of RC frame with buckling restrained braces in zigzag configuration. Earthquake Engineering and Structural Dynamics 2013; 42(7): 1087-1102. **[2]** T. Takeuchi, K. Yasuda, M. Iwata. Seismic retrofitting using energy dissipation façade. ATC-SEI09 Conference on Improving the Seismic Performance of Buildings and Other Structures, San Francisco., December 9-11, 2009. **[3]** A. Naeem, J. Kim. Seismic retrofit of structures using rotational friction dampers with restoring force. Advances in Structural Engineering, 2020. S. Yildirim et al. **[4]** Retrofit of a reinforced concrete building with friction dampers. Second European Conference on Earthquake Engineering and Seismology, Istanbul, August 25-29 2014.

The example of the 1st retrofitted 2-story RC school l building with BRBs, Chaing Rai, Thailand (in 2019)

(a) Target 2-story bare RC school building (b) Retrofitted building with BRBs

A total of 8 BRBs.

4 BRBs with the capacity of 160 kN in the longitudinal direction of the frame.

and

4 BRBs with the capacity of 275 kN in the transverse direction of the frame.

Reference: W. Wararuksajja, S. Leelataviwat, P. Warnitchai. L. Bing, H. Tariq and N. Naiyana1. Seismic Strengthening of Soft-Story RC Moment Frames. The 25th National Convention on Civil Engineering, July 15-17, 2020, Chonburi, Thailand.

東京工業大学
Tokyo Institute of Technology

Seismic retrofit of RC building method with BRBs and elastic steel frame (SF) from Takeuchi lab, Tokyo Institute of Technology

Reference: https://www.titech.ac.jp/

Preliminary retrofit design method

Evaluation of non-retrofit structure based on Equivalent Linearization

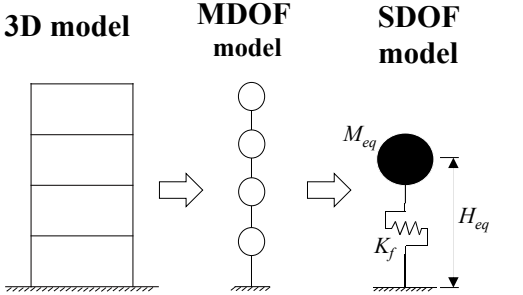

Structural model of non-retrofit model (RC frame)

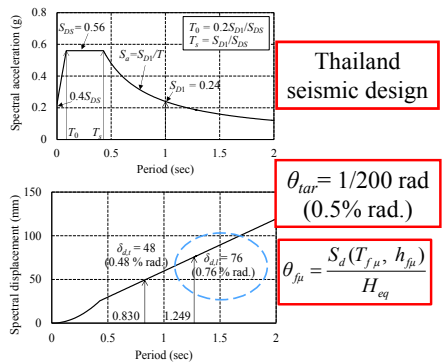

Thailand seismic design

θ_{tar}= 1/200 rad (0.5% rad.)

$\theta_{fu} = \frac{S_d(T_{f\mu}, h_{f\mu})}{H_{eq}}$

Displacement 5% damped response spectra

$SDR_{fu} > SDR_{tar}$ → Required to retrofit

Constant drift (CD) method for preliminary design

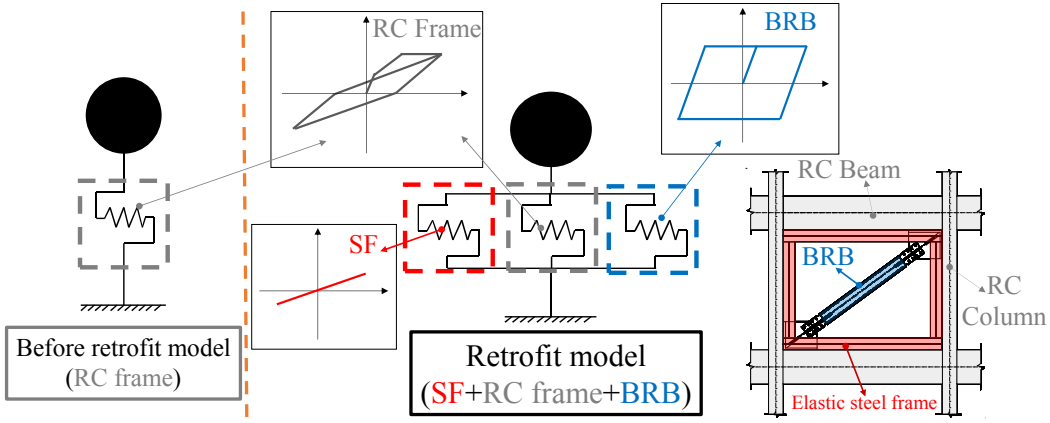

A design method without iteration to control SDR_{max} close to SDR_{tar}

Retrofit concept of CD method

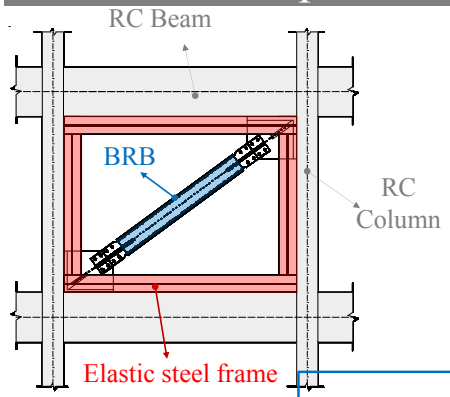

- Outline of retrofit -

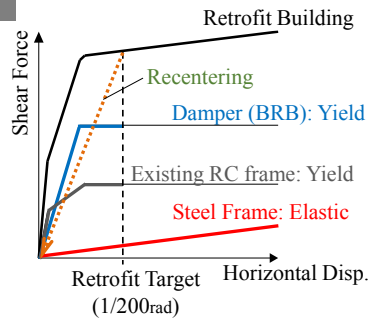

Total behavior of retrofit model using BRB and SF

Key parameters

1. K_{BRB} = BRB stiffness 2. K_f = Story stiffness of bare RC frame
3. γ_s = Stiffness ratio of SF to BRB (5%)

Previous experiment from Takeuchi lab and ITU

(a) R-specimen
[Bare RC frame specimen]

(b) RS-specimen
[RC frame specimen retrofitted with only SF]

(c) RSB-specimen
[RC frame specimen retrofitted with SF and BRB]

Composite behavior

Combined lateral stiffness of the RS-specimen is higher than the simple sum of RC frame and SF stiffnesses $(K_{RC,i} + K_{SF,i})$

Detail of RSB specimen, connection zone cross-section

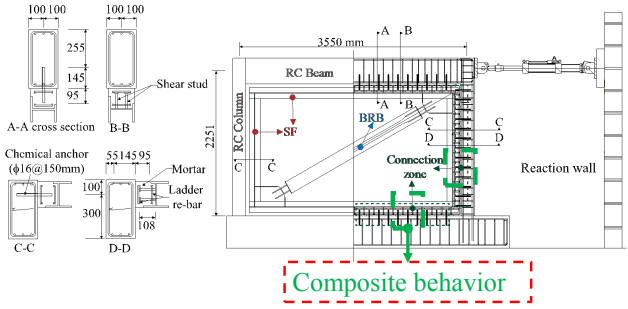

Detail of RSB specimen, connection zone cross-section

Retrofit concept including effect of composite behavior

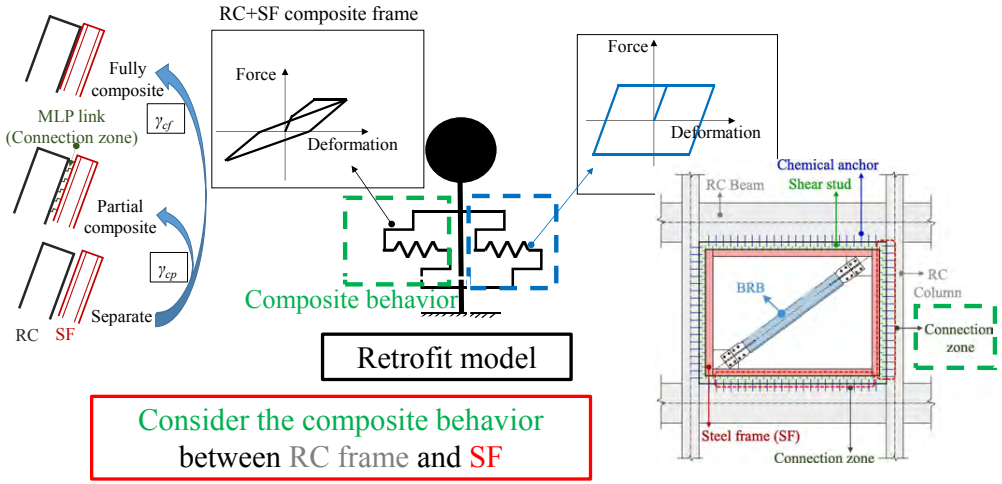

Retrofit concept

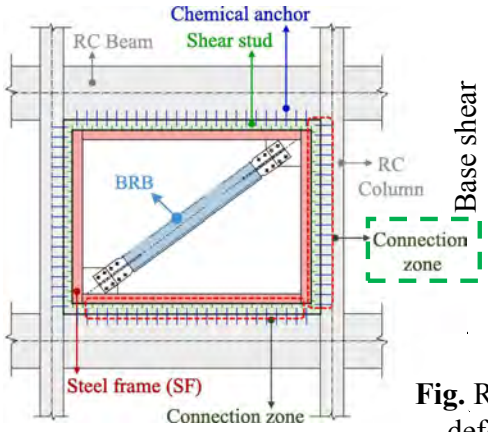

Fig. Outline of retrofit -

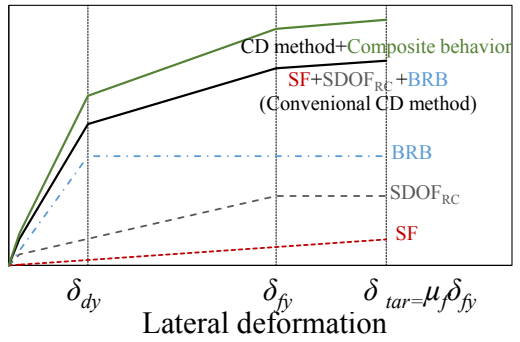

Fig. Relationship between base shear and lateral deformation of the retrofitted SDOF model

Calibration numerical models with experimental results

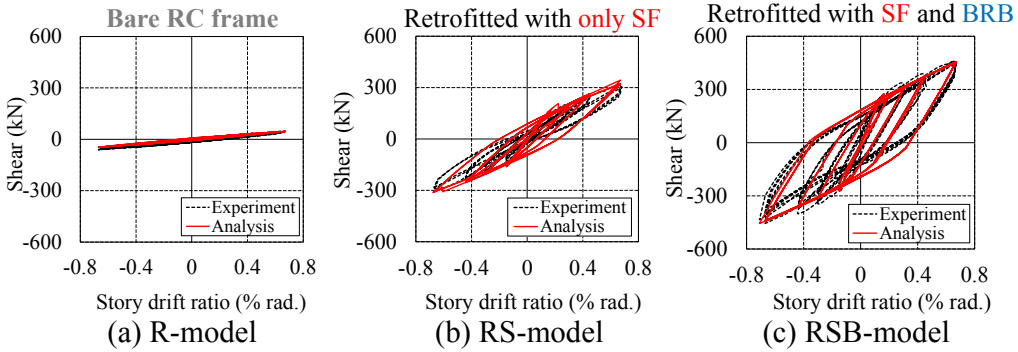

(a) R-model (b) RS-model (c) RSB-model

Performed **cyclic nonlinear pushover analysis on the numerical models** and calibrated against **quasi-static cyclic loading tests**.

Investigate of the composite behavior in multi-story building

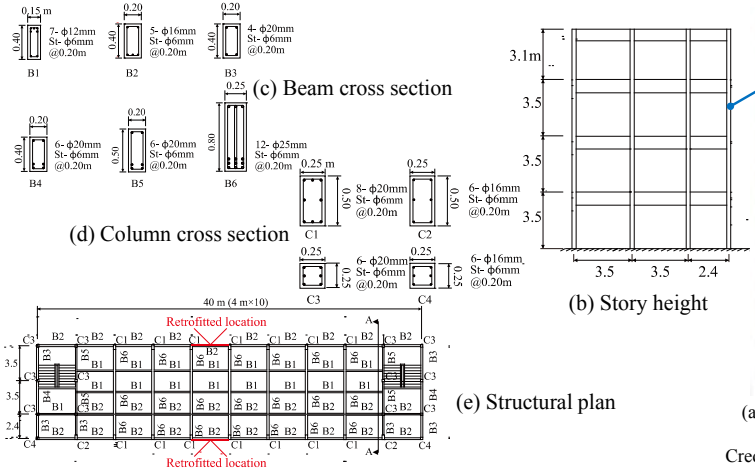

(e) Structural plan (b) Story height

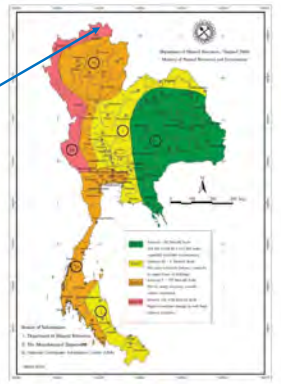

(a) Seismic Hazard Map of Thailand (Mercalli scale)
Credit: Department of Mineral Resources

Illustration of the analytical model for computing the elastic stiffness

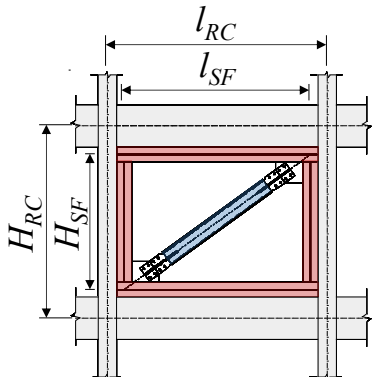

(a) Story height and spans

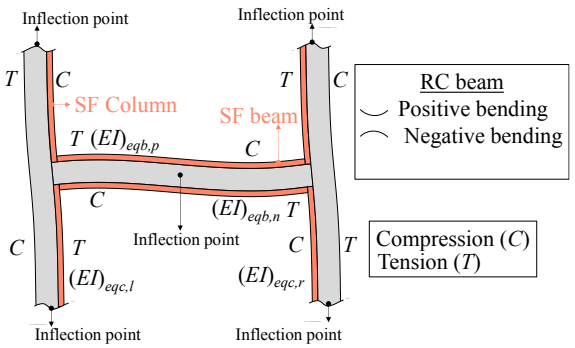

(b) Deformed shape

Design recommendations

1. Perform the pushover analysis to obtain bare RC frame story stiffness ($K_{f,i}$)
2. Calculate $K_{BRB,i}$ based on $K_{f,i}$ from the preliminary design (Conventional CD method).
3. Select the SF section and calculate $K_{SF,i}$ from Eq. (3), that $K_{SF,i}$ is either equal or slightly greater than 5% of $K_{BRB,i}$.
4. Obtain $K_{RC,i}$ for each retrofitted frame using Eq. (2) or by performing pushover analysis.
5. Calculate the $K_{BRBc,i}$ from Eq. (6) that satisfied the required stiffness, considering the composite behavior between the RC frame and SF.

Retrofit design results

Table. Design results

Story	Before retrofit	CD method	Proposed method				
	$K_{f,i}$ (kN/mm) Pushover analysis	$K_{BRB,i}$ (kN/mm)	$K_{RC,i}$ (kN/mm) (Equation 4)	$K_{RC,i}$ (kN/mm) Pushover analysis	$\delta_{dy,i}$ (mm)	$K_{SF,i}$ (kN/mm)	$K_{BRBc,i}$ (kN/mm)
4th	39.6	34.8	4.1	3.7	-	-	-
3rd	32.2	34.8	3.2	3.0	3.5	2.0	26.5
2nd	32.1	65.4	3.2	3.1	3.5	3.8	53.9
1st	45.3	43.7	3.2	4.3	3.5	2.0	28.7

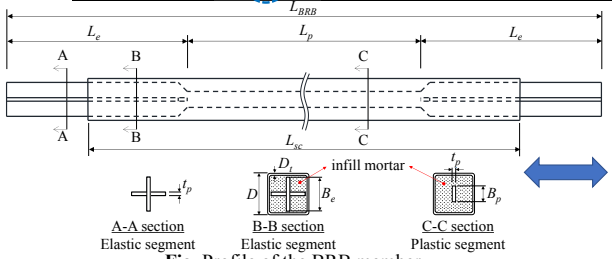

Fig. Profile of the BRB member

Based on the example building, the **BRBs steel tonnage** can be **reduced by 20%** as compared to a retrofit design that **does not consider composite behavior**.

Analysis: 3D-Numerical models

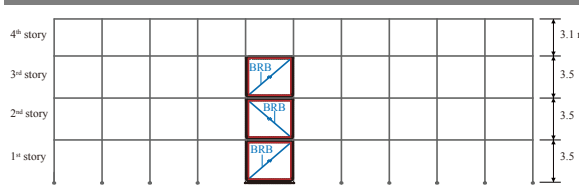

(a) Structural elevation with the components of the retrofitted bay

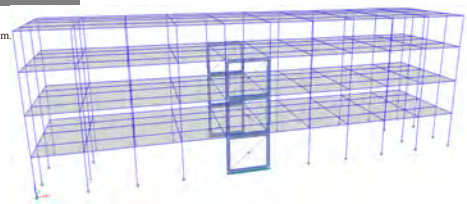

(b) 3-D view of the analysis model

(a) 3D-R model = Non-retrofit RC frame (Bare RC frame)

(b) 3D-RSB model = Retrofitted by BRB and SF neglecting composite behavior ($K_{BRB,i}$)

(c) 3D-RSCB model = Retrofitted by BRB and SF considering composite behavior ($K_{BRBc,i}$)

$$K_{BRB,i} > K_{BRBc,i}$$

Nonlinear response history analysis (NLRHA)

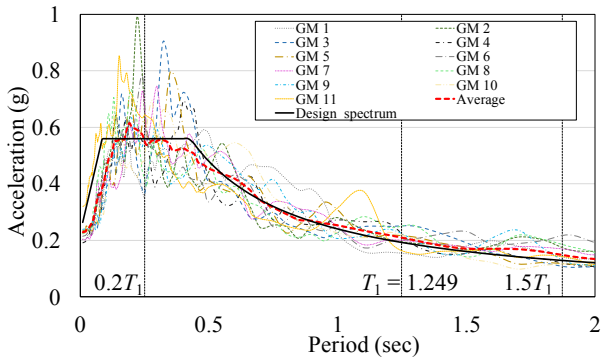

11 Ground motions for NLRHA

NLRHA results

Maximum story drift ratio (SDR_{max})

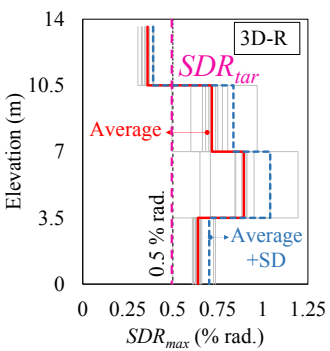

(a) Non-retrofit RC frame

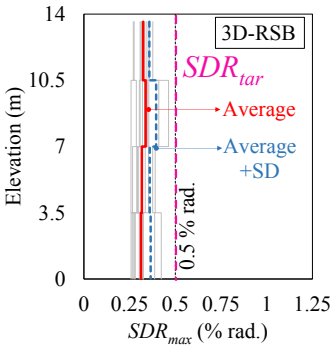

(b) Retrofitted by BRB and SF neglecting composite behavior

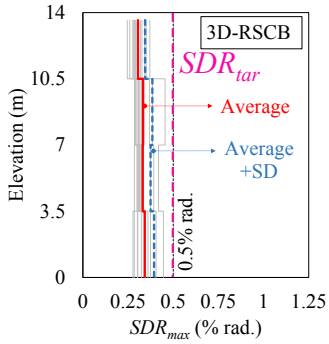

(c) Retrofitted by BRB and SF considering composite behavior

Viscous damper

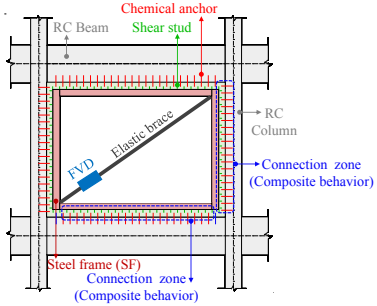

Extend the CD method and effect of composite behavior to viscous damper

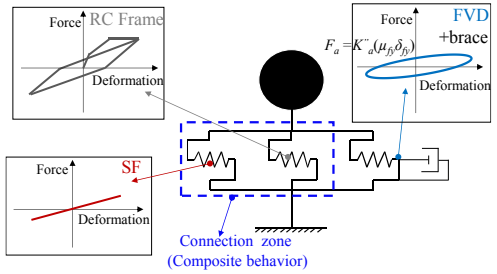

Retrofit model (SF+RC frame+braced FVD)

Key parameter : K''_a = Loss stiffness of the viscous damper

Friction damper

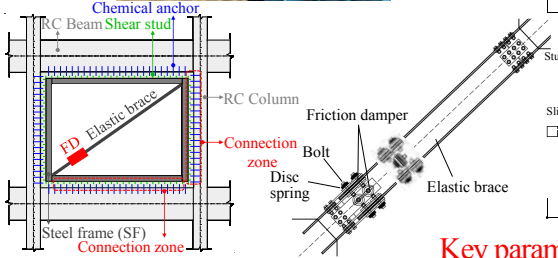

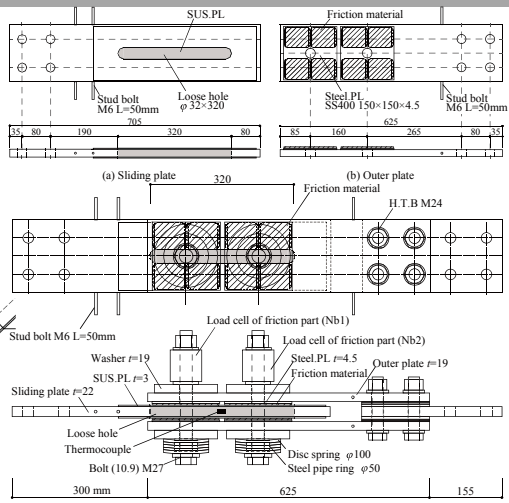

Key parameter : F_d = Slip force of friction damper

Department of Civil Engineering, King Mongkut's Institute of Technology Ladkrabang (KMITL), Thailand

To achieve SDGs at Department of Civil Engineering, School of Engineering, KMITL

11. Sustainable Cities and Communities

Reference: https://www.sdgmove.com/aboutsdgs/

Structural laboratory (STR Lab), Department of Civil Engineering, KMITL

Location

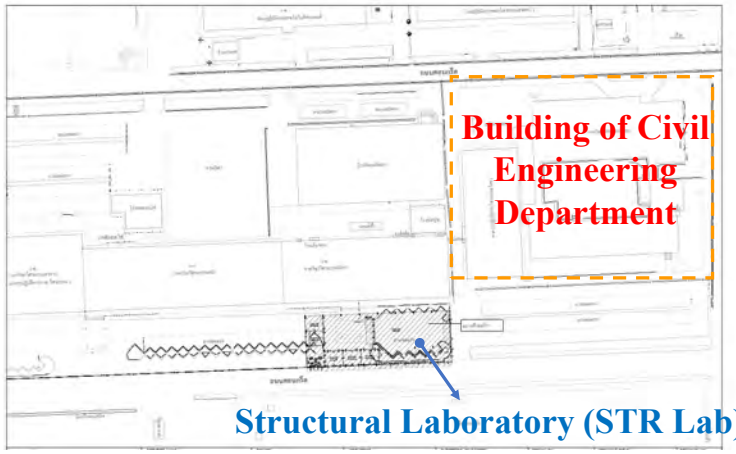

Outside structural laboratory building

Inside structural laboratory building

1st Structural laboratory plan

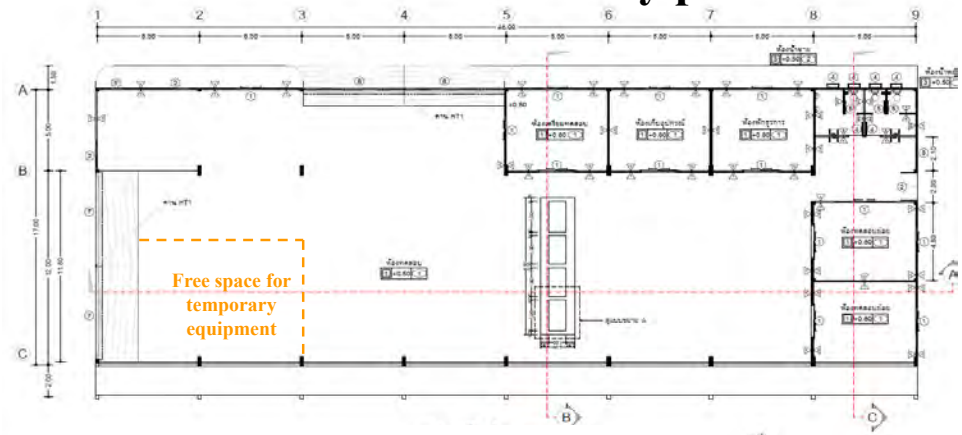

Plan view

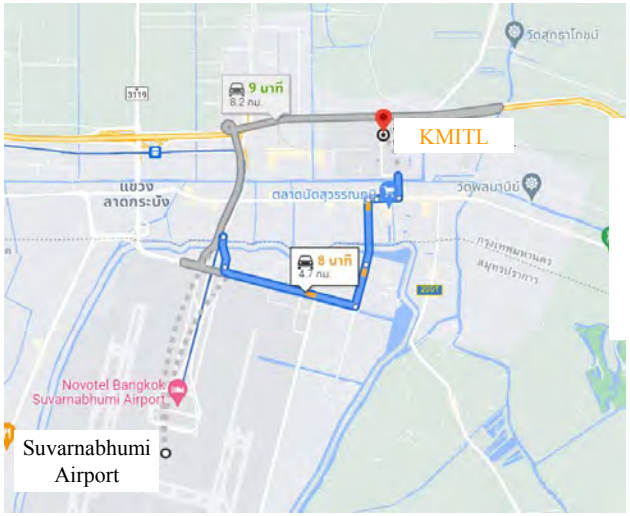

KMITL to Suvarnabhumi airport (Thailand's main international airport) is about 10 mins by car.

Reference: Google map.

If buildings and infrastructure are protected against disasters such as an earthquake, cities will become sustainable communities.

Reference: https://www.sdgmove.com/aboutsdgs/

References:

1) Y. Dou, Q. Huang, C. He, S. Meng and Q. Zhang. Rapid Population Growth throughout Asia's Earthquake-Prone Areas: A Multiscale Analysis. International Journal of Environmental Research and Public Health v.15(9); 2018 Sep.
2) Council of Engineers, Thailand.
3) Professor Amorn PIMANMAS. Department of Civil Engineering, Kasetsart University
4) https://www.wbdg.org/resources/seismic-design-principles
5) Panitan Lukkunaprasit, Anat Ruangrassamee, Tirawat Boonyatee, Chatpan Chintanapakdee, Kruawun Jankaew, Nuttawut Thanasisathit & Tayakorn Chandrangsu. Performance of Structures in the Mw 6.1 Mae Lao Earthquake in Thailand on May 5, 2014 and Implications for Future Construction
6) Concept in Earthquake Behavior of Building, C.V.R. Murty Asso and GOV of Gujarat. Nitikorn Sangswang Infra Group Knowledge Sharing Topic: Earthquake and Sesimic Design per DPT 1301/1302-61.
7) K.Kazuhiko Kasai. Tokyo Institure of Technology.
8) Announcement of the Ministry of Interior. November 2021. and American Society of Civil Engineers (ASCE).
9) American Society of Civil Engineers (ASCE). Minimum Design Loads for Buildings and Other Structures 2016 (ASCE/SEI 7-22).
10) https://www.youtube.com/watch?v=ufOtpGS9fRM
11) https://www.youtube.com/watch?v=ovfLDAI3BWM
12) https://www.youtube.com/watch?v=LVhKat3FMaA
13) V.R. Gharehbaghi, E. N. Farsangi, M. Noori, T. Y. Yang,· S. Li, A. Nguyen, C. M. Chuquitaype, P. Gardoni and S. Mirjalili. "A Critical Review on Structural Health Monitoring: Definitions, Methods, and Perspectives" Archives of Computational Methods in Engineering (2022) 29:2209–2235
14) Rytter A (1993) Vibrational based inspection of civil engineering structures. Fract Dyn R9314(44)

Thank you very much for your attention

ขอบคุณครับ

Name: Asst.Prof.Dr. Panumas Saingam
Department of Civil Engineering
School of Engineering
King Mongkut's Institute of Technology Ladkrabang
E-mail: panumas.sa@kmitl.ac.th
Website: https://civil.kmitl.ac.th/dr-panumas-saingam/

Enabling Integrated Measurement and Control Solutions for Railway by Garry Tjhin

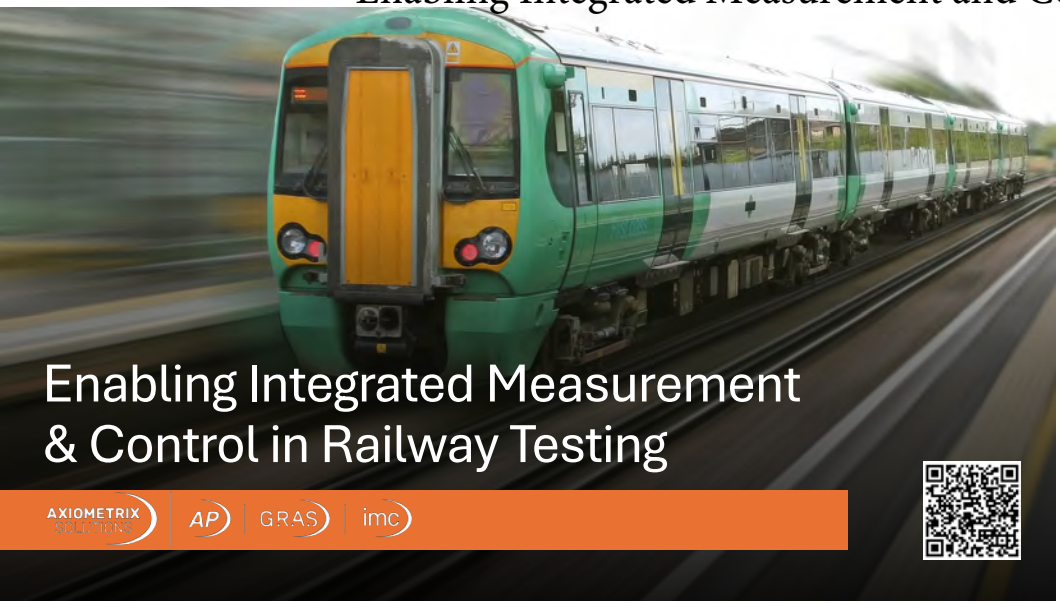

AXIOMETRIX SOLUTIONS | tme

AXIOMETRIX SOLUTIONS

KEY TAKEAWAYS

MEASUREMENT REQUIREMENTS
DECENTRALISED, REMOTE, INTEGRATION, CONTROL

USE CASES
WHEELSET, PANTOGRAPH, PASSENGER COMFORT, NOISE

COMPLEXED TESTING IN RAILWAY INDUSTRY

Expertise in mobile applications

- Passenger comfort
- Investigation of vehicle behavior (e.g., wheel flange strength)
- Commissioning tests
- Crash tests
- Climate testing
- Brake testing
- Testing at high speeds
- Derailment testing

Expertise in stationary applications

- Structural testing of components (e.g., wheels, bogies, railroad car bodies)
- Structural analysis of the complete train
- Structural tests on railway tracks
- Structural analysis of inter-carraige bridges
- Air-pressure measurement in tunnels
- Testing noise barriers
- Pantograph tests (on test stands and mobile)

NEED FOR DECENTRALISED & REMOTE TEST & MEASUREMENT

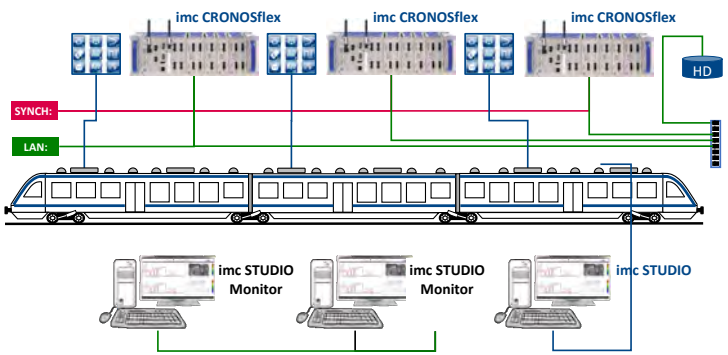

2KM
LONG TRAIN

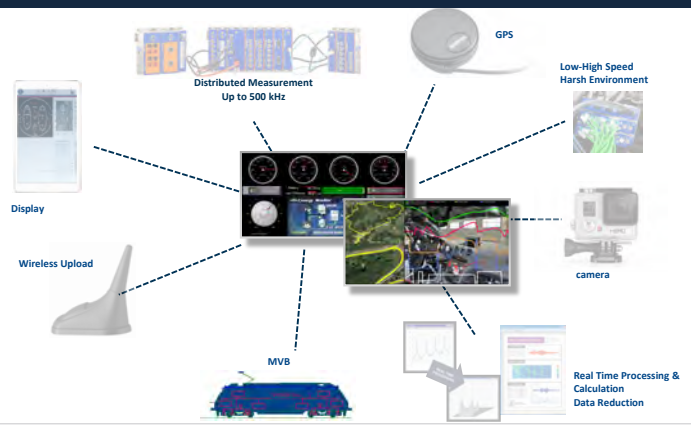

Complex Testing that requires integration and real time processing

PREFERRED TEST & MEASUREMENT PROVIDER FOR MAJOR STAKEHOLDERS WORLDWIDE

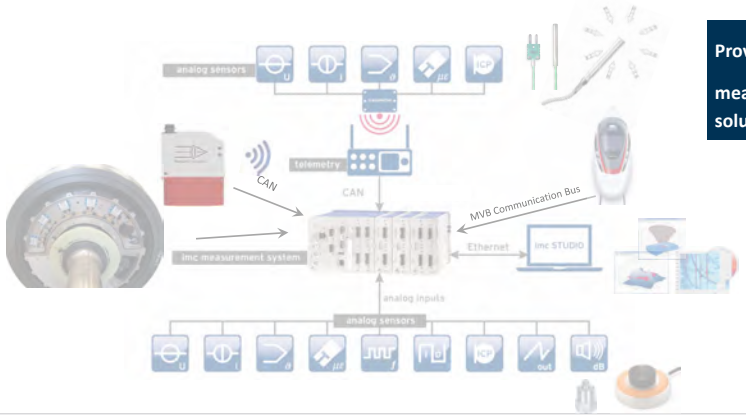

Providing Integrated measurement and Control solution

- Analog Sensors
- Telemetry (rotating parts)
- Vehicle Dynamics Sensors
- Digital Fieldbuses
- Sequence and Triggers *via Software
- Real time Processing

THALES · Hitachi Rail STS · SBB CFF FFS · Kawasaki Powering your potential · JR CENTRAL · ALSTOM · TÜV SÜD · PJM · CRH · SIEMENS · KNORR-BREMSE · STADLER · GE Transportation · PROSE · ZF · cetest · ITALCERTIFER GRUPPO FERROVIE DELLO STATO ITALIANE · 中国中车 CRRC · CARS · SNCF · vossloh

COMPREHENSIVE INSPECTION TRAIN

- **CIT - Comprehensive Inspection Train** - a huge device for infrastructure state detection and integrating various testing equipment
  - Detection of **rail geometry, conditions of catenary, communication, signal, environment around the rail** and other infrastructure conditions
  - Detection of **dynamic performance of high-speed trains such as wheel-rail contact status and the accelerations**
- imc Solution: CRONOS SL/ CRONOSflex-400
  - UNI2-8 MTC Version for Wheel force and Acceleration.
  - ***MTC series* (protection module)** are intended for applications in electrically harsh environments, electric motor train applications are characterized by possible transient input voltage conditions, both common mode and differential mode
    - Destructive transient overvoltage
    - ESD discharge processes
  - ENC-4 for Speed & Distance
  - CAN bus for distance stamp

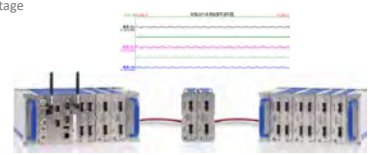

WHEELSET

MEASURING STRAIN ON ROTATING PARTS

Fatigue, Wear, Cracks

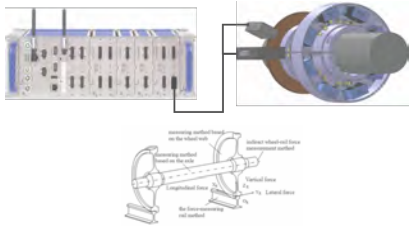

Why do the wheelsets of rail-bound vehicles have to be tested?

- **Detection of material fatigue:**
  Wheelsets are exposed to extreme loads, which can lead to material fatigue.
- **Monitoring wear:**
  Wear on wheel treads and other wheelset components can affect driving safety
- **Detecting cracks:**
  Cracks in wheels or axles can have catastrophic consequences
- **Checking the lubrication:**
  Insufficient lubrication of bearings and other moving parts leads to increased friction and wear.

TELEMETRY FOR WHEELSETS

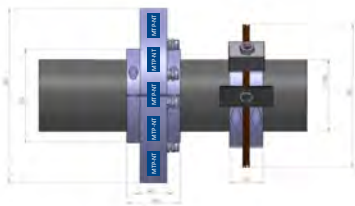

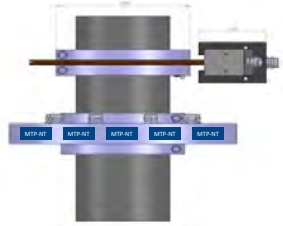

- Strain gauge sensors (350 Ω):
  For monitoring loads and stresses in the wheelset.
- Temperature sensors:
  For detecting temperature changes that indicate lubrication problems or excessive friction.
- IEPE vibration sensors:
  For measuring vibrations that indicate imbalances, bearing problems or other mechanical defects.

TELEMETRY FOR WHEELSETS

- **Summary**

  Regular and accurate wheelset inspections are essential for the safety and reliability of rail transportation.
  By using the latest measurement technologies and robust system setups, potential problems can be identified and rectified at an early stage, leading to a significant improvement in operational performance and safety

- **USPs:**

  All signals are measured synchronously, whether wireless via MTP-NT telemetry or wired or signals from the digital rail bus

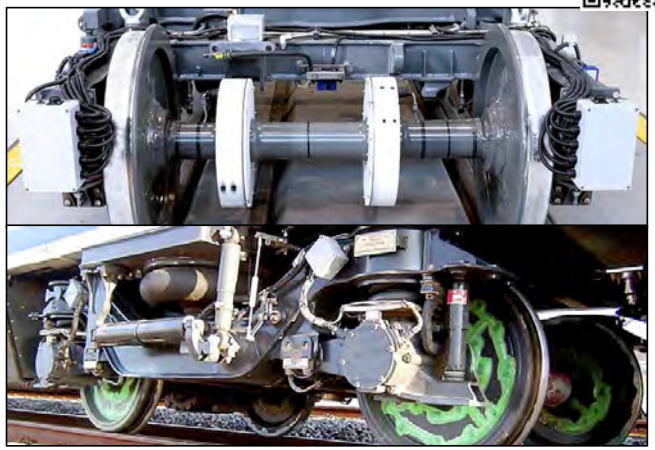

TELEMETRY FOR WHEELSETS

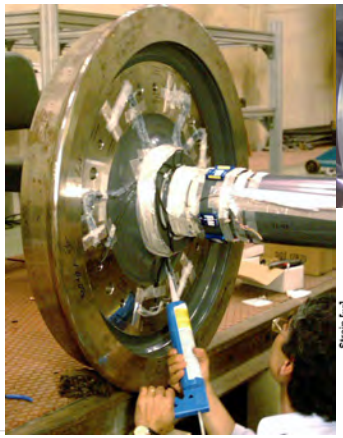

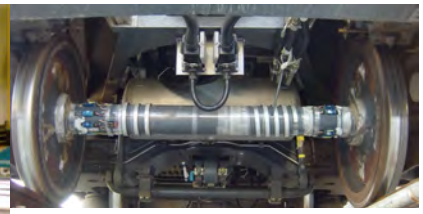

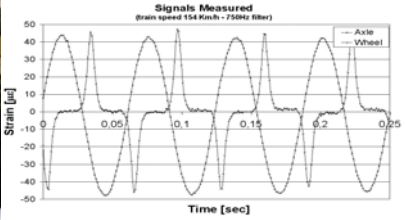

PANTOGRAPH

PANTOGRAPH

- Measure the dynamic behavior of the pantograph
- Force applied on the catenary by the contacts strips
- Displacement of the upper and lower arms
- Vertical acceleration of the contact strips
- Voltage and flowing current

STRUCTURAL AND DERAILMENT TEST

STRUCTURAL AND DERAILMENT TEST

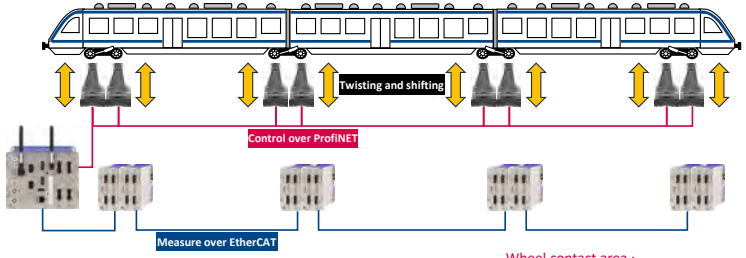

Each twisting element has several drives:

- 2x lifting drive (1x drive per contact surface) to adjust the torsion
- 2x lateral adjustment to move the train in and out
- 1x travel drive to position the elements
- 1x relief drive to lift the torsion element from the rail

- The test stand consists of 8 twisting elements mounted between 2 rails. These elements are each made up of 2 height-adjustable wheel contact surfaces.
- Each side can lift up to 175 kN=17 t, is independent of each other and is controlled via ProfiNET

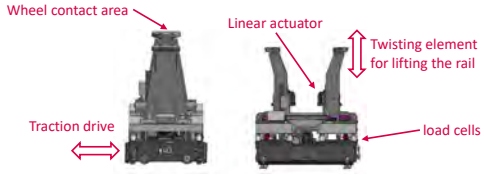

CONDITION MONITORING

TRACK TRACER

TRACK TRACER

- Measure vibration and angular velocity
- Use of standalone CS4108 imc systems

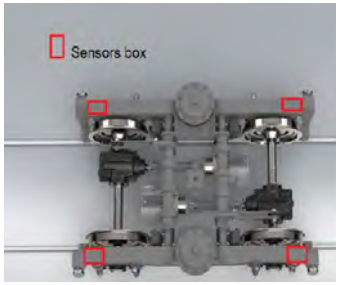

TRACK TRACER

- Position with GPS
- High precision distance and speed sensors *optical
- VLAN or 4 G connection
- imc Link automatic upload software

Proprietary - Company Confidential ©2022 Axiometrix Solutions Holdco LLC

AXLE LOAD CHECKPOINT

AXLE LOAD CHECKPOINTS (ALC)

- Wheel Damage: measuring the vertical wheel forces
- Infrastructure Damage: measuring shear stress with strain gauges

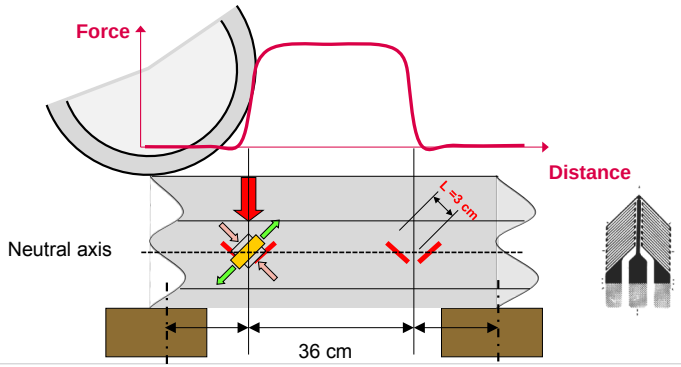

AXLE LOAD CHECKPOINTS (ALC)

- Noise / Vibrations / Damage to infrastructure

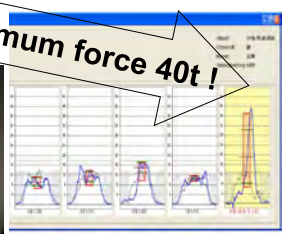

- Destruction of infrastructure
- Irreversible damage to permanent structures (bridges)
- Inevitably leads to bearing damage -> running hot

BRIDGE MONITORING

BRIDGE MONITORING

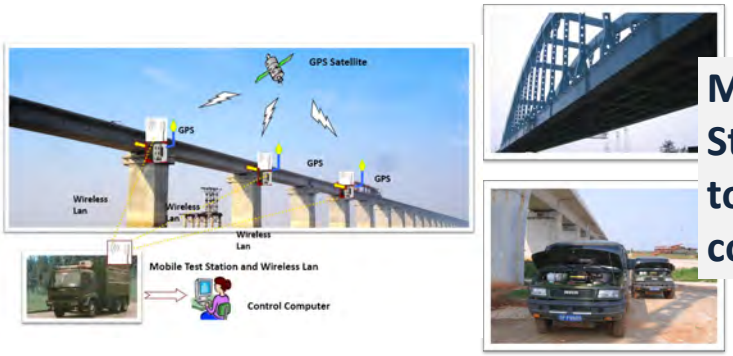

Mobile Test Station deployed to analyse bridge condition

SENSORS

NOISE MEASUREMENT

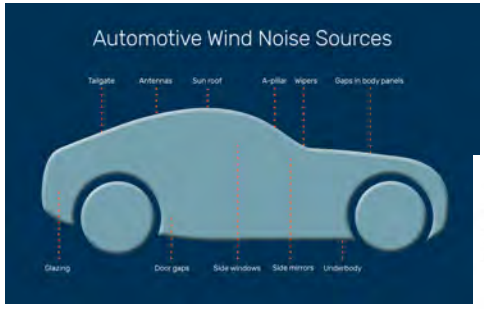

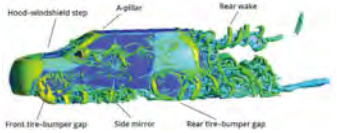

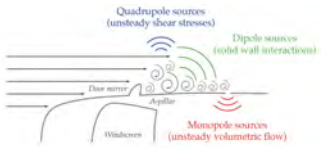

Aeroacoustic Sensors for the Railway Industry

Aeroacoustic

Low Profile
With a height of 1 mm the door opens to a whole new world of what can be measured in boundary layers and turbulent flow.

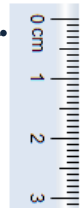

Flow-optimized Fairings
The fairing has a rise angle of 7.5° ensuring minimal disturbance to the sound field/airflow.

Frequency range:	20 Hz - 40 kHz (± 1 dB)
	10 Hz - 70 kHz (± 3 dB)
Dynamic range:	54 dB(A) - 170 dB
Sensitivity:	0.6 mV/Pa (± 3 dB)

GRAS Sound & Vibration

AXIOMETRIX SOLUTIONS

IN CABIN MEASUREMENT – ISO 3381 STANDARD

Requirements and challenges to measure inside noise

- Noise emissions from rail vehicles are an important aspect of rail transportation, affecting both the environment and the quality of life of local people.
- ISO 3095 is the internationally recognized standard that regulates the measurement and assessment of noise emissions from rail vehicles
- Requirements and challenges when carrying out noise emission measurements

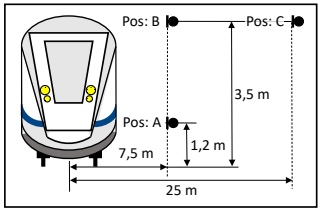

Requirements and challenges to measure emitted noise

- Noise measurements inside rail vehicles are standardized in the international ISO 3381.
- Challenges for the measurement and evaluation of noise inside rail vehicles
- Requirements for measurement technology for measuring the speech intelligibility of loudspeaker announcements in accordance with ISO 60268-16

AXIOMETRIX SOLUTIONS | AP | GRAS | imc

AXIOMETRIX SOLUTIONS

IN CABIN MEASUREMENT – ISO 3381 STANDARD

Overview of ISO 3381 INSIDE

- The ISO 3381 is an international standard for the measurement and assessment of noise inside railbound vehicles
- The goal is to provide standardized procedures for measuring and evaluating interior noise
- An additional goal is to measure and evaluate the speech intelligibility of loudspeaker announcements in accordance with ISO 60268-16

Summary:

- With the help of imc you can measure and evaluate according to ISO 3381
- By complying with this standard, manufacturers and operators can ensure that passenger comfort is guaranteed, and passenger acceptance is increased

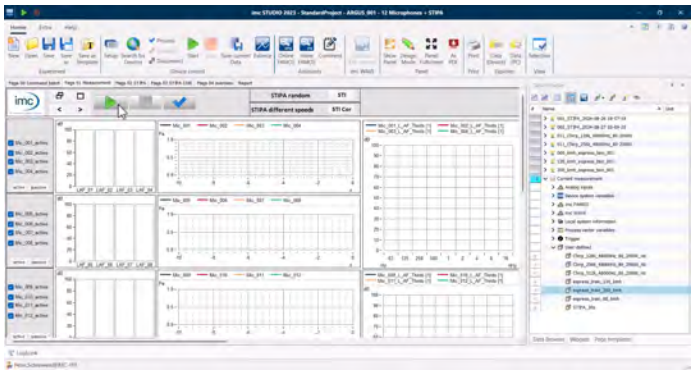

AXIOMETRIX SOLUTIONS | AP | GRAS | imc

AXIOMETRIX SOLUTIONS

IN CABIN MEASUREMENT – ISO 3381 STANDARD

Overview of ISO 3095 OUTSIDE

- ISO 3095 specifies the procedures for measuring the noise generated by railbound vehicles
- The goal is to collect uniform and comparable data in order to assess noise exposure and, if necessary, take measures to reduce noise
- Suitable for all types of railbound vehicles, including high-speed trains, goods trains and trams

Summary:

- With the help of imc you can measure and analyze according to ISO 3095
- By complying with it, manufacturers and operators can ensure that noise emissions remain within acceptable limits and thus contribute to reducing noise pollution in the environment

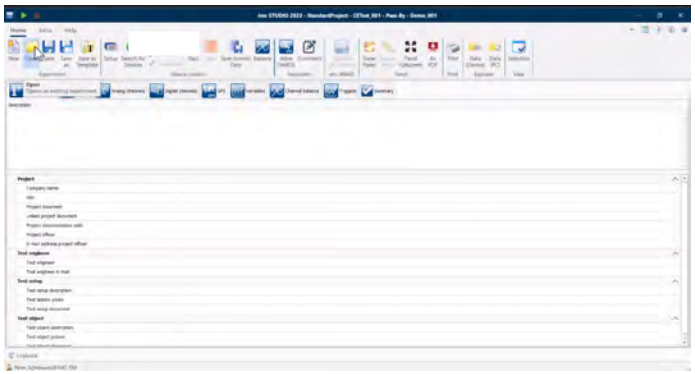

AXIOMETRIX SOLUTIONS | AP | GRAS | imc

PASSENGER COMFORT

- Measure vibration on car body and bogie
- Use of multi axial accelerometers
- Use of GPS positioning and speed measurements
- Stand alone systems

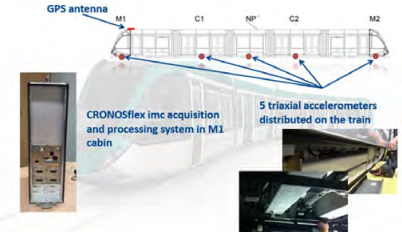

PASSENGER COMFORT

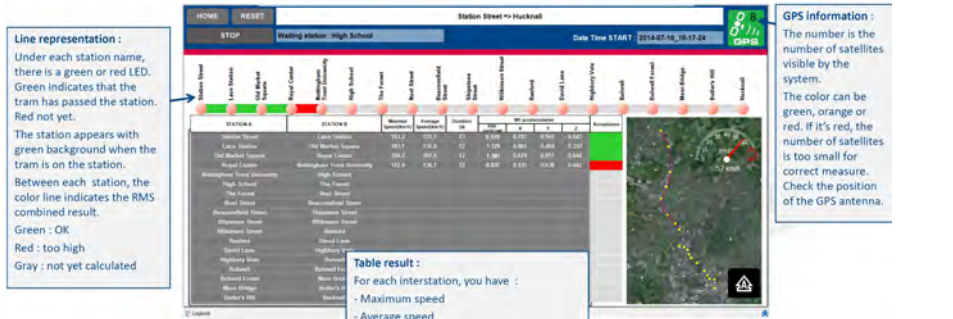

PASSENGER COMFORT

END OF DAY MEASUREMENT

- Black box recording without PC
- End of the day analysis (imc FAMOS)
- Report of all the recorded

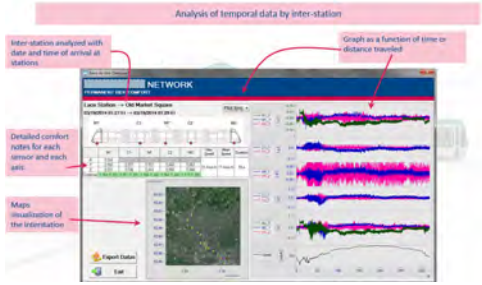

Comfort evaluation

Vibration and shock with respect to human beings

Evaluation based on standard:

- ENV 12299 (dynamic behavior): 1999
- UIC – Kodex 513 E : 1994
- Special BOMBARDIER requirements

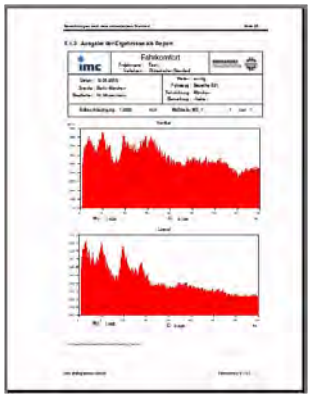

Comfort note seated

$$N_{VA} = 4 \cdot \left(a_{ZP95}^{Wab}\right) + 2 \cdot \sqrt{\left(a_{XP95}^{Wad}\right)^2 + \left(a_{ZA95}^{Wab}\right)^2} + 4 \cdot \left(a_{XD95}^{Wac}\right)$$

ab = vertical direction Wab = Wa x Wb
ad = horizontal direction Wad = Wa x Wb
ac =in longitudinal direction backrest Wac=Wa x Wc
k = 95 for 95. Quantil

N<1 very comfortable
1 ≤ N < 2comfortable
2 ≤ N < 4on average
4 ≤ N < 5uncomfortable
N > 5 very uncomfortable

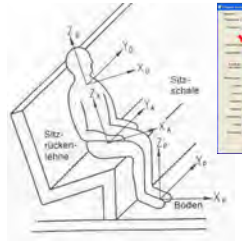

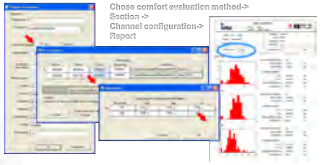

29.09.2024

Derailment test

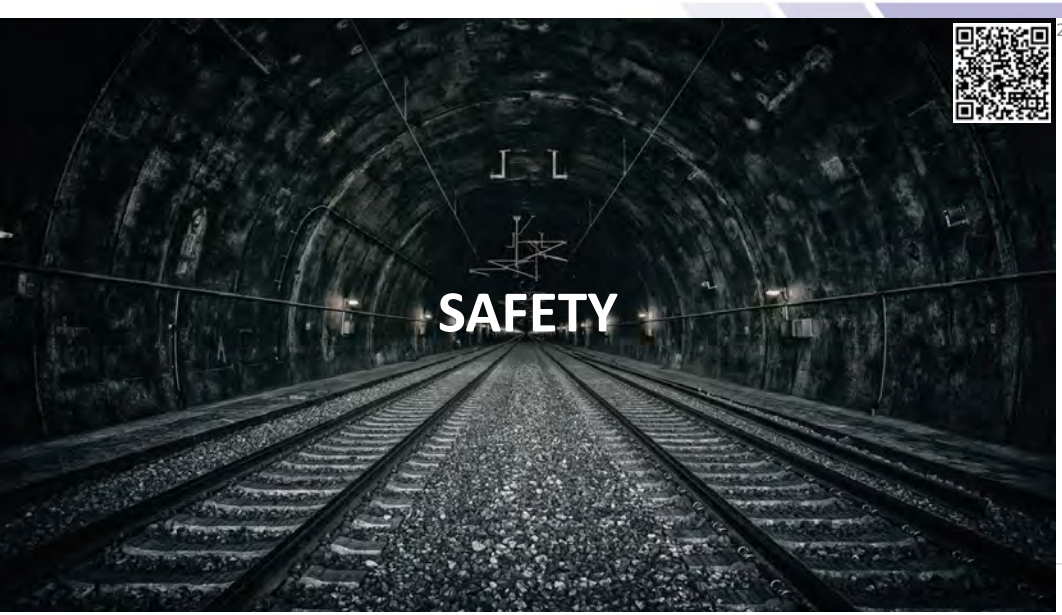

Derailment test

An unidentified derailment often results in extreme consequential damage which, if detected at an early stage, could have been almost completely avoided. Safety, especially in the case of hazardous goods, can be substantially improved by fitting derailment detectors on freight wagons and making use of telematics …

Technische Universität Berlin

FACHBEREICH 10
VERKEHRSWESEN UND
ANGEWANDTE MECHANIK

Institut für Straßen-
und Schienenverkehr

Fachgebiet Schienenfahrzeuge

Prof. Dr.-Ing. Markus Hecht

Tel.: +49 (0)30 314 25150

Derailment test

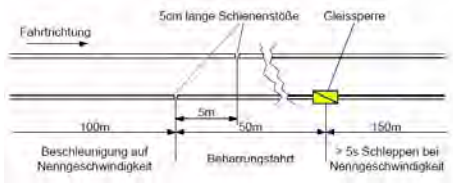

Derailment test

Measurement system and position of accelerometers

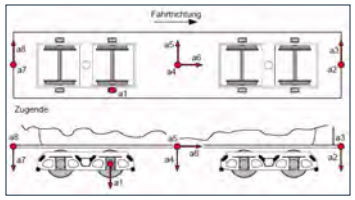

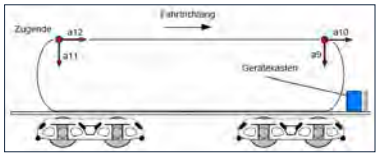

Derailment test

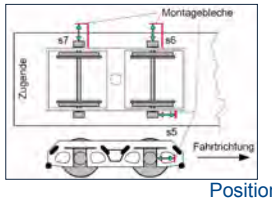

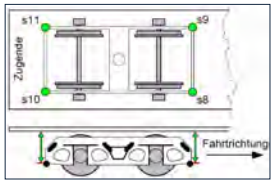

Position of displacement sensors

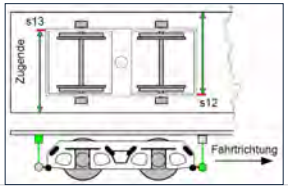

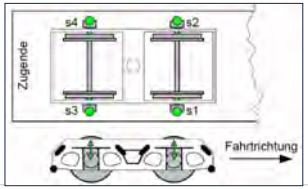

Derailment test

YOUR PREFERRED SOLUTION PARTNER

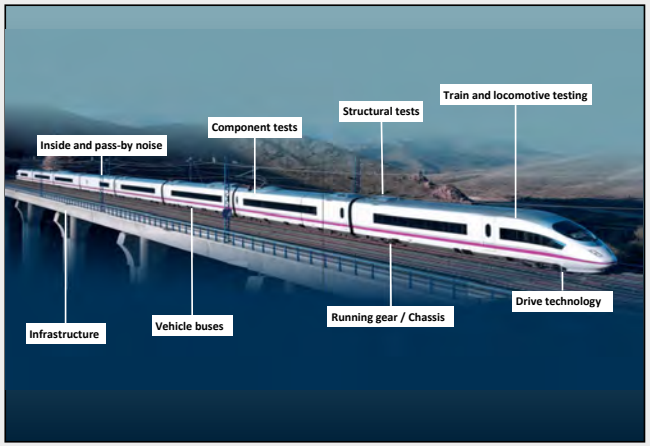

Solutions for:

- **Inside and pass-by noise**
  ISO 3095, ISO 3381, IEC 60268-16
- **Component tests**
  Pantograph, air conditioning + clutch, brake
- **Structural tests**
  Car body, bogie, overrun tests + derailment test
- **Train and locomotive testing**
  acceptance, approval runs + brake tests
- **Drive technology**
  Electric traction + combustion engines
- **Running gear / Chassis**
  Wireless wheelset, bogie testing (telemetry)
- **Vehicle buses**
  MVB, CAN, TRDP (IPTCom), PROFINET or Modbus
- **Infrastructure**
  Wheel load checkpoints + detection of wheel defects

CASE STUDIES

***confidential**

Projects Examples

SBB, Switzerland
Trackside Measurement and Assessment

“Yellow Doctor”, China
Train based infrastructure measurement and monitoring

Passenger Comfort, UK
Realtime assessment of passenger comfort from tram network.

SBB in Switzerland

Axle Load Checkpoints (ALC)

The Goal: Safer Railways

Monitoring Safety Critical Load Data at Wheel Load Measurement Points

Measurements

- Maximum Permissible Axle Load
- Unbalanced Load Detection
- Deviation from Declared Weight
- Wheel Flat Spots

SBB Switzerland: Axle Load Checkpoints (ALC)

- Instrumented track sections in 20 locations around the network.
- Measure at normal train speed.
- Data transmitted to central control room.
- Information available in real time.
- Allows immediate action to be taken.
- Trains may be slowed down or stopped.

System Requirements

- runs 24 hours a day,
- 7 days a week
- works in real time
- is largely automated
- reliably detects technical problems before they turn into dangerous situations.

Technical Solution

- Rail sections - instrumented to measure load with strain gauges.
- imc CRONOSflex – PC independent, decentralized, distributable measurement system with direct online analysis of measurement data.
  - imc CRONOSflex
  - Two 8-channel strain gauge bridge amplifiers
  - One universal measurement amplifier for temperature acquisition
- Software integration via imc DEVICES and imc COM

Typical Report

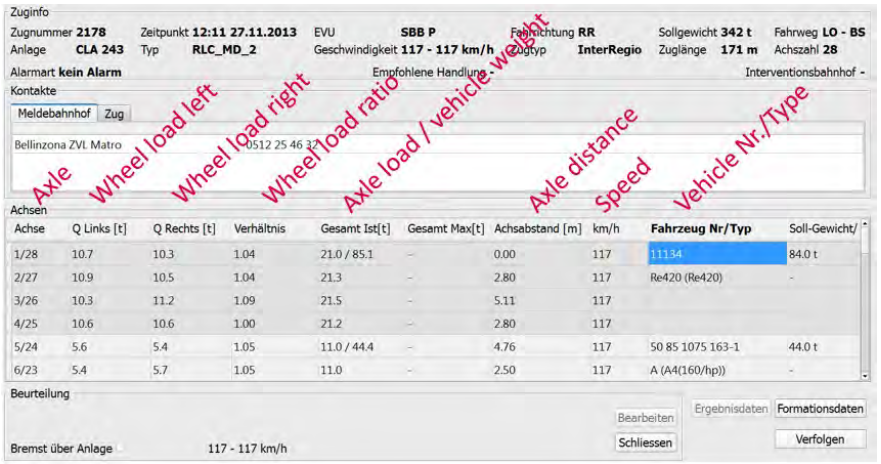

Wheel Defect Detection

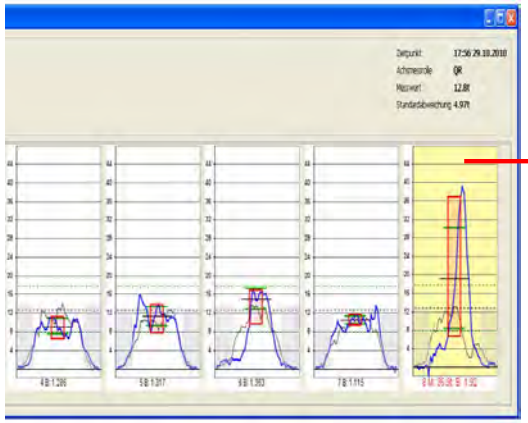

Conclusion

- SBB operates 20 wheel-load checkpoints that allow for automated monitoring of all the trains on the Swiss rail network.
- The quality of the primary acquired measurement signals – for example with resolution, precision and bandwidth – is improved tenfold over previously used methods .
- More accurate diagnosis can be provided, thus, increasing the quality of the available information.
- The trains are safer, have fewer breakdowns and save time and money for the SBB and their customers.

©2024 Axiometrix Solutions Holdco LLC

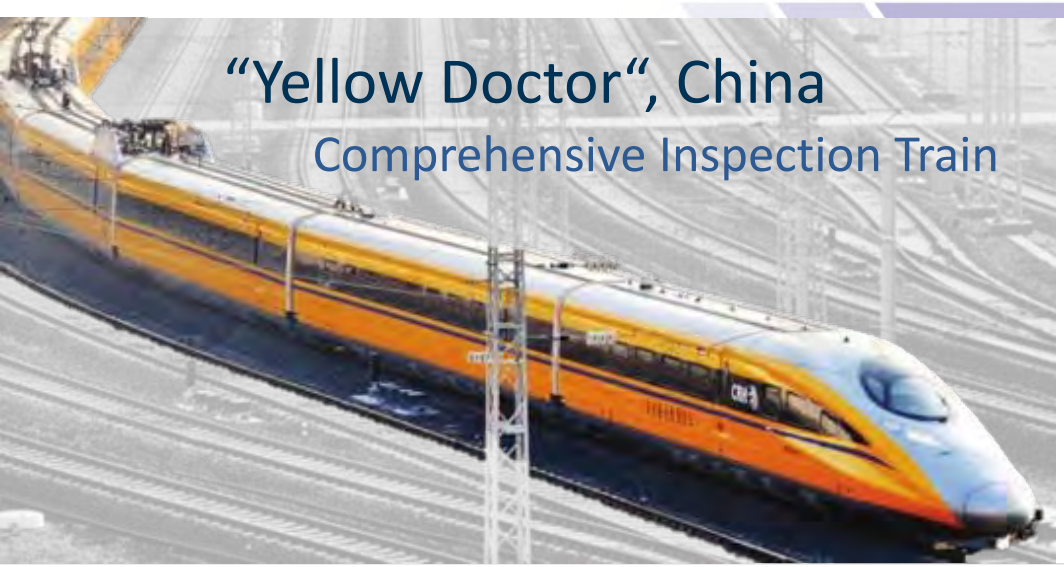

“Yellow Doctor“, China

Comprehensive Inspection Train

Railway Infrastructure in China

1. By the end of 2015, China had a 121,000 km operating railway network, including 19,000 km of high-speed railway.
2. This is projected to be 175,000 km and 38,000 km by 2025.
3. At present, there are more than 4,500 EMUs running on the high-speed railway every day.

©2024 Axiometrix Solutions Holdco LLC

©2024 Axiometrix Solutions Holdco LLC

Challenge – Effective Safety Testing of New Routes

- "Yellow Doctor" – Dedicated rolling railway laboratory.
- High Speed, Capable of 250km/h
- Diverse range of operating terrain
- Wide range of operating temperature (-40°C to +45°C)
- Large and varied channel count.
- Many measurement locations
- Signal Synchronisation
- Dynamics detection system – wheel and rail force, acceleration, etc.
- Comfort evaluation – vibration, acceleration
- Traction tests – network voltage and current, motor current, etc.
- Acoustical testing – microphone
- Pantograph test
- Bogies, body chassis dynamic stress test

Distributed and Decentralized Measurement System

- Standardised "Measurement Clusters" for bogie based on robust imc C series devices
- CRONOSflex modular measurement system allows connection of all types of sensors and signals.
- Sample rates up to 100 kHz
- All devices controlled from common software platform.

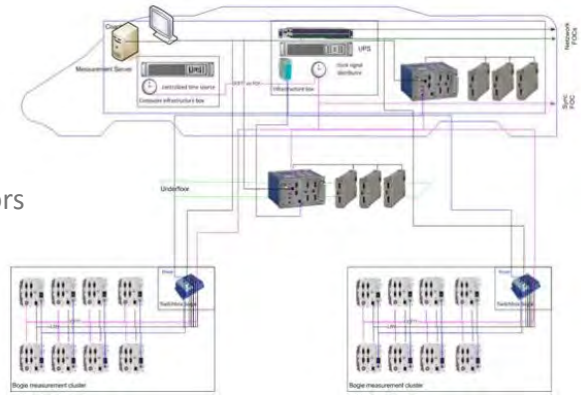

©2024 Axiometrix Solutions Holdco LLC

Hardware Designed for Rail Applications

CRONOS SL/ CRONOSflex-400

UNI2-8 MTC Version for Wheel force and Acceleration.
MTC series **(motor train cars)**
are intended for applications in electrically harsh environments,electric motor train applications in particular.
are characterized by possible transient input voltage conditions, both common mode and differential mode, of different types:
- **Destructive transient overvoltage**
- **ESD discharge processes**

ENC-4 for Speed & Distance

CAN bus for Distance synchronization

Conclusion

In the past 15 years, great progress has been made in the construction of Chinese railways, especially high-speed rail.

It has not only shortened the distances between cities, but also profoundly changed the way people live and work.

The advanced, feature-rich data acquisition equipment from imc Test & Measurement can meet the needs of China's high-speed rail test mission.

In the future, imc will continue to support the Chinese railway industry to expand the development and construction of one of their largest infrastructures.

©2024 Axiometrix Solutions Holdco LLC

United Kingdom, Tram Network

Permanent Ride Comfort

Tram Network – Permanent Ride Comfort

System Requirements

- Autonomous Operation
- Transparent to passengers
- Comfort Evaluation to International Standards
- Offline Analysis (full recording). Analysis is done at the tram's end station.
- Online Analysis (always at every station the tram arrived).

Source : Transport Focus, Tram Passenger Survey – April 2019

©2024 Axiometrix Solutions Holdco LLC

AXIOMETRIX SOLUTIONS | AP | GRAS | imc

Tram Network – Permanent Ride Comfort

System Configuration

- 5 x Accelerometers
  - Car body and bogie vibration measurement
- 1 x GPS receiver
  - Speed and position data
- imc CRONOSflex system
  - Data Acquisition
  - Online data processing

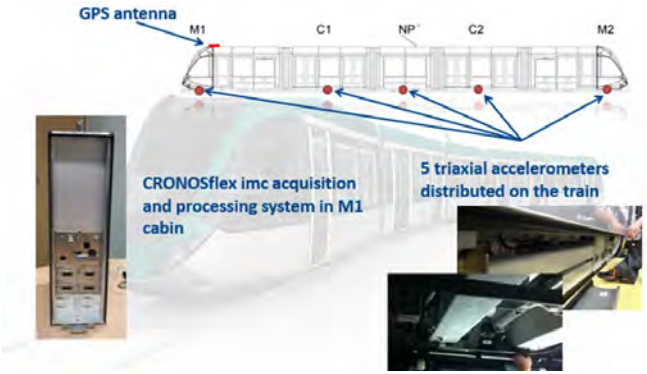

Tram Network – Inter Station Report

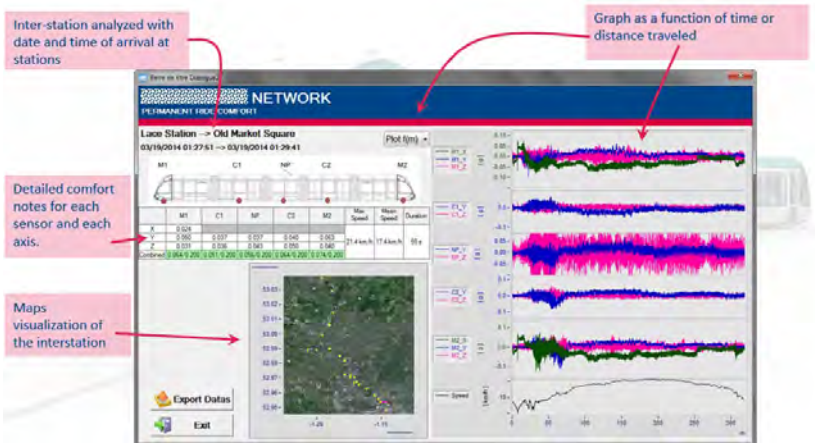

©2024 Axiometrix Solutions Holdco LLC

AXIOMETRIX SOLUTIONS | AP | GRAS | imc

Tram Network – Report for Complete Route

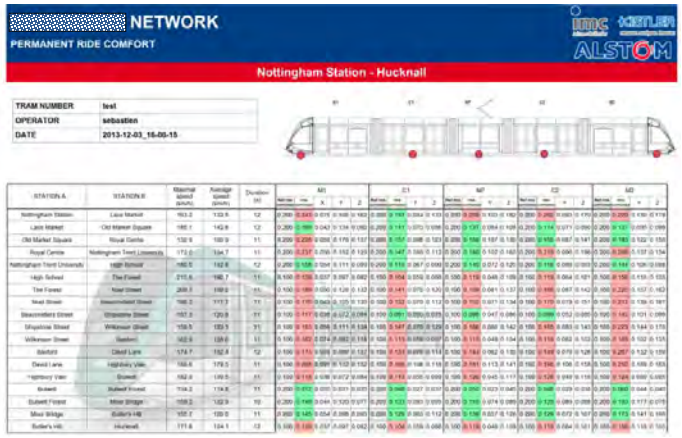
NETWORK
PERMANENT RIDE COMFORT
Nottingham Station - Hucknall

TRAM NUMBER	test
OPERATOR	sebastian
DATE	2013-12-03_16-00-15

AXIOMETRIX SOLUTIONS

LET'S CONNECT!

GARRY TJHIN
International Sales Manager (Asia-Pacific)